Lignin fibres prepared by coagulation : a promising precursor for carbon fibres

Marie Föllmer

université de BORDEAUX

THÈSE PRÉSENTÉE

POUR OBTENIR LE GRADE DE

DOCTEUR DE L'UNIVERSITÉ DE BORDEAUX

ÉCOLE DOCTORALE DES SCIENCES CHIMIQUES

SPÉCIALITÉ: Chimie-Physique

Par: Marie Föllmer

Lignin Fibres Prepared by Coagulation: a Promising Precursor for Carbon Fibres

Sous la direction de: Philippe Poulin

Co-directeur: Célia Mercader

Soutenue le 15 novembre 2018

Membres du jury :

M. Juan José Vilatela	Directeur de Recherche, IMDEA Madrid	Président du jury
Mme Sylvie Bonnamy	Directeur de Recherche, CNRS Orléans	Rapporteur
M. Wolfgang Maser	Directeur de Recherche, CSIC Zaragoza	Rapporteur
M. Alain Derré	Chargé de Recherche, CNRS Bordeaux	Examinateur
Mme Célia Mercader	Ingénieur de Recherche, CANOE (ADERA)	Examinateur
M. Philippe Poulin	Directeur de Recherche, CNRS Bordeaux	Directeur de thèse

Title: Lignin Fibres Prepared by Coagulation: a Promising Precursor for Carbon Fibres

Abstract:

Carbon fibres are currently used in composite materials for the aerospace, transportation and energy sectors. Their application in mass markets however is hindered by the high cost of the fibre raw materials. Therefore, alternative and inexpensive precursor materials are in high demand. Especially lignin, a widely abundant natural resource containing high quantities of carbon, is considered as an important candidate. So far, lignin fibres have mostly been prepared by melt-spinning and by blending with thermoplastic polymers to enhance their spinnability and mechanical properties, but strongly lowering their carbonization yields and raising their price. We propose lignin-based precursor fibres obtained through a continuous wet-spinning process. In combination with only small ratios of polyvinyl alcohol, highly flexible and infusible composite fibres, containing up to 70-90 % of industrial lignin, can be obtained. Our development enables us to manufacture carbon fibres in high yields which exhibit promising properties. Until now, lignin-based carbon fibres reported in literature do not reach the mechanical properties required for high-performance applications due to their amorphous carbon structure. However, by incorporation of liquid crystalline graphene oxide flakes or cellulose nanocrystals into our lignin precursor fibres, we are able to improve the orientation of the carbon planes obtained after carbonization. Our lignin-based fibre systems with enhanced structuration thus represent an important step towards the industrial implementation of lignin as “green” precursor material for low-cost and high-strength carbon fibres.

Keywords: Lignin, Fibre, Precursor, Wet-spinning, Coagulation, Carbon, Graphene Oxide, Liquid Crystals

---

Titre: Fibres de lignine préparées par coagulation: un précurseur prometteur pour fibres de carbone

Résumé:

Les fibres de carbone sont actuellement utilisées dans les matériaux composites pour les secteurs de l'aérospatiale, l’aéronautique et les sports de compétition. Leur application sur les marchés de grande consommation est toutefois entravée par le coût élevé des matières premières et le procédé de carbonisation, notamment l’étape de stabilisation. Par conséquent, les matériaux précurseurs alternatifs et peu coûteux sont très demandés. La lignine, une ressource naturelle très abondante contenant de grandes quantités de carbone, est considérée comme un bon candidat. Jusqu'à présent, les fibres de lignine ont été principalement préparées par filage en voie fondue et en mélange avec des polymères thermoplastiques pour améliorer leur aptitude au filage et leurs propriétés mécaniques, mais en réduisant fortement leurs rendements de carbonisation et en augmentant leur prix. Nous proposons dans cette thèse des fibres précurseur à base de lignine obtenues par un procédé de filage en continu par coagulation. En combinaison avec de petites proportions d'alcool polyvinylique, on obtient des fibres composites hautement flexibles et infusibles, contenant

jusqu'à 70-90 % de lignine industrielle. Notre développement nous permet de fabriquer des fibres de carbone avec des rendements de l'ordre de 30 % qui présentent des propriétés prometteuses. Jusqu'à présent, les fibres de carbone à base de lignine mentionnées dans la littérature n'atteignent pas les propriétés mécaniques requises pour des applications à hautes performances en raison de leur structure de carbone amorphe. Cependant, en incorporant des cristaux liquides de feuillets d'oxyde de graphène ou des nanocristaux de cellulose dans nos fibres précurseurs de lignine, nous pouvons améliorer l'orientation des plans de carbone obtenus après la carbonisation. Nos systèmes de fibres à base de lignine avec une structuration améliorée représentent donc une étape importante vers la mise en œuvre industrielle de la lignine en tant que matériau précurseur «vert» pour les fibres de carbone à faible coût et à haute résistance.

Mots clés: Lignine, Fibre, Précurseur, Voie Solvant, Coagulation, Carbone, Oxyde de Graphène, Cristaux Liquides

Centre de Recherche Paul Pascal

[Groupe Nanotubes & Graphène, Avenue Dr. Albert Schweitzer, 33600 Pessac]

Plateforme CANOE (ADERA)

[Groupe Fibres & Carbone, ENSCBP Cheminnov, 16 Avenue Pey Berland, 33600 Pessac]

Acknowledgements

I would like to express my sincere gratitude to Célia Mercader for her supervision at CANOE and for her unlimited support during these three years. I also would like to thank my PhD supervisor Philippe Poulin for his advice and expert guidance throughout my work at any time. It was a real pleasure to work with these two people.

Furthermore, I would like to thank the reviewers and the members of my jury (Sylvie Bonnamy, Wolfgang Maser, Juan José Vilatela and Alain Derré) for their evaluation of this work.

I am deeply grateful for the opportunity of doing my PhD in Bordeaux and I would like to thank all the people who contributed to this amazing experience. My achievements would not have been possible without them.

Special thanks go to my colleagues Simon Jestin and Hubert Thuillier with whom I shared the office and who never let me down when I encountered technical or personal difficulties. I especially appreciated Simon's helpful feedback on my writing, experiments and presentations. Furthermore, I would like to say "Merci beaucoup!" to Patrice Gaillard and the whole team of engineers and technicians at CANOE for their support and exceptional kindness. In particular, it was my pleasure to collaborate with Robin Pellissard and Aurélie Milani, who considerably participated in the positive outcome of my thesis. I also would like to thank my intern Chloé Pablos for her assistance in some of my experiments.

Besides, I would like to thank the people from CRPP who welcomed me among them without hesitation. A big part of my experiments would not have been possible without the advice and help of Wilfrid Neri and Ahmed Bentaleb. Furthermore, I would like to thank Alain Derré and Isabelle Ly for their assistance in my experiments. I also would like to acknowledge some people from the FORCE project (Julien Roman, Van Son Vo and Fernando Torres-Canas) who exchanged their results, experience and fruitful discussions with me.

I am very thankful to have been part of the group of PhD students and postdocs in the CRPP who shared some of my problems and who somehow made me feel more at home in this country. Thank you for being there for me, for constant advice and for the nice moments we spent together outside of the lab.

My special gratitude also goes to the Marie Curie ITN "DiStruc", who provided funding for my work. Thank you to all the people involved and especially to the ESRs for the awesome times we spent together during the meetings. I am grateful for the scientific and personal exchange with students and supervisors.

Finally, I would like to thank Christophe for always standing by my side, especially during tough periods of my PhD. I am really lucky to have met you. I also would like to express my particular gratitude towards my parents, my sister and my grandfather, who always supported me throughout my studies and, even from far away, throughout this thesis.

Résumé: Fibres de lignine préparées par coagulation - un précurseur prometteur pour fibres de carbone

Les fibres de carbone sont un moyen efficace de renforcement structurel des matériaux composites. Largement appliquées aux pièces composites dans les secteurs de l'aérospatiale, du transport et de l'énergie, ces fibres sont extrêmement demandées. De nos jours, l'industrie cherche à étendre son utilisation à des applications de grande consommation. La mise en œuvre est toutefois fortement entravée par le coût élevé des matières premières classiques utilisées comme précurseurs. Depuis plusieurs décennies, la recherche de matériaux précurseurs alternatifs, dont des bio polymères, et à bas coûts est en cours. La cellulose a été largement étudiée en tant que précurseur bio sourcé et les fibres de carbone résultantes sont relativement bien développées. Cependant, comparées aux fibres de carbone classiques, elles présentent des propriétés mécaniques plutôt faibles. De plus, la cellulose ne présente que de faibles rendements de carbonisation d'environ 15 %. Un autre candidat prometteur pour les fibres de carbone dérivées de ressources renouvelables est la lignine. Considérée comme un déchet dans l'industrie du papier et des biocarburants, la lignine est une ressource naturelle très abondante contenant de grandes quantités de carbone. Le filage des fibres à partir de la lignine est difficile en raison de sa faible masse moléculaire et de sa structure non linéaire ramifiée. Cependant, la lignine est parfaitement adaptée au traitement par pyrolyse thermique lors de la carbonisation grâce à sa structure aromatique, déjà partiellement réticulée. En théorie, la lignine présente des rendements de carbonisation élevés d'environ 40 %.

La plupart des fibres de lignine présentées dans la littérature ont été préparées par filage à l'état fondu. Un inconvénient évident des fibres filées à l'état fondu est leur fusibilité, qui est inappropriée pour subir un traitement à haute température pendant la carbonisation. Cette opération nécessite donc au préalable une stabilisation thermique sous oxygène. Afin d'éviter cette étape, nous avons choisi une approche de filage de la lignine par coagulation en voie solvant. Cette approche permet l'utilisation de grades de lignine infusibles, telles que la lignine Kraft de résineux. Cette lignine infusible ne requiert pas de stabilisation, ce qui rend sa carbonisation moins coûteuse en temps et en énergie.

L'objectif de ce travail était d'explorer les possibilités de fabrication de fibres de carbone bio sourcées à des coûts de matières premières et de production peu élevés, adaptées à une production à grande échelle. D'autre part, une nouvelle approche pour améliorer la structure des fibres de lignine a été proposée et étudiée. La combinaison des deux aspects représente une étape importante vers la mise en œuvre industrielle de la lignine en tant que matériau précurseur « vert » pour les fibres de carbone à bas coût et à haute résistance.

Les fibres à base de lignine ont été préparées via une méthode de filage humide simple et économique. Une lignine Kraft a été utilisée sans modification chimique préalable, et les fibres précurseur obtenues ont présenté des rendements autour de 30 % lors de la carbonisation. De petites quantités d'alcool polyvinylique (APV) ont été introduites dans les fibres pour faciliter

la formation des fibres pendant le filage, mais elles ont été maintenues aussi basses que possible. Ceci contraste avec les fibres de lignine fabriquées par filage en voie solvant dans la littérature. Des travaux à plusieurs échelles ont été effectués, allant du filage manuel (à l'échelle du laboratoire) au filage en continu de mono-filaments (à l'échelle intermédiaire) et enfin au filage des multi-filaments (à l'échelle pilote). Les essais de filage à l'échelle pilote ont été réalisés avec un grade de lignine commercial. Les fibres obtenues ont été caractérisées sous plusieurs aspects: miscibilité des polymères lignine et APV, morphologie et propriétés thermiques et mécaniques. En outre, les conditions de carbonisation ont été déterminées et les fibres de carbone résultantes ont été caractérisées par rapport à leur morphologie, la structure du carbone, l'orientation cristalline et encore leur propriétés mécaniques et électriques.

Les résultats obtenus ont montré que les deux polymères, la lignine et l'APV, ne sont que partiellement miscibles en solution et qu'ils forment des mélanges homogènes métastables dans les films et les fibres solides. Les fibres précurseur contenant un ratio lignine-PVA de 70:30 ont été filées en continu dans des conditions optimisées. Leurs propriétés mécaniques se sont avérées appropriées pour la carbonisation. Au moyen de l'analyse thermogravimétrique, un programme de température sur mesure a été créé. Les fibres de carbone obtenues présentent une résistance à la traction allant jusqu'à 400 MPa et des modules de Young à 50 GPa. En ce qui concerne les structures du carbone, les résultats de diffraction des rayons X (DRX) ont révélé du carbone désordonné et mal orienté. Cette structure est liée à la nature amorphe de la lignine elle-même, et est considérée comme la principale raison des propriétés mécaniques et électriques plutôt faibles des fibres. Les approches pour améliorer la structure et les propriétés mécaniques des fibres de carbone dans des études à venir comprennent une diminution du diamètre du filament, une carbonisation sous tension mécanique et une éventuelle graphitisation à haute température.

Des feuillets d'oxyde de graphène (GO) agencés en phase cristal liquide ont ensuite été ajoutés aux solutions de lignine afin de former un carbone plus structuré dans les fibres. Cette approche s'est avérée efficace. Contrairement au graphène, le GO peut être facilement dissous dans l'eau et dans les solvants organiques polaires, dans lesquels il forme des phases cristallines liquides. En utilisant les solutions de GO en voie solvant, elles peuvent être filées en fibres de GO. La structure et les propriétés résultantes de ces fibres sont prometteuses en raison de l'alignement des feuillets de GO dans l'axe de la fibre induit par l'écoulement pendant le filage.

Différents mélanges de lignine Kraft et de lignosulfonate avec du GO ont été préparés en solutions et sous forme de films et fibres solides. Les propriétés des films et fibres de lignine-GO ont été caractérisées par microscopie électronique, analyse DRX et conductivité avant et après carbonisation. Des images de microscopie optique des solutions sous lumière polarisée ont révélé un alignement des feuillets de GO en présence de lignine et la formation d'une phase nématique. Il est montré par DRX que cette phase favorise la structuration du carbone lors de la carbonisation des systèmes. En outre, une conductivité électrique de 10^4 S m^{-1} indique une cristallinité accrue dans les échantillons.

Cependant, une microporosité élevée a été détectée à la surface des films et des fibres carbonisés en raison des réactions de dégradation pendant la carbonisation. La porosité était principalement influencée par la quantité d'impuretés à l'intérieur de la lignine et par la vitesse de chauffe utilisée pour la carbonisation. Son impact sur la structure et les propriétés du carbone a été démontré par des pics de DRX plus larges et des conductivités électriques réduites. La microporosité du carbone amorphe étant une contrainte générale pour les applications structurelles, une caractérisation plus détaillée devrait être réalisée afin de mieux comprendre les mécanismes qui la créent. Une réduction de la porosité pourrait également être obtenue par une étape de stabilisation sous air avant la carbonisation.

En ce qui concerne les applications de filage par voie solvant, l'approche d'un renforcement par utilisation de GO est prometteuse car elle conduit à des fibres de lignine avec une structuration améliorée. Malgré de bonnes performances de filage, les fibres de lignine-GO, spécialement fabriquées à partir de lignine Kraft, ont montré une grande fragilité à l'état sec. La fragilité de ces fibres peut être considérée comme une restriction importante pour les applications industrielles. Les propriétés mécaniques des fibres de lignine-GO ne pouvaient pas être caractérisées en raison de leur grande fragilité et d'une quantité limitée d'échantillon. Par conséquent, l'utilisation d'un plastifiant s'est avérée nécessaire pour obtenir des fibres flexibles pouvant être manipulées plus facilement jusqu'au procédé de carbonisation. Les premières tentatives de création de ces fibres ont été effectuées dans la troisième partie expérimentale de cette thèse. De ce fait, les deux idées principales de cette thèse, filage en voie solvant en présence d'APV comme plastifiant et amélioration par addition de GO, sont directement combinées.

Des solutions de filage à base de diméthylsulfoxyde (DMSO), contenant de la lignine Kraft, de l'APV et des nanoparticules carbonées, à savoir des feuillets d'oxyde de graphène (GO) et des nanocristaux de cellulose (NCC), ont été utilisées pour préparer des films et fibres nanocomposites. Il a été montré que les nanoparticules étaient assemblées, au moins partiellement, dans des phases cristallines liquides au sein des solutions de filage. Lors de l'évaporation du DMSO, des films nanocomposites ont été préparés à partir des solutions de filage. Ces solutions ont également été utilisées pour la coagulation dans l'isopropanol afin de préparer des fibres nanocomposites. Les films et les fibres obtenus ont été soumis à un traitement de carbonisation. La structure et les propriétés résultantes, avant et après carbonisation, ont été caractérisées.

Le rendement de carbonisation des films nanocomposites est considérablement augmenté par l'addition de feuillets de GO à l'intérieur de la matrice lignine-APV. En outre, une cristallinité accrue a été trouvée pour les films contenant 5 et 10 % de GO. Cela a été mis en évidence par une augmentation de la conductivité électrique de 10^3 S m^{-1} à 10^4 S m^{-1} et par des spectres DRX indiquant des domaines graphitiques dans les échantillons. Des résultats similaires ont été obtenus pour la structure des films composites contenant des NCC, bien que l'effet de structuration ait été jugé moins prononcé.

En ce qui concerne le procédé de filage par voie solvant de fibres nanocomposites, l'isopropanol a été validé comme coagulant approprié pour les fibres lignine-APV-NCC. Cependant, la coagulation des solutions lignine-APV-GO s'est avérée plus difficile dans l'isopropanol, probablement en raison d'une force ionique insuffisante pour coaguler le GO. Les essais de traction des fibres précurseurs ont révélé des contraintes à la rupture et des modules d'Young plus élevés en y incorporant des charges de nanoparticules. Après carbonisation des fibres filées en continu, les propriétés mécaniques des fibres de carbone ex-lignine ont été améliorées avec seulement 5 % de NCC ou de GO. Le GO semble notamment être un renforcement prometteur, conduisant à des contraintes à la rupture allant jusqu'à 650 MPa pour les fibres de carbone à base de lignine Kraft, soit une amélioration des performances de plus de 100 %.

Afin d'améliorer encore les propriétés des fibres lignine-APV-GO, des essais d'optimisation futurs devraient inclure une méthode alternative de préparation de la solution de filage à des concentrations plus élevées. Différentes sources de GO avec des tailles de feuillets plus grandes pourraient également améliorer les propriétés des solutions de filage et des fibres. En outre, un contre-solvant plus approprié pour la coagulation des fibres nanocomposites contenant du GO est nécessaire pour évaluer le potentiel d'un procédé de filage par voie solvant à l'échelle industrielle.

Les résultats de cette thèse démontrent une préparation réussie des fibres de lignine-APV au moyen de la coagulation. Les fibres à base de lignine obtenues peuvent être transformées en fibres de carbone «vertes» et à faible coût. Les propriétés de ces fibres peuvent être adaptées en optimisant les paramètres de filage, en adaptant le procédé de carbonisation et en incorporant des charges nanocarbonés de renforcement tels que l'oxyde de graphène (GO) et les nanocristaux de cellulose (NCC). Grâce à un intérêt croissant de l'industrie papetière et composite, les futures recherches basées sur cette thèse incluront très probablement la lignine comme matériau précurseur prometteur pour les fibres de carbone.

Table of Contents

Chapter II: Preparation of Lignin Precursor Fibres by Coagulation and their Carbonization

Chapter III: Structuration of Lignin Through Liquid Crystalline Graphene Oxide

List of Abbreviations

CNCs	Cellulose nanocrystals
Dex	Dextran
DMA	Dynamic Mechanical Analysis
DMEU	Dimethyl ethylene urea
DMF	Dimethyl formamide
DMSO	Dimethyl sulfoxide
DR	Draw ratio
DSC	Differential Scanning Calorimetry
EDS	Energy dispersive Spectroscopy
EtOH	Ethanol
GO	Graphene oxide
IAT	IndulinAT®
KL	Kraft Lignin
LS	Lignosulfonate
L9	Lignin Grade Number 9 = IndulinAT®
L12	Lignin Grade Number 12 = LS from Tembec
L16	Lignin Grade Number 16 = KL from FCBA
NMMO	4-methylmorpholine N-oxide
p.	page
PAN	Polyacrylonitrile
PE	Polyethylene
PEG	Polyethylene glycol
PEO	Polyethylene oxide
PET	Polyethylene terephthalate
POM	Polarized Optical Microscopy
PP	Polypropylene
PVA	Polyvinyl alcohol
PVP	Polyvinylpyrolidone
rGO	Reduced graphene oxide
SAXS	Small angle X-ray scattering

SDS	Sodium dodecyl sulfate
SEM	Scanning Electron Microscopy
TEM	Transmission Electron Microscopy
T_g	Glass transition temperature
TGA	Thermogravimetric Analysis
T_m	Melting temperature
TPU	Thermoplastic polyurethane
wt%	Percent in weight
XRD	X-ray diffraction

Introduction

Carbon fibres are considered a powerful tool for the structural reinforcement of composite materials. Widely applied in composite parts for high performance sectors such as aerospace, military or nuclear engineering, these fibres are in extremely high demand. Nowadays, industry seeks an expansion of their use onto commercial applications. The implementation however is strongly hindered by the high cost of conventional fibre raw materials. For several decades, the search for alternative and inexpensive precursor materials has been ongoing and has also included biopolymers. Cellulose was extensively studied as a bio-based precursor and the resulting carbon fibres are relatively well developed. The fibres show a high thermal conductivity, but compared to conventional carbon fibres they exhibit rather weak mechanical properties. Besides, cellulose bears only low carbonization yields of around 15 %. Another promising candidate for carbon fibres derived from renewable resources is lignin. Considered as a waste product in the paper- and biofuel industry, lignin is a widely abundant natural resource containing high quantities of carbon. Fibre spinning from lignin is difficult because of its low molecular weight and branched, non-linear structure. However, lignin is highly suitable for the thermal pyrolysis treatment during carbonization thanks to its aromatic structure, which is already partially cross-linked. In theory, lignin bears elevated carbonization yields of around 40 %.

Most of the lignin fibres reported in literature have been prepared by melt-spinning. A clear drawback of melt-spun fibres is their fusibility, which is inappropriate to undergo the high temperature treatment during carbonization and which necessitates a thermal stabilization under oxygen. Therefore, our chosen approach is the preparation of lignin fibres by coagulation or wet-spinning, allowing the use of infusible lignin grades. These grades may not need a stabilization at all, thus rendering their carbonization process less time- and energy consuming.

The first chapter introduces the topic of this thesis by providing detailed background information about lignin, the most common fibre spinning techniques and carbon fibres in general. It includes an overview over already existing lignin-based carbon fibres. The second chapter is focused on the fabrication trials of lignin-based fibres via a simple wet-spinning method. The lignin was used without any prior chemical modification and the obtained precursor fibres showed high yields upon carbonization. Small amounts of polyvinyl alcohol (PVA) were introduced into the fibres to assist the fibre formation during spinning, but they were kept as low as possible. This stands in contrast to previously reported lignin-based fibres made by wet-spinning. The obtained fibres were characterized regarding polymer miscibility, morphology, thermal- and mechanical properties. Besides, the carbonization conditions have been determined and the resulting carbon fibres were characterized regarding morphology, structure, crystal orientation, mechanical- and electrical properties.

The prepared carbon fibres based on lignin were found to consist of amorphous carbon which is only poorly organized and bears only low electrical- and mechanical properties. Therefore, attempts to enhance the carbon structure of lignin by means of graphene oxide (GO) flakes

were made in the third chapter. Unlike graphene, GO can be easily dissolved in water and in polar organic solvents, in which it forms liquid crystalline phases. By using GO solutions as spinning dopes, they can easily be wet-spun into GO fibres. The resulting structure and properties of these fibres are extremely promising due to the alignment of GO flakes in fibre axis induced by the flow during spinning. Carbon nanotubes exhibit similar spinning performances. However, due to the fact that they are already reported in literature as filler for lignin fibres, this thesis is solely focused on GO. Its mixing behaviour with lignin was studied in solution prior to preparation of solid lignin-GO films and –fibres. The impact of the GO flakes on the lignin structure and on its resulting properties was characterized by electron microscopy, X-ray diffraction- and conductivity measurements.

Since the approach led to promising results, the preparation and characterization of nanocomposite films and –fibres consisting of lignin, PVA and nanoparticle fillers (GO or cellulose nanocrystals) is presented in the fourth and last chapter of this thesis. It thereby represents a combination of the approaches shown in chapter two and three. On the one hand, the preparation of low-cost carbon fibres based on lignin and PVA prepared by a continuous and scalable wet-spinning process. On the other hand, the reinforcement of these fibres by incorporation of GO liquid crystalline particles.

The aim of this work was to explore the possibilities of manufacturing bio-based carbon fibres at low raw material costs and low production costs, which are suitable for a large-scale production. Furthermore, a novel approach towards lignin-based fibre systems with enhanced structuration was proposed and studied. The combination of both aspects represents an important step towards the industrial implementation of lignin as “green” precursor material for low-cost and high-strength carbon fibres. Thanks to an increasing interest from side of the papermaking- and composite industry, future research is very likely to include lignin as a promising precursor material for carbon fibres.

The work presented in this thesis has been carried out at the Research and Technology Transfer Platform CANOE for Organic Nanostructured Composites in collaboration with the group Nanotubes and Graphene of the Paul Pascal Research Centre in Pessac, Bordeaux. Funding has been provided by the European Union within the framework of the Marie Skłodowska-Curie Innovative Training Network “DiStruc” (*Di*rected *Struc*ture at the mesoscale). In collaboration between academia and industry, the network consists of 15 PhD projects at 9 host institutions in 6 different European countries which cover theory, simulations and novel applications of liquid crystalline phases.

Chapter I Theoretical Background and State of the Art

This chapter provides fundamental background information for the topic presented and evaluated in this thesis. An overview over the material class of lignin including its structure, properties, industrial extraction techniques and applications is given in the first part. The most common spinning techniques for the production of polymer fibres are presented in the second part. The third part covers important facts about conventional carbon fibres and shows their processing steps, their properties and their current applications. Finally, the last part gives a summary of the state of the art on lignin-based carbon fibres, which are already reported in literature. The chapter is concluded by the motivation and the aims of the work presented in this thesis.

I.1 Lignin

An overview over the material class of lignin is given in the following sub-chapters, including its general structure and properties, the main extraction techniques used in industry and possible applications for this type of polymer.

I.1.1 General Introduction

Lignin is one of the building blocks present within the cell walls of trees and plants, along with cellulose and hemi-cellulose. The latter two polymer materials have a rather linear structure and cellulose is arranged as fibrils on the micro- and nanoscale. Both cellulose and hemi-cellulose are surrounded by lignin, an aromatic bio-polymer formed as a 3-dimensional network holding the fibrils together and giving them strength and rigidity (see Figure I-1). Lignin represents about 20 % of the mass composition within wood. Since forests cover around one third of the earth's land surface area, lignin is known to be the most abundant aromatic bio-polymer on earth. Hence, it is both a widely available resource and a renewable material.[1–4]

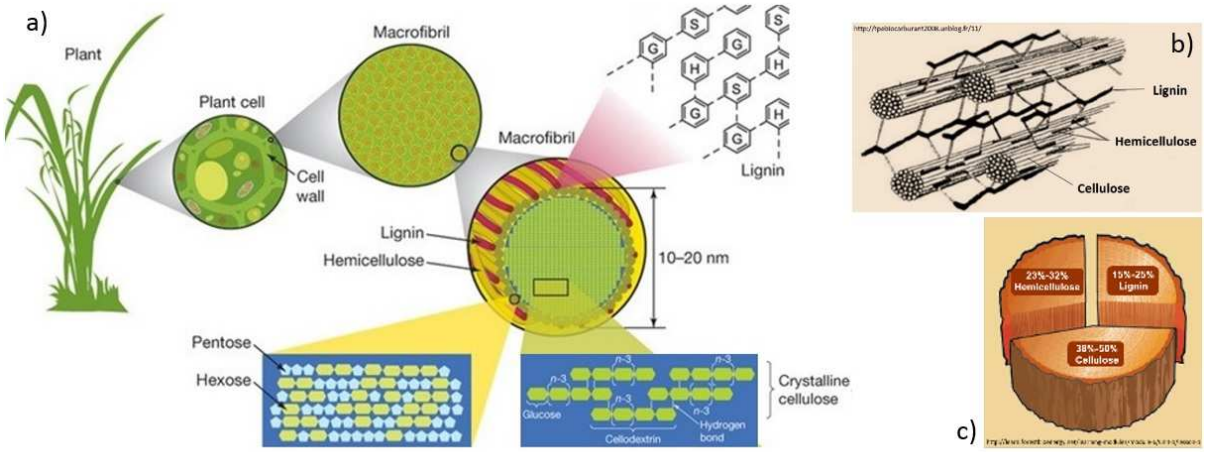

Figure I-1: *Cell wall components of plants (a), schematic 3D-structure of cellulose, hemi-cellulose and lignin (b), Composition of wood (c) [1]*

More than 50 million tons of lignin are extracted per year, mainly as by-product from bio-fuel- and paper production. Large quantities of the resulting lignin are used as internal energy source, but there is an increasing interest in utilizing it for applications of higher value as well. During the last decades, a lot of research and new developments in chemistry and material science have been dedicated to the material class of "ligno-cellulosic biomass". This includes especially lignin due to the fact that in industry, it is considered as a waste product. Nowadays only 2 % of the produced lignin is actually commercialized, hence there is a huge market potential. Along with other possible applications, researchers have been considering lignin as an important candidate for producing "green" carbon fibres. In addition to its low raw material cost (< 1 € kg^{-1}, Alibaba.com, Mai 2018), the high carbon content within the structure of lignin

(60-65 %) promises rather high carbonization yields upon pyrolysis of the precursor fibre (see *chapter I.3* and *I.4*).[5]

I.1.2 Structure and General Properties

Lignin is an amorphous polyol made from branched methoxylated phenylpropane units with a three-dimensional structure (see Figure I-2), whose shape and constitution are determined by the type of plant and the extraction process used in order to separate lignin from cellulose. Consequently, there are large variations in its molecular structure, which lead to completely different chemical- and physical properties between different lignin grades.

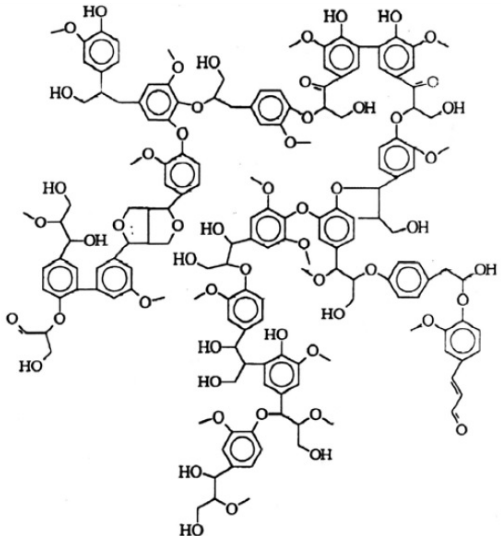

Figure I-2: *Example structure of lignin [6]*

Lignin grades can generally be classified into three main types according to their biomass origin: softwood, hardwood and grass lignin. Depending on the origin, the lignin structure is primarily composed of specific building blocks, so-called monolignols, in different ratios. The monolignols consist of: *p-coumaryl alcohol, coniferyl alcohol and sinapyl alcohol* (see structures in Figure I-3). Lignin can hence be classified according to its content of monolignols. Softwood lignin mainly consists of coniferyl alcohol with small amounts of p-coumaryl alcohol, hardwood lignin contains both coniferyl- and sinapyl alcohol whereas grass lignin contains all three types of monolignols (see Table I-1).[3, 7]

Table I-1: Abundance of lignin monomers in different types of plants [7]

Plant	p-coumaryl alcohol (%)	coniferyl alcohol (%)	sinapyl alcohol (%)
Coniferous softwood	< 5	> 95	only traces
Broadleaf hardwood	0-8	25-50	46-75
Grasses	5-33	33-80	20-54

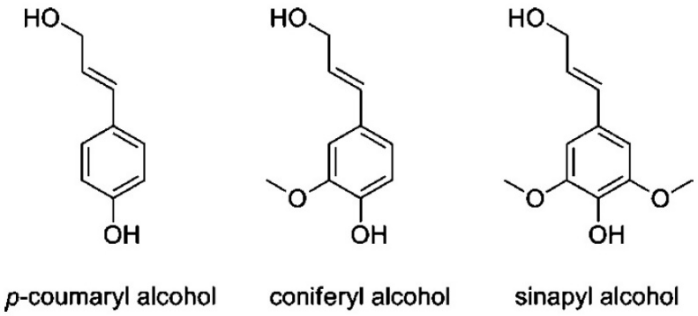

***Figure I-3**: The three monomer building-blocks of lignin [8]*

Generally, lignin monolignols are linked by ether- or carbon-carbon bonds. It is important to note that besides the monolignol units, also other molecular structures can be found within lignin polymers. Softwood lignin contains more resistant linkages compared to hardwood lignin types because the C_5 positions within the coniferyl alcohol units are available for coupling. The sinapyl alcohol units in hardwood have C_5 positions which are sterically hindered, hence resulting in the fact that hardwood lignin has a lower degree of condensation than softwood lignin. Thus, hardwood lignin is fusible and can be used for melt-spinning, whereas the stronger bonds of softwood lignin generally make it an infusible material (see *chapter I.4*).[9]

Due to the fact that the structure of lignin is aromatic and branched and constructed as a three dimensional network, lignins are generally insoluble in the most common solvents. What serves as protection and resistance for a plant, results in a material that is rather unsuitable for chemical reactions or fermentation into other products.[8]

The structure and properties of lignin are not only determined by the type of plant it comes from, but also by the treatment performed on naturally occurring lignin. In most cases, lignin is separated from cellulose for industrial purposes. The specific extraction techniques are described in the following subchapter. For instance in paper production, where the long and linear molecular chains of cellulose are required, the molecular network of lignin is cut in order to separate the two components. Hence, the resulting molecular weights for the recovered lignin are rather low and within a wide range from approximately 2000 to 25000 g mol^{-1}.

Unlike cellulose, lignin does not have a long and linear architecture. Using lignin as a polymer for fibre spinning thus represents a real challenge. Due to its three dimensional and branched molecular structure, lignin is a very brittle material that cannot be easily aligned or stretched as it would be necessary to produce fibres with a high toughness (see *chapter I.2*). Therefore, examples in literature usually show spinning of lignin fibres only with addition of plasticizers (see *chapter I.4*).[10]

I.1.3 Extraction Techniques

The main industrial sources for lignin can be found in the pulp- and paper industry (e.g. Kraft lignin, lignosulfonate and Soda lignin) and in bio-refineries (e.g. Organosolv lignin). The

extraction technique used to separate cellulose from lignin is a major factor determining the structure and properties of the resulting lignin material.

- Kraft Pulping:

  The most frequently used extraction technique is the Kraft pulping process or sulfate process used in industrial paper production. The resulting lignin material is called “Kraft lignin” or “alkali lignin” and consequently it is the most abundant industrially produced grade compared to other lignin types.

  During the Kraft pulping process, wood is dissolved in so-called white liquor containing aqueous sodium hydroxide (NaOH) and sodium sulfide (Na_2S) at a high pH of 13 and high temperatures (140-180 °C) for about 2 hours. During this cooking process, degradation and dissolution reactions break the bonds of lignin and hemi-cellulose to separate it from cellulose. The treatment results in two obtained products: wood pulp containing cellulose fibres for paper production and so-called black liquor. It contains lignin (29-45 %), carbohydrates and a high amount of inorganic materials. After collection of the solid pulp used for paper making, the solvent of the black liquor is evaporated in a step-wise process. The remaining, highly viscous part is then regenerated and typically used as combustion for the recovery boiler. If lignin is to be extracted, black liquor is treated with acids in order to precipitate the lignin (at pH 9) and recover it by filtration. Generally, the obtained Kraft lignin is insoluble in water and has only low impurity contents of up to 3 %.[3, 8, 11]

  In the commercial LignoBoost® technique, the black liquor is treated with carbon dioxide gas in order to decrease its pH to 9 (see Figure I-4). The precipitated lignin is filtered afterwards and re-dispersed several times in slightly acidic conditions (H_2SO_4). This milder treatment of the black liquor generates small and uncrosslinked precipitates, thus lignin of higher quality of higher molecular weight and elevated glass transition temperature.[12]

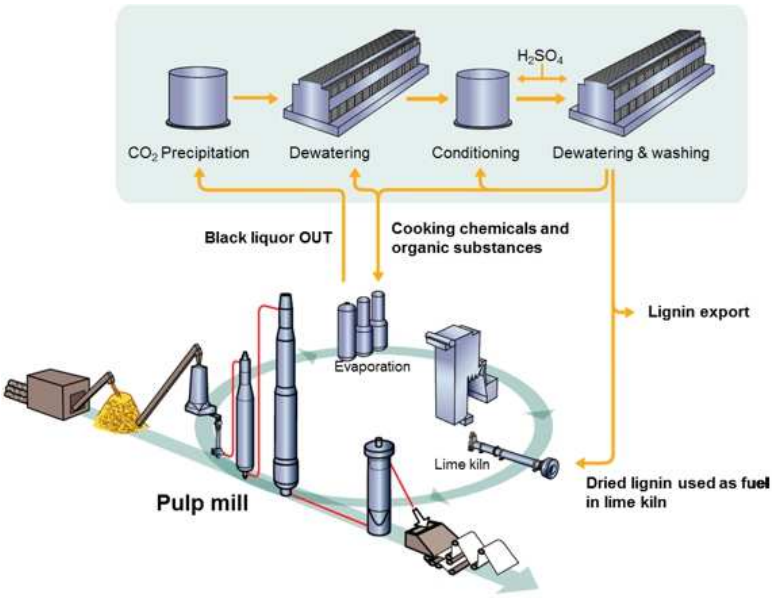

Figure I-4 : *Schematic of lignin extraction of Black liquor via the Lignoboost® process* ***[13]***

- Sulfite Pulping:

  In order to dissolve lignin and separate it from wood, the sulfite pulping process uses heated aqueous solutions of sulfite or bisulfite and calcium, magnesium, sodium or ammonium as the counter-ions, resulting in so-called “lignosulfonates”. The process is conducted at various pH values (1-13) and relatively common in the pulp- and paper industry. It bears lignin grades that are usually soluble in water and in some highly polar organic solvents. Lignosulfonates from sulfite treatment commonly exhibit higher average molecular weights than other lignin grades because of the incorporation of sulfonate groups into their molecular structure. Typically, lignosulfonates exhibit high sulfur contents (3.5-8 %) and rather high amounts of inorganic impurities. Thanks to their solubility in water, lignosulfonates have already been used for solution-based spinning processes such as wet-, dry- and electrospinning (see chapter I.2). The incorporated sulfur also generates potential active sites for modification.[8, 14, 15]

- Soda Pulping:

  “Soda lignin” originates from the Soda pulping process, where lignocellulose is cooked at 160 °C in an aqueous solution of sodium hydroxide (NaOH) dissolving lignin. This lignin type is free of sulfur and, in contrast to other lignin grades, mostly obtained from non-wooden plants. Soda lignin has a high purity, but at the same time it exhibits rather low molecular weights.[14, 15]

- Organosolv Process:

  In the Organosolv process, aqueous organic solvents are used to solubilize lignin from wood and to isolate separate streams of cellulose, hemi-cellulose and lignin. It is hence considered more environment-friendly because it is lacking sulfites and the harsh conditions used in Kraft- and sulfite pulping. For instance the Alcell® process developed in 1989 uses ethanol at low pH for the pulp cooking. Typically, “Organosolv lignin” thus contains extremely low sulfur contents and only very small amounts of inorganic compounds, making it a lignin grade of very high purity. However, up to now this process, which is used both in paper industry and in bio refineries, is still rather expensive due to a limited solvent recovery.[8, 14, 15]

Additionally, there are other extraction techniques such as extraction by hydrolysis or steam-exploded extraction of lignin. Besides the type of extraction influencing the structure and properties of lignin grades, it is possible to tailor their properties by purification or chemical modification.

Purification of technical lignin grades is generally performed by washing with distilled water or diluted acids to decrease the amount of impurities (e.g. ash, salts or sugar residues).[16] Purification can also be performed by precipitation, as it is the case in the Lignoboost® process. Another way to purify technical lignin is fractionation in order to obtain polymer

materials with a narrower molecular weight distribution and hence lower polydispersity. Fractionation can be performed chemically (with solvents) or physically (by filtration with membranes).[3]

The molecular structure of lignin grades can be modified either by chemical modification or chemical reactions such as functionalization, grafting or co-polymerization. For instance acetylation can change the solubility, fusibility or compatibility of lignin with other polymers.[17] However, chemical modification of lignin is a very expensive treatment and cannot be used for applications with critical cost factors.

I.1.4 Applications

Lignin has only a few commercial uses, which are listed and shortly described in this subchapter.

As already mentioned, lignin within black liquor is converted into thermal energy to help running recovery boilers for the pulp- and paper production. Besides its use for combustion, it can be converted into chemicals such as synthetic vanillin or the solvent dimethylsulfoxide (DMSO). However, about three quarters of all commercial products containing lignin are dispersants, emulsifiers, binders and complexing agents. Other applications include adhesives and filler materials. For these applications, lignin is mostly used without any modification.[6]

All of these examples represent applications of rather low value. However, the current research goes towards the use of lignin as a novel precursor material for carbon fibres, hence transforming lignin into a promising candidate of higher value (see Figure I-5). The idea of the work presented in this thesis is thus to develop a novel and simple approach to spin lignin fibres, which are suitable for a subsequent carbonization in order to obtain low-cost and “green” carbon fibres.

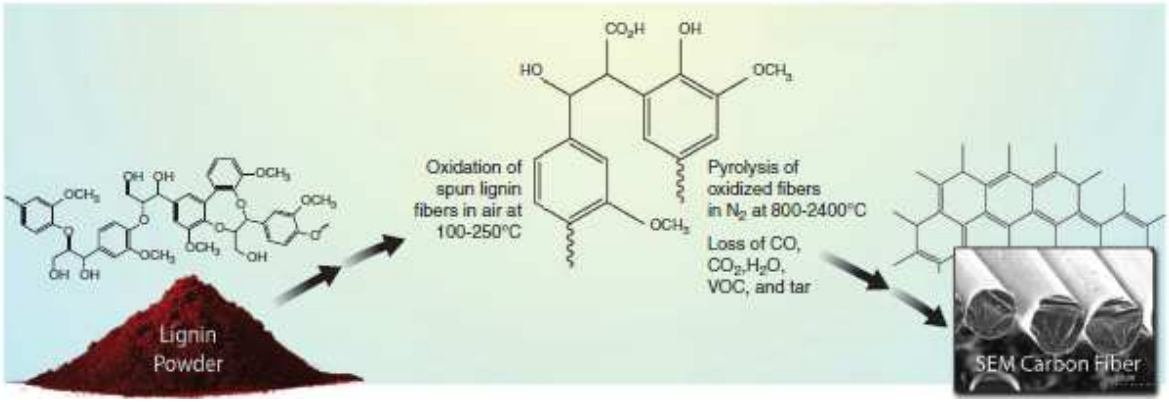

Figure I-5 : *Conversion of raw material into commercial carbon fibres: a novel desired application for lignin [18]*

I.2 Fabrication Principles of Polymer Fibres

Nowadays, tremendous research and development is dedicated to so-called high performance fibres. These fibres are being developed with unique structure and properties in order to match the required performances such as high strength- and stiffness (e.g. carbon-, aramid fibres), high thermal- or chemical resistance (e.g. Teflon) or "smart" properties (thermal, electrical, magnetic or mechanical response to external stimuli). High performance fibres generally include, but are not limited to: commercial nylon- and polyester fibres, glass fibres, steel fibres, aramid fibres (Kevlar®/Twaron®), carbon fibres and ceramic fibres.[20, 21] They are often used as reinforcement in composite materials to build strong structures at light weight.

Within this work, we focus on carbon fibres and their fabrication principles. Since carbon cannot directly be produced into a fibre form, a suitable polymer material is first processed into a precursor fibre. This precursor is then subjected to a pyrolysis treatment above 1000 °C whereby all elements except carbon are removed from the fibre. The following sub-chapters give a broad overview over the most common principles used to produce precursor fibres that are suitable for subsequent carbonization.

I.2.1 Melt-Spinning

During melt-spinning, a polymer material is typically molten by means of an extruder and subsequently drawn into fibres throughout a spinneret which contains small holes (see Figure I- 6). Upon exiting the spinneret, solid filaments are formed from the melt upon cooling. In many cases, a spin finish is applied onto the fibres before they are wound up and collected onto spools. The most important processing parameters are the extrusion temperature and -rate (material throughput), the winding speed and the drawdown ratio.[21]

Nowadays, melt-spinning is the most common commercial process to spin polymer fibres at very high speeds.[14, 23] Typical examples of melt-spun synthetic fibres are made from polyester (e.g. polyethylene terephthalate (PET)), polyolefins (e.g. polyethylene (PE) or polypropylene (PP)), nylon and polyphenylene sulfide (PPS).[22] Moreover, the second most common precursor material for carbon fibres, namely pitch, is produced by melt-spinning (see chapter I.3.2).

Melt-spinning does not need any solvents, it is thus considered an environmentally friendly process.[10] Besides, the fabrication step itself is considered as rather simple because the material only melts and solidifies into a fibre state. The spun fibres usually exhibit a high molecular orientation due to the draw-down movement during their fabrication.[23] However, clear drawbacks of this technique are the high energy costs for heating and the limitation to fusible polymer materials forming stable melts. Regarding carbon fibre production, a further drawback is the necessity to cross-link the fibres after spinning by means of a thermo-oxidation treatment to prevent them from melting during carbonization.[10, 24]

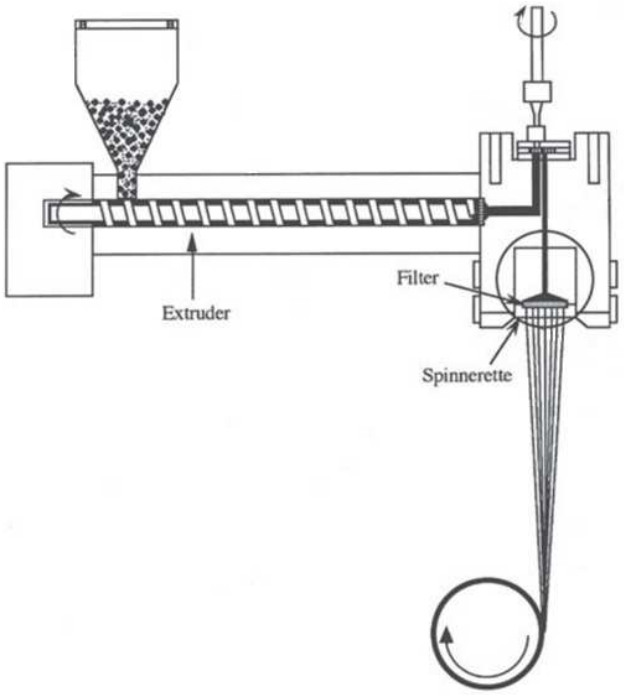

Figure I-6: *Melt-spinning principle (basic image taken from* ***[25]****)*

In the case of lignin, crucial factors for melt-spinning are their thermal- and rheological properties. As lignin generally is an amorphous material it does not melt in a classic sense, but rather softens above its glass transition where it can be processed via melt-spinning. The temperature window to process lignin fibres is quite narrow, as at low temperatures fibres may not be formed, whereas at too high temperatures the lignin may chemically degrade. Therefore, pretreatments or blending with other substances are commonly used to decrease the lignin's glass transition temperature and to facilitate the spinning process. Besides, the residence times within the extruder should be limited for lignin in order to prevent cross-linking of OH-groups or thermal degradation during processing.[26] In many cases, lignin powders are pelletized by extrusion prior to melt-spinning to facilitate their handling during production.[14]

I.2.2 Dry-Spinning

In contrast to melt-spinning, dry-spinning is a solution-based spinning method. Thereby, a polymer solution is extruded through a spinneret into a heated gas chamber, in which the solvent evaporates while a solid fibre is formed (see Figure I-7). Thus, three phenomena are taking place simultaneously: the flow of a non-Newtonian solution during extrusion, a mass transfer during fiber solidification and a heat transfer during solvent evaporation.[27]

The temperature of the gas containing chamber depends on the solvents used and is an important variable for the process. Other crucial processing parameters are the polymer solid content in solution and the resulting viscosity, the injection rate of the solution and the drawing rate of the solid fibres.[27] Typical dope concentrations are within a high range of 25-45 % of dissolved polymer. The cross-section of the spun fibre depends on the rate of diffusion and the rate of evaporation of the solvent. In only rare cases, when both rates are equilibrated, the

fibre cross-section will have a circular shape, otherwise it can be flat, bean-shaped or crenulated.[28]

Commercially, dry-spinning is used for the production of cellulose acetate fibres. The spinning solution of cellulose acetate and acetone is heated to decrease its viscosity and filtered by a very small spinneret hole size (30-50 µm). The vaporized acetone is removed by hot air flow.[29]

In order to dry-spin lignin fibres, the lignin grade should be soluble in a volatile solvent which exhibits a high vapor pressure. The most common solvent is acetone, but also water, dimethylformamide (DMF) or other solvents are being used.[10, 29] The first and only carbon fibres based on lignin that were commercially available in the 1970s were produced by dry-spinning (see *chapter I.4*).

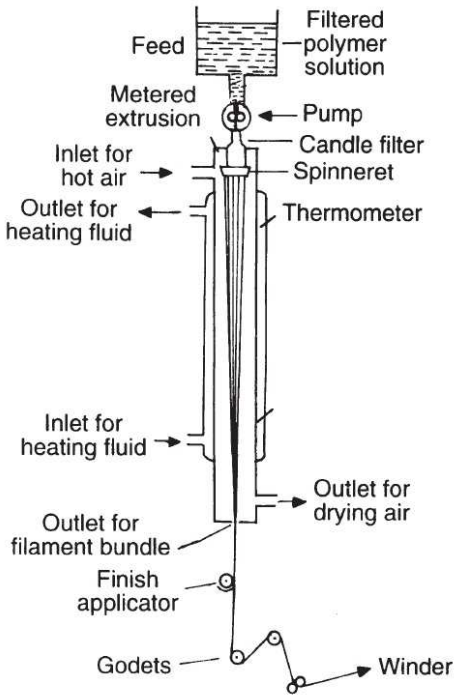

Figure I-7 : *Dry-spinning principle* ***[28]***

A similar solution-based fabrication principle is the so-called electrospinning. This technique can be considered a niche process at rather small scales. Commonly, it is used to prepare fibre mats containing nanofibres. In principle, a polymer solution is drawn into filaments by means of electrostatic forces. The polymer solution exiting from a syringe or capillary tube is exposed to an electric field and hence electrically charged. As soon as the electrical repulsion forces overcome the forces of the solution's surface tension, a jet is ejected from the syringe tip. Electrostatic repulsion makes the jet bend and the solvent evaporate so that tiny polymer filaments are formed. Ultimately, the jet arrives at a collector where the mat containing nanofibres is deposited.[30-31]

Compared to conventional spinning processes, the obtained fibres have smaller diameters within the nano range and higher surface areas. Regarding carbon fibres, their applications

thus rather focus on energy storage, membranes and other devices based on highly porous structures instead of structural reinforcement.[10]

I.2.3 Wet-Spinning

Another common spinning technique in industry based on solution spinning is wet-spinning. Thereby, fibres are formed by extrusion of a polymer solution through a spinneret into a so-called coagulation bath (see Figure I-8). The bath contains a counter-solvent of the polymer, thus upon contact with the polymer solution (namely: spinning dope), a solvent exchange takes place and provokes the precipitation (coagulation) of the polymer. The interchange between the spinning dope and the coagulation bath is diffusional. The coagulant from the coagulation bath diffuses into the fibre, while solvent from the polymer solution is removed from it. The solvent and counter-solvent should thus be miscible systems. Following the diffusion process, it becomes clear that coagulation occurs at first at the fibre surface. Depending on the coagulation rate, the resulting fibre cross-sections may have different shapes. A very fast coagulation typically leads to skin-core structures.[28]

After passing the coagulation bath, the fibre is typically guided through other coagulation- and/or washing baths in order to fully remove the solvent. After drying with hot air or infrared light, the fibre can be hot- or cold-stretched and can undergo finishing treatments prior to winding (see Figure I-8).

Along with the coagulation rate, the spinning dope concentration (usually 10-30 wt%), injection speed and drawing speed are important processing parameters. Spinnerets used for wet-spinning typically comprise several hundred up to 1000 holes of 20-200 µm in diameter. The spinneret can either be placed inside the coagulation bath or slightly above, leaving a small gap between the spinneret exit and the surface of the coagulation bath. This “air-gap” is typically used in dry-jet wet-spinning to enhance the molecular orientation of the polymer chains by aligning them inside the gap. The air-gap usually consists of only a few millimeters. Dry-jet wet-spinning can thus be considered a mixture between wet-spinning and dry-spinning.[28]

Fibres obtained by wet-spinning are usually high quality products suitable for mass production.[26] Besides, temperature or heat transfer only play a minor role, which is a clear advantage with respect to melt- and dry-spinning.[32] However, the adjustment of processing parameters and the coagulation process itself is complex and still not fully understood.

Typical products of commercial wet-spinning are aramid fibres (Kevlar®, Twaron®), cellulose fibres, carbon nanotube fibres, polyvinylalcohol (PVA) fibres and polyacrylonitrile (PAN) fibres. The latter is the most common precursor material for carbon fibres (see *chapter I.3*).

In order to wet-spin lignin fibres, the lignin raw material should typically be blended with high molecular weight polymers to enable its spinnability and to adjust the viscosity of the spinning dope.[26] However, the dissolution of lignin and a plasticizing polymer in common solvents at high concentrations is considered rather difficult.

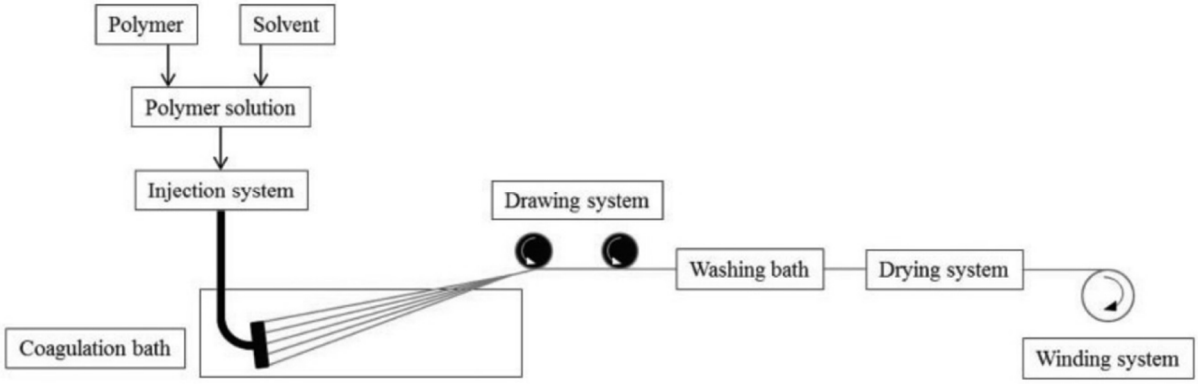

Figure I-8 : *Wet-spinning principle* ***[32]***

Different fabrication techniques used to spin precursor fibres for subsequent carbonization have been presented in this chapter. Melt-spinning, dry-spinning and wet-spinning are equally used to produce conventional precursors. Regarding the spinning of lignin fibres, the most frequently used technique until today is melt-spinning. However, also the other methods can be found more and more in literature. A detailed overview of these developments will be given in chapter I.4.

I.3 Carbon Fibres

I.3.1 Introduction

By definition, carbon fibres are prepared from a polymeric precursor fibre or from carbon allotrope building blocks and they consist of carbon by at least 92 %. Generally, carbon fibres are known to exhibit high strength and high stiffness at very light weight. The carbon fibre industry is principally located in Japan (Toray, Toho Tenax, Mitsubishi Rayon) and in the United States (Hexcel), but there is also some production in Europe (Toray and Hexcel in France, SGL Group in Germany). The most commonly used raw materials for carbon fibre production are polyacrylonitrile (PAN) (about 90 %) and mesophase pitch (about 9 %). Carbon fibres are principally used in high value sectors such as aerospace, military, construction, windpower, luxury automobile, medical- and sporting goods. There is a constantly growing demand for carbon fibres (see Figure I-9). However, mass market applications of carbon fibres are still hindered due to the high precursor fibre costs and the lack of high speed production techniques.[33–35]

Historically, carbon fibres have been invented by Thomas Edison in 1878 in his quest for incandescent lamp filaments. At the time, he converted cotton and bamboo fibres into carbon. The first practical use of carbon fibres started in the 1950s, when viscose fibres were carbonized for missile applications in the military sector. In the 1960s, polyacrylonitrile (PAN)-based carbon fibres were commercialized, which nowadays represents the technical breakthrough for high performance carbon fibres. In the following years, tremendous efforts were made to improve the performance-price ratios of carbon fibres. These activities are still ongoing today.[36-37]

The strongly increasing demand for carbon fibres of lower cost has been driving the search for alternative raw materials as precursor fibres. Especially renewable, biogenic resources such as cellulose and lignin have come into focus of researchers and engineers. However, these developments do not yet meet the properties of the PAN-based reference fibres.

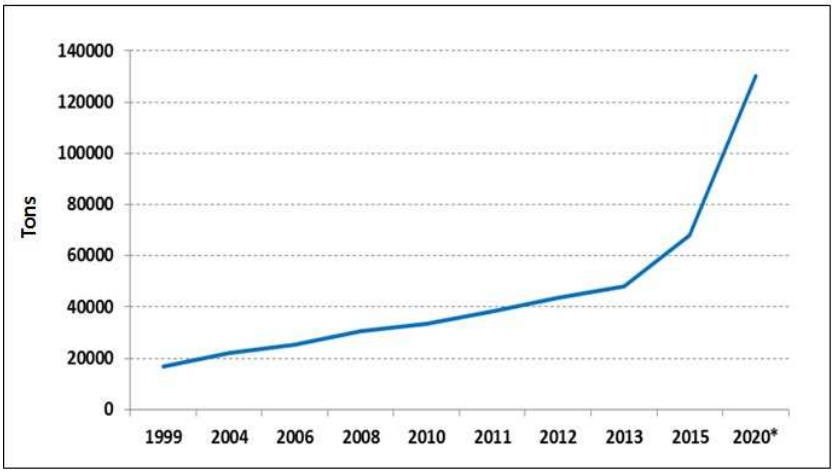

Figure I-9: *Global demand for carbon fibres per year, *estimated (data from **[38]**)*

I.3.2 Processing

The basic processing sequence of a conventional carbon fibre production as shown in Figure I-10 always begins with the spinning of the precursor fibre. Afterwards, the obtained fibre is heated up to 200-300 °C under air for stabilization and cross-linking to make it infusible. Then, the actual carbonization step is performed, where the fibre is heated to 1200-1600 °C under an inert atmosphere (nitrogen or argon). In some cases, the fibre is heated further up to 3000 °C for graphitization, which improves the ordering of the carbon planes along the fibre axis and bears especially high mechanical properties. The processing steps for PAN-and pitch-based carbon fibres are explained in the following paragraphs.[35, 38]

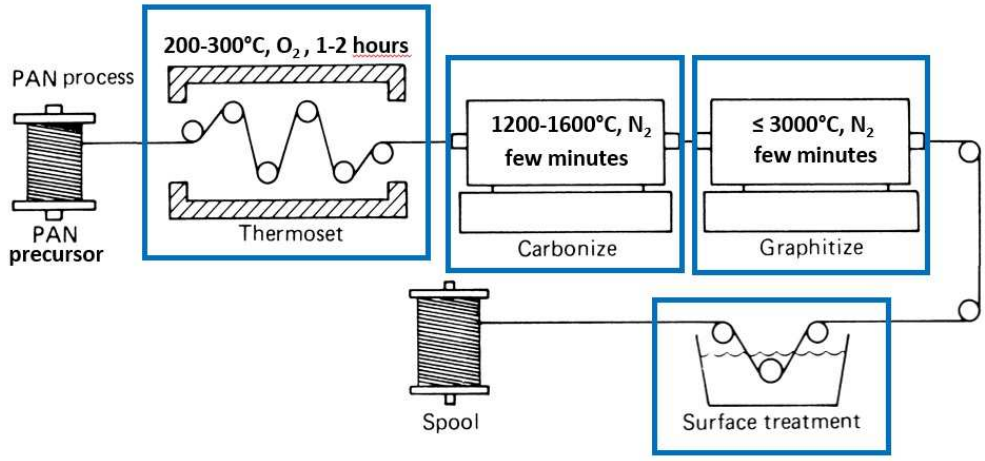

Figure I-10 : *Schematic representation of PAN-based carbon fibre production*

- ***Spinning of PAN- and Pitch Precursor Fibres***

a) PAN Processing

Currently, polyacrylonitrile (PAN) is the most widely used polymeric precursor material for carbon fibres. In most cases, its monomer acrylonitrile is polymerized by initiators through addition polymerization in solution or suspension, either as batch or continuously. It is important to remove the remaining AN-monomers from the dope since they are toxic and carcinogenic. The PAN fibres are traditionally spun through wet-spinning or dry-jet wet-spinning (see *chapter I.2*). Thereby, the dissolved polymer (in DMAc, DMF, DMSO) precipitates by passing through several baths at different temperatures and compositions. The most critical factors for the PAN fibre production are the temperature and the diffusion- and coagulation rates in both dope and baths, which are difficult to equilibrate. These factors determine the obtained fibre properties. Besides, to increase molecular orientation, the fibres can be spun by means of an air gap or be stretched under steam directly after spinning. Before further heat treatments, the fibres can be coated with a finishing oil (silicon oil, fatty acids).[33-34]

Because of its polar nitrile groups, strong intermolecular interactions usually take place between adjacent PAN chains. Therefore, small ratios of co-monomer are often added to reduce the interactions and facilitate the production of PAN fibres. The obtained molecular weights are usually within the range of 70,000-260,000 g mol^{-1}. PAN contains 68% of carbon.[33]

b) Pitch Processing

After PAN, pitch is the second most frequently used precursor material for carbon fibres. Pitch is a viscoelastic, tarry material which in its natural form originates from the distillation of petroleum or coal. Synthetic pitch is produced from pyrolysis of polymers and aromatic compounds. It has an inhomogeneous, polyaromatic structure and low molecular weights of around 1000 g mol^{-1}, which strongly depend on its origin. For instance, pitch obtained from coal has a more aromatic structure than petroleum pitch. Less aromatic pitches are generally preferred for carbon fibre production. Pitch can contain more than 80 % of carbon.

Pitch precursor fibres can be prepared by melt-spinning, either from isotropic pitch or from anisotropic, so-called mesophase pitch. The latter one is preferred for carbon fibre production because it usually leads to fibres with extremely high strength and high modulus. Mesophase pitch is obtained by heating isotropic pitch to 350-500 °C under an inert atmosphere, resulting in a disk-like liquid crystalline phase. The melt-spinning process of mesophase pitch is extremely difficult and expensive. The low molecular weight of the pitches results in very low viscosities and hence the production temperatures are relatively difficult to adjust and require a strict control of the spinning conditions, increasing the costs.[33-34]

Pitched-based precursor fibres have lower raw material costs, higher carbonization yields and higher degrees of orientation in fibre direction, which results in higher elastic moduli and higher conductivities compared to PAN-based fibres. However, their production costs are much higher than those of PAN fibres, which is due to purification, formation of the mesophase as well as the complexity of fibre spinning from pitch.[33]

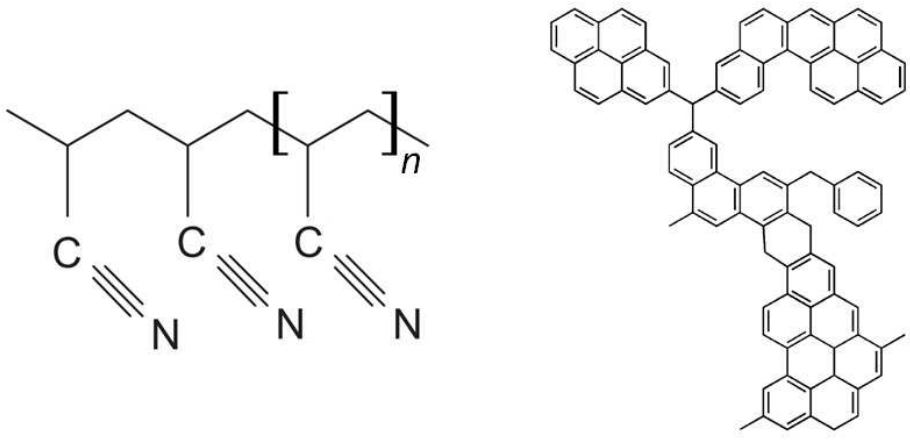

Figure I-11: *Linear structure and repeat unit of PAN (left) and example structure of aromatic pitch (right)*

- ***Thermo-Stabilization of Precursor Fibres***

During the stabilization/oxidation process, the as-spun precursor fibres pass under tension through an oven heated at 200-300 °C under an oxidizing atmosphere. Typically, the oven contains different air-heated zones gradually increasing in temperature. The air flow thereby provides oxygen for the reaction, heats the fibre and removes gases created during the treatment. The stabilization process includes highly exothermic reactions and the heat released needs to be controlled in order to avoid fibre defects.[33-34]

In the case of PAN, the stabilization treatment provokes a reorganization of linear chains into a cyclized structure. Besides, cross-linking reactions take place which are triggered by oxygen molecules in an exothermic manner. This new cross-linked PAN structure protects the fibre from decomposing in the subsequent pyrolysis steps at even higher temperatures, thus its structure is preserved. Stabilization times vary from 25 minutes up to several hours, depending on the diffusion rate of oxygen into the fibre. The treatment is usually carried out under tension to avoid fibre shrinkage. For PAN-based fibres, the density usually increases from 1.18 to 1.36 g cm^{-3}. The exact reaction mechanisms strongly depend on the co-monomers introduced prior to the PAN precursor fibre spinning.[33-34]

Pitch-based precursor fibres are generally stabilized in the same way as PAN fibres. The oxidative treatment at 250-350 °C (below the material's glass transition) provokes cross-linking and hence the fibres become infusible.[33]

Alternative ways for stabilization or cross-linking of precursor fibres are plasma-, electron beam- or microwave treatments. Besides, stabilization processes induced by UV- or gamma ray radiation are reported.[14, 34, 39]

It is important to note that certain infusible precursor fibres (prepared by wet- or dry spinning) do not need to undergo this procedure, but they can directly be carbonized without any prior treatment. The most important example of this work is infusible Kraft lignin.

- ***Carbonization***

The carbonization process consists of a thermal pyrolysis, in which the fibres are heated in an inert atmosphere (nitrogen or argon) to temperatures ranging from 1000-1500 °C. The process takes only a few minutes at the highest temperature, during which the fibres are kept under tension at all times. Upon heating, non-carbon elements are removed step by step from the fibre until there are only very small fractions of nitrogen and hydrogen left. The non-carbon elements are usually volatile compounds, which include HCN, H_2O, O_2, H_2, CO, NH_3, CH_4 etc. Due to this removal, the fibre diameter decreases drastically during carbonization and the fibre loses approximately 50 % of its weight.[34]

The heating rates during carbonization are of critical importance since they determine the morphology of the obtained carbon fibre. If the rate is too fast, defects and pores within the fibre structure will occur upon heating. However, if it is too slow, too much nitrogen will be

eliminated from the fibres at lower temperatures. In small amounts, nitrogen atoms provide a certain level of molecular flexibility required for the rearrangement at higher temperatures.[33] Besides, very low heating rates can lead to the creation of macropores.[5, 16]

The molecular rearrangement of PAN starts around 400-500 °C by dehydrogenation reactions. Thereby, the cyclized PAN structure obtained from the oxidative stabilization process is linked up into graphite-like ribbons. Upon further heating between 600 and 1300 °C the formed ribbons are combined into planar structures by denitrogenation. At even higher temperatures, additional condensation reactions create the so-called turbostratic carbon structure, graphite-type carbon layers intertwined by cross-links, but still highly oriented along the fibre axis.[33] The mechanisms are presented in Figure I-12. It has to be noted that the nitrile groups within PAN generate toxic hydrogen cyanide during carbonization, which is another reason why researchers started looking for alternative precursors.[10]

In the case of mesophase pitch, the elimination of hydrogen atoms creates covalent bonds starting from 350 °C. Upon further heating to 1300 °C and above, further hydrogen, oxygen and nitrogen atoms are removed from the structure, resulting in a carbon yield of 80-85 %.[33-34]

In general, the degree of orientation of the obtained carbon planes within the fibre gets higher at higher carbonization temperatures, which also increases the fibre's strength.

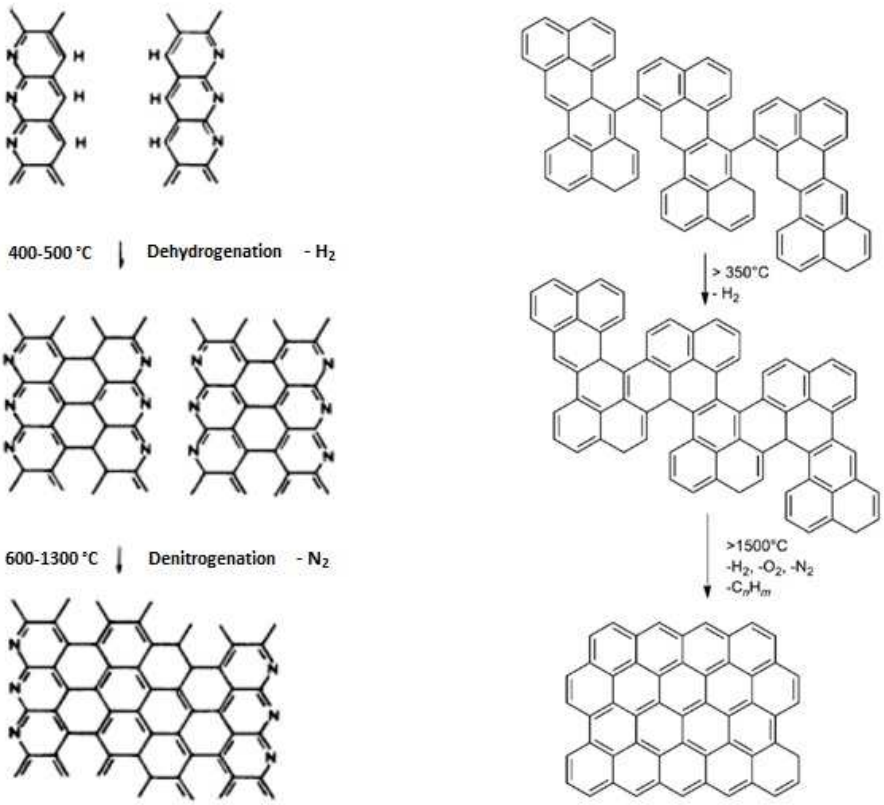

Figure I-12: *Formation of the graphite structure during carbonization for PAN (left side) and pitch-based fibres (right side)* ***[33-34]***

- ***Graphitization***

The final stage of the pyrolysis treatment for carbon fibres is called graphitization. Thereby, the carbonized fibres are further heated up to 3000 °C under argon (since nitrogen would react with the carbon structure). This final treatment leads to the growth of an ordered carbon structure in fibre thickness and area, thus in axial and transverse direction. Specifically, the crystalline orientation gets increased and the interlayer spacing between the carbon planes as well as the void contents get reduced.

Graphitization is usually used to obtain high modulus carbon fibres, although it simultaneously leads to lower tensile strengths.

In summary, it has been shown that the processing of carbon fibres from PAN and pitch is complex and energy consuming. The high raw material costs (PAN) and the high processing costs (pitch and PAN) represent the largest contributors (50 %) to the final price of conventional carbon fibres, which nowadays is too high for mass market applications. The price of PAN-based carbon fibres lies at 13-17 € kg^{-1}[40] (in 2016), whereas pitch-based carbon fibre costs are much higher depending on their desired performance (80-1000 € kg^{-1}). Carbon fibres of much lower costs are necessary for a use in mass market applications.

I.3.3 Structure and Properties

PAN- and pitch-based carbon fibres have outstanding properties due to their unique microstructure in both axial and transverse direction. However, the properties of carbon fibres strongly depend on factors such as crystallinity, molecular orientation or amount of defects. Thus, they do not depend on the precursor material itself, but rather on its molecular structure and the resulting fibre morphology.[33, 37]

The internal structure and morphology of conventional carbon fibres is quite complex. According to a model proposed in the 1970s, it consists of intertwined ribbon-like crystallites in axial direction, which are oriented more or less parallel to the fibre axis. The ribbons itself consist of multiple layers made of carbon arranged in a hexagonal lattice, just like planes of graphene. It thus resembles the structure of graphite, although the layer spacing within carbon fibres is much higher than in actual graphite.[37] Generally, the width of the ribbons, the number of graphene layers within it, the length of the ribbons and their degree of orientation determine the properties of the carbon fibre.[37] The graphene planes making up the internal structure of a carbon fibre can be arranged in different ways:

Graphitic structure → layer planes are completely parallel to each other in a regular fashion; can be found in pitch-based carbon fibres

Turbostratic structure → layer planes are parallel but irregularly stacked, bent, folded, tilted or split, increasing the layer spacing; usually found in PAN-based carbon fibres

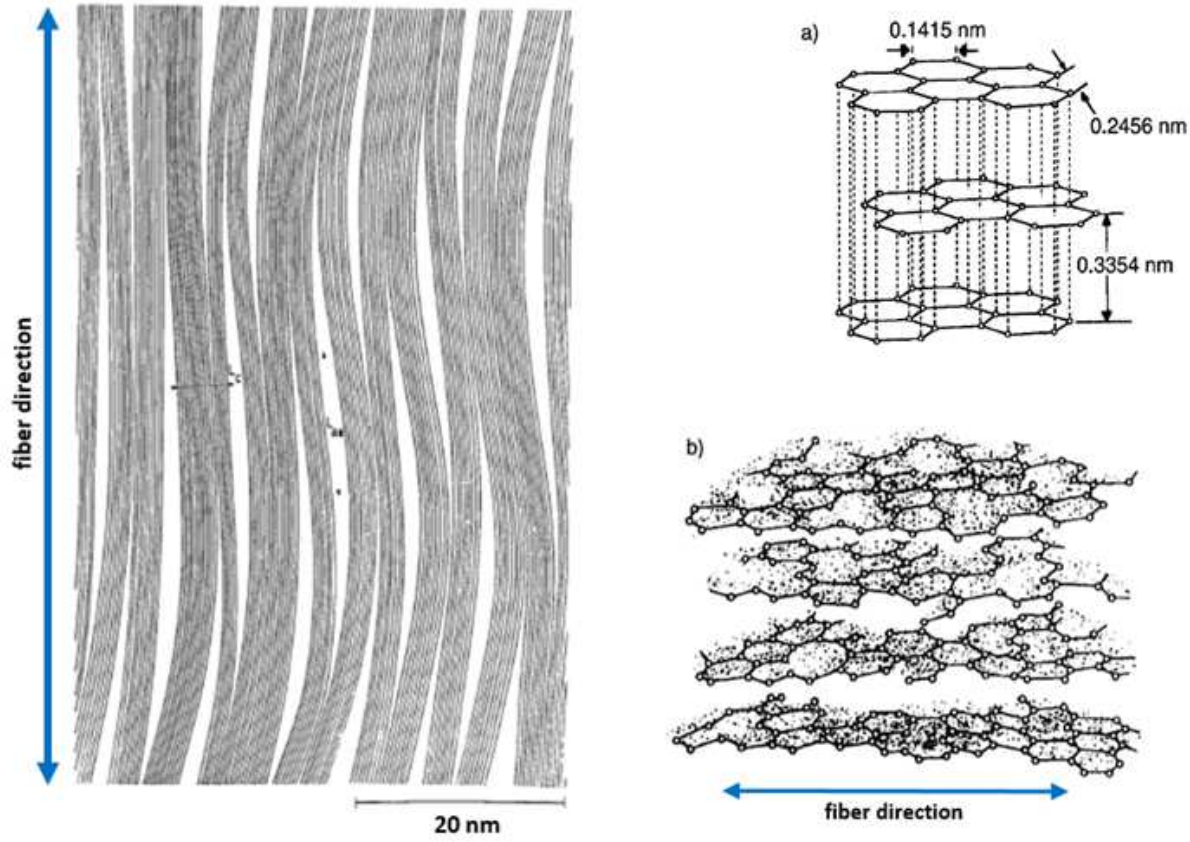

Figure I-13: *Model of ribbon-like microstructure for carbon fibres (left); graphitic carbon structure (a) and turbostratic carbon structure (interlayer spacing ≥ 0.344 nm) (b) of graphene planes within carbon fibres* ***[33-34]***

The layer spacing between graphene planes decreases with increasing temperature during the heat treatment. Thus, graphitization at 2000-3000 °C typically leads to increased mechanical properties. Improved molecular orientation and hence higher mechanical properties can also be obtained by mechanical stretching of the fibre during the stabilization and/or graphitization process.[37]

The extremely high strength and stiffness of carbon fibres are due to the covalent sp^2 C-C bonds within the graphene planes. However, the layer planes are only bound by rather weak van-der-Waals forces, thus the fibres usually exhibit a poor shear resistance. Despite the layer spacing between graphene planes, the fibres are thermally and electrically conducting since loose electrons can move freely within them.[37]

The long-range ordering within the fibres, thus the length and orientation of the ribbons, determines the elastic modulus. Fibres classified as “ultra-high modulus” (> 500 GPa) can only be made from mesophase pitch precursors, which are present in a disk-like liquid crystalline phase orienting upon fibre spinning (see Figure I-14). Besides, given the turbostratic carbon structure and the higher amount of microvoids within PAN-based fibres, they usually exhibit a lower density (1.8 g cm^{-3}) than pitch-based fibres (2-2.15 g cm^{-3}).

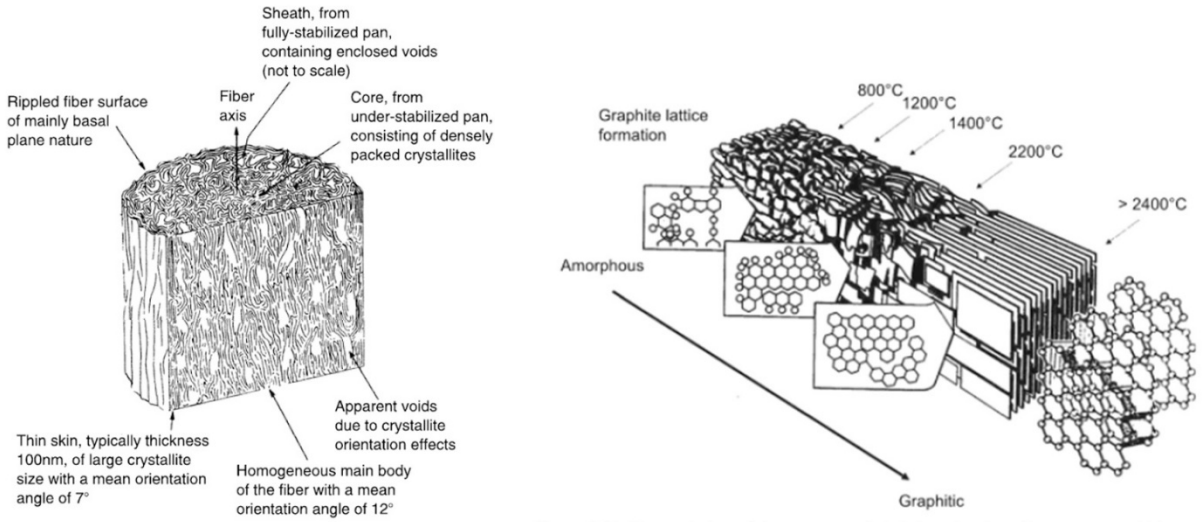

Figure I-14: *Models of carbon plane orientation within PAN-based (left) and mesophase pitch based carbon fibres (right)* ***[19, 41]***

In summary, the most important properties of carbon fibres (both PAN- and pitch-based) are[37]:

- Very high modulus (=stiffness) ⟶ 230-450 GPa (PAN); up to 750 GPa (pitch)
- High tensile strength ⟶ up to 5.5 GPa (PAN); up to 3 GPa (pitch)
- High conductivity in fibre direction:
  - thermal conductivity ⟶ 21-125 W $m^{-1}K^{-1}$ (PAN); 500 W/mK (pitch)
  - electrical conductivity ⟶ 5-6x10^4 S m^{-1} (PAN); 2-3x10^5 S m^{-1} (pitch)
- Low compressive strength
- High fatigue- and creep resistance
  (In composites: no stress rupture, complete elastic recovery upon unloading)
- Resistance to moisture and chemicals

As has been shown previously, carbon fibres underly a crucial structure-property relationship. The mechanical properties and conductivity of carbon fibres depend on the graphene layer orientation within them. This molecular orientation is completely determined by the spinning process and not by the carbonization itself. In order to achieve moderate and high mechanical properties, the molecular chains within the precursor should have the same orientation. Consequently, an amorphous precursor material will form rather glassy carbon instead of highly oriented and large carbon crystallites. Amorphous precursor materials thus generally exhibit only weak mechanical properties.[34]

The well-ordered turbostratic structure of PAN-based carbon fibres leads to a good balance in properties and is responsible for their dominance in structural applications. Given the elevated

price of highly oriented pitch-based carbon fibres, they are primarily used for high value applications.

I.3.4 General Applications

Nowadays, carbon fibres are mainly used as reinforcements in composite materials. These fibre-reinforced materials are typically used as a replacement for metals in order to save weight. The properties of the respective carbon fibres are usually tailored according to their application in two different approaches (see Figure I-15).

In the high technology sectors such as aerospace, military or nuclear engineering, a maximum performance of the composite materials is required. At the same time, the production requirements or the cost factors are less important and the composite pieces are considered as high value products. For these applications, the most expensive carbon fibres with the highest mechanical properties can be used.[36] In aerospace applications, the main objective is usually to save weight. Carbon fibres are in demand due to their high specific strength and specific stiffness at light weight. For instance, satellites contain high modulus pitch-based fibres, partly due to the high stiffness-to-weight ratio and partly due to their negative axial coefficient of thermal expansion.[37]

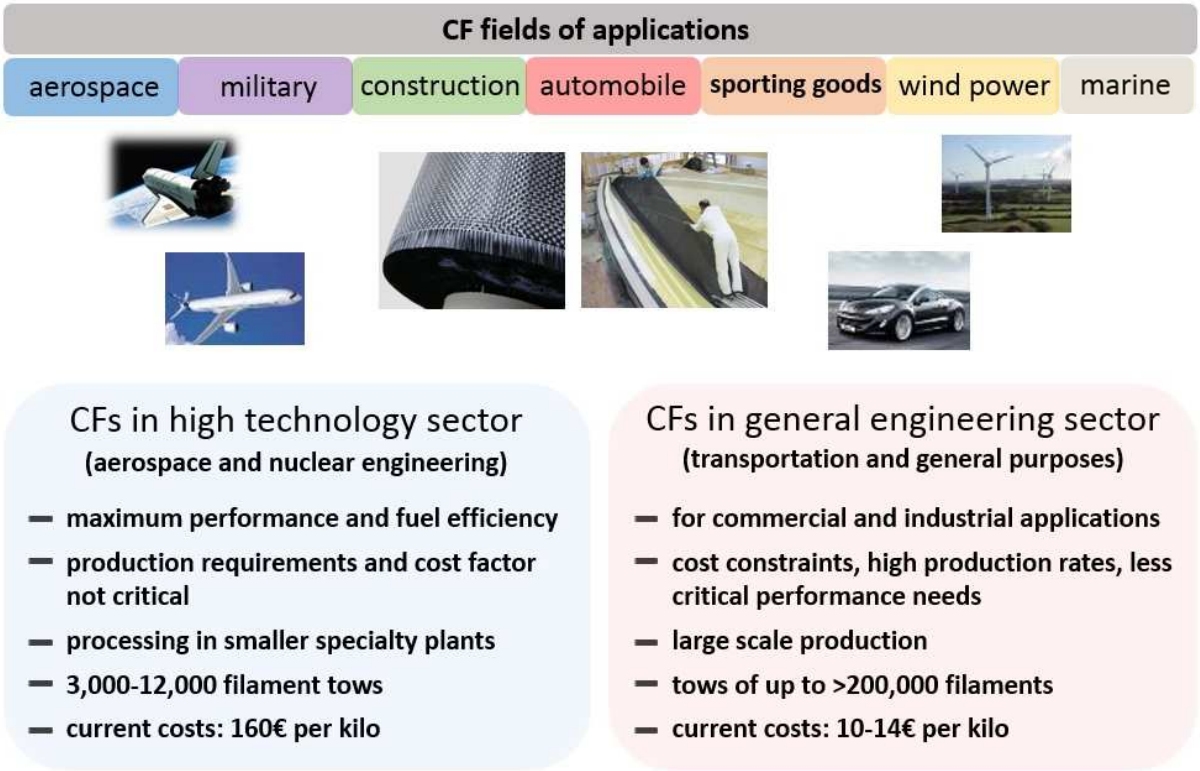

Figure I-15: *Overview of current applications for carbon fibres*

The sector of transportation and general engineering applications is the fastest growing sector demanding for carbon fibres with intermediate performances. These fibres are targeted for commercial and industrial applications, where high production rates and rather low material costs are required. Typical examples for this sector are the automobile-, marine-, wind power- and sporting goods industry (see Figure I-15). Oil pipes made from carbon fibre reinforced composites can support their own weights in deeper water when hanging from the platform. Besides, machine parts generally can contain carbon fibre pieces for static discharge purposes. Regarding sporting goods, the largest application within this field is golf club shafts. Because of their lighter weight at higher stiffness, more weight can be placed into the club head, which increases its speed and improves the resulting distances of the ball. Other sporting goods are made from carbon fibres principally because of their light weight and sensitive touch.[37]

So-called “activated” carbon fibres containing a high amount of pores and microvoids are typically used for gas absorption applications.[33] Besides, there are new trends going towards the use of renewable carbon fibres for battery electrodes and electronic applications.[42]

In order to incorporate carbon fibres into composite parts, the fibres are first woven into fabrics, which are then combined with polymer resins in so-called layup processes inside a mould (see Figure I-15). Another fabrication technique is the combination of carbon fibre strands with thermoplastic polymers in order to produce so-called tapes. In this case, the composite parts are created by arranging the tapes in the desired way and melting the polymer, which then solidifies into the final shape. It has to be noted that surface treatments of the carbon fibre fabrics are necessary prior to their combination with polymer resins. Through active groups such as hydroxyls, carboxyls and carbonyls, bridges are formed between the fibres and the resins. Thereby, the number of created bonds is more important than their strength in order to achieve a strong interface. The surface of the fibres can also be etched and roughened in order to increase the surface area available for interfacial bonding.[34, 37]

Within a composite material, the strength of a single carbon fibre is generally averaged over the bundles containing thousands of fibres.[37]

From the estimated production capacities for the following years (see Figure I-16), the increasing interest and demand for carbon fibres tailored for this sector becomes clear. Nowadays, the existing commercial products containing carbon fibres are regarded as luxury considering their elevated prices. One of the targets of the automobile industry is therefore to decrease the raw material price of carbon fibres in order to implement them in commercial cars. The French project FORCE for instance is aiming for carbon fibres from alternative ressources at a raw material price of around 8 € kg^{-1}.[36-37] This development towards a strong cost decrease initialized a new trend in the carbon fibre industry. In order to respond to the high demand and to new developments made in carbon fibre research, the production capacities and hence the actual supply need to be adjusted (see Figure I-16). Further production plants adapted to high throughputs and to novel precursor materials are necessary in the near future.

Carbon fiber demand and supply, metric tonnes (MT)			
	Carbon fiber demand	Carbon fiber supply (nameplate)	Carbon fiber supply (actual)*
2010	48,370	79,650	47,790
2015	82,400	143,595	93,171
2020 (est.)	150,200	180,600	129,965
*Actual output is less than nameplate, due to capacity knockdown.			

Figure I-16: *Trend of global carbon fiber demand and –supply in metric tons until 2020 (**[43]**, data from "Composites Forecasts and Consulting LLC")*

I.3.5 Alternative Precursor Materials

The price of conventional carbon fibres made from polyacrylonitrile (PAN) and mesophase pitch currently hinders their industrial growth since it is too high for implementation in mass market applications. The high raw material- as well as the high production costs are the largest price contributors to the final fibre (up to 50 %). As a consequence, research activities on low-cost precursor materials have been ongoing for several decades. In this subchapter, a small selection of possible alternative precursor materials is presented.

- *Cellulose*

The idea of using cellulose as a precursor material already existed in the 1950s. However, back at the time, researchers stopped their activities because they obtained only low carbon yields and the production costs were too high compared to the more promising results for PAN-based precursors. Nowadays, the interest in cellulose as "green" and widely available precursor material has arisen again. Rayon fibres have been the most studied until today. Their carbonization yield typically ranges between 10 and 20 %, depending on the heating rates. During their thermal decomposition, a complex mechanism of reactions takes place. An oxidative stabilization as well as very slow processing are required to avoid material degradation. Besides, tension should be applied during carbonization and graphitization in order to obtain acceptable mechanical properties. These processing parameters drastically increase the fibres' prices.[33, 34, 36]

The challenges to be resolved for this precursor material are the low carbonization yields and the weak mechanical properties compared to conventional carbon fibres.

- *Polyethylene*

Polyethylene (PE) generally is a promising precursor material due to its rather low raw material- and low production costs. However, in order to reach elevated carbon yields, it has to be chemically treated to stabilize its carbon backbone. This stabilization can for instance be achieved by replacing some of the hydrogen atoms by heteroatoms. Typically, concentrated

sulfuric acid (H_2SO_4) serves as oxidizing agent to remove hydrogen and add sulfur atoms in a suitable way. This so-called sulfonation takes place directly after melt-spinning of PE, followed by carbonization.

Besides polyethylene, also other synthetic polymers are being considered as alternative precursor materials for carbon fibres. These include, but are not limited to: syndiotactic 1,2-poly(butadiene), poly(p-phenylene benzobisoxazole) (PBO), polyamide, polyphenylene, polyvinylalcohol and polystyrene.

Although considerable progress has been made on alternative and renewable carbon fibre precursors over the last decades, these materials do not yet compete with PAN- or pitch derived carbon fibres in terms of strength and stiffness, thus the properties required for large market applications. The general drawbacks and challenges are summarized in Table I-2.

Table I-2: Structures of polymer precursors and resulting conditions for carbon fibre production

Precursor backbone	Advantages and drawbacks for carbon fibre production
Aromatic structure	+ high carbonization yields - either high material costs or low mechanical properties
Linear structure	+ theoretically high mechanical properties - low carbonization yields and required treatment prior to carbonization

- *Graphene*

All of the carbon fibres presented in this chapter so far have a common production procedure. The conventional as well as the alternative precursors are organic materials which are subjected to a pyrolysis treatment, inevitably resulting in polycrystalline structures within the carbon fibres. However, this polycrystalline internal structure might be overcome by the nanotechnology of carbon allotropes, more precisely by carbon nanotubes and graphene.[44]

Graphene flakes are independent carbon crystals with two dimensions and they possess long-range order up to the micro- and millimeter scale. Graphene is known for its extremely high mechanical properties (130 GPa tensile strength and 1100 GPa elastic modulus), high electrical and thermal conductivity and excellent flexibility against deformation. The concept of a so-called “bottom-up assembly” hence tailors the creation of an ordered state within a carbon fibre by arranging individual carbon building blocks with high precision. The spinning of graphene fibres allows the regular and continuous alignment of graphene flakes in uniaxial direction. A long-range order with covalent crystalline structure is thus translated into macroscopic fibres which do not show any grain boundaries anymore. This improved carbon structure might even overcome the properties of current carbon fibres.[44-45]

For the fabrication of graphene fibres, melt-spinning cannot be chosen since graphene does not melt. However, in order to use solution-based spinning techniques, graphene needs to be

dispersed in a solvent. Graphene is very difficult to disperse, unless graphite is exfoliated in superacids and then spun directly into fibres. Another possible way is the functionalization of graphene flakes, for instance by oxidation. The obtained graphene oxide flakes can easily be dissolved in water and organic solvents into individual flakes. Thanks to numerous oxygen groups on their surface, they can easily be processed and are compatible with other materials. Besides, graphene oxide flakes are known to form liquid crystalline phases in solutions. Thanks to their asymmetry (anisotropic flakes) and good solubility within solvents, they show liquid crystalline behaviour, hence spontaneous arrangement in orientational and positional order.[44]

In polymer technology, the concept of producing fibres from liquid crystals is already established (e.g. see pitch processing in chapter I.3.2). During wet-spinning of graphene oxide solutions, a flow-induced alignment of the GO flakes occurs upon their injection into a coagulation bath. As depicted in Figure I-17, this arrangement is kept during the coagulation and solidification process. As a last step, the readily spun graphene oxide fibres are transformed into graphene fibres by chemical- or thermal reduction to recreate a conjugated structure. In this case, no further carbonization or graphitization step is needed to obtain well-structured carbon fibres.[44, 46]

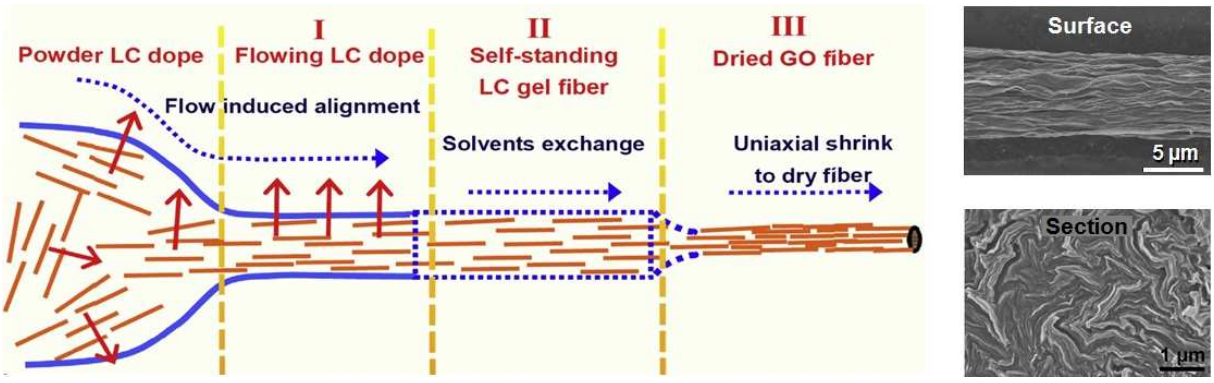

Figure I-17: *Liquid-crystal based wet-spinning of graphene oxide (GO) fibres and their structural evolution (left), surface and cross-section of a graphene fibre (right, SEM images) (images from **[44]**)*

In terms of mechanical properties, the tensile strength and elastic modulus of graphene fibres reported in literature are not yet comparable to those of conventional carbon fibres. It has been found that the stacking of graphene sheets within the fibres is relatively loose, which results in decreased mechanical properties.[45] By combining small- and large sized graphene flakes, the internal fibre structure can be densified considerably.[47] Besides, the use of very large graphene flakes (24 µm average width) in wet-spinning leads to a very high lateral crystal size of the carbon sheets within the fibres, which can be up to three times higher compared to conventional carbon fibres. Using this concept, **Xu et al. (2016)** recently obtained record mechanical properties of 1.45 GPa tensile strength and 282 GPa tensile modulus.[46] This rapid improvement in mechanical strength has been achieved after only three years, which underlines the high potential of graphene fibres.[44] In addition to wet-spinning, also dry-spinning has been demonstrated as efficient technique to fabricate graphene fibres with promising properties.[48]

The density of graphene fibres (< 1 g cm^{-3}) is still much lower than that of conventional carbon fibres (1.7-1.9 g cm^{-3}) or of ideal graphite crystals (2.2 g cm^{-3}). Although at the moment graphene fibres are much more expensive than conventional carbon fibres due to small scale manufacturing, a clear advantage is their simple fabrication and the lack of oxidation and thermal pyrolysis treatment required for organic precursors. Another advantage is the unique structure of graphene fibres.[44]

Furthermore, the rich functionalities of graphene fibres lead to more versatile applications compared to conventional carbon fibres. Applications proposed in literature are lightweight conductive cables, knittable supercapacitors, wearable textiles containing solar cells, micro-motors or actuators responding to environmental conditions. Composite fibres such as graphene-cellulose fibres (groups of Dai, Li and Hu[49] and Jiang et al.[50]), cellulose-graphene fibres (Tian et al.[51]) or graphene-PVA fibres (groups of Coleman[52], Gao[53] and Nishino[54]) further increase the number of possible applications.[44-45] **Shin et al. (2012)** even produced graphene-CNT-PVA nanocomposite fibres with significantly improved strength compared to pure PVA nanofibers.[55] These examples also demonstrate the attractiveness of graphene as a filler material for polymer composite fibres with enhanced mechanical and electrical performances.

There is another important material class that came into focus for renewable carbon fibres, a bio-polymer of extremely high availability, very low raw material costs and high carbon contents. Lignin is one of the most promising candidates for a “green” precursor fibre production in the future. The current developments and state of the art of lignin-based carbon fibres are explained in detail in the following subchapter.

I.4 Lignin-Based Carbon Fibres

Comprising carbon contents of 60-65 %, lignin generally represents a promising precursor material for low-cost and green carbon fibres. During the past decade, numerous research activities have been ongoing in this field, as it becomes clear from the increasing number of publications (see Figure I-18). Regarding the spinning techniques chosen to prepare the lignin fibres, melt-spinning and wet-spinning are the most frequently used, along with some rare cases of dry-spinning. However, current developments have not yet successfully reached industrial markets because of different limitations summarized in the following.

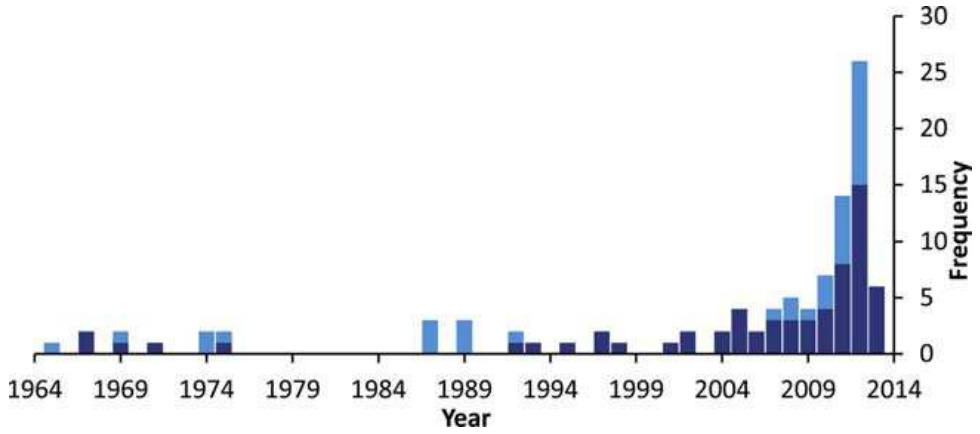

Figure I-18: *Frequency of journal articles (dark) and patents (light) about lignin-based carbon fibres over the past 50 years* ***[5]***

The very first attempts to develop lignin-based carbon fibres started in the 1960s and 1970s, when **Otani** patented a rather general "method for producing carbonized lignin fibres" in **1969** (US 3461082).[56] No limitations regarding the lignin type (from the group of alkali lignin, lignosulfonate or mixtures thereof) or the processing method (dry-, wet- or melt-spinning) were mentioned. Besides, the addition of high molecular weight materials to the lignin raw material, in particular polyvinylalcohol (PVA), polyacrylonitrile (PAN) and viscose, was described for dry-spinning.[5, 56] Otani also reported wet-spinning from solutions containing viscose, requiring thus solvents in which viscose is soluble such as carbon disulfide (CS_2).[56] Unfortunately, the use of CS_2 makes the process costly and toxic.

Shortly afterwards, lignin-derived carbon fibres under the name of "Kayacarbon" became commercially available for a short time. These fibres developed by the Nippon Kayaku company (**Fukuoka & Mikawa, 1970**) were processed by dry-spinning of a hot alkaline lignosulfonate-PVA solution based on highly concentrated aqueous NaOH, with subsequent carbonization of the obtained fibres.[34, 57] Ultimately, other precursor materials like PAN and pitch developed more rapidly and at lower costs, so that Kayacarbon eventually disappeared from the market.[5]

I.4.1 Melt-Spun Lignin Precursor Fibres

In contrast to wet-spinning, which returned into the focus of research only a few years ago, melt-spinning is the most studied technique for the production of lignin-based precursor fibres. However, regarding the final application of melt-spun lignin carbon fibres for structural applications, no significant progress could be made until today.

Since the end of the 1980s, the process of lignin melt-spinning has been studied extensively. **Sudo & Shimizu (1987-1992)** described the melt-spinning of hardwood lignin isolated by a steam treatment under high pressure and temperature with subsequent hydrogenation to lower its softening point.[58] To further increase the carbonization yields of the obtained carbon fibres, they added a treatment in a phenolic solvent followed by thermostabilization under inert atmosphere prior to melt-spinning (US 5344921, **1994**).[6, 59] Especially the work of Sudo can be found among the first accessible publications about the preparation of carbon fibres from lignin.[5]

Uraki et al. (1995) used a hardwood-based lignin extracted by aqueous acetic acid pulping (Organosolv lignin) for melt-spinning because it was directly suitable for processing due to its partial acetylation. Later on, they compared the fusibility of hardwood and softwood Organosolv lignin. The study was concluded by **Kubo et al. (1998)**, who succeeded in melt-spinning hardwood-based lignin fibres, whereas softwood lignin could not be processed in its pure form, but only after removal of its infusible fraction.[6, 34, 60]

Later works rather focused on combining lignin with different polymers as plasticizing agents and the subsequent melt-spinning into lignin-blend fibres including their carbonization. **Kadla & Kubo (2002-2005)** worked on this topic over several years. Their blends of lignin (Kraft and Organosolv) and 3-5 wt% polyethylene oxide (PEO) led to higher ease of spinnability. However, the fibres' mechanical properties did not improve significantly.[34, 61] They also investigated the compatibilities between lignin and PVA, polyethylene (PE), polypropylene (PP) and polyethylene terephthalate (PET). They found miscibility and good spinning properties of lignin with PVA and PET, but immiscibility of lignin with PE and PP due to their non-polar nature, leading to inhomogeneous fibre structures and poor mechanical properties.[61] PET (5-25 wt%) within hardwood Kraft lignin-PET blends improved the tensile strength of the carbonized fibres by 10-17 %.[62] For lignin-PVA fibre blends however, hardwood Kraft lignin served mostly as plasticizing agent to improve the melt-spinnability of PVA.[63] Comparatively high mechanical properties (tensile strengths up to 1.03 GPa, Young's moduli up to 109 GPa) were achieved by **Compere et al. (2005)**, who carbonized melt-spun fibres of Soda hardwood lignin and PET.[6, 34, 64] However, these fibres still do not meet the desired properties for an application in the automotive industry (tensile strength: 1.72 GPa, Young's modulus: 172 GPa).[5]

In addition to lignin blends with high molecular weight polymers, purified or modified lignin grades were used for melt-spinning and alternative stabilization techniques prior to carbonization (UV-, electron beam- and plasma treatment) were tested.[34] In **2010, Tomani** (Innventia, Sweden) developed the "LignoBoost" purification process resulting in high purity

lignin, which by now has been commercialized to large-scale productions in the USA and Finland.[65] The Innventia company (Sweden) has been working on the use of lignoboost-purified lignin for melt-spinning ever since (patent US 9446955B2 in **2016**)[66], also in cooperation with Oak Ridge National Laboratory (USA). Blends of purified hardwood and softwood lignin for instance already led to carbon fibres from lignin **(Norberg, 2013**).[11] Lignin-lignin blends were also studied by **Warren (2008), Baker et al. (2010-2012)**[16] and **Nordström (2011)**[67], where for instance infusible softwood Kraft lignin could be melt-spun with small portions of fusible hardwood Kraft lignin as plasticizer. Regarding the final application of melt-spun lignin-based carbon fibres however, no significant progress could be made.

An alternative approach, mostly to improve the mechanical properties of lignin-based carbon fibres, is the use of nanoparticles serving as fibre reinforcement. **Baker et al. (2010)** added up to 15 wt% multi-walled carbon nanotubes to different lignin precursor materials and produced nanocomposite fibres by melt-spinning (patent in 2011)[68]. The nanotubes increased the fibres' tensile strengths by 20 % and their moduli by 50 %.[5, 57] **Sevastyanova et al. (2010)** added organoclay particles to Organosolv hardwood lignin and found improved melt-spinnability and strongly increased tensile strengths.[57]

The most recent work focused on melt-spinning of lignin precursor fibres has been carried out by **Steudle et al. (2017)**. Softwood Kraft Lignin (IndulinAT) was chemically modified and these lignin derivatives (especially percynnamoylated lignin) were melt-spun under addition of vanillin (5 wt%) and ethylene glycol dimethacrylate (EGMA, 5 wt%) as spinning aids. Very small precursor fibre diameters of up to 17 µm could be achieved on pilot scale. After a long oxidative stabilization treatment (0.25 °C min^{-1} up to 250°C), the precursor fibres were carbonized at different temperatures between 1000 °C and 2200 °C. Besides turbostratic carbon structures with some graphitic domains obtained at high carbonization temperatures, the group reports carbon fibres with relatively high mechanical properties (tensile strength of up to 750 MPa, elastic modulus of up to 40 GPa). Steudle et al. claim to further improve these values in the near future.[69]

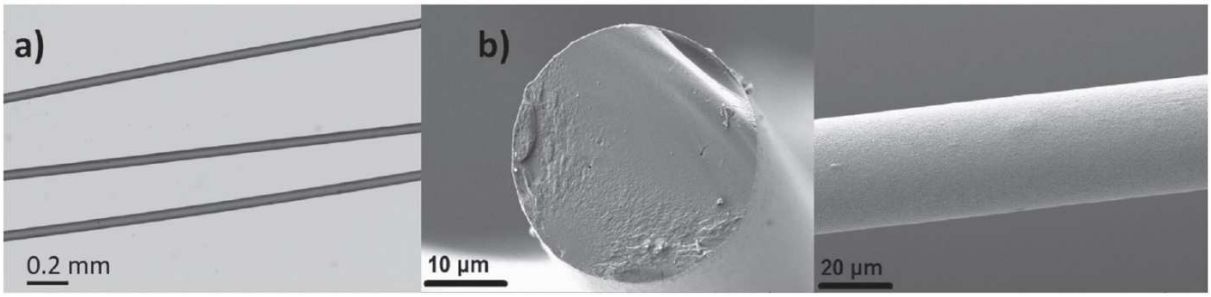

Figure I-19: *Optical micrograph (a) and SEM micrographs (b) of melt-spun fibres prepared from lignin, 5% vanillin and 5% EGMA (diameter: 32 µm) by Steudle et al.* ***[69]***

Despite these developments, the use of melt-spinning remains delicate because melt-spun fibres are brittle unless a large amount of plasticizer is introduced. The use of large amounts of plasticizers however makes the carbonization stage more difficult and less efficient. In

addition, the main limitation of melt-spinning is the use of fusible lignin grades, which by definition implicates the need of a long, difficult and costly stabilization stage prior to carbonization. For instance, if stabilization under air up to 250 °C is performed at a heating rate of 0.1 °C min^{-1}, the length of the treatment is around 36 hours. A heating rate of 0.25 °C min^{-1}, as used by Steudle et al., corresponds to 15 hours. At large scale production, this stage thus represents an extremely high cost factor.

I.4.2 Wet-Spun Lignin Precursor Fibres

After the patent of Otani in 1969[56] and the commercialized "Kayacarbon" fibres of the company Nippon Kayaku (Fukuoka)[70] which could not compete with the upcoming PAN- and pitch-based fibres, only very few research activities on the spinning of infusible lignin were carried out. Furthermore, fusible lignin grades appeared on the market in the 1980s and hence new developments focused almost exclusively on melt-spinning of lignin fibres and their thermostabilization.[6, 34] Only since 2011, also wet-spun fibres appeared again in literature. These research activities mainly comprise lignin-PAN blends and –co-polymers developed by **Seydibeyoglu et al. (2012)**[71], **Maradur & Kim (2012)**[72], **Bissett & Herriott** (patent in **2012**)[73], **Dong et al. (2015)**[26], **Liu et al. (2015-2016)**[74-75] **Xia et al. (2015)**[76], **Jia et al. (2016)**[77], as well as lignin-PAN-cellulose mixtures patented at **Fraunhofer** Institute (WO 2012156443 A1, **2013**)[78-79] and spun by **Ma et al. (2015)**[80] and **Olsson et al. (2017).**[35]

Regarding lignin-PAN blends, these processes unfortunately suffer from the high cost of the PAN precursor material. Besides, lignin-PAN copolymers require additional reaction times, increasing their cost even further. Using cellulose for carbon fibres is a less expensive approach regarding fibre raw material costs. However, given the poor carbon yield of cellulose, its combination with lignin is rather limiting. Another limitation of this approach is the use of cellulose as fibre forming component since dissolution of cellulose is generally difficult. In addition, a large fraction of cellulose is needed so that fibres can be manipulated and treated. The above mentioned research activities are described in detail within the following paragraphs.

Seydibeyoglu et al. investigated PAN-lignin blends in cast films and found a high miscibility between the two polymers. They stated the blends as promising precursor material for carbon fibres, but they did not do any actual fibre spinning trials. **Maradur & Kim** synthesized a PAN-lignin copolymer dissolved in DMSO with subsequent wet-spinning into fibres by coagulation in water. The obtained fibres were stabilized during two hours prior to carbonization.[71-72] Besides the cost factor of this procedure, the synthesis of copolymers is a very costly approach for lignin-based fibres since it imposes an additional production step.

Bissett & Herriott (Weyerhaeuser, USA) patented a technique for solution- or dry-jet wet-spinning of PAN or PAN-copolymers, whereby they added lignin (10-45 wt% of solids content) to the spinning dope to lower its viscosity while maintaining a high solid content. This technique allows wet-spinning of PAN-lignin blend fibres at lower temperatures and hence lower cost. The prepared fibres were subsequently stabilized and carbonized.[73] However, lignin was

described to be “not the main ingredient in the fibre”, considering that the lignin content remains below 45 %. Since PAN thus represents the main component, these fibres still have elevated prices.

Dong et al. used PAN and lignosulfonate dissolved in DMSO for wet-spinning into blend fibres by coagulation in water.[26] However, the lignin contents were limited to 47 % and although thermogravimetric measurements were performed up to 320 °C, no carbonization of the fibres was performed yet.

Liu et al. mainly focused on PAN within PAN-softwood Kraft lignin blends as well, because lignin contents did not exceed 25 %. Blends were made by dissolving lignin and PAN in DMF and coagulation was performed in methanol at -50 °C. Besides, the fibres were kept inside the coagulation bath during 36 h at -30 °C for gelation.[75] Methanol is highly toxic and the chosen processing parameters with numerous steps make it a complicated procedure. In another study, Liu et al. used PAN-lignin blends containing 30 % of lignin by dissolving both components in dimethylacetamine (DMAc). Additionally, they added 3 % of carbon nanotubes to the blend solutions. Coagulation was again performed in methanol, by the same hazardous procedure as described above.[74]

Lehmann et al. patented another wet-spinning technique for lignin-PAN blend fibres.[78] Within their claims, they do not limit the possible lignin content within the fibres (1-99 %), but given examples do not describe lignin contents higher than 47.3 %. Besides, the solvents used in the examples include dimethylacetamine (DMAc) and, to dissolve lignin with PAN and cellulose, 1-butyl-3-methylimidazolium chloride, which is also used at 15 wt% in an aqueous solution for coagulation.[78] These solvents are toxic, making the procedure hazardous and costly.

Globally, the use of PAN always remains critical for low-cost carbon fibres because of environmental and cost factors. Acrylonitrile is a toxic and carcinogenic monomer, which needs to be treated accordingly during polymerization and any residues need to be carefully removed from the spinning dope to minimise risks. Besides, during the stabilization and carbonization of PAN fibres, toxic by-products such as hydrogen cyanide (HCN) and nitrous gases are generated.[28, 35] Additionally, the raw material costs for PAN are high compared to other possible fibre-forming polymers (> 6 € kg^{-1}, Alibaba.com, Aug. 2018), limiting their use for carbon fibres at reduced prices.

Xia et al. synthesized a novel precursor material made from a lignosulfonate-PAN copolymer. Fibres were formed by dissolving the copolymer in DMSO and coagulation in a DMSO-water mixture. The fibres were subsequently stabilized and carbonized. The prepared copolymer leads to only partially bio-based carbon fibres exhibiting only medium mechanical properties.[76]

Jia et al. found a method to produce hollow fibres based on blends of purified lignin and PAN by means of wet-spinning with a diffusion-controlled coagulation bath containing water and DMSO. By gradually increasing the amount of water, solid fibres can be turned into hollow fibres. Besides, the addition of formaldehyde (HCHO) inside the coagulation bath showed a

positive effect on the fibres' elastic modulus and their thermal stability. However, the group did not yet perform any carbonization tests on these fibres.[77]

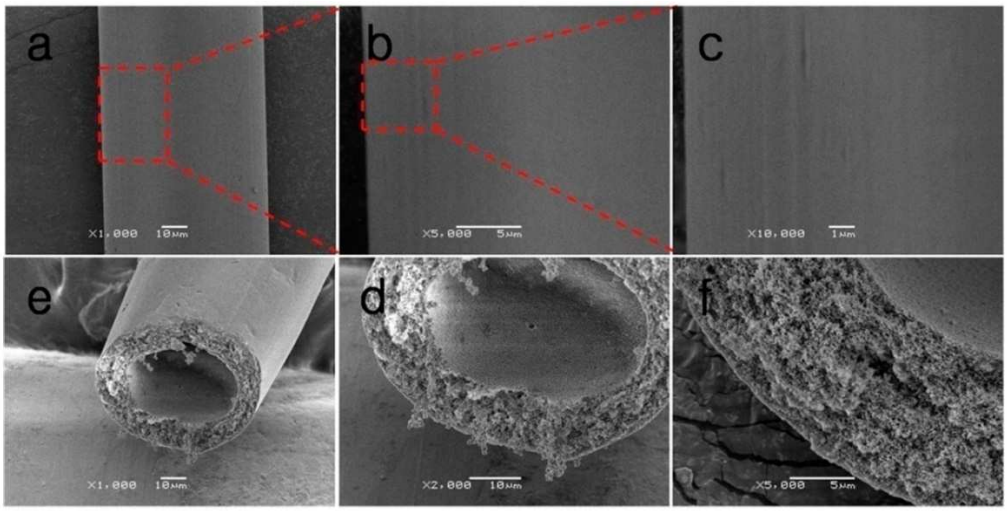

Figure I-20: *SEM images of the surface and cross-sections of wet-spun hollow lignin-PAN blend fibres prepared by Jia et al.* ***[77]***

The above mentioned process by **Lehmann et al.** has also been patented with cellulose instead of PAN, this time in collaboration with Stora Enso (Sweden).[79] In contrast to PAN, cellulose is a renewable material, but it does not lead to high carbon yields upon carbonization compared to lignin. In addition, cellulose, just like PAN, has to be used at large weight fractions so that fibres can be produced. Using cellulose instead of PAN clearly represents an important cost advantage for the final carbon fibres. However, low carbon yields are also limiting the approach of cellulose-lignin blend fibres with only low lignin contents (< 50 %).

The combination of lignin and cellulose has also been pursued by the group of **Ma et al**. who produced composite fibres from different cellulose-lignin blends dissolved in ionic liquid solutions by dry-jet wet-spinning. Thereby, the lignin contents did not exceed 50 %, hence resulting in cellulose-based fibres with a slightly higher carbon yield, but lower mechanical properties compared to pure cellulose fibres. The loss of crystallinity and orientation with increasing lignin content was stated, but no actual carbonization tests have been performed.[80]

Olsson et al. have recently been working on precursor fibres based on Kraft lignin (extracted with Lignoboost®) and paper grade Kraft pulp (containing different polysaccharides) at high lignin contents of up to 70 %. Both components have been dissolved in an ionic liquid solvent ([EMIm] [OAc]) and spun by dry-jet wet-spinning (air gap 10 mm) into smooth and flexible multi-filaments (diameter 10-12 µm), whereby coagulation was performed in acidic water (pH 5). Washing, drying and conditioning of the fibres were performed over a long time and in a discontinuous manner. After stabilization and carbonization, the obtained fibres exhibit a very high tensile strength of up to 780 MPa and a modulus of up to 68 GPa. This result is claimed to be due to a high draw ratio (of 5) within the air-gap, increasing the fibers' orientation. The authors state that there is still a high potential for improvements. However, it needs to be kept

in mind that the use of ionic liquid solvents remains costly, even though their prices are said to decrease in the future.[35]

Recently, **Lu et al.**[81], published a method of “gel-spinning” of PVA as the polymer matrix in combination with lignin for the first time. As shown in Figure I-21, PVA and lignin were both dissolved in DMSO and subsequently spun through an air-gap (3-5 mm) into a coagulation bath containing methanol/acetone mixtures at -25 °C. The spun and wound-up fibres were then kept inside a coagulation bath at 5 °C for 24 h. Afterwards, the fibres were unwound and stretched after passing them through a silicone oil bath heated to 90-240 °C. The maximum lignin content tested was 50 % when using a 15/85 methanol/acetone coagulation bath.[81] However, Lu et al. did not carbonize the obtained PVA-lignin fibres. It is believed that the carbonization would actually be impossible considering the insufficient amount of lignin.

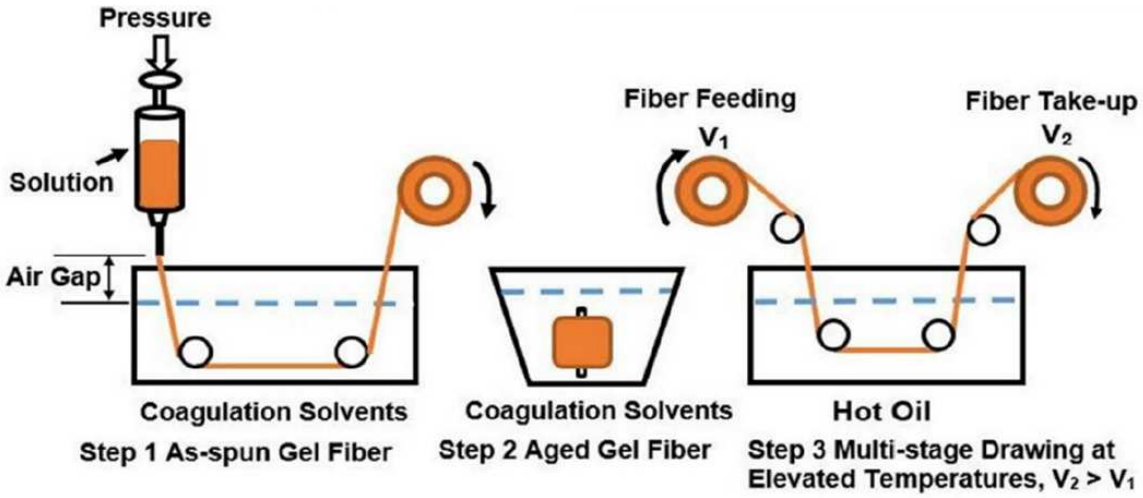

Figure I-21: *Scheme of gel-spinning for PVA-lignin fibres used by Lu et al.* ***[81]***

However, the use of PVA as reinforcing polymer for lignin fibres is a highly cost-effective approach, given the fact that its current market price lies between 1.3-2 € kg^{-1} (Alibaba.com, Aug. 2018) which is 3-4 times below the price of PAN polymers (currently > 6 € kg^{-1}). As in the work of Lu et al., the current work is focused on the use of PVA as well. Regarding the production of low-cost carbon fibres however, a very important factor is the obtained yield after carbonization. In order to keep both a high carbon yield and low raw material costs, there is an interest in keeping the lignin content inside the precursor fibres as high as possible. Lignin-PVA fibres should thus contain lignin contents above 50 %. Other disadvantages of the method by Lu et al. are the use of methanol and acetone for coagulation and their discontinuous process, which both increases the fibres’ production costs.

The approach for wet-spinning of infusible lignin grades is a promising perspective, given the fact that these precursors can be carbonized directly without prior stabilization. Examples of wet-spun lignin fibres reported in literature always include a thermostabilization step and none of them have been commercialized so far.

I.4.3 Dry-Spun Lignin Precursor Fibres

As already mentioned in a previous chapter, the commercialized Kayacarbon fibres were produced by dry-spinning of lignosulfonate-PVA solutions. Shortly afterwards in 1973-1974, **Mansmann et al.** patented two methods to prepare lignosulfonate fibres blended with polyethyleneoxide (PEO) and acrylic acid-acrylamide copolymers.[14, 82]

The most recent research activities on dry-spinning of lignin fibres have been performed by **Zhang & Ogale (2014-2016)**. They dissolved partially acetylated softwood lignin (IndulinAT) in acetone (at 75 wt%) which was subsequently dry-spun into fibres with a spinning barrel at constant throughput. The obtained fibres were then stabilized at 0.2 °C min^{-1} and carbonized. However, non-circular but crenulated cross-sections were obtained for the fibres due to an irregular out-diffusion of acetone (see Figure I-22). Although the crenulations generally being a disadvantage for the mechanical properties of the carbon fibre, bonding with a matrix for composites would be improved due to an increased surface area. The mechanical properties of the obtained carbon fibres were high (strength 1.04 GPa and modulus 52 GPa). Besides, lignin fibres carbonized under tension were found to exhibit a higher molecular orientation. A clear drawback of this method however is the long stabilization time.[27, 83]

Therefore, they showed in a following study that the slow stabilization times used before can be significantly decreased by a 15 minute UV-irradiation treatment below 50 °C. After the performed UV-irradiation, stabilization times could be decreased from 40 hours to 4 hours.[84] The results obtained were very encouraging. However, it has to be mentioned that the UV treatment clearly decreased the mechanical properties of the fibres compared to those stabilized over a long time (strength 0.9 GPa and modulus 34 GPa).[10, 27]

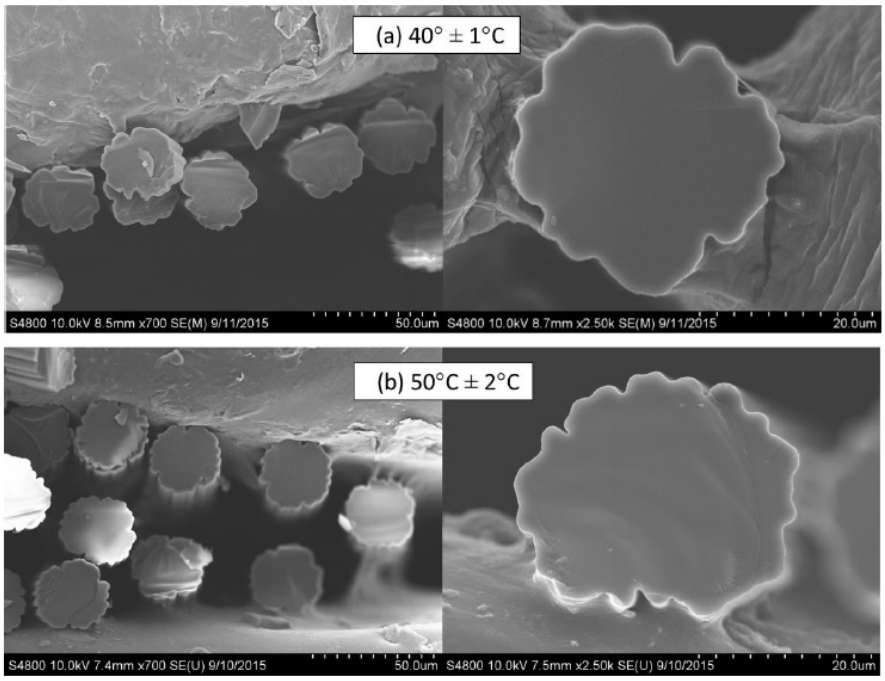

Figure I-22: *Acetylated softwood Kraft lignin fibres obtained by dry-spinning at 40°C (a) and 50°C (b)* ***[27]***

I.5 Conclusion and Aim of This Thesis

It can be concluded that numerous developments have been dedicated to the preparation of lignin-based carbon fibres during the last decades. As explained in *chapter I.1*, lignin exhibits an amorphous and three-dimensional structure at low molecular weights due to its extraction from cellulose, e.g. in paper production. The fabrication of fibres (*chapter I.2*) from a non-linear polymer is generally difficult because its molecular chains cannot be aligned along the fibre axis. This lack of orientation results in a very high fibre brittleness of pure lignin fibres. Besides, *chapter I.3* demonstrated that an amorphous structure within a precursor is preserved during the carbonization process. Thus, the obtained carbon fibres lack highly oriented structures and strong properties, as it has been explained in *chapter I.4*. This stands in contrast to conventional carbon fibres prepared from PAN and pitch precursor fibres which exhibit a high orientation, turbostratic and graphitic carbon crystallite structures and thus excellent properties (see Figure I-23).

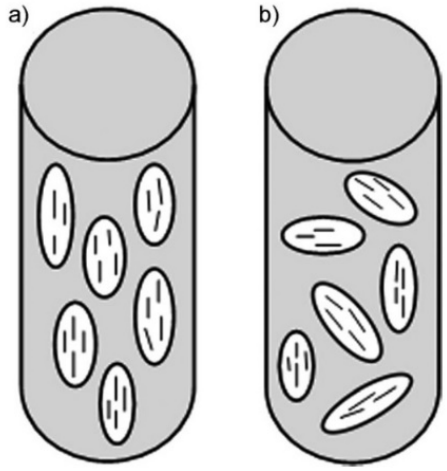

Figure I-23: *Crystallites within PAN-based (a) and lignin-based carbon fibres (b) and their degree of orientation* ***[34]***

In order to overcome the brittleness of pure lignin fibres, the addition of linear polymers with high molecular weights (e.g. PE, PAN, PET, PVA, among others) is a common approach (*chapter I.4*). Blending with the latter typically facilitates the spinning process and allows fibre drawing during their production, which is important for handling and mechanical stability during the subsequent stabilization and carbonization processes. Besides, drawn fibres generally comprise higher molecular orientation which can possibly be transferred to the obtained carbon fibres. It is important to note that some plasticizing polymers added to the lignin raw material do not contribute to the carbon fibre formation, nor to the carbonization yield. Due to their non-aromatic nature and chemical compositions, some of them do not form any carbon residues, but decompose under volatilization upon thermal pyrolysis. Mainly the carbon atoms present within the aromatic lignin polymer chains can resist the high temperature treatment. This is why the amount of lignin within the precursor fibre should be kept as high as possible.

Therefore, one of the approaches of the work presented in this thesis consists of using unmodified commercial softwood Kraft lignin, which can be wet-spun into fibres upon combination with PVA as a plasticizing polymer. The PVA content is kept as low as possible between 15 and 30 %. In contrast to existing inventions, the wet-spun fibres do not contain any PAN. Lignin-PVA fibres thus represent less hazardous conditions for the environment during fibre processing and an important cost advantage for the final carbon fibres.

Another important advantage is the use of infusible softwood Kraft lignin. Melt-spun lignin fibres can only be produced from fusible lignin grades and these are thermally instable for the subsequent carbonization step. The stabilization procedures prior to carbonization for fusible fibres are complex and time- and energy consuming, hence significantly raising the fibres' prices. The experiments performed for this thesis are thus aiming for the wet-spinning or coagulation of infusible fibres based on softwood Kraft lignin, which do not necessitate a costly stabilization process.

Additionally, a combination of lignin with carbonaceous filler materials, namely graphene oxide (GO) and cellulose nanocrystals (CNCs) is proposed in this thesis. Due to the amorphous nature of lignin, its carbon structure within fibres is disordered and usually lacking crystallinity and a clear orientation along the fibre axis. By introducing liquid crystalline GO particles into lignin solutions, they should align during wet-spinning due to their anisotropic shape and hence improve the molecular orientation within the lignin-based fibres. Neither carbon nanotubes nor graphene have been considered for this approach. Nanotubes show similar performances in wet-spinning, but they have already been used as reinforcement in lignin fibres. Graphene is very difficult to disperse in solvents, in which it does not show spontaneous liquid crystalline behaviour. Therefore, this thesis is focused on GO and CNCs as filler materials. The platelet shape of GO and the rod shape of CNCs could induce graphitic domains within lignin-based carbon. Theoretically, the reinforcement of lignin with nano-sized carbon materials should also increase their carbonization yield.

The preparation of continuously wet-spun lignin-based fibre systems with enhanced structuration would represent an important step towards new perspectives for the market. Numerous possible applications such as electronics, energy storage (e.g. anodes of porous carbon[42]) and intermediate structural applications underline the importance of an implementation of lignin-based carbon fibres for industrial applications on a larger scale.

References

[1] M. Madadi and A. Abbas, 'Lignin Degradation by Fungal Pretreatment: A Review', *J. Plant Pathol. Microbiol.*, vol. 8, pp. 1–6, 2017.

[2] A. G. Vishtal and A. Kraslawski, 'Challenges in industrial applications of technical lignins', *BioResources*, vol. 6, no. 3, pp. 3547–3568, 2011.

[3] I. Brodin, 'Chemical properties and thermal behaviour of kraft lignins', 2009.

[4] Michael Carlowicz, 'Seeing Forests for the Trees and the Carbon: Mapping the World's Forests in Three Dimensions', *earthobservatory.nasa.gov*, vol. Feature Jan 9, 2012.

[5] D. A. Baker and T. G. Rials, 'Recent advances in low-cost carbon fiber manufacture from lignin', *J. Appl. Polym. Sci.*, vol. 130, no. 2, pp. 713–728, 2013.

[6] J. M. Rosas, R. Berenguer, M. J. Valero-Romero, J. Rodríguez-Mirasol, and T. Cordero, 'Preparation of Different Carbon Materials by Thermochemical Conversion of Lignin', *Front. Mater.*, vol. 1, p. 29, 2014.

[7] M. Ek, G. Gellerstedt, and G. Henriksson, *Wood chemistry and biotechnology*, vol. 1. Walter de Gruyter, 2009.

[8] J. Zakzeski, P. C. A. Bruijnincx, A. L. Jongerius, and B. M. Weckhuysen, 'The Catalytic Valorization of Lignin for the Production of Renewable Chemicals', *Chem. Rev.*, vol. 110, no. 6, pp. 3552–3599, Jun. 2010.

[9] C. Li, X. Zhao, A. Wang, G. W. Huber, and T. Zhang, 'Catalytic Transformation of Lignin for the Production of Chemicals and Fuels', *Chem. Rev.*, vol. 115, no. 21, pp. 11559–11624, Nov. 2015.

[10] A. A. Ogale, M. Zhang, and J. Jin, 'Recent advances in carbon fibers derived from biobased precursors', *J. Appl. Polym. Sci.*, vol. 133, no. 45, p. n/a–n/a, 2016.

[11] I. Norberg, 'Carbon fibres from kraft lignin', 2012.

[12] P. Fatehi and J. Chen, 'Extraction of technical lignins from pulping spent liquors, challenges and opportunities', in *Production of Biofuels and Chemicals from Lignin*, Springer, 2016, pp. 35–54.

[13] Valmet, 'First LignoBoost plants producing large volumes of kraft lignin to the market place'. [Online]. Available: http://www.valmet.com/media/articles/up-and-running/new-technology/PEERS1stLignoBoostPlants/.

[14] W. Fang, S. Yang, X.-L. Wang, T.-Q. Yuan, and R.-C. Sun, 'Manufacture and application of lignin-based carbon fibers (LCFs) and lignin-based carbon nanofibers (LCNFs)', *Green Chem*, vol. 19, no. 8, pp. 1794–1827, 2017.

[15] B. M. Upton and A. M. Kasko, 'Strategies for the Conversion of Lignin to High-Value Polymeric Materials: Review and Perspective', *Chem. Rev.*, vol. 116, no. 4, pp. 2275–2306, Feb. 2016.

[16] D. A. Baker, N. C. Gallego, and F. S. Baker, 'On the characterization and spinning of an organic-purified lignin toward the manufacture of low-cost carbon fiber', *J. Appl. Polym. Sci.*, vol. 124, no. 1, pp. 227–234, 2012.

[17] J. Sameni, S. Krigstin, and M. Sain, 'Solubility of Lignin and Acetylated Lignin in Organic Solvents', *BioResources*, vol. 12, no. 1, pp. 1548–1565, 2017.

[18] A. J. Ragauskas *et al.*, 'Lignin Valorization: Improving Lignin Processing in the Biorefinery', *Science*, vol. 344, no. 6185, May 2014.

[19] G. Bhat, *Structure and Properties of High-Performance Fibers*. Woodhead Publishing, 2016.

[20] J. W. Hearle, *High-performance fibres*. Elsevier, 2001.

[21] D. D. Edie and M. G. Dunham, 'Melt spinning pitch-based carbon fibers', *Carbon*, vol. 27, no. 5, pp. 647–655, 1989.

[22] T. Takajima, K. Kajiwara, and J. E. McIntyre, *Advanced fiber spinning technology*. Woodhead Publishing, 1994.

[23] D. D. Edie, N. K. Fox, B. C. Barnett, and C. C. Fain, 'Melt-spun non-circular carbon fibers', *Carbon*, vol. 24, no. 4, pp. 477–482, 1986.

[24] V. B. Gupta, 'Melt-spinning processes', in *Manufactured Fibre Technology*, V. B. Gupta and V. K. Kothari, Eds. Dordrecht: Springer Netherlands, 1997, pp. 67–97.
[25] L. R. P. de Andrade Lima and A. D. Rey, 'Computational modeling of ring textures in mesophase carbon fibers', *Mater. Res.*, vol. 6, pp. 285–293, 2003.
[26] X. Dong, C. Lu, P. Zhou, S. Zhang, L. Wang, and D. Li, 'Polyacrylonitrile/lignin sulfonate blend fiber for low-cost carbon fiber', *RSC Adv.*, vol. 5, no. 53, pp. 42259–42265, 2015.
[27] M. Zhang, 'Carbon Fibers Derived from Dry-Spinning of Modified Lignin Precursors', 2016.
[28] V. Gupta and V. Kothari, *Manufactured fibre technology*. Springer Science & Business Media, 2012.
[29] J. A. Kent, *Handbook of industrial chemistry and biotechnology*. Springer Science & Business Media, 2013.
[30] N. Bhardwaj and S. C. Kundu, 'Electrospinning: A fascinating fiber fabrication technique', *Biotechnol. Adv.*, vol. 28, no. 3, pp. 325–347, 2010.
[31] S. Ramakrishna, *An introduction to electrospinning and nanofibers*. World Scientific, 2005.
[32] P. Weisser, G. Barbier, C. Richard, and J.-Y. Drean, 'Characterization of the coagulation process: wet-spinning tool development and void fraction evaluation', *Text. Res. J.*, vol. 86, no. 11, pp. 1210–1219, 2016.
[33] X. Huang, 'Fabrication and Properties of Carbon Fibers', *Materials*, vol. 2, no. 4, pp. 2369–2403, 2009.
[34] E. Frank, L. M. Steudle, D. Ingildeev, J. M. Spörl, and M. R. Buchmeiser, 'Carbon Fibers: Precursor Systems, Processing, Structure, and Properties', *Angew. Chem. Int. Ed.*, vol. 53, no. 21, pp. 5262–5298, 2014.
[35] Olsson Carina, Sjöholm Elisabeth, and Reimann Anders, 'Carbon fibres from precursors produced by dry-jet wet-spinning of kraft lignin blended with kraft pulps', *Holzforschung*, vol. 71, no. 4, p. 275, 2017.
[36] S. Chand, 'Review carbon fibers for composites', *J. Mater. Sci.*, vol. 35, no. 6, pp. 1303–1313, 2000.
[37] P. J. Walsh *et al.*, *ASM handbook Composites: Carbon Fibers*, vol. 21. ASM international Materials Park, OH, USA, 2001.
[38] M. Holmes, 'Carbon fibre reinforced plastics market continues growth path (Part 1)', 07-Jan-2014. [Online]. Available: https://www.materialstoday.com/carbon-fiber/features/carbon-fibre-reinforced-plastics-market-continues/.
[39] H. K. Shin, M. Park, H.-Y. Kim, and S.-J. Park, 'An overview of new oxidation methods for polyacrylonitrile-based carbon fibers', *Carbon Lett.*, vol. 16, no. 1, pp. 11–18, 2015.
[40] A. S. Gill, D. Visotsky, L. Mears, and J. D. Summers, 'Cost Estimation Model for PAN Based Carbon Fiber Manufacturing Process', presented at the ASME 2016 11th International Manufacturing Science and Engineering Conference, 2016, p. V001T02A044-V001T02A044.
[41] P. Morgan, *Carbon fibers and their composites*. CRC press, 2005.
[42] S. Chatterjee *et al.*, 'Conversion of Lignin Precursors to Carbon Fibers with Nanoscale Graphitic Domains', *ACS Sustain. Chem. Eng.*, vol. 2, no. 8, pp. 2002–2010, 2014.
[43] 'Supply and demand: Advanced fibers (2017)'. [Online]. Available: https://www.compositesworld.com/articles/supply-and-demand-advanced-fibers-2016.
[44] Z. Xu and C. Gao, 'Graphene fiber: a new trend in carbon fibers', *Mater. Today*, vol. 18, no. 9, pp. 480–492, 2015.
[45] H. Cheng, C. Hu, Y. Zhao, and L. Qu, 'Graphene fiber: a new material platform for unique applications', *NPG Asia Mater.*, vol. 6, no. 7, p. e113, 2014.
[46] Z. Xu *et al.*, 'Ultrastiff and strong graphene fibers via full-scale synergetic defect engineering', *Adv. Mater.*, vol. 28, no. 30, pp. 6449–6456, 2016.
[47] G. Xin *et al.*, 'Highly thermally conductive and mechanically strong graphene fibers', *Science*, vol. 349, no. 6252, pp. 1083–1087, 2015.
[48] Q. Tian *et al.*, 'Dry spinning approach to continuous graphene fibers with high toughness', *Nanoscale*, vol. 9, no. 34, pp. 12335–12342, 2017.

[49] Y. Li *et al.*, 'Hybridizing wood cellulose and graphene oxide toward high-performance fibers', *NPG Asia Mater*, vol. 7, p. e150, Jan. 2015.
[50] H. Jiang, W. Yang, S. Chai, S. Pu, F. Chen, and Q. Fu, 'Property enhancement of graphene fiber by adding small loading of cellulose nanofiber', *Nanocomposites*, vol. 2, no. 1, pp. 8–17, 2016.
[51] M. Tian *et al.*, 'Enhanced mechanical and thermal properties of regenerated cellulose/graphene composite fibers', *Carbohydr. Polym.*, vol. 111, pp. 456–462, 2014.
[52] C. S. Boland, S. Barwich, U. Khan, and J. N. Coleman, 'High stiffness nano-composite fibres from polyvinylalcohol filled with graphene and boron nitride', *Carbon*, vol. 99, pp. 280–288, 2016.
[53] L. Kou and C. Gao, 'Bioinspired design and macroscopic assembly of poly(vinyl alcohol)-coated graphene into kilometers-long fibers', *Nanoscale*, vol. 5, no. 10, pp. 4370–4378, 2013.
[54] S. Morimune, T. Nishino, and T. Goto, 'POLY (VINYL ALCOHOL)/GRAPHENE OXIDE FIBER PREPARED BY GEL PROCESS'.
[55] M. K. Shin *et al.*, 'Synergistic toughening of composite fibres by self-alignment of reduced graphene oxide and carbon nanotubes', *Nat. Commun.*, vol. 3, p. 650, Jan. 2012.
[56] S. Otani, Y. Fukuoka, B. Igarashi, and K. Sasaki, 'Method for producing carbonized lignin fiber', 12-Aug-1969.
[57] R. Paul, A. Naskar, N. Gallego, X. Dai, and A. Hausner, 'Treatment of Lignin Precursors to Improve their Suitability for Carbon Fibers: A Literature Review', GrafTech International Holdings Inc., 2015.
[58] K. Sudo and K. Shimizu, 'A new carbon fiber from lignin', *J. Appl. Polym. Sci.*, vol. 44, no. 1, pp. 127–134, 1992.
[59] K. Sudo and K. Shimizu, 'Method for manufacturing lignin for carbon fiber spinning', 06-Sep-1994.
[60] S. Kubo, Y. Uraki, and Y. Sano, 'Preparation of carbon fibers from softwood lignin by atmospheric acetic acid pulping', *Carbon*, vol. 36, no. 7–8, pp. 1119–1124, 1998.
[61] J. F. Kadla, S. Kubo, R. A. Venditti, R. D. Gilbert, A. L. Compere, and W. Griffith, 'Lignin-based carbon fibers for composite fiber applications', *Carbon*, vol. 40, no. 15, pp. 2913–2920, 2002.
[62] S. Kubo and J. F. Kadla, 'Lignin-based Carbon Fibers: Effect of Synthetic Polymer Blending on Fiber Properties', *J. Polym. Environ.*, vol. 13, no. 2, pp. 97–105, 2005.
[63] S. Kubo and J. F. Kadla, 'The Formation of Strong Intermolecular Interactions in Immiscible Blends of Poly(vinyl alcohol) (PVA) and Lignin', *Biomacromolecules*, vol. 4, no. 3, pp. 561–567, 2003.
[64] A. Compere, W. Griffth, C. Leitten Jr, and J. Pickel, 'Evaluation of lignin from alkaline-pulped hardwood black liquor', *ORNL*, vol. 118, pp. 6–97, 2005.
[65] P. Tomani, 'The lignoboost process', *Cellul. Chem. Technol.*, vol. 44, no. 1, p. 53, 2010.
[66] E. Sjholm, G. Gellerstedt, R. Drougge, I. Norberg, and Y. Nordstrom, 'Method for producing a lignin fiber', 20-Sep-2016.
[67] Y. Nordström, I. Norberg, E. Sjöholm, and R. Drougge, 'A new softening agent for melt spinning of softwood kraft lignin', *J. Appl. Polym. Sci.*, vol. 129, no. 3, pp. 1274–1279, 2013.
[68] F. S. Baker, D. A. Baker, and P. A. Menchhofer, 'Carbon nanotube (cnt)-enhanced precursor for carbon fiber production and method of making a cnt-enhanced continuous lignin fiber', 24-Nov-2011.
[69] L. M. Steudle *et al.*, 'Carbon Fibers Prepared from Melt Spun Peracylated Softwood Lignin: an Integrated Approach', *Macromol. Mater. Eng.*, vol. 302, no. 4, pp. 1600441–n/a, 2017.
[70] Y. Fukuoka, 'Carbon fiber made from lignin (Kayacarbon)', *Jap Chem Quart*, 1969.
[71] M. Ö. Seydibeyoğlu, 'A Novel Partially Biobased PAN-Lignin Blend as a Potential Carbon Fiber Precursor', *J. Biomed. Biotechnol.*, vol. 2012, p. 8, 2012.

[72] S. P. Maradur, C. H. Kim, S. Y. Kim, B.-H. Kim, W. C. Kim, and K. S. Yang, 'Preparation of carbon fibers from a lignin copolymer with polyacrylonitrile', *Synth. Met.*, vol. 162, no. 5–6, pp. 453–459, 2012.
[73] P. J. Bissett and C. W. Herriott, 'Lignin/polyacrylonitrile-containing dopes, fibers, and methods of making same', Jan-2012.
[74] H. C. Liu, A.-T. Chien, B. A. Newcomb, Y. Liu, and S. Kumar, 'Processing, Structure, and Properties of Lignin- and CNT-Incorporated Polyacrylonitrile-Based Carbon Fibers', *ACS Sustain. Chem. Eng.*, vol. 3, no. 9, pp. 1943–1954, 2015.
[75] H. C. Liu, A.-T. Chien, B. A. Newcomb, A. A. B. Davijani, and S. Kumar, 'Stabilization kinetics of gel spun polyacrylonitrile/lignin blend fiber', *Carbon*, vol. 101, pp. 382–389, 2016.
[76] K. Xia, Q. Ouyang, Y. Chen, X. Wang, X. Qian, and L. Wang, 'Preparation and Characterization of Lignosulfonate–Acrylonitrile Copolymer as a Novel Carbon Fiber Precursor', *ACS Sustain. Chem. Eng.*, vol. 4, no. 1, pp. 159–168, 2016.
[77] Z. Jia, C. Lu, Y. Liu, P. Zhou, and L. Wang, 'Lignin/Polyacrylonitrile Composite Hollow Fibers Prepared by Wet-Spinning Method', *ACS Sustain. Chem. Eng.*, vol. 4, no. 5, pp. 2838–2842, 2016.
[78] A. Lehmann, H. Ebeling, and H. P. Fink, 'Method for the production of lignin-containing precursor fibres and also carbon fibres', 19-Dec-2013.
[79] A. Lehmann, H. Ebeling, and H.-P. Fink, 'Method for the production of lignin-containing precursor fibres and also carbon fibres', 16-May-2012.
[80] Y. Ma *et al.*, 'High-Strength Composite Fibers from Cellulose-Lignin Blends Regenerated from Ionic Liquid Solution', *ChemSusChem*, vol. 8, 2015.
[81] C. Lu, C. Blackwell, Q. Ren, and E. Ford, 'Effect of the Coagulation Bath on the Structure and Mechanical Properties of Gel-Spun Lignin/Poly(vinyl alcohol) Fibers', *ACS Sustain. Chem. Eng.*, vol. 5, no. 4, pp. 2949–2959, Apr. 2017.
[82] M. Mansmann, G. Winter, P. Pampus, H. Schnoring, and N. Schon, 'Stable lignin fibers', 1974.
[83] M. Zhang and A. A. Ogale, 'Carbon fibers from dry-spinning of acetylated softwood kraft lignin', *Carbon*, vol. 69, pp. 626–629, 2014.
[84] M. Zhang, J. Jin, and A. A. Ogale, 'Carbon fibers from UV-assisted stabilization of lignin-based precursors', *Fibers*, vol. 3, no. 2, pp. 184–196, 2015.

Chapter II Preparation of Lignin Precursor Fibres by Coagulation and their Carbonization

In this chapter, lignin fibres prepared by coagulation spinning which are suitable as precursor material for low-cost carbon fibres are presented under several different aspects. The wet-spinning trials performed within the framework of this thesis, including discontinuous and continuous monofilament spinning on laboratory scale and multifilament spinning on pilot scale, are described in detail. The miscibility of the chosen blend system lignin-polyvinyl alcohol is characterized in solution and in solid films and fibres. Furthermore, the properties of the as-spun lignin-polyvinyl alcohol fibres are shown with respect to their morphology, structure, thermal- and mechanical properties. The subsequent carbonization process of the obtained lignin-based precursor fibres is demonstrated and the resulting properties of the carbon fibres are presented. The chapter thus represents the entire development process from the raw materials to the final carbon fibres.

II. 1 Wet-spinning of Lignin-based Fibres on Laboratory Scale

The approach for producing lignin fibres by means of coagulation (wet-spinning) chosen for the work presented in this thesis is based on numerous small-scale experiments. These experiments led the way to a system that allows the wet-spinning of lignin-based fibres suitable as carbon fibre precursors. The obtained fibres prepared from the chosen system were thoroughly characterized in this work. The development stages from the raw materials until definition of the final system are shown in this chapter and consists of: dissolution and coagulation trials of lignin, combination of lignin with other polymers as spinning aids and characterization of the chosen Kraft lignin-polyvinyl alcohol blend system.

II.1.1 Dissolution and Coagulation of Lignin

The principle of polymer wet-spinning is generally based on the solubility and insolubility of the polymer in two different solvents. As described in *chapter I.2*, a polymer material is first dissolved in a solvent and then injected into a counter-solvent whereby fibres are formed by coagulation of the polymer. Thus, a crucial condition in wet-spinning of polymer fibres is the choice of a suitable solvent and a counter-solvent. As it was shown in *chapter I.1*, the dissolution of lignin has been found a challenge in literature.[1] The structure of every lignin grade is slightly different depending on the origin and extraction technique and thus may also contain different functional groups. Due to the fact that a polymer's solubility is mostly determined by its chemical structure, functional groups and molecular weight,[2] the solubility of a lignin grade can only partially be foreseen and its description by solubility parameters (e.g. Hansen) is very complex. Since a detailed lignin characterization was not within the focus of this thesis, the chosen approach was rather experimental. Hence, numerous dissolution experiments were performed in order to find a suitable solvent which completely dissolves the respective lignin grades, if possible in high concentrations. In order to screen a broad range of raw materials, 20 different lignin grades were tested regarding their solubilities in various solvents (see Table II-1). The grades included lignin extracted from softwood, hardwood and annual plants by means of different pulping processes such as Kraft, sulfite, Organosolv or Soda (*see chapter I.1.3*). Consequently, different suppliers were chosen accordingly. Among the tested grades was commercially available lignin, such as IndulinAT® Kraft softwood lignin (Mead WestVaco) or Kraft lignin purchased from Sigma Aldrich. Other lignin grades were provided by research institutions such as Fraunhofer or FCBA who received the raw materials from paper manufacturers (e.g. Smurfit Kappa) and extracted the lignin, for instance from black liquor.

The lignin grades in powder form were dissolved in different solvents at room temperature by means of magnetic stirrer bars. Solubility was first evaluated by eye (see Figure II-1) and then solutions at lignin concentrations of ≥ 5 wt% were investigated more closely by optical microscopy regarding non-dissolved particles (see Figure II-1). If the solution was found homogeneous, the lignin concentration was increased to its limit for the respective cases by stirring for several hours at room temperature.

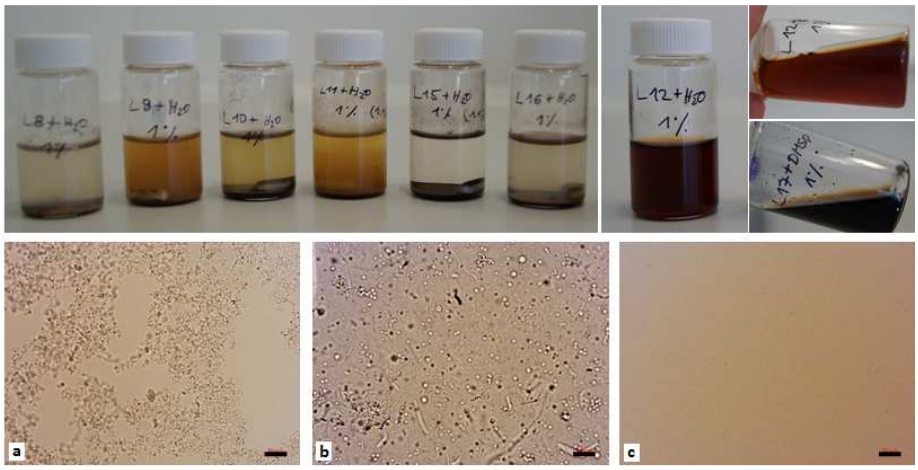

***Figure II-1**: Dissolution trials of lignin (above) and optical microscopy images of promising solutions (below, scale bars 20 µm): undissolved Organosolv lignin particles (L2) at 10 wt% in DMSO (a), Kraft lignin solution (L8) at 5 wt% in DMSO with impurities (b) and homogeneous Kraft lignin solution (L16) at 30 wt% in DMSO (c)*

As it can be seen from the results of the screening, the majority of the lignin grades exhibited at least partial solubility in the tested organic solvents (dimethyl sulfoxide (DMSO), dimethyl ethylene urea (DMEU) and ethylene glycol). Besides, the lignosulfonate grades were found to be soluble in water, which is in agreement with literature[1, 3] (see *chapter I.1.3*). Since 4-methylmorpholine N-oxide (NMMO) was present in an aqueous solution at 50 wt%, only a few more lignin grades, additionally to the lignosulfonate grades, were found to be soluble. None of the lignin grades were found to be soluble in ethanol and four of the chosen grades could not be dissolved in any of the tested solvents. Although certain tendencies can be recognized from Table II-1, the final solubility properties for each of the lignin grades depend on its molecular structure and functional groups, its origin, extraction technique and molecular weight. Generally, the evaluation of lignin solubility is very complex and since only limited structural characterizations of the lignin grades were performed for this thesis, more detailed explanations about their dissolution behaviour cannot be provided. One of the main goals of this work being the spinning of low-cost precursor fibres, no chemical modifications or purifications of the lignin grades were performed in order to keep the raw material cost as low as possible. Since the polymer solubility represents a crucial parameter for the wet-spinning process, the results of the screening trials presented in Table II-1 represent the basis for all subsequent experiments comprised in this thesis.

Some simple approaches to improve the quality of lignin solutions have been evaluated. By heating the solvent, dissolution seemed to be realized faster for some cases. However, the general dissolution ability of the solvent was not found to be modified at increased temperatures. A Kraft lignin solution consisting of IndulinAT® (L9 or IAT) at 14 wt% in DMSO (see Table II-2) was heated to different temperatures up to 100 °C for 1-3 h. After evaluation by optical microscopy, the lignin solution was found thermally stable since no degradation could be observed. Besides, the use of ultrasound (ultrasonic bath and -tip) has been tested to improve the dissolution behaviour of lignin in given solvents, but no significant difference was found. Filtration experiments performed with syringe filters at pore sizes of 0.45-5 µm revealed that the homogeneity of lignin solutions can be increased by removal of impurities.

After their extraction, residual cellulose and hemicellulose as well as inorganic particles (coming from ash or salts) can typically be found within lignin grades.[3-4] The exact composition and the amount of these impurities depend on the respective extraction process (see *chapter I.1.3*). However, the filtration of impurities from lignin solutions needs to be adjusted to the used solvent (e.g. glass fibre filters are compatible with DMSO) and the process may generally increase the spinning costs at high impurity contents.

Only lignin solutions which were found homogeneous and which could be highly concentrated were chosen for the coagulation trials. Homogeneity is an essential condition since undissolved lignin particles or impurities of > 1/10 of the fibre diameter may break the fibre during spinning or cause clogging of the filters in the spinning apparatus. Besides, at low lignin concentrations the spinning dope may not coagulate inside the counter-solvent because the solid content of the dope is not high enough. As a consequence, only the lignin solutions given in Table II-2 were considered for spinning applications.

Table II-1: Solubility of lignin grades 1-20 in water, ethanol, dimethyl sulfoxide (DMSO), dimethyl ethylene urea (DMEU), 4-methylmorpholine N-oxide (NMMO, solution of 50% in water) and ethylene glycol with respective maximum concentrations (values are given in wt%). The respective type, source, extraction process and molecular weight for each lignin grade is given (if known). Filtration of some solutions is recommended (*)

Lignin grade	Water	Ethanol	DMSO	DMEU	NMMO	Ethylene Glycol	Type	Source	Extraction Process	M_w (g/mol)
L1			< 9	20		< 10	Organosolv	beech	Alcell	4200
L2			< 5	< 5			Organosolv	straw	Alcell	3400
L3			< 1	< 9			Organosolv	spruce	Alcell	26400
L4			< 9	40			Organosolv	spruce	Alcell	7100
L5			20	< 5	10*	< 5	Soda	annual plants	SODA	5600
L6			30*	20	< 10	< 5	Soda	annual plants	SODA	6000
L7			< 13	< 13	30*	10*	Soda	annual plants	SODA	5400
L8			< 5	20*		10*	Kraft		Kraft	9200
L9			13*	20*		30*	Kraft	pine	SODA	10800
L10			< 1	< 9			Organosolv	wheat straw	Formacell	1850
L11			< 13	< 5	< 5	< 5	Kraft	pine	Kraft	
L12	40		40		20	< 10	Lignosulfonate	maritime pine	Sulfite	
L13	< 23		< 9		20*	< 10	Lignosulfonate	maritime pine	Sulfite	
L14	< 33		< 1		30*	30	Lignosulfonate	maritime pine	Sulfite	
L15									acid solvent	5800
L16			35	35		< 1	Kraft	maritime pine	Kraft	
L17										
L18			5	1	1		Organosolv	wheat straw		
L19										
L20										

The lignin solutions listed in Table II-2 were used for the coagulation trials, whereby they were manually injected through a syringe needle into several different solvents in a coagulation bath and their behaviour was evaluated. The chosen solvents for coagulation were water, ethanol and different salts in aqueous solutions (of different valencies, see Table A-II-1 in annex). In some cases, the lignin solutions simply dissolved inside the coagulation bath, whereas in other cases they started to solidify, but without keeping a defined shape. When the solutions solidified while forming fibres through the injection, the case was considered as a suitable system of solvent and counter-solvent for the respective lignin grade. The three different cases are illustrated in Figure II-2 and the results of the coagulation screening are demonstrated in Table A-II-1 (see annex).

In the case of a good coagulation behaviour, it can be assumed that solvent and counter-solvent are exchanged, whereby the solvent diffuses into the counter-solvent while the counter-solvent diffuses to the lignin molecules. The insolubility of lignin inside the counter-solvent should then provoke solidification under flow into a fibre. The solution of lignosulfonate (L12) in DMSO for instance showed this behaviour in ethanol. However, it did not coagulate in water or aqueous salt solutions due to the fact that the lignosulfonate was found soluble in water. The Soda lignin grade L7 showed a good coagulation behaviour at high salt concentrations in aqueous solutions. In this case, it can be assumed that the coagulation of Soda lignin was rather triggered by interacting ions and not necessarily by the counter-solvent. The chosen Organosolv lignin grade (L4) seemed to show coagulation in water and in some of the salt water solutions, but not in all of them, which indicates a dependency on the ion valencies. Both of the softwood Kraft lignin grades (L16 and L9) showed coagulation or partial coagulation in water or saltwater. Thereby, the IndulinAT® (L9) solution based on ethylene glycol was rather found to form fibres at higher salt concentrations, whereas the softwood Kraft lignin L16 dissolved in DMSO showed good coagulation behaviour in all cases as soon as water was present in the system. This suggests that the coagulation of IndulinAT® in ethylene glycol could be supported by ions, whereas L16 in DMSO mostly needed water as a counter-solvent for coagulation.

These observations suggest that coagulation was determined on the one hand by the functional groups of the lignin grades and their ionic nature. Counter-ions within the counter-solvent thus potentially enhance the coagulation behaviour of these lignin grades. On the other hand, the coagulation was found to be determined by the solvents used for the lignin solutions, since different solvents may have different mixing affinities with different counter-solvents. In conclusion, the coagulation trials have shown that the process is of high complexity and that a tailor-made system of solvent and counter-solvent is necessary for a lignin grade in order to spin lignin from it.

Table II-2: Lignin grades and respective solvents for solutions chosen for coagulation trials (commercial lignin grade)*

Lignin Grade	Type	Source	Supplier	Solvent	Maximum concentration in solution [wt%]
L4	Organosolv Alcell	spruce	Fraunhofer CBP	DMEU	30
L6	Soda	Annual plants	Green Value (Protobind 2400)	DMSO	30
L7	Soda	Annual plants	Green Value (Protobind 6000)	NMMO	20
L9*	Kraft, softwood	pine	Mead WestVaco (IndulinAT®)	Ethylene glycol	20
L12	Lignosulfonate	Maritime pine	Tembec	Water / DMSO	40
L16	Kraft, softwood	pine	FCBA / Smurfit Kappa	DMSO	35

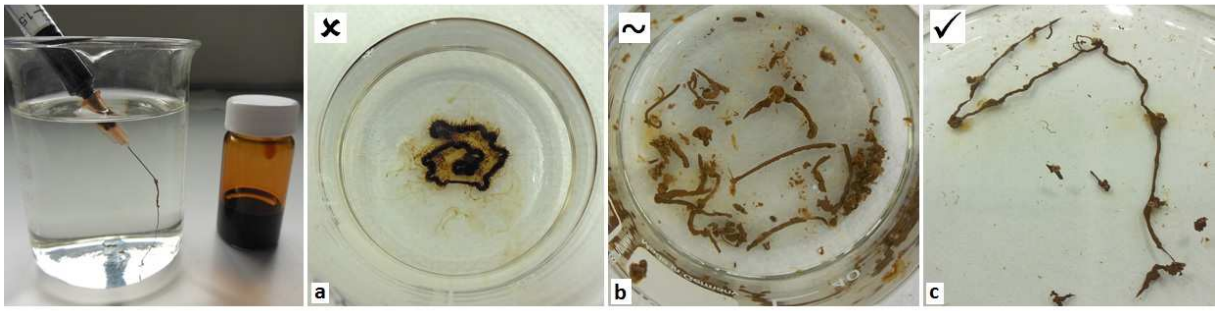

***Figure II-2** : Coagulation screening by injection of lignin solutions into coagulation baths (as shown on the left): dissolution (a), partial coagulation (b) and coagulation into fibre (c)*

Some selected fibres obtained from the coagulation screening were characterized by means of scanning electron microscopy (SEM) in order to investigate their morphology. The microscope HITACHI TM3030 was used to take the images of the lignin fibres. Prior to the SEM observation, the samples were coated with a thin gold-palladium (Au-Pd) layer by means of plasma metallization with a Quorum SC7620. The fibres were attached to the sample holder in a way that both their cross-sections and their surfaces could be evaluated. As can be seen from Figures II-3 and II-4, the lignin fibres coagulated in different solvents all exhibit a highly porous structure. Besides this morphology, the fibres showed a very brittle behaviour during sample preparation, which is in agreement with literature, where the high brittleness of lignin fibres is already stated.[3–5]

A typical example of a fast coagulation can be seen in the fibre cross-section in Figure II-4-c.1, whereby the coagulant visibly penetrated the fibre and migrated along its cross-section in a symmetrical manner.

The highly porous morphology of the obtained lignin fibres led to an extremely high brittleness, making it very difficult to manipulate the fibres. Due to the fact that at least a small amount of mechanical stability is necessary to handle the fibres and bring them to the carbonization step, the need of a reinforcing element became evident. The most common reinforcements proposed in literature are linear polymers of high molecular weight which are suitable for the spinning process and thus facilitate the spinning of lignin fibres. The search for a suitable polymer as spinning aid for lignin and the respective results are shown in the following subchapter.

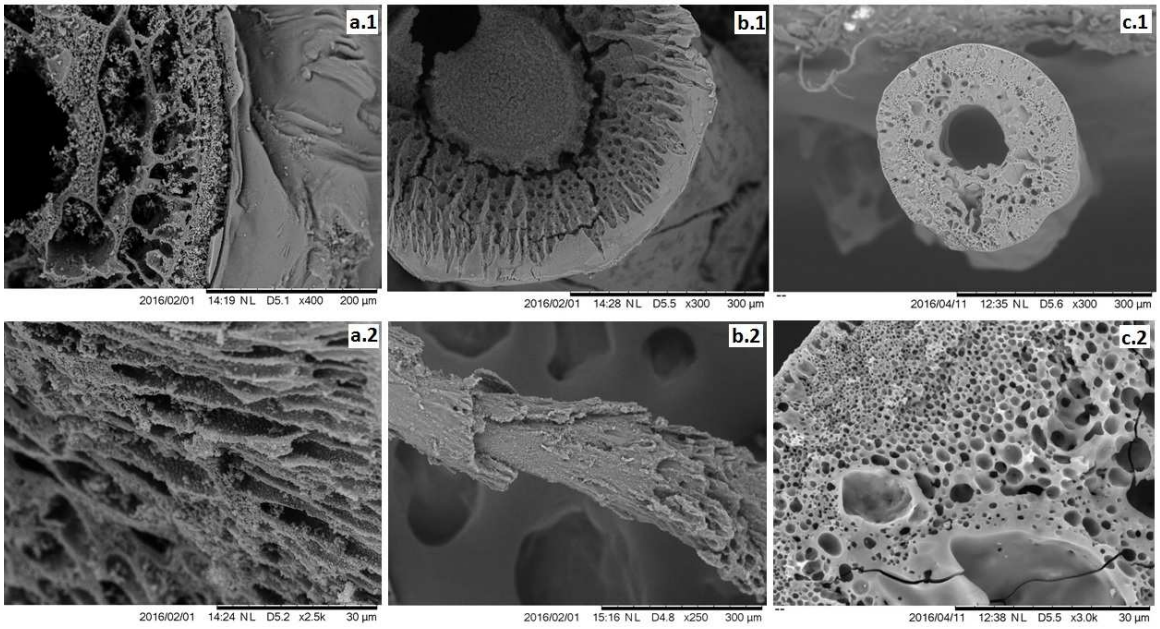

Figure II-3: *Lignin fibres coagulated in different solvents: Organosolv lignin (L4) coagulated in aqueous $(NH_4)_2SO_4$ (a), Soda lignin (L6) coagulated in aqueous $(NH_4)_2SO_4$ (b) and lignosulfonate (L12) coagulated in ethanol (c)*

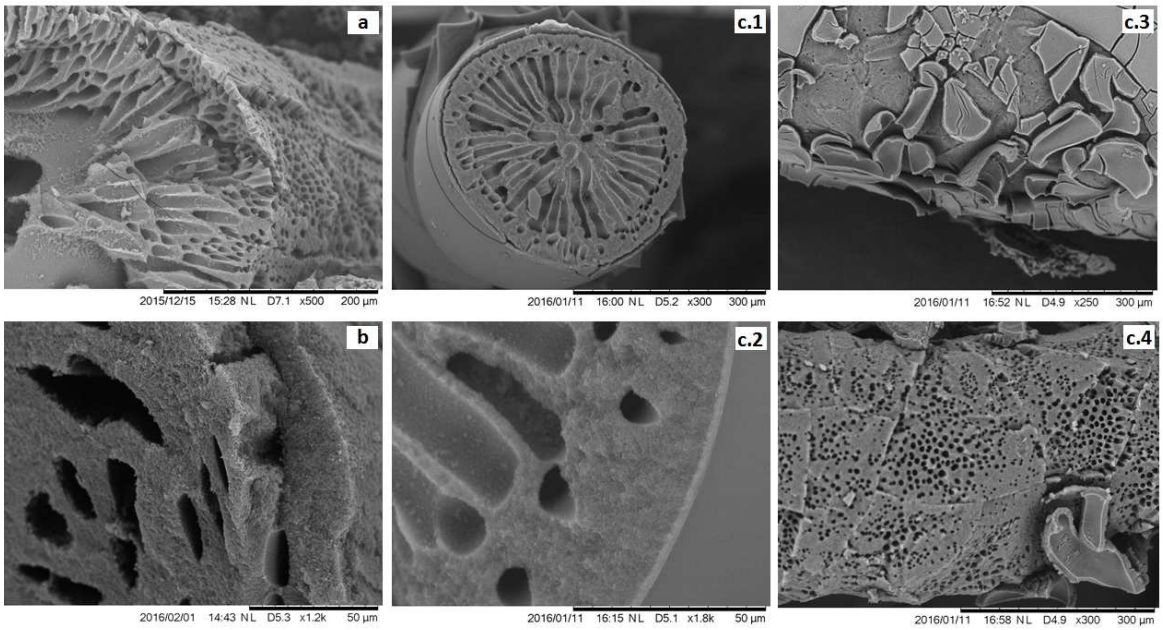

Figure II-4: *Kraft lignin fibres (L16) coagulated in different solvents: water (a), aqueous Na_2SO_4 (b) and aqueous $Al_2(SO_4)_3$ (c)*

II.1.2 Combination of Lignin with Other Polymers for Spinning Applications

As shown in *chapter I.4,* the combination of lignin with high molecular weight polymers to facilitate fibre spinning is a common approach in literature. In particular polyacrylonitrile (PAN), polyethylene (PE), polyethylene oxide (PEO), polyethylene terephthalate (PET), polyvinyl alcohol (PVA) and cellulose have been reported in combination with lignin. Regarding wet-spinning applications, the most common spinning aid for lignin is PAN, along with some cases of cellulose. Crucial conditions for the wet-spinning of polymer blends are that both polymers are soluble in the same solvent and that the mixture is homogeneous. Due to the fact that after the solubility- and coagulation screening the pure lignin fibres were found to exhibit extremely high brittleness, different polymers were evaluated which can be dissolved in the same solvents as the lignin grades in order to prepare blend fibres. In most cases, lignin- and polymer solutions were prepared separately and mixed only after dissolution in order to ensure homogeneous mixtures.

Some of the combinations investigated for this thesis were Lignosulfonate (L12, see Table II-2) and Alginate, Kraft lignin IndulinAT® (L9, see Table II-2) and Polyvinylpyrolidone (PVP) and Kraft lignin L16 (see Table II-2) and PEO. In the first two cases, blend solutions based on one common solvent could be prepared (Lignosulfonate and Alginate in water, Kraft lignin and PVP in DMSO), but no suitable counter-solvents were found for coagulation. In the case of Kraft lignin and PEO, which had been mixed by extrusion beforehand, no suitable solvent was found for dissolution of the granules. Besides, the Kraft lignin L16 and thermoplastic polyurethane (TPU) could both be mixed by dissolution in dimethyl formamide (DMF) and the solution was found to coagulate in a mixture of DMF and water (40:60). Flexible fibres could be obtained, showing a rubber-like behaviour in dried state. However, no further trials were performed since the system was based on DMF and the use of toxic solvents did not match with the scope of this thesis.

- Lignosulfonate-Polyvinyl Alcohol-Water System

Despite its high impurity content of around 22 % (see Figure A-III-2-a in annex), the lignosulfonate grade from Tembec (L12) being soluble in water was considered for an aqueous system in combination with polyvinyl alcohol (PVA). PVA is a common polymer used in fibre wet-spinning, thus a promising candidate for fibre reinforcement. The mixture of an aqueous lignosulfonate solution (at 40 wt%) and an aqueous PVA solution (at 10 wt%, molecular weight: 61000 g mol^{-1}) was found to form an emulsion, thus exhibiting two separate phases. Coagulation trials were performed in an aqueous solution of sodium sulphate (Na_2SO_4) at 300 mg ml^{-1} heated to 40 °C. This coagulation medium is one of the most commonly used systems for the wet-spinning of PVA fibres.[6-7] Flexible lignosulfonate-PVA fibres could be spun by manual injection into the heated solution inside a large petri dish (see Figure II-5). By addition of small concentrations of sodium tetraborate salt ($B_4Na_2O_7$) into the dope solution at pH 5 and injection into a coagulation bath (Na_2SO_4 at 300 mg ml^{-1}, 40 °C) at pH 10, spinning was facilitated and even more flexible fibres could be obtained. This is due to the fact that sodium tetraborate usually cross-links the molecular chains of PVA, thus reinforcing the

fibres.[8] A clear drawback of this system however was found to be the water-solubility of lignosulfonate, hindering the salt removal from these fibres. Residues of Na_2SO_4 salt crystals could be recognized by eye and evidenced by SEM imaging (see Figure A-II-1, in annex). A solution for washing without removing lignosulfonate from the fibres could not be found. Even an immersion of the as-spun fibres in an aqueous glutaraldehyde solution for further cross-linking of PVA did not lead to significantly improved fibre properties.

From an industrial point of view, the use of lignosulfonate for fibre spinning on the one hand is critical due to its high amount of inorganic impurities (salt residues and ashes). On the other hand, the use of water-soluble polymers is generally preferred in industry due to their low impact on the environment.

- Kraft Lignin-Polyvinyl Alcohol-DMSO System

The combination of Kraft lignin and PVA dissolved in DMSO represents the most promising approach within this thesis. Solutions of PVA (molecular weights 61000 g mol^{-1} and 195000 g mol^{-1}) were prepared at 10 wt% in DMSO at 90 °C under strong stirring. After cooling down to room temperature, it was mixed with a Kraft lignin L16 solution at 35 wt% in DMSO (prepared under stirring at room temperature), resulting in a homogeneous spinning dope in the form of an emulsion. The dope containing a Kraft lignin- and a PVA phase (17.5 wt% of lignin and 5 wt% of PVA, see Figure II-6) could be easily coagulated into fibres by means of a syringe needle as illustrated in Figure II-5. The used coagulation baths for the tests contained water, a calcium chloride ($CaCl_2$) solution at pH 10, an aqueous sodium tetraborate ($B_4Na_2O_7$) solution, acetone, ethanol or isopropanol. The approach led to very flexible fibres with lignin contents of up to 80 %, which could be easily manipulated. Directly after coagulation, the humid fibres could be manually stretched, whereby their diameter was reduced by more than three times. Thin fibre diameters are important in order to obtain higher mechanical properties.

The best conditions for coagulation were found in ethanol- and isopropanol baths. After manual stretching, the fibres were attached to a metal bar and thus dried under tension at room temperature for several hours under a fume hood (see Figure II-5). The stretching step could not be performed after coagulation in e.g. water, due to a lack of elasticity of the obtained fibres. Stretching of the blend fibres was found easier when PVA with higher molecular weight (195000 g mol^{-1}) was used.

Despite its excellent spinning properties right after mixing, the solution of Kraft lignin and PVA in DMSO was not found to be stable over time. Depending on the lignin-PVA ratios, the overall dope solid content and the chosen lignin- and PVA grades, the stability of the spinning dope varied between a few hours up to a few weeks before the mixture was found to form a gel. During gelation of PVA solutions, a cross-linking mechanism by the formation of hydrogen bonds typically creates a network of polymer chains. The process can e.g. be triggered by chemical cross-linkers or by dehydration of pure PVA solutions.[9-10] A full gelation of lignin-PVA solutions over time thus suggests H-bonding between the two components. The gelation process typically occurred faster at elevated dope concentrations and higher PVA molecular

weights, thus accelerating the cross-linking. The use of different lignin grades was also found to influence the process. In some cases, the gels could be re-dissolved by stirring the mixtures at elevated temperatures. However, this treatment usually led to a decreased spinning performance compared to a freshly prepared dope solution. A fast gelation of the dope solution can generally be considered as a constraint for wet-spinning since it clogs the apparatus and it hinders a stable coagulation process.

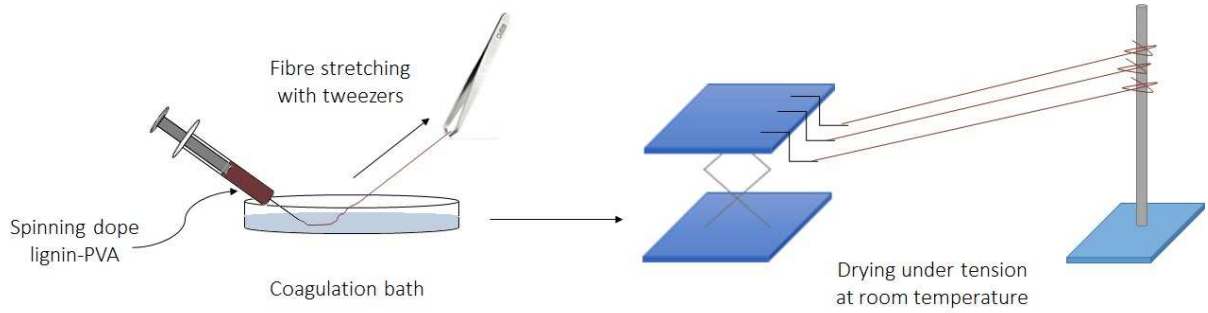

Figure II-5 *: Principle used for manual discontinuous wet-spinning of Kraft lignin-PVA fibres (on laboratory scale)*

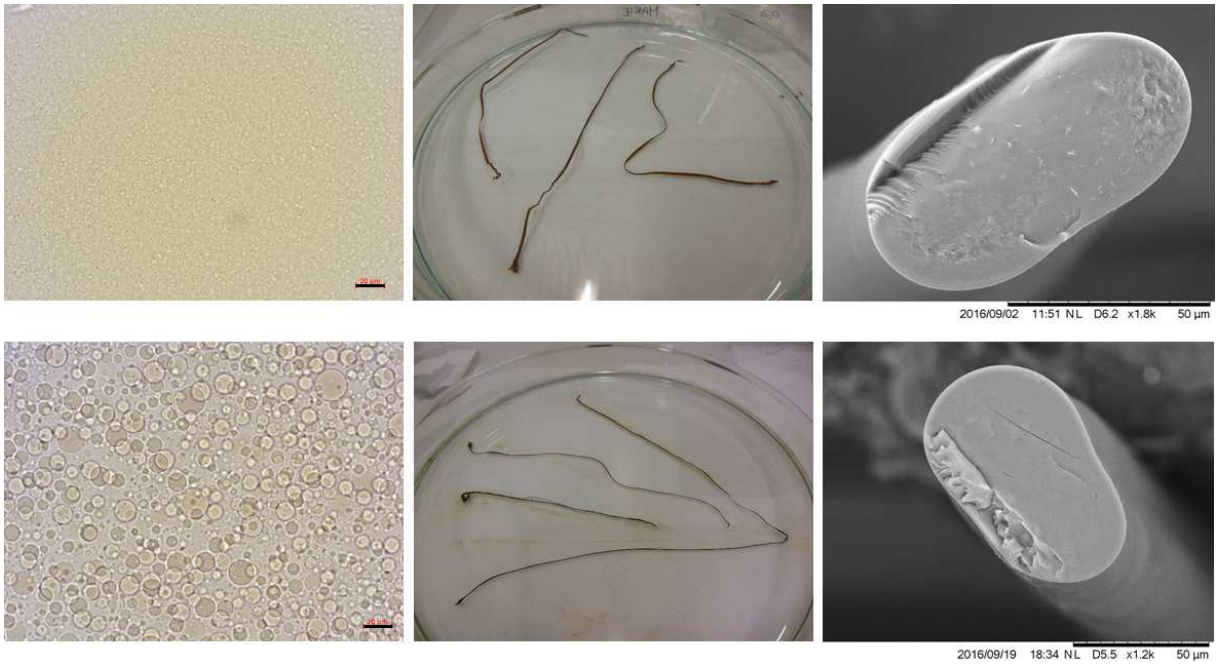

Figure II-6*: Spinning dope of Kraft lignin (L16)-PVA61K (17.5wt%-5wt%) with coagulation in aqueous $CaCl_2$ (above) and Kraft lignin (L16)-PVA195K (17.5wt%-5wt%) with coagulation in isopropanol (below), micrograph scale bars 20µm*

The as-spun fibres (Figure II-6) were found to be stable when heated to 280 °C, they did not melt, nor degrade. This is an important condition for the processing of carbon fibres, as polymeric precursor fibres that will undergo carbonization should not melt during the treatment. It has to be noted that the addition of PVA as a spinning aid allows the preparation of lignin precursor fibres which can easily be manipulated. However, PVA itself does not contribute to

the carbonization yield due to its high content of oxygen groups, which is why its ratio inside the fibres should be kept as low as possible.

In conclusion, the use of Kraft lignin (L16 or IndulinAT®) is preferred compared to lignosulfonate (L12) because of its higher purity. In combination with PVA in DMSO, the softwood Kraft lignin fibres represent the most promising approach to produce a low cost precursor material for carbon fibres on a larger scale and in an economical way. This system was thus studied in more detail (see *chapter II.1.3*) and chosen for spinning trials on larger scale (see *chapter II.2*).

II.1.3 Miscibility of Lignin and Polyvinyl Alcohol

The spinning of lignin solutions into fibres generally represents a challenge due to the fact that the solutions have relatively low viscosities even at high concentrations. The low viscosity is directly linked to the low molecular weight of lignin molecules (see *chapter I.1.2*). However, a certain viscosity is needed in order for the solution to coagulate under the form of a fibre during the wet-spinning process. A solution of softwood Kraft lignin at 35 wt% in DMSO (0.4±0.1 Pa.s at shear rate 1 s^{-1}) was thus mixed with a PVA solution at 10 wt% in DMSO (7.3 Pa.s at shear rate 1 s^{-1}) to increase the overall viscosity of the spinning dope to 4.0±0.1 Pa.s (at shear rate 1 s^{-1}). The initial solutions were prepared as described in *chapter II.1.2* and the viscosities of lignin- and PVA solutions as well as their mixtures are presented in Figure A-II-2 (see appendix). Moreover, the wet-spinning of PVA fibres is a well-known industrial process and thus this polymer is believed to assist the fibre formation and the processability of lignin. The miscibility of hardwood Kraft lignin-PVA blends has already been investigated by Kubo and Kadla in melt-spun fibres[11]. In this thesis, the miscibility of softwood Kraft lignin-PVA blends both in solution and in solid films was investigated. Two different types of softwood Kraft lignin were used for the trials. On the one hand L16 from FCBA, in the following called “KL” and on the other hand IndulinAT® from MeadwestVaco, in the following called “IAT”. The systems were later used for fibre spinning trials (see *chapter II.2* and *II.3*).

- Miscibility in Solution

The phase behaviour of the evaluated blend solutions was demonstrated by means of ternary phase diagrams taking into account the three components of the system: Kraft lignin, PVA and DMSO. Spinning dopes for wet-spinning applications typically have solid contents of 10-30 %. Therefore, several sample solutions were prepared within this concentration range and after mixing was completed, images were taken by optical microscopy in transmission mode. For higher clarity, the phase diagrams were only partially illustrated with the axes displaying 0-30 wt% of lignin and PVA and 70-100 wt% of DMSO (as depicted in Figure II-7).

Three different states were found for lignin-PVA solutions by optical microscopy. At low polymer concentrations, the solutions were found to be homogeneous and completely miscible. The mixtures were found to be in a monophasic state. With increasing PVA- and total concentrations, the systems turned into a biphasic state whereby the two combined polymer

solutions formed an emulsion upon mixing. Besides, an intermediate state was found, in which the emulsion-like appearance starts to form. The blend solutions were prepared using a PVA solution at ≤ 10 wt%, because the solution viscosity at higher concentrations would have been too high for homogeneous mixing (see right side of the phase diagram, Figure II-7).

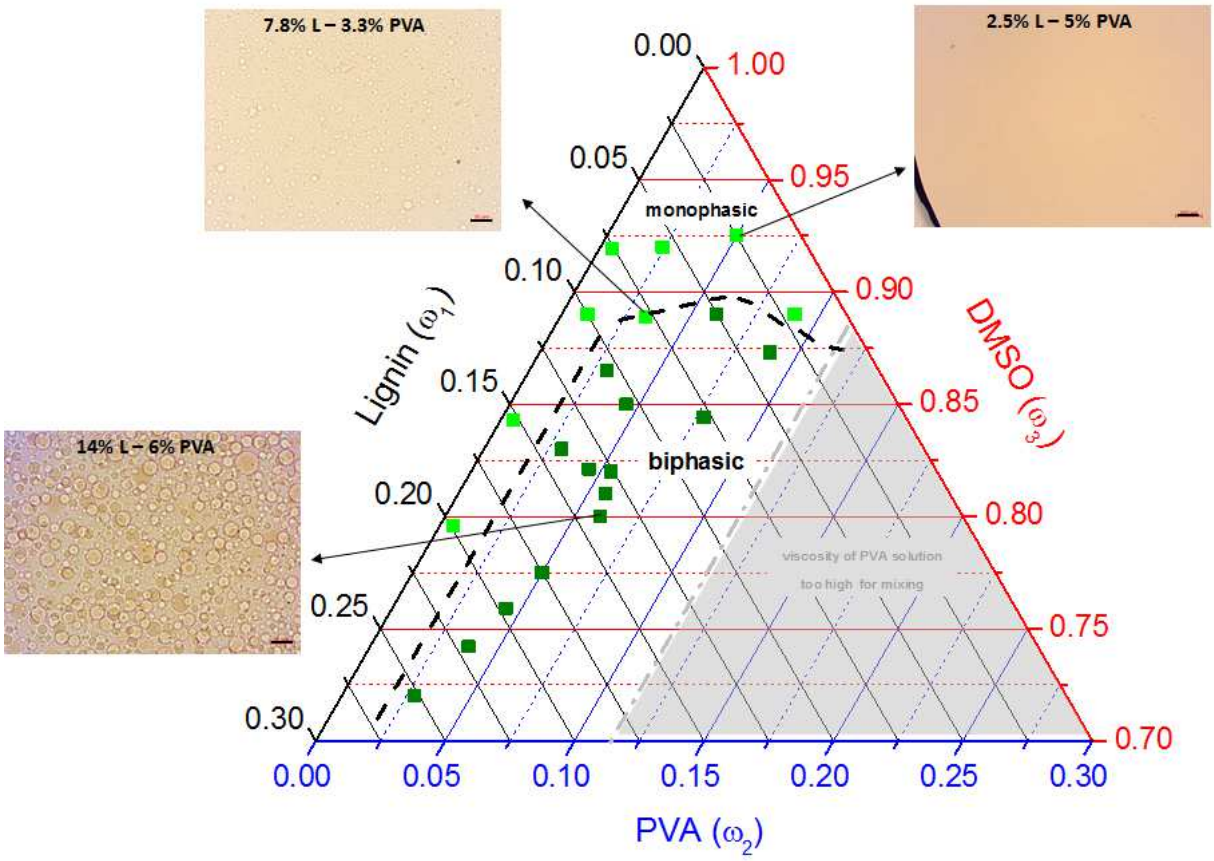

Figure II-7: *Phase diagram of Kraft lignin (KL)- and PVA solutions in DMSO (given in weight fractions ω_1, ω_2 and ω_3, only partially illustrated: the grey area represents the composition domain with too high viscosity for mixing and spinning). Scale bars of microscopy images are 20 µm.*

Although the use of monophasic spinning dopes is generally preferred for wet-spinning applications, the monophasic region in the case of KL and PVA (195000 g mol^{-1}) (see Figure II-7) is present at only very low concentrations. By changing the Kraft lignin grade, the PVA grade or the sample preparation method, it has been found possible to expand the monophasic region within the lignin-PVA-DMSO phase diagrams. Examples are provided in Figure II-8, showing the blends of IAT-PVA-DMSO prepared by mixing in cold (“C”) or in hot state (“H”) and the blends IAT-PVA2-DMSO using a PVA grade with lower degree of hydrolysis (88 %, 205000 g mol^{-1}). For the solution prepared in hot state, lignin powder was directly dissolved inside the PVA solution in DMSO at 90 °C at the desired concentrations. It can be recognized that the modification of components inside the blends or of the preparation method led to a different phase behaviour compared to the reference system KL-PVA-DMSO.

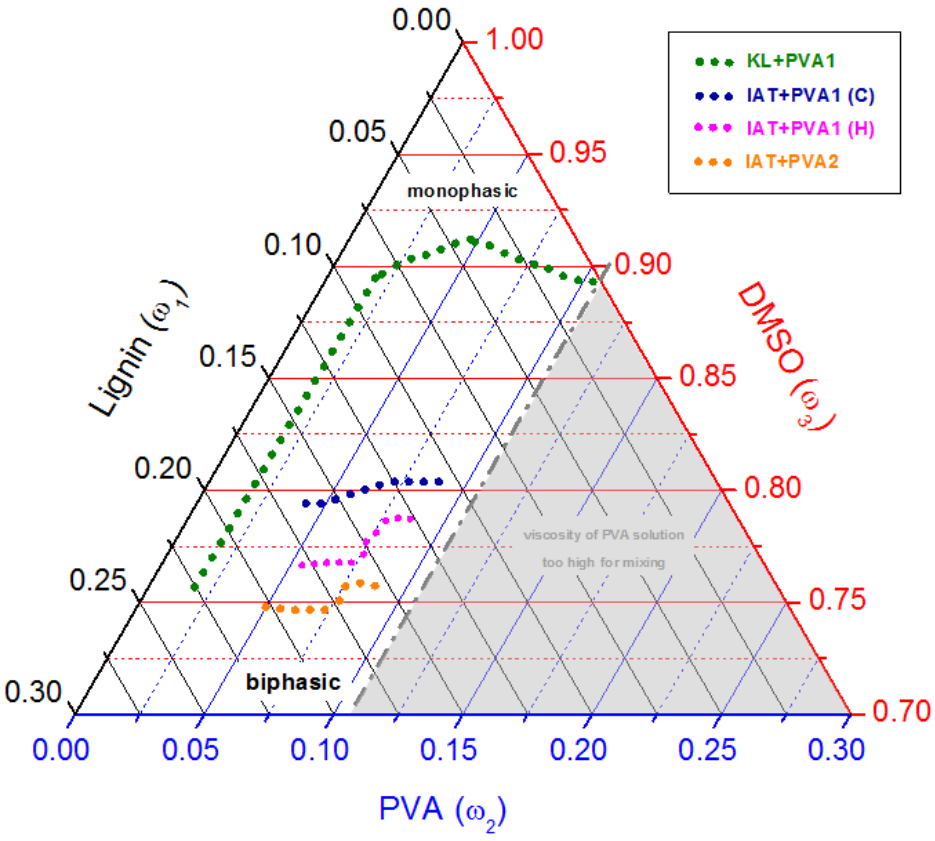

Figure II-8 *: Influence of Kraft lignin grade, dope preparation method and PVA grade on monophasic – biphasic transition of lignin-PVA spinning solutions based on DMSO (phase diagram of lignin, PVA and DMSO given in weight fractions ω_1, ω_2 and ω_3, only partially illustrated)*

- Miscibility in Solid Films

Films consisting of pure lignin and pure PVA, as well as films at different lignin-PVA ratios (70-30, 50-50 and 30-70), were characterized for two different lignin grades (KL and IAT). In order to prepare these films, a lignin solution at 35 wt% in DMSO and a PVA solution at 10 wt% in DMSO (preparation see *chapter II.1.2)* were mixed in specific ratios indicated in Table A-II-2 (see annex). After stirring at room temperature for 30 min with a magnetic stirrer bar, the solutions were filled into a Teflon mould or onto a polyethylene sheet. The films were dried at 80 °C for 3 days under ventilation.

Differential Scanning Calorimetry (DSC) measurements were performed on the films using a Mettler Toledo DSC 1 STARe System instrument and software. Two heating and cooling cycles were recorded at 5 °C min^{-1} from -20 °C to 200 °C under nitrogen for each film. Additionally, Dynamic Mechanical Analysis (DMA) was performed on a Mettler Toledo DMA 1 STARe System in tension mode. The amplitude used was 3 µm at a frequency of 10 Hz. The same heating and cooling cycles were applied as in the DSC measurements. After each DMA measurement, the films were collected and analysed with a transmission electron microscope (TEM). Prior to observation, the samples were cut into thin slices, put onto grids and stained with ruthenium tetroxide (RuO_4).

In solution, the blends based on KL were found to be biphasic, whereas the blends of IAT and PVA were monophasic for the ratios 30-70 and 50-50 and biphasic for 70-30 (see Figure II-8, blue line). The prepared films were investigated by means of differential scanning calorimetry (DSC) and the results are presented in Figure II-9. The endothermic peak found for all samples between 180 °C and 200 °C corresponds to the evaporation of residual DMSO (boiling point 189 °C). Therefore, peaks above 200 °C are considered as melting of PVA crystalline domains (melting temperature around 220 °C). Regarding the samples containing Kraft lignin (KL) and PVA, a clear melting of crystalline domains only occurred for pure PVA and for 70 % PVA within the blend, but the peak disappeared with higher KL contents. This stands in contrast to IAT-PVA blends, which exhibited fusion of PVA within all blend films. However, compared to pure PVA, the peak is broadened and shifted towards lower temperatures for all lignin-PVA blends. Kubo and Kadla[11] thermally blended hardwood Kraft lignin with two different PVA grades and obtained similar results. The existence of the melting peak of PVA indicates crystalline domains within the films, thus immiscible systems. However, the shift of the PVA melting temperature towards lower temperatures and the peak broadening indicate a partial miscibility of amorphous PVA fractions with lignin. The shift of the melting temperature can be considered as dilution effect.[12-13] The crystallinity of the PVA fraction seems reduced since crystalline domains of PVA do not seem completely separated from lignin. In the case of KL-PVA 50-50 and 70-30, the crystalline phase of PVA seems to have completely disappeared due to a high miscibility with KL.

The glass transitions of both lignin and PVA within the blends were found to be difficult to evaluate via DSC measurements due to a lack of clear signals (Figure A-II-3, see annex). Therefore, dynamic mechanical analysis (DMA) was performed on the 70:30 and 30:70 blends. As already found within the DSC results, DMSO residues were present within the films, modifying their thermal properties (see 1st curve in Figure II-10). In order to completely remove the remaining DMSO from the films, the DMA measurements were performed in cycles with isotherms at 180 °C for 30 minutes and 1 h respectively. As shown in the graphs in Figure II-10, the glass transition is shifted to higher temperatures after the isotherms, suggesting a thermal cross-linking reaction within KL and IAT. Besides, the shift of T_g towards higher temperatures was accompanied by an increase of the storage modulus *E'*, as shown for the KL-PVA blends in Figure A-II-4 (see annex). The same trend was observed for the IAT-PVA blends.

Figure II-11 illustrates the 70:30 and 30:70 blends after the second round of a DMA cycle from -20 to 200 °C at 5 °C min^{-1}. In other words, the films were heated to 200 °C for complete removal of DMSO, then cooled down to -20 °C and heated again to 200 °C (see Figure II-11). This method (fast heating to high temperature and fast subsequent cooling) allowed an investigation of the thermal properties of the blends without the influence of DMSO and without structural modification (cross-linking) of lignin. The obtained results clearly demonstrate two glass transitions for IAT-PVA blends and only one for KL-PVA 30:70. No sign of glass transition was found for KL-PVA 70:30. Two glass transition temperatures (T_gs) within the blends suggest amorphous domains where either lignin chains or PVA chains are dominant. In the case of

IAT-PVA blends, also crystalline domains of PVA chains with some incorporated lignin can be found, as proposed by DSC results (Figure II-9). For KL-PVA 30:70, amorphous domains and crystalline domains seem to coexist. This system is considered as partially miscible. KL-PVA 70:30 represents a fully miscible system since no thermal signature of PVA, be it amorphous or crystalline, can be found by means of DSC and DMA. Surprisingly, no glass transition could be found for this blend below 230 °C, presumably due to a low signal. To conclude, some of the blends form immiscible systems, while others show partial miscibility.

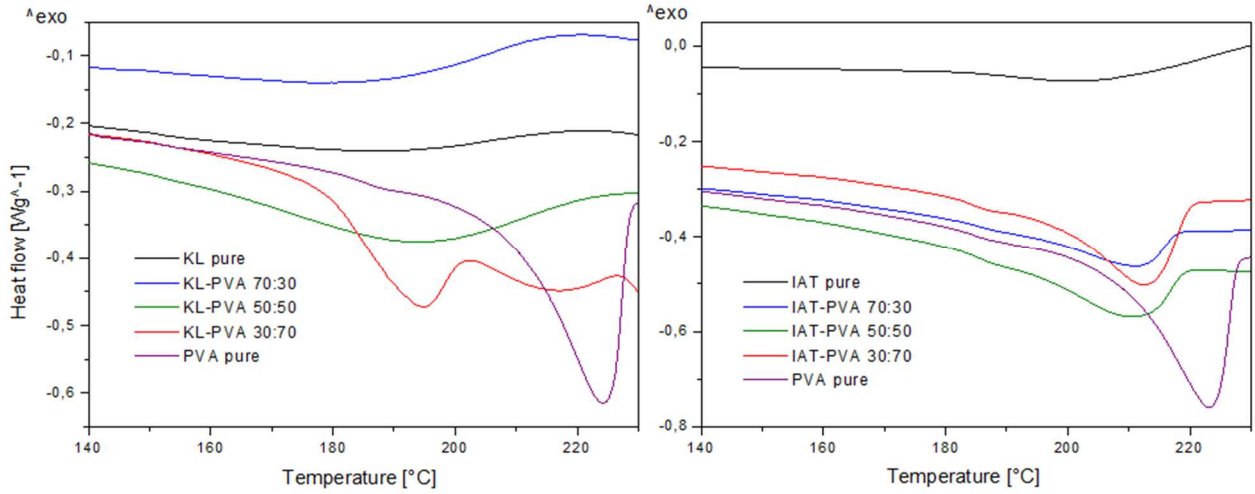

***Figure II-9**: DSC results (2nd heating cycle) of Kraft softwood lignin (KL)-PVA films (left) and IndulinAT Kraft softwood (IAT)-PVA films (right)*

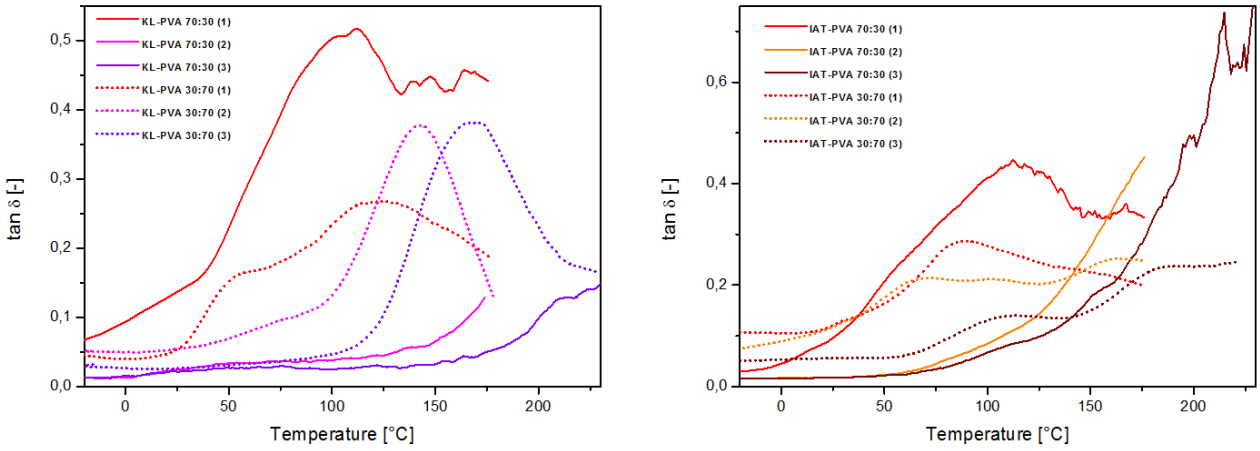

***Figure II-10**: DMA heating cycles of films KL-PVA 70:30 and 30:70 (left) and of films IAT-PVA 70:30 and 30:70 (right): samples have been heated from -20 °C to 180 °C, directly (1), after 30 minutes isotherm at 180 °C (2) and after 1 hour isotherm at 180 °C (3)*

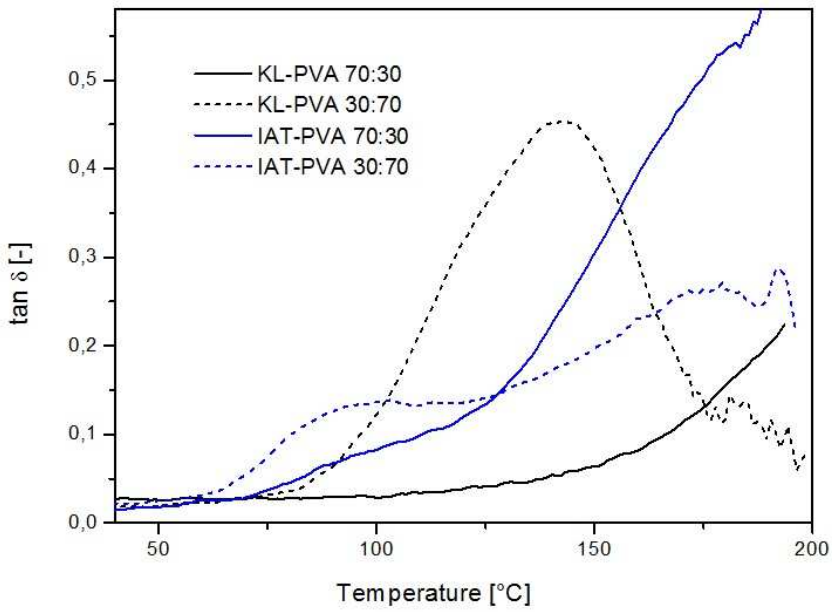

***Figure II-11**: DMA results (2nd heating cycle) of KL- and IAT-PVA blends at ratios of 70:30 (full line) and 30:70 (dashed line)*

In order to confirm the obtained results, the films were investigated by transmission electron microscopy (TEM) at high magnification to image their structure. The TEM images allow a clear distinction between lignin and PVA domains thanks to prior treatment of the films with ruthenium tetroxide (RuO_4) which marked exclusively the aromatic molecular groups, thus contrasting lignin without modifying PVA. Figure II-12 shows that the blends of IAT and PVA are immiscible since separate domains of IAT-lignin and PVA in different proportions can be distinguished. At low magnification, the blends of KL and PVA are homogeneous in comparison with IAT-PVA blends. However, at high magnification and adjustment of contrast, two separate domains become visible as well, although at much smaller sizes. The blends of KL-PVA are somewhat more “dispersed”, demonstrating that KL is still more compatible with PVA than IAT. These findings are in good agreement with the obtained DSC and DMA results.

After a detailed characterization of the blends consisting of Kraft lignin-PVA-DMSO in solution as well as in solid films, the system was transferred to the spinning of precursor fibres by means of a continuous wet-spinning process, as presented in the following subchapter.

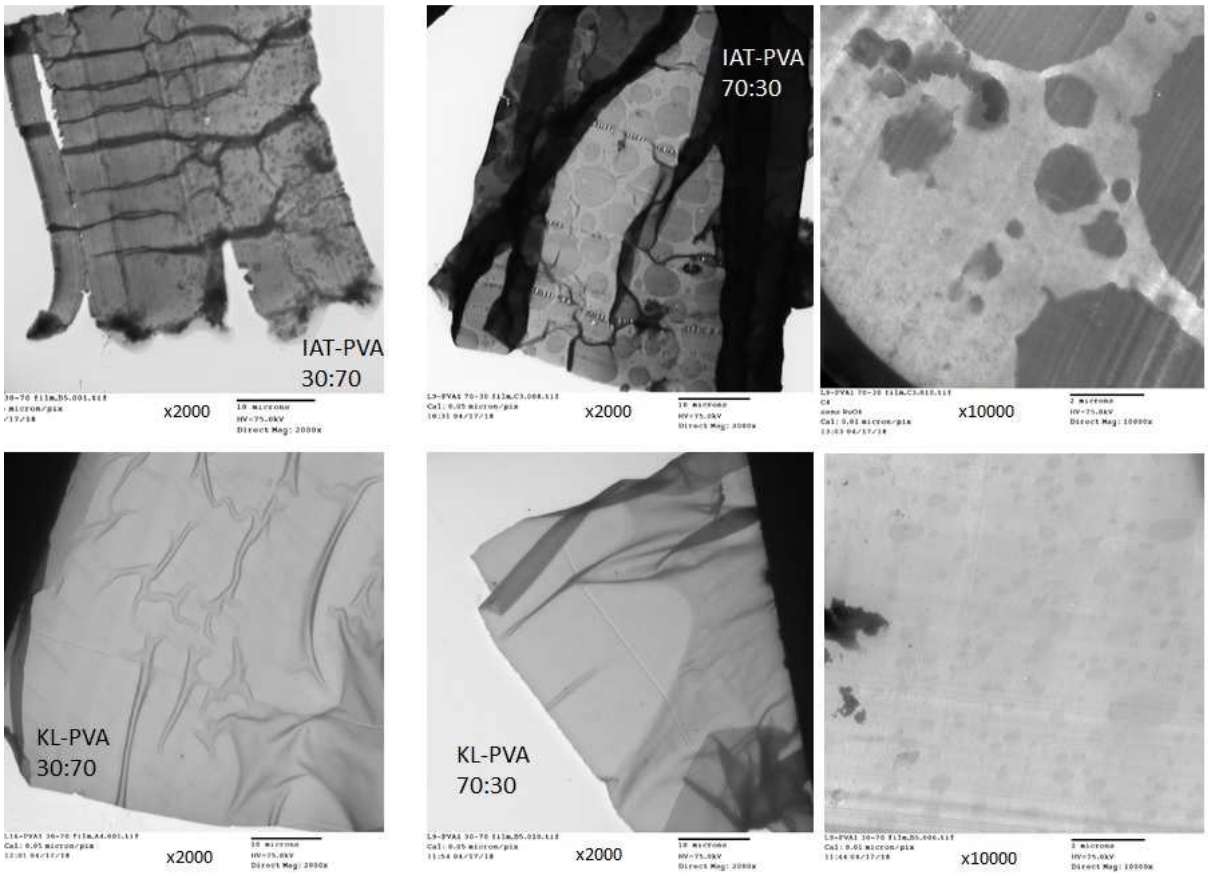

***Figure II-12**: TEM images of lignin-PVA films (samples have been cut into thin slices and marked with RuO_4 so that lignin is illustrated as darker areas). Images of IAT-PVA films 30:70 and 70:30 (above) and KL-PVA films 30:70 and 70:30 (below) have been taken at magnifications of 2000 (scale bar 10 µm) and 10000 for ratios 70:30 (scale bar 2 µm).*

II.2 Continuous Wet-Spinning and Characterization of Lignin-Polyvinyl Alcohol Fibres

The main goal of the work presented in this thesis is to prepare wet-spun precursor fibres containing high lignin contents in order to increase the potential carbon yields obtained after their carbonization. Pure lignin fibres were found to be unspinnable due to high brittleness (see *chapter II.1.1*). Therefore, PVA was added as a spinning aid and the fibre spinning ability was first tested manually on laboratory scale (see *chapter II.1.2*). Due to the promising properties of the obtained fibres, continuous wet-spinning trials were performed as well, which are presented in this subchapter. The preparation method of lignin-PVA wet-spinning into continuous fibres developed within the framework of this thesis has been filed for a patent application in October 2017.[14]

II.2.1 Spinning Conditions

The dope solutions used for continuous wet-spinning of lignin-PVA fibres were based on DMSO and prepared in the same way as the ones used for manual spinning (see *chapter II.1.2,* p. 57) and for lignin-PVA films (see *chapter II.1.3*). Precisely, separate solutions of Kraft lignin and PVA were prepared prior to mixing at the desired ratios. As described in *chapter II.1*, Kraft lignin powder (KL, FCBA or IAT, MeadwestVaco) was fully dissolved in DMSO under constant stirring at room temperature at a concentration of 35 wt%. A PVA solution of 10 wt% was prepared by stepwise addition of PVA flakes (Mowiol® 56-98,195 kg mol^{-1}, 99 % hydrolysis degree, Sigma Aldrich) into DMSO at 90 °C under strong stirring until dissolution was completed. The solution was cooled down to room temperature and mixed with the lignin solution in ratios x + y as indicated in Table II-3. The resulting concentrations of lignin (L) and PVA inside the spinning dopes and inside the dried fibres can be calculated as

$$C_{dope} = \%L_{dope} + \%PVA_{dope} = x * \frac{C_{L\text{-}solution}}{\left(\frac{m_{dope,\,total}}{100}\right)} + y * \frac{C_{PVA\text{-}solution}}{\left(\frac{m_{dope,\,total}}{100}\right)} \qquad (II\text{-}1)$$

$$C_{fibre} = \%L_{fibre} + \%PVA_{fibre} = \%L_{dope} * \left(\frac{100}{\%_{dope,\,total}}\right) + \%PVA_{dope} * \frac{100}{\%_{dope,\,total}}) \qquad (II\text{-}2)$$

By choosing the amount of lignin- and PVA solution forming the mixture, their respective concentration both inside the spinning solution and inside the final fibre can be tuned.

Example for a spinning dope resulting in a lignin-PVA fibre at ratio 70-30:

$\%L_{dope}$ = 4g * 0.35 / (10g/100) = 14 wt%
$\%PVA_{dope}$ = 6g * 0.1 / (10g/100) = 6 wt%
$\%L_{fibre}$ = 14 wt% * (100/20 wt%) = 70 %
$\%PVA_{fibre}$ = 6 wt% * (100/20 wt%) = 30 %

Different lignin-PVA ratios were tested step by step for spinning, along with the dope solid contents shown in Table II-3. Based on the DSC, DMA and TEM results for lignin-PVA films (see *chapter II.1.3*), the softwood Kraft Lignin KL (from FCBA) was chosen as the most suitable lignin grade for fibre spinning due to a high compatibility with PVA195K. Only the PVA with a molecular weight of 195000 g mol^{-1} was considered for the trials, since it showed a better spinning performance than other PVA grades. A compromise between a high lignin content and sufficiently high spinning ability obtained by PVA addition was found with the ratio KL-PVA 70:30.

The as-prepared spinning solutions were continuously injected into a coagulation bath containing isopropanol through a 1-hole spinneret (diameter 300 µm), in which the solutions formed fibres only at sufficiently high concentration and PVA content. The obtained fibres were directly washed in isopropanol, dried in an infrared oven at 90 °C and wound up at different draw ratios as explained by equation II-3 and Table II-3. The spinning principle is shown in Figure II-13.

At a spinning solution concentration of 20 wt%, the spinning process could be optimized in a way that high draw ratios (of 2-4) could be applied on the fibres, decreasing their diameter and increasing their mechanical properties, as will be discussed later. The washing baths were mainly used to facilitate the fibre stretching while keeping the fibres in wet state (unless hot-stretching was applied in a post-treatment). The applied draw ratios in wet state (DR_1) and during the drying stage (DR_2) were calculated from the linear velocity gradients V_{ii}/V_i of the draw roll velocities V_1, V_2 and V_3 as:

$$DR_1=\frac{V_2}{V_1} \text{ and } DR_2=\frac{V_3}{V_2} \qquad (II\text{-}3)$$

However, it has to be mentioned that the spinning of monophasic lignin-PVA solutions was not possible under the chosen conditions. The biphasic spinning dope thus potentially rendered the obtained fibres less homogeneous. An overview of the obtained fibres and of their morphology investigated by SEM is given in Figure II-14.

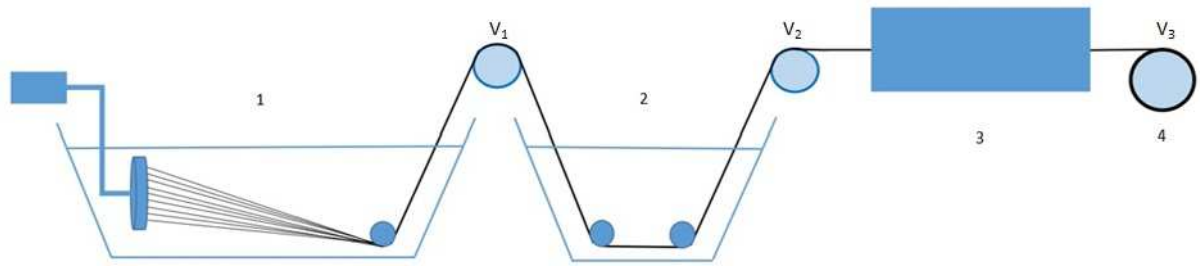

***Figure II-13**: Schematic principle of continuous lignin fibre spinning: coagulation (1), washing (2), oven-drying (3), winding (4), linear velocity of draw rolls 1-3 (V_1, V_2, V_3) [14]*

Table II-3: Feasibility of lignin-PVA fibre spinning with respective processing parameters

Lignin content [%]	PVA content [%]	Dope composition Lignin + PVA [wt%]	Spinning conditions
90	10	25.2 + 2.8 (28)	No coagulation achieved
85	15	22.2 + 3.8 (26)	Coagulation possible but unstable, only discontinuous spinning possible (DR_1 = 1.36, DR_2 = 2.37)
82	18	19.7 + 4.4 (24)	Coagulation rather unstable, fibre breaks easily during spinning (DR_1 = 1.36, DR_2 = 2.37)
78	22	17.5 + 5.0 (22.5)	Coagulation and spinning stable (DR_1 = 1.2, DR_2 = 2.35)
75	25	13.4 + 4.5 (17.9)	Coagulation and spinning stable, winding at 6-8 m min^{-1} (DR_1 = 1.7, DR_2 = 2.8)
70	30	14.0 + 6.0 (20)	Coagulation stable, spinning under tension is possible (DR_1 = 2.2, DR_2 = 4)

II.2.2 Fibre Morphology

The morphology of the obtained fibres was visualized with a scanning electron microscope (SEM) HITACHI TM3030 after gold-palladium metallization with a Quorum SC7620 to enhance the image contrast. The samples were fixed on a sample holder in a way that the fibre cross-sections, but also the fibre surfaces could be characterized.

No significant differences were observed between the morphologies of fibres containing 85 % and 70 % of lignin. The investigated fibres' cross-sections were defect-free and their surfaces of a smooth morphology (see Figure II-14-a-c+g). The impact of the coagulation bath on the shape of the fibre cross-section became clear as well. At a high concentration of isopropanol (in the beginning of the spinning trial), the obtained fibre cross-section was found as bean-shaped, reflecting a quick coagulation at the surface of the fibre followed by a decrease of the fibre diameter by diffusion of the inner solvent (see Figure II-14-d). However, with increasing DMSO concentration within the static coagulation bath towards the end of the spinning trial, the fibre cross-sections became perfectly round, reflecting now a slower coagulation due to the decreasing efficiency of the coagulating medium with operating time (see Figure II-14-e).[13-14] By adjusting the solvent ratios within the coagulation bath, the cross-section shape can thus be tailored. Besides, the metastable state within the lignin-PVA fibres became visible on their cross-section after mechanical testing: the forced fracture led to phase separation of lignin and PVA (see Figure II-14-f), which did not occur when fibres were broken carefully under liquid nitrogen (see Figure II-14-a-e). From high resolution SEM images (see Figure II-15) and TEM images of the lignin-PVA fibres (see Figure II-16), two different phases can clearly be distinguished. However, the global fibre morphology looks homogeneous with well-mixed lignin and PVA phases.

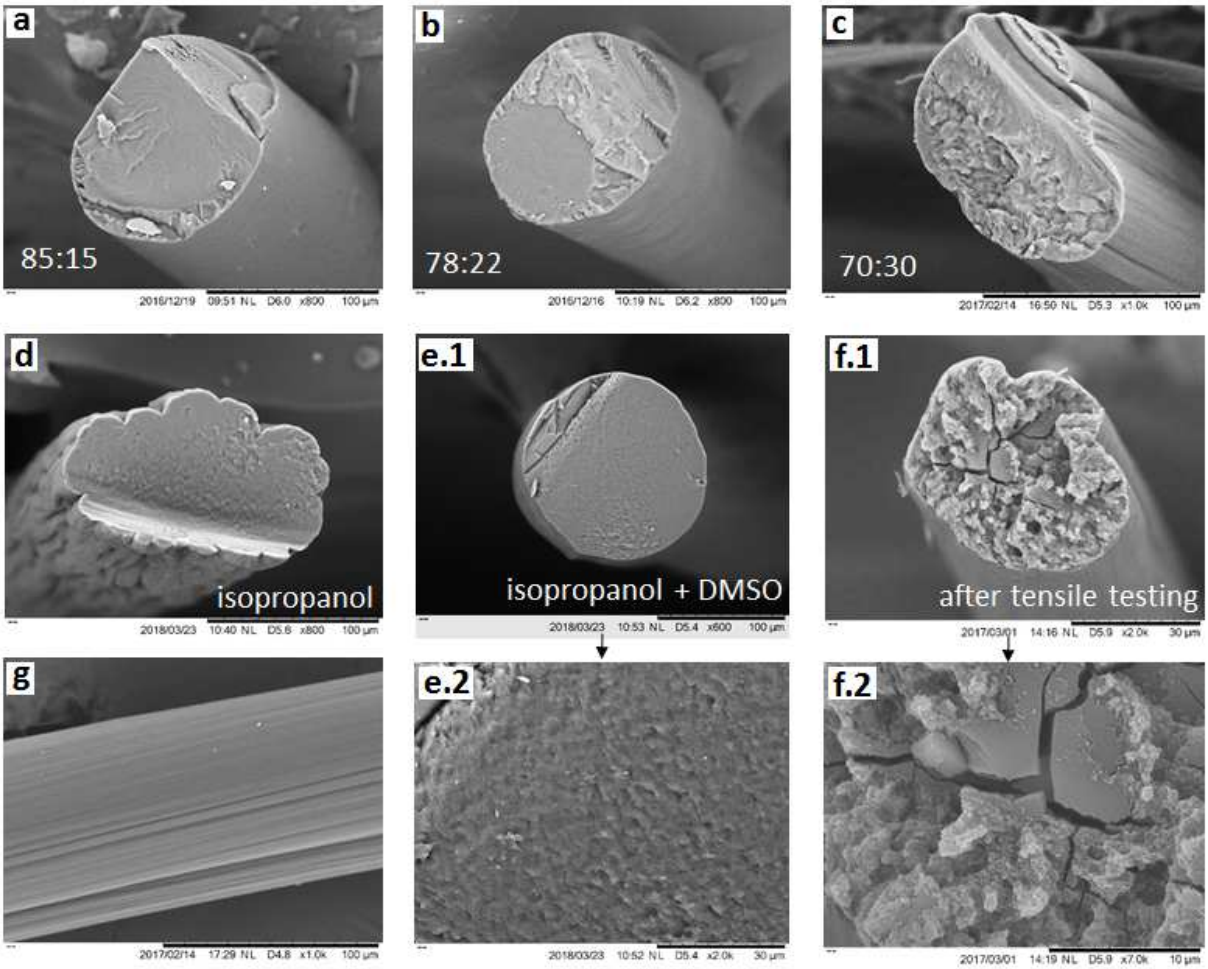

***Figure II-14**: SEM images of lignin-PVA fibre cross-sections: different KL-PVA ratios of 85:15 (a), 78:22 (b), 70:30 (c); different coagulation bath compositions (for ratio 70:30) containing isopropanol (d) and isopropanol + DMSO (e); cross-section after tensile test (f) and fibre surface (g)*

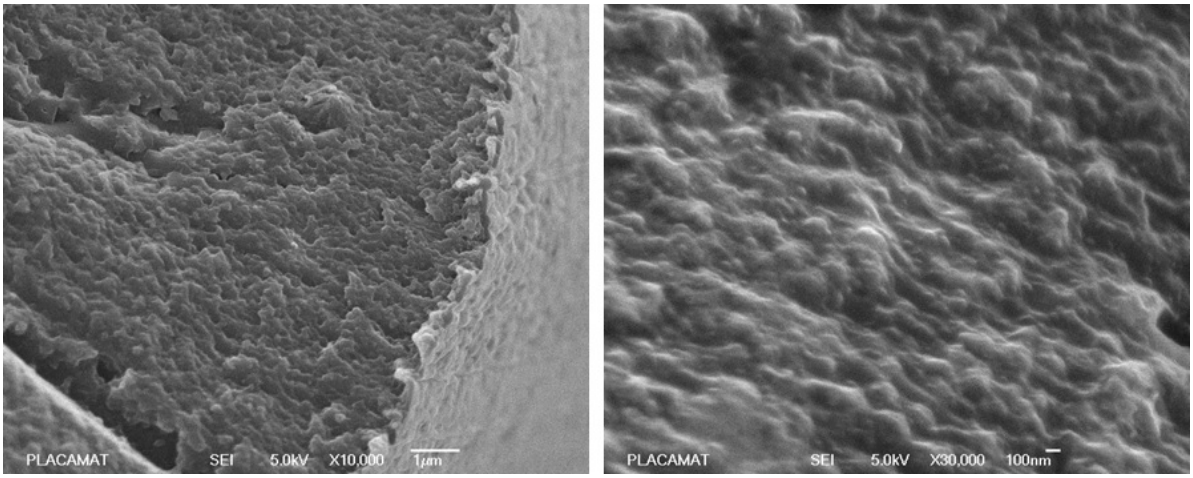

***Figure II-15** : High resolution SEM images of reference precursor fibre KL-PVA 70:30, scale bars 1µm (left) and 100nm (right)*

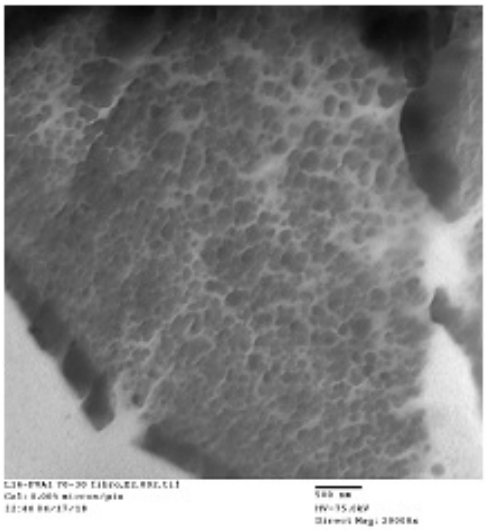

***Figure II-16**: TEM images of reference precursor fibres KL-PVA 70:30 in biphasic state (scale bars 500 nm, samples have been cut into thin slices and stained with RuO_4 to contrast aromatic groups within lignin, corresponding to the darker areas)*

II.2.3 Thermal Properties of Precursor Fibres

The as-spun lignin-PVA fibres being intended as renewable precursor material for carbon fibres, their behaviour upon thermal treatment was characterized by thermogravimetric analysis (TGA). The measurements were performed on a Mettler Toledo TGA 2 STARe instrument. The samples were heated in a sapphire pan from 25 °C to 1000 °C at a heating rate of 10 °C min^{-1}. The derivative was calculated from the obtained curve by the TGA 2 STARe software. Based on the mass losses upon heating, an adapted temperature program was defined for carbonization.

The precursor fibre with a lignin-PVA ratio of 70:30 was subsequently chosen as a reference for the carbonization trials (see *chapter II.4*). Compared to the fibres containing higher lignin ratios, this fibre showed excellent flexibility and sufficiently high mechanical properties due to optimized processing conditions. Moreover, it still led to elevated carbon residues of 28.2 % (Figure II-17 and Table II-4) which are advantageous for the subsequent carbonization process. The obtained TGA results show that upon pyrolysis the blend fibres behave differently from the pure components. The high mass loss around 190 °C, which is not found for pure KL or pure PVA, could be attributed to DMSO residues within the fibres. In this case, the weight loss and the residues after TGA measurements do not correspond to the actual carbonization yields. The potential of the precursor fibres would thus be underestimated.

Besides the ratio 70:30, also fibres with higher PVA contents have been considered for the carbonization tests. However, these fibres have not been found resistant enough, meaning they broke during the treatment under tension. Due to the fact that PVA alone almost completely decomposes into gaseous species upon carbonization (2.4 % residue, see Figure II-17), fibres with PVA contents above 30 % may not provide enough matter necessary for the process, thus they are not suitable as precursor material. Generally, the lignin contents should

be kept as high as possible in order to obtain high carbonization yields and to keep the process economical.

Based on the derivative of the obtained TGA graph for lignin-PVA 70:30, a tailor-made temperature program was designed for the carbonization of this fibre. The process is explained in more detail in *chapter II.4*.

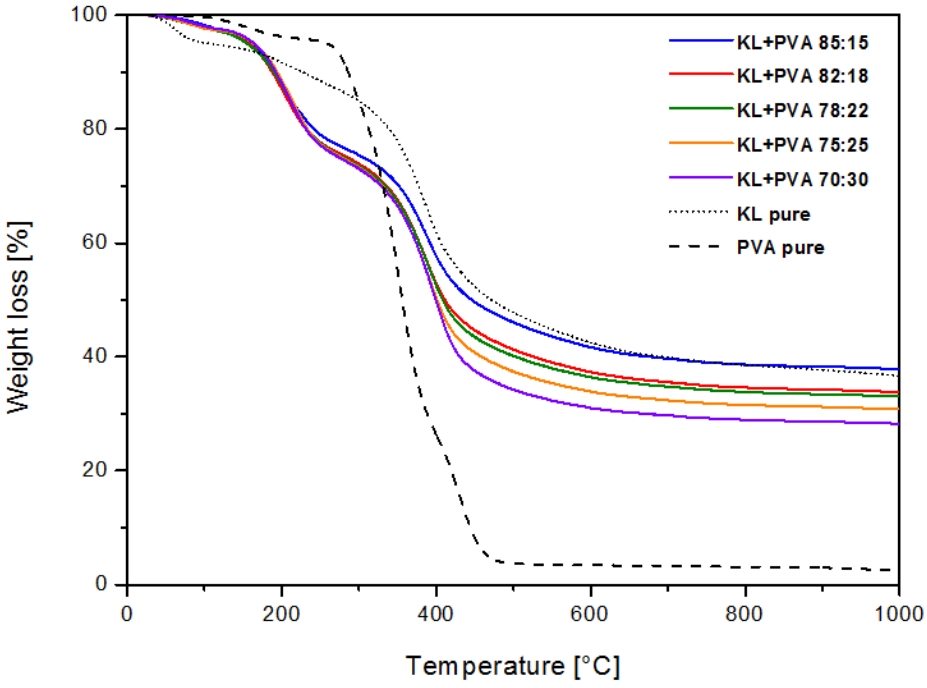

***Figure II-17**: Thermogravimetric analysis of pure KL, pure PVA and KL-PVA fibres in different ratios, heated under nitrogen from 25 °C to 1000 °C at 10 °C min^{-1}*

Table II-4: TGA results of KL-PVA fibres and pure components (heated under N_2, 10 °C min^{-1})

Sample	TGA residue at 1000°C [wt%]
KL-PVA 85:15	37.9
KL-PVA 82:18	33.7
KL-PVA 78:22	33.0
KL-PVA 75:25	30.8
KL-PVA 70:30	28.2
KL pure	36.7
PVA pure	2.4

II.2.4 Structure of Precursor Fibres

Structural characterizations have been performed on as-spun lignin-PVA precursor fibres and on hot-stretched precursor fibres by means of X-ray diffraction (XRD) measurements. The XRD spectra were obtained from a Bruker Nanostar instrument operating at a wavelength of 1.54 Å and measuring under vacuum.

The XRD measurements performed on the precursor fibres demonstrate the orientation of crystalline domains induced exclusively by PVA. As depicted for the reference fibre (black curve in Figure II-20), the obtained peaks of the diffraction pattern after azimuthal integration are wide and of high intensity. This result suggests that the PVA crystallites are only visible throughout the amorphous domains of lignin (70 %), which diffract and thus “dampen”/weaken the signal. A possible structure of the reference fibre as obtained by the XRD measurements is depicted in Figure II-19-b No. 4 on the right side. It becomes clear that the fibres exhibit a poor orientation along the fibre axis. Therefore, the impact of fibre drawing on the molecular orientation of the precursor fibres has been studied.

Hot-stretching of fibres can be described as a drawing process in solid state since it is performed above the glass transition T_g, but below the melting temperature T_m. During the process, the molecular chains within a fibre are typically aligned in the fibre axis (see Figure II-18). The increased temperatures facilitate the structural rearrangement due to a higher molecular mobility. Post-stretching treatments in solid fibres are usually much more effective than stretching of polymer melts or fibres in gel state.[7, 17] In the case of pure PVA fibres, hot-stretching is a common tool to increase the orientation of the linear PVA chains in fibre axis, which usually also leads to an increase in mechanical properties. PVA being a semi-crystalline material, not only the crystalline regions, but also the amorphous parts are considered to be aligned. Typical draw factors for hot-stretched PVA fibres lie within a range of 100-800 % up to more than 1000 %,[18] which drastically improves the alignment of chains and molecular crystals, thus resulting in high-strength fibres. The drawing is usually performed at temperatures above the glass transition (T_g) and below the melting temperature (T_m) of PVA, hence within ranges of 100-200 °C. The T_g and T_m of PVA have been determined from DSC measurements (see Figure II-9). The T_g of the raw material lies at around 75 °C, meaning that the material softens above this temperature due to increased mobility of the amorphous molecular chain fraction. Melting of the crystalline fraction then occurs around 220 °C.

The hot-stretching tests of lignin-PVA precursor fibres within the framework of this thesis were performed at 120-180 °C by means of a Zwick Roell Tensile Testing Machine Z010. The fibres were stretched at 100 % min^{-1} to 100 % of their initial length (e.g. from 20 mm to 40 mm). Hot-stretched KL-PVA fibres have been compared with reference fibres regarding their molecular structure and their mechanical properties (see *chapter II.2.5*).

By means of hot-stretching treatments of the precursor fibres performed at 180 °C, the orientation of crystallites was increased significantly (see Figure II-20, red curve). These results suggest an increased alignment of PVA chains within the stretched fibres, as depicted

in Figures II-18 and II-19-a No. 3. The performed hot-stretching of the reference fibres can thus be considered as reinforcement, since the precursor fibres exhibit a higher orientation along the fibre axis.

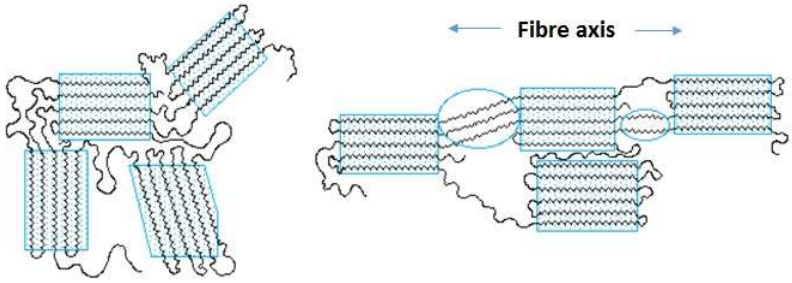

***Figure II-18**: Crystalline- and amorphous domains within PVA fibres: randomly oriented crystals (left) and aligned crystals in fibre direction (right) [from **16**]*

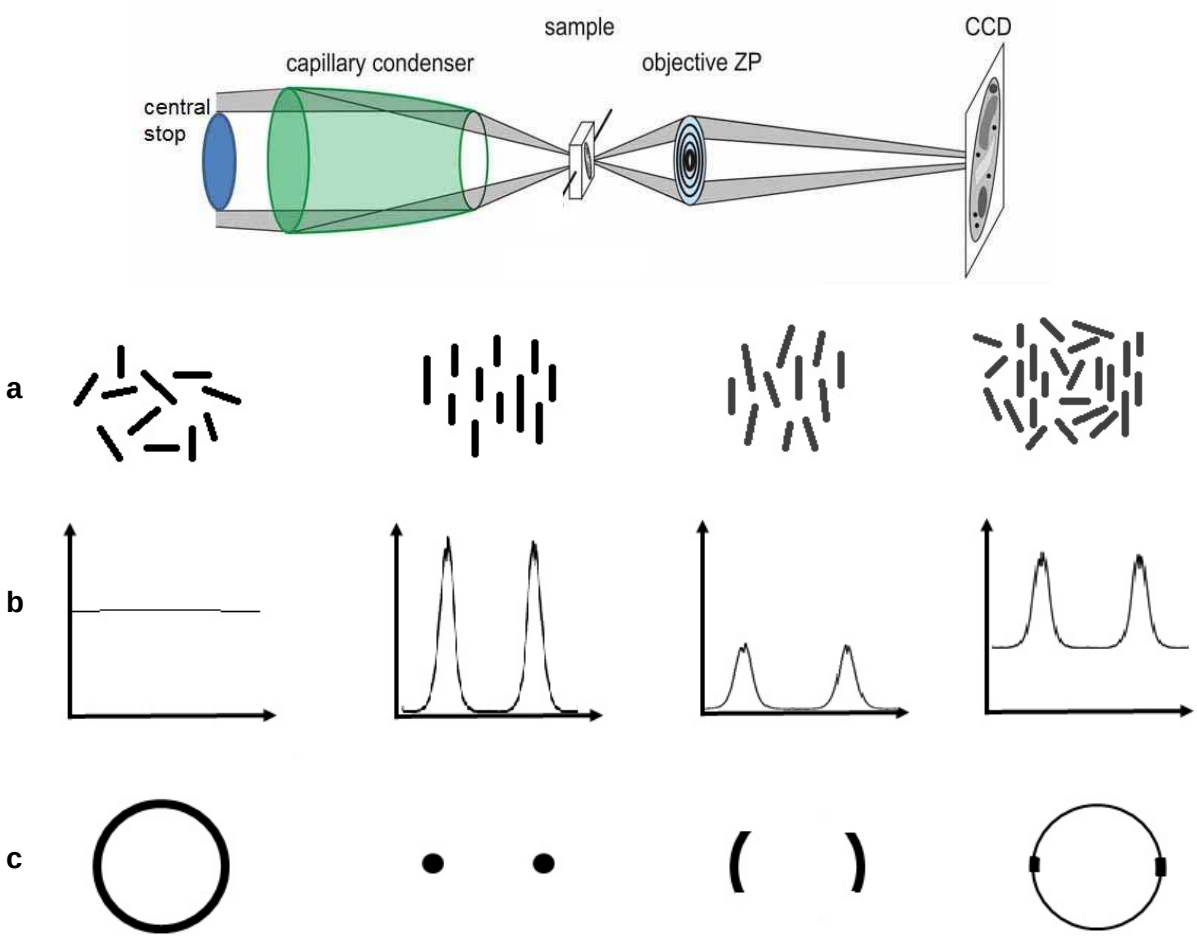

***Figure II-19**: Above: X-ray diffraction setup (from [19]), below: possible crystalline structures within samples (a) with resulting azimuthal integration of the diffraction pattern (b) and resulting image on CCD detector (c)*

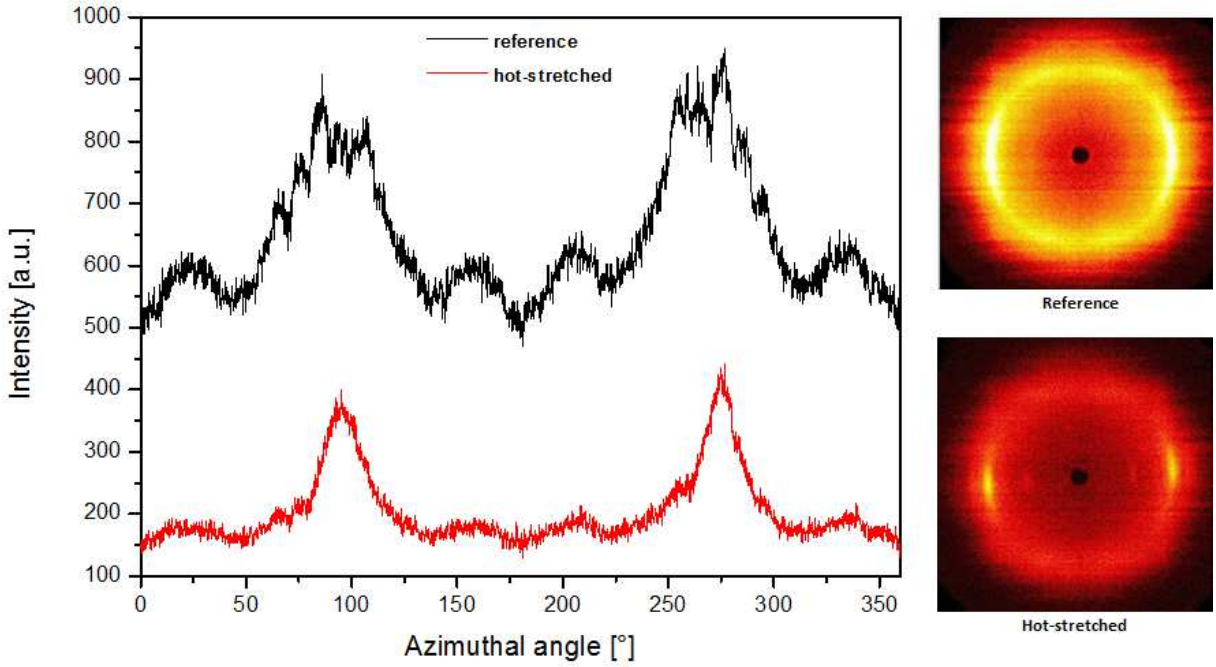

***Figure II-20**: Crystalline orientation of as-spun lignin-PVA precursor fibres (reference curve in black) and of hot-stretched precursors (curve in red). The 2D diffraction patterns were treated by azimuthal averaging over 2-Theta = 0.02-28°.*

II.2.5 Mechanical Properties of Precursor Fibres

Fibres based on lignin are known for rather weak mechanical properties, which is mainly linked to the amorphous structure and low molecular weight of the material. In literature, numerous examples of lignin blend fibres prepared from melt-or wet-spinning exist at rather low lignin ratios (see *chapter I.4*). As a consequence, intermediate up to high mechanical properties have been obtained for the precursor fibres.

The mechanical properties of lignin-PVA monofilaments were measured on a Zwick Roell Z010 tensile testing machine according to ISO 5079. The sample length was 20 mm, strain rate 10 mm min^{-1} or 50% min^{-1} and a preload of 0.05 N was applied prior to testing in order to tighten the fibre inside the clamps. The force at rupture and elongation of the fibre were measured. The cross-section surfaces of the fibres were measured after the test by optical or electron microscopy. The tensile stress was calculated by normalization of the force to the surface cross-section as indicated below and stress-strain curves were obtained. The Young's modulus *Y* was calculated from the slope of the curves between strain values of 0.05-0.25 %.

$$\sigma = \frac{F}{A} \qquad (II\text{-}4)$$

(where σ is the tensile stress, F is the force and A the surface cross-section)

Since the approach of this thesis was to keep high lignin contents within the precursor fibres, the obtained tensile strengths, Young's moduli and elongations at break were found to be rather low. As demonstrated by XRD spectra (see previous subchapter), the amorphous structure of lignin shows a poor orientation along the fibre axis, leading to poor mechanical properties. These properties however were found to improve with increasing PVA contents in a monotonic way (see Figure II-21-a). PVA possesses linear molecular chains and a higher molecular weight than lignin. It thus introduces a certain degree of molecular alignment in fibre axis into the otherwise amorphous structure of the fibres. As it is commonly known, the mechanical properties of polymer fibres increase with increasing degree of orientation. At a fixed lignin-PVA ratio of 70:30, the fibres showed a tensile strength of around 80 MPa and a Young's modulus of around 4 GPa at a fibre diameter of around 80 µm (see Figure II-21-b). At this given ratio, the mechanical properties of the precursor fibres could be further improved by optimization of their processing parameters. For instance with increasing draw ratios, a decrease in diameter from 80 µm to 55 µm could be realized, leading to an increased tensile strength of 150-160 MPa and a higher Young's modulus of around 6 GPa. Through hot-stretching treatments after the spinning process, which typically provoke an alignment of PVA chains (see *chapter II.2.4*), the tensile strength could be increased up to 200 MPa and the Young's modulus up to 6.5 GPa.

Generally, a tensile strength of ≥ 100 MPa for a precursor fibre is considered as sufficient for withstanding a carbonization process. Therefore, the reference fibre KL-PVA 70:30 was chosen for carbonization tests under different conditions and the resulting mechanical properties were compared afterwards. The resulting lignin-based carbon fibres and their properties are presented in *chapter II.4*.

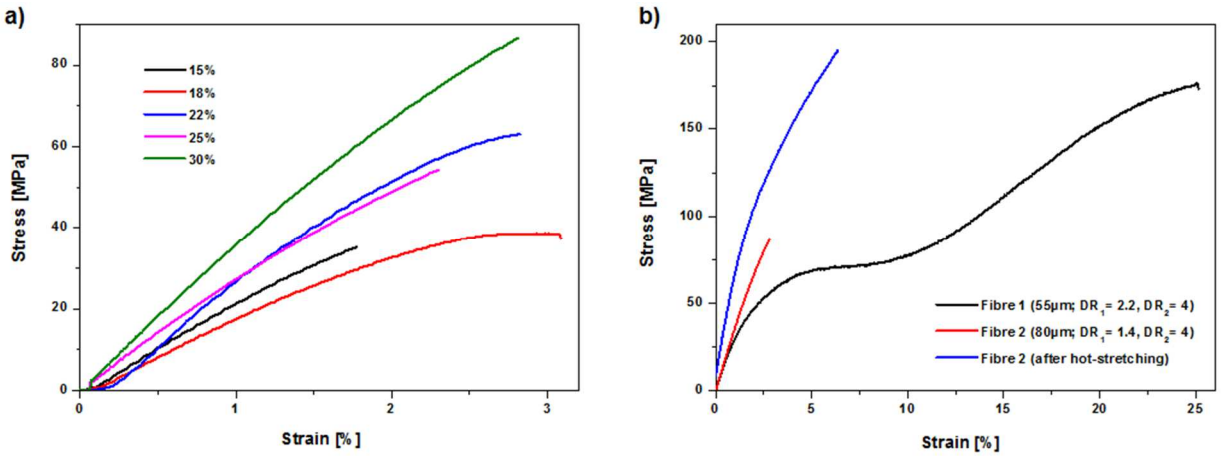

Figure II-21*: Mechanical properties of KL-PVA precursor fibres: increase of tensile strength and stiffness with PVA content (a) and dependency of processing parameters such as draw ratio and hot-stretching on KL-PVA fibres at a fixed ratio of 70:30 (b)*

II.3 Multifilament Spinning Trials – Transfer to Pilot Scale

Commercial polymer fibres typically consist of several hundred filaments combined to a fibre bundle or –strand of 3000-48000 filaments. Conventional carbon fibres made from polyacrylonitrile and pitch are produced as so-called multifilaments prior to combination with polymer resins in composite materials. In literature, a few examples of multifilament spinning are reported for lignin fibres obtained by melt-spinning, wet-spinning and dry-spinning[20–24] (see *chapter I.4*). As shown in *chapter II.2*, the system of softwood Kraft lignin and PVA in DMSO was found to be suitable for continuous fibre spinning by coagulation. The obtained fibres could potentially be used as bio-based precursor for carbon fibres, which is why the upscaling potential of this system has been investigated as well. The transfer to pilot scale is of crucial importance to demonstrate the system's potential for a future large-scale production and implementation in industry.

II.3.1 Setup and Spinning Parameters

The multifilament spinning trials were performed at the Research and Technology Platform CANOE on a pilot wet-spinning line (Fourné Polymertechnik GmbH) with a capacity of up to 500 filaments spun at 30 m min^{-1}. The minimum amount of dope solution needed for one spinning trial was 5-8 litres. Due to a limited amount of softwood Kraft lignin raw material provided from FCBA, commercially available lignin grades had to be chosen in order to produce dope solutions in higher quantities. Softwood Kraft lignin grades were thus purchased from Meadwestvaco (IndulinAT®) and Sigma Aldrich. Due to their extraction from softwood, the structures of these lignin grades were considered as similar to the Kraft lignin grade "KL" (or L16) from FCBA. However, slight differences regarding their solubility in DMSO could still be observed. Therefore, small-scale dissolution experiments of the commercial lignin grades were performed, but the systems were not studied in detail.

Since several litres of dope solution were necessary to perform the spinning trials, the preparation method was simplified and scaled up as well. A solution of PVA 195K (56-98 Mowiol®, Sigma Aldrich) at 6 wt% in DMSO was prepared under strong stirring with a mixer at 90 °C. Once dissolved, the solution was cooled down to room temperature and lignin powder was added directly into the PVA solution up to 14 wt%. The concentrations of the two components were chosen based on the spinning trials presented in *chapter II.2*. Optical microscopy images of used spinning dopes are shown in Figure II-25.

The prepared lignin-PVA dope solutions were filled into a reactor connected to a spinneret, fed by a gear pump. The reactor was first put under vacuum to degas the spinning dope. By increasing the pressure up to 270 kPa (2.7 bar), the spinning dope was then injected through a spinneret of 100 holes (hole diameter 90 µm) into a coagulation bath (40 litres) containing alcohols (ethanol, isopropanol or butanol). After coagulation, the filaments were guided through 1-2 washing baths (also containing alcohols), in between which the filaments were kept under tension and stretched, if possible. Drying of the filaments was performed via an

oven under ventilation at 180 °C. After passing the drying stage, the filaments were wound up onto a bobbin. The principle of the pilot wet-spinning line is depicted in Figures II-22 and II-23.

Substantial differences between the spinning of lignin-PVA multifilaments on pilot scale and monofilament spinning (see *chapter II.2*) were noticed. Observations made before, which did not hinder the process for monofilaments, were amplified on larger scale, thus complicating the multifilament spinning and decreasing the quality of the obtained fibres.

Due to impurities inside the lignin raw material (97 % purity according to data sheet, to be compared with Figure II-25) and possibly undissolved parts inside the spinning dope, the filter placed between the reactor vessel and the spinneret got blocked very easily. Upon injection, these particles blocked the access to the spinneret after some time, thus breaking the fibre during the spinning process. Besides, a suitable counter-solvent was found crucial for the coagulation stage since the filaments need to be resistant enough to reach the end of the spinning line (4-5 meters). Isopropanol and butanol were found to be the most suitable solvents for coagulation, since the injection was stable over the whole time period of the trial. The washing baths were found to be an important tool to keep the filaments flexible and elastic before the drying stage, also to perform drawing in wet state. Mostly isopropanol and butanol were used for washing.

Another crucial factor for fibre spinning on larger scales was the long-term stability of the dope solution. As already mentioned in *chapter II.1*, the lignin-PVA dope solutions formed a gel at high concentrations over time. The dope solution of 21 wt% Kraft lignin (Aldrich) and 9 wt% PVA195K (see Figure II-25) formed a gel overnight inside the reactor and the pipes, hence blocking the spinneret. Removing and re-dissolving of the gel caused a high cleaning effort and delayed the spinning process.

During the spinning trials, the influence of several different spinning parameters on the obtained multifilaments was tested. In addition to the fact that two different lignin grades were used, the following parameters were varied: dope concentration, counter-solvents for coagulation- and washing, injection speed and dope temperature. The quality of the obtained multifilaments was evaluated mostly by scanning electron microscopy.

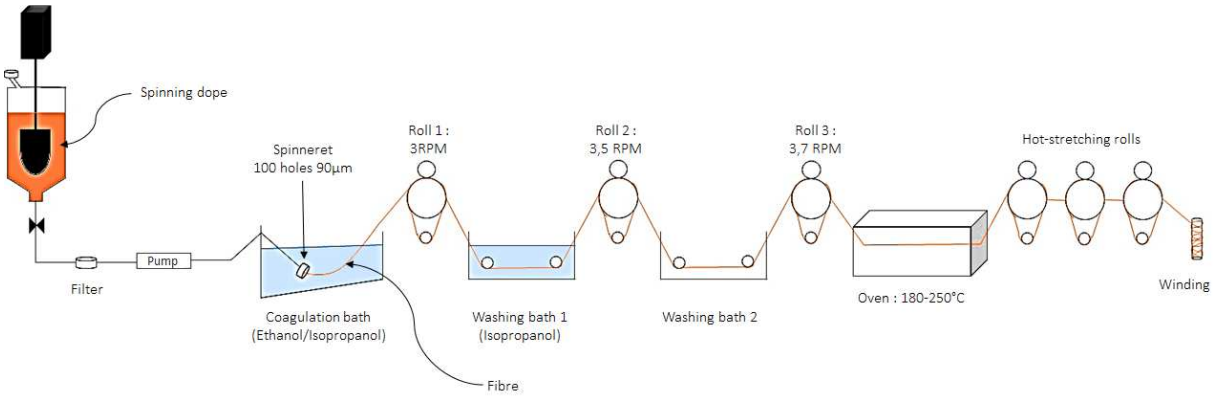

***Figure II-22**: Principle of continuous wet-spinning line on pilot scale*

As shown in the SEM images, a variation of the dope injection towards higher speeds led to more distinct filaments (see Figure II-24-a compared to II-24-b), which could be related to a faster coagulation of each single filament. However, an increase of the dope temperature at high injection speeds led to partial adhesion of the filaments towards the outer layers of the strand. This result could be related to the fact that the temperature gradient between dope solution and coagulation bath was too high ("collapsing" of the filaments on the outside). Upon injection into cold coagulation baths and thus even higher gradients, the effect was found amplified since all the filaments were found attached to each other into a thick strand showing extremely high brittleness.

The viscosity of the spinning dope depending on shear and temperature was characterized by rheology measurements (see Figure A-II-2 in appendix). The lignin-PVA dope solution showed shear thinning behaviour and a strong viscosity decrease with increasing temperature. The viscosity of the dope solutions being high at room temperature (3.5 Pas at 10 s^{-1}), the spinning at a dope temperature of 70 °C has been tested to facilitate its flow (0.5 Pas at 10 s^{-1}) and to study the impact on the resulting filaments (see Figure II-24-c). However, a decreased viscosity upon heating of the dope was not found to have an impact on the spinning performance.

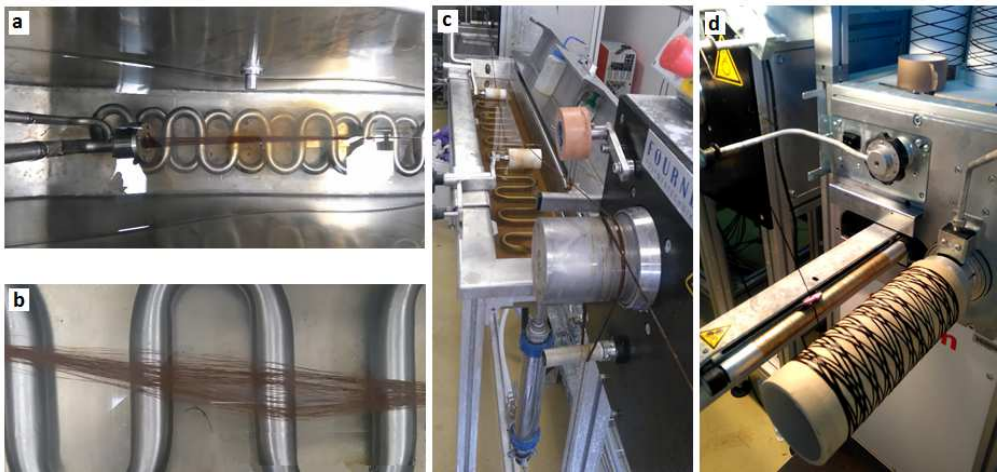

***Figure II-23**: Coagulation bath and obtained lignin-PVA multifilaments in wet state (a+b), washing bath (c) and wound-up dried multifilaments (d)*

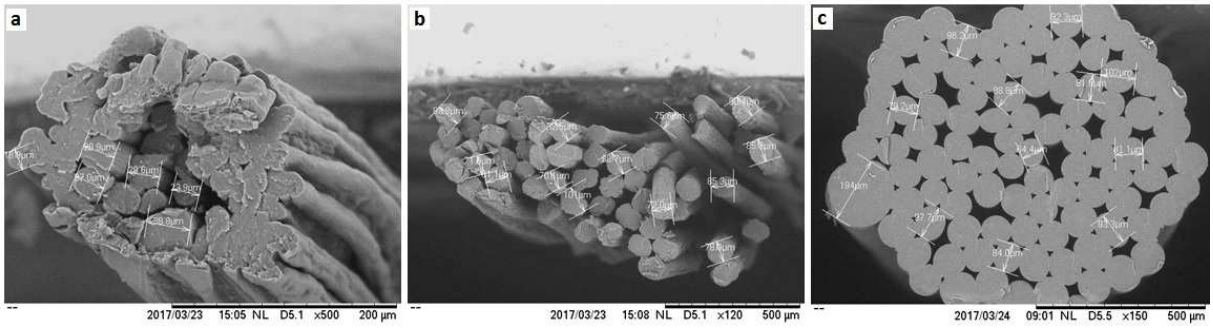

***Figure II-24**: SEM micrographs of Aldrich Kraft lignin-PVA 195K (70:30) multifilaments: low injection speed under room temperature (a), high injection speed under room temperature (b) and high injection speed at 70°C (c)*

II.3.2 Optimization of Spinning Process

Based on the problems encountered, tests on smaller scale were performed between several series of spinning trials in order to adapt the spinning parameters and improve the filament properties. The system-related challenges mainly include the leaching of lignin and the separation of single filaments.

- Lignin Leaching

Leaching describes the diffusion of lignin into the coagulation- or washing baths due to a partial solubility. At high rates, this behaviour may lower the lignin concentration inside the filaments and block the coagulation process. Suitable counter-solvents normally hinder leaching effects. However, due to a high polydispersity index of lignin (see *chapter I.1*), high molecular weight fractions may be insoluble inside a given solvent, whereas low-molecular weight fractions may dissolve. To prevent the dissolution of low-molecular weight fractions, alcohols of higher molecular weights were considered for coagulation (e.g. change from isopropanol to butanol). Besides, purification or fractionation of the lignin raw material and thus removal of these fractions prior to dissolution in DMSO could decrease the leaching effect. Washing of lignin with low molecular weight alcohols (e.g. ethanol) or filtration of the lignin solution are possible approaches.

On the other hand, pure alcohols like isopropanol or butanol may still possess partial solubility with lignin, given the fact that they are polar solvents. During dissolution tests at smaller scale, other counter-solvents have been found which dissolve less lignin or none at all. These include, but are not limited to: 2-ethyl-1-hexanol, diethyl ether, cyclopentane and other nonpolar solvents. Due to their elevated prices however, they should rather be combined with e.g. isopropanol in mixtures of 50:50 for the coagulation bath in order to keep the processing costs as low as possible (volume of coagulation bath: 40 litres; solvent prices Sigma Aldrich: isopropanol 26 € l^{-1}, diethyl ether 38 € l^{-1}, cyclopentane 180 € l^{-1}). Besides, the toxicity of solvents regarding health and safety should generally be considered for large-scale spinning applications.

Optical microscopy images of the spinning dopes containing IndulinAT® Kraft lignin and PVA195K revealed a high amount of undissolved parts which appear at a certain concentration threshold. It is possible that above this threshold, lignin starts to precipitate from the dope because the solubility limit (e.g. induced by the presence of PVA) is reached (here: 8 wt% of lignin and 6 wt% of PVA, but also happens for pure lignin solutions at ≥ 30 wt%). In theory, this insoluble fraction could then diffuse from the filaments into the counter solvent upon contact.

However, both approaches – purification of lignin and use of different counter solvents – drastically increase the spinning costs and thus need to be considered carefully.

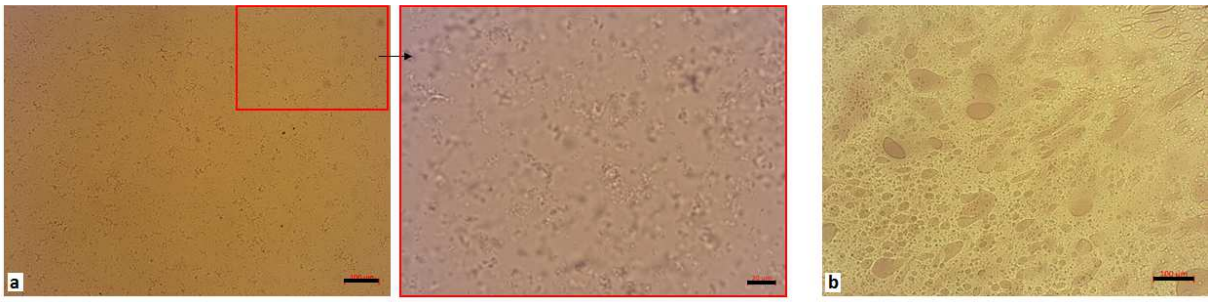

***Figure II-25**: Optical microscopy images of spinning dopes for multifilament trials: IndulinAT®+PVA195K (14wt%+6wt% in DMSO) forming a "network", scale bars 100µm and 20µm (a) and Aldrich Kraft lignin+PVA195K (21wt%+9wt% in DMSO) re-dissolved after gel formation, scale bar 100µm (b)*

- Separation of Filaments

Multifilaments of small diameters (5-30 µm) combined to a fibre strand are usually produced in order to facilitate the manipulation and to amplify the mechanical properties compared to monofilaments of larger diameter. A crucial condition for this amplification however is that the filaments are separated and thus can "act" individually. One of the challenges in multifilament spinning is thus the simultaneous coagulation of hundreds of filaments without them sticking together at any moment during the production process. The two most important stages regarding the separation of single filaments are the coagulation- and drying process.

In order to assist the coagulation process, aqueous solutions of sodium tetraborate salt ($Na_2B_4O_7$) and boric acid (H_3BO_3) were tested for coagulation and/or washing of the filaments. Sodium tetraborate, also called "Borax" is commonly used to reinforce PVA fibres through cross-linking. However, upon contact with the solutions, the filaments seemed to soften and partially dissolve. This observation was also made when the lignin-PVA filaments were brought in contact with pure water right after coagulation. Possible reasons for these observations could lie in the composition of the fibres. It is possible that DMSO was not fully removed from the fibres during coagulation/washing due to a low solubility of DMSO in isopropanol and/or butanol. This hypothesis is supported by TGA results (high weight loss at the boiling point of DMSO) and a high flexibility of the precursor fibres (DMSO residues acting as plasticizer). DMSO is a highly hygroscopic solvent. As a consequence, it is possible that the DMSO residues inside the filaments could attract water from the Borax- and boric acid solution. The diffusion of water into the filaments could thus be responsible for a weakening of PVA, which would explain the softening and rupture of the filaments. In this case, the attraction of water by DMSO would be higher than the cross-linking reaction between PVA and boric acid.

During the course of the spinning trials, it became clear that the lignin-PVA-DMSO system should not be brought in contact with water at any time before drying since it weakens the filaments. As a consequence, further tests should be performed using boric acid solutions based on alcohol. In concentrations of up to 4 wt%, the acid has been found miscible with butanol. A coagulation in butanol could hence be reinforced by cross-linking of PVA through the acid. Used for coagulation and/or washing, this system could lead to a better filament

separation and also prevent lignin leaching and poor mechanical properties of the resulting fibres at the same time.

Another approach to separate the filaments in a better way could be an optimization of their drying process. The temperatures and the duration of the drying process have been varied to study their impact on the filament quality. As shown by SEM images, the best result regarding separated filaments was obtained with a fast drying process at ≥ 180 °C directly after coagulation and washing (see Figure II-26-b). At lower temperatures, DMSO residues were not removed sufficiently, which led to adhesion of the filaments. Similarly, a long drying process over 24 h at room temperature provoked adhesion (see Figure II-26-a) and even direct drying at 180 °C with subsequent storage at 30 °C for 2 days led to adhesion of once separated filaments (see Figure II-26-c). These results indicate that the DMSO removal had not been successful before. Ideally, the drying of the filaments should thus happen around the boiling temperature of DMSO (189 °C) over a long time, which could not be realized within the framework of this thesis due to limitations of the setup. However, a possible solution for the filament drying on larger scale could be an integration of the carbonization process right after the precursor spinning.

The draw-ratios applied during spinning were also found to influence the filament separation. Tendencies could be observed that the filaments became more distinct with increasing draw ratios. Besides, high draw-ratios are generally advantageous for the precursor spinning in order to obtain small diameters and increased molecular orientation along the fibre axis. During our spinning trials, it was possible to decrease the diameter of the filaments to 50 µm. The aim would be to reach diameters of 15 µm (as for commercial precursors) since thinner filaments would lead to higher mechanical properties after carbonization.

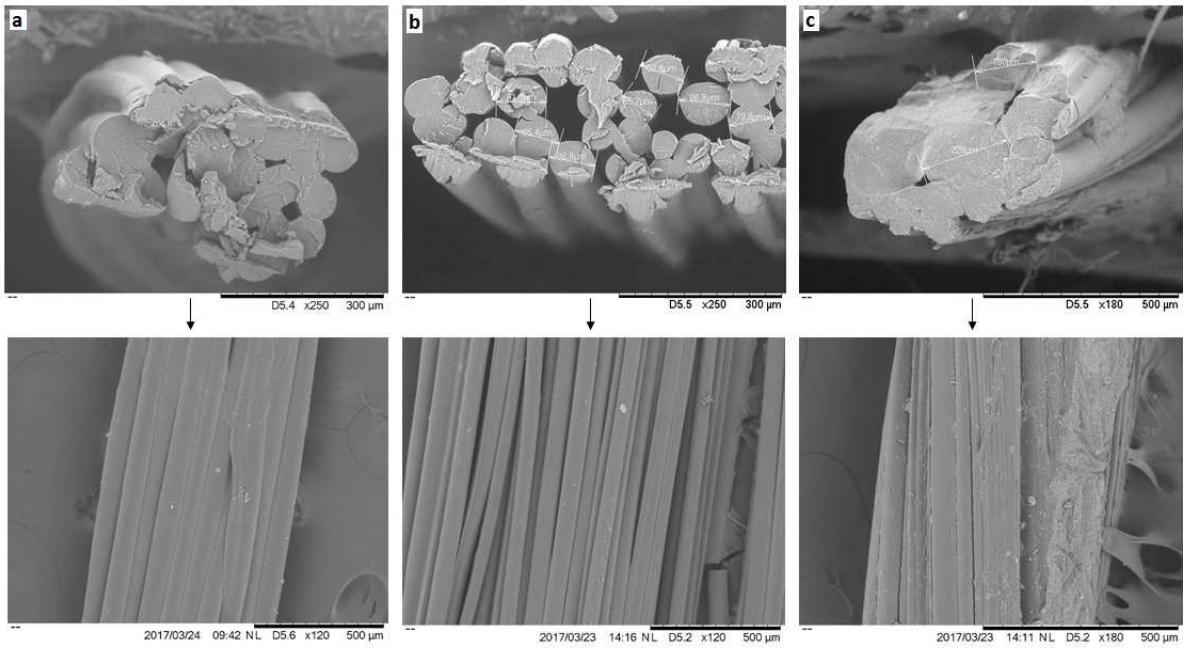

***Figure II-26**: Cross-sections and surfaces of lignin-PVA multifilaments dried under different conditions: drying for 24h at room temperature (a), direct drying at 180°C (b) and direct drying at 180°C + drying at 30°C for 2 days (c)*

II.4 Carbonization of Lignin-Polyvinyl Alcohol Precursor Fibres

After the wet-spinning of lignin-PVA precursor fibres and their characterization, the carbonization process represents the final stage within the development of lignin-based carbon fibres. The process itself as well as the resulting structure and properties of lignin-based carbon fibres are presented in this subchapter.

II.4.1 Optimization of Carbonization Process

The thermal properties of precursor fibres are directly linked to their behaviour during the subsequent carbonization process. Therefore, it is necessary to perform thermogravimetric measurements of the precursor fibres (see *chapter II.2.3*) in order to evaluate their degradation process and to define an adapted temperature program for carbonization. Based on the derivative of the obtained TGA graph for the precursor fibre lignin-PVA 70:30, a tailor-made temperature program was designed for the carbonization of this specific fibre (see Figure II-27). At the respective temperature ranges where high mass losses occurred, the heating rates were either decreased or isotherms were integrated into the carbonization treatment. Besides, the effect of thermo-oxidation under air at up to 250 °C on the fibre morphology was investigated. Possible pathways for an adapted carbonization program are shown in Figure II-27-b (blue line or blue + green line).

The proposed temperature programs have been tested by means of TGA measurements under inert atmosphere, simulating a carbonization process on the precursor fibre “IndulinAT®-PVA 195K” at a ratio of 70:30. The highest value of the TGA residues was considered as best result, given the fact that the smallest weight loss corresponds to the “heaviest” obtained carbon. A heavier residue implies less porosity and a dense structure within the sample, which theoretically represents carbon of high quality. Moreover, high carbon residues (and hence high carbonization yields) are desired in industry since the process is aimed to be as economical as possible. A list of the TGA measurements performed on a TGA 5500 instrument under argon and under air (light blue fields) with the corresponding carbon residues is given in Table II-5.

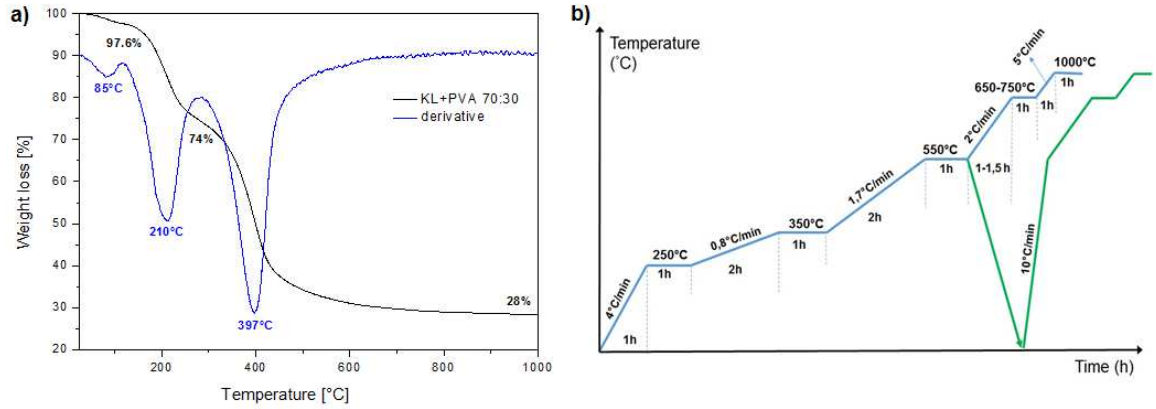

***Figure II-27**: Possible tailor-made temperature programs for carbonization of KL-PVA 70:30 (right) based on derivative of weight loss as a function of temperature (blue line, left).*

Table II-5: Conditions and results of TGA performed on IAT-PVA195K 70:30 precursor fibres (fields marked in light blue correspond to measurements under air)

Stabilisation				Carbonisation			TGA Residue (%)
N°	Heating Rate (°C min^{-1})	Temperature (°C)	Duration (h)	Heating Rate (°C min^{-1})	Temperature (°C)	Duration (h)	
1	5	300	0	5	1000	1	**33.5**
2	1	300	0	5	1000	1	**33.6**
3	1	300	0	5	1000	1	**37.6**
4	3	300	0	5	1000	1	**36.5**
5	3	250	0	5	1000	1	**33.5**
6	3	200	0	5	1000	1	**33.1**
7	1	250	0	5	1000	1	**34.5**
8	3	250	1	5	1000	1	**37.2**
9	1	300	1	5	1000	1	**39.5**
10	2	300	1	5	1000	1	**39.5**
11	2	300	1	10	1000	1	**39**
12	2	300	1	2	1000	1	**43**
13	1	250	1	5	1000	1	**37.5**
14	5	300	1	5	1000	1	**39**
15	4	300	1	5	1000	1	**40.4**
16	2	300	1	2+5	550+1000	1	**44.1**
17	2	330	1	5	1000	1	**42.7**

According to the results given in Table II-5, the highest carbon residues were obtained with the following temperature program:

- **stabilization under air**: heating to 300 °C at 2 °C min^{-1} + 1 h isotherm at 300 °C
- **carbonization under argon**: heating to 550 °C at 2 °C min^{-1} + heating to 1000 °C at 5 °C min^{-1} + 1 h isotherm at 1000 °C

Due to simplicity, this program was chosen over the one proposed in Figure II-27-b. It has been used for the carbonization processes of all lignin-PVA precursor fibres presented in this subchapter. The fibres were first attached with carbon-based glue to a graphite frame and afterwards they were subjected to the stabilization- and carbonization stage under tension, fixed by the glue and the frame. A fibre deformation (shrinkage or expansion) during carbonization was thus avoided by the attachment to the frame. Besides, it has been shown in literature that thermal pyrolysis under tension leads to higher molecular orientation along the fibre axis.[3] However, by using the graphite frames, the applied tension could not be controlled.

Stabilization under air is known to be an important tool to improve the quality of the obtained carbon. Table II-5 shows that the residues at 1000 °C after a stabilization under air are much higher than those after a stabilization under argon. This could indicate a cross-linking process happening under air between 100-300 °C, thus reinforcing the fibre for the subsequent

carbonization step by formation of additional carbonyl and carboxyl groups[25] (see *chapter I.3.2*). As a consequence, a slow oxidative stabilization process might also lead to lower porosity on the fibre surfaces. Due to its amorphous and branched structure, lignin bears disordered and porous carbon structures. During the thermal treatment, water and gases such as methanol, methane and carbon oxides are removed from the fibres, possibly leading to pores within the structures.[3] Although stabilization is not necessary to obtain carbon fibres from softwood lignin (due to a higher cross-linking degree compared to other lignin grades, see *chapter I.1.2*), the treatment can still significantly improve the fibres' properties and decrease their porosity. Another approach to decrease porosity is to remove metals, volatile organic compounds and impurities (e.g. ash) in advance from the precursor fibres before they can create pores during carbonization.[21] The porosity of a fibre can be characterized by X-ray scattering measurements at small angles (SAXS). However, the investigation is very complex and difficult to evaluate.

The thermal reactions of lignin during stabilization and carbonization have been investigated by Brodin et al.[25], Norberg et al.[26] and Olsson et al.[21]. At first, physically adsorbed water is removed from the material, which is followed by the formation of ketones and double bonds in dehydration reactions. Afterwards, numerous radical reactions lead to a molecular rearrangement and further removal of water and hydrogen from lignin,[26] resulting in a "pure" carbon structure (see Figure II-28-f). As can be recognized from SEM images, the optimized temperature program for the carbonization process led to lignin-based carbon fibres with less porosity on the fibre surface (see Figure II-28-a-d). Besides, the cross-sections of carbonized fibres were found to exhibit the same shape as the precursor fibres (bean-shaped or round).

Elemental analysis (EDS) of precursor- and carbon fibres was performed on images taken by a scanning electron microscope Jeol 6700F. As also shown in Figure II-28-e and -f, the EDS performed on the obtained images revealed a carbon content of 98 % after carbonization, indicating a very high purity.

In order to define a final carbonisation program, a compromise between high carbonization yields and good macroscopic properties (porosity, mechanical properties) needs to be found. Due to a high complexity and limited time, these investigations have not been performed within the framework of this thesis.

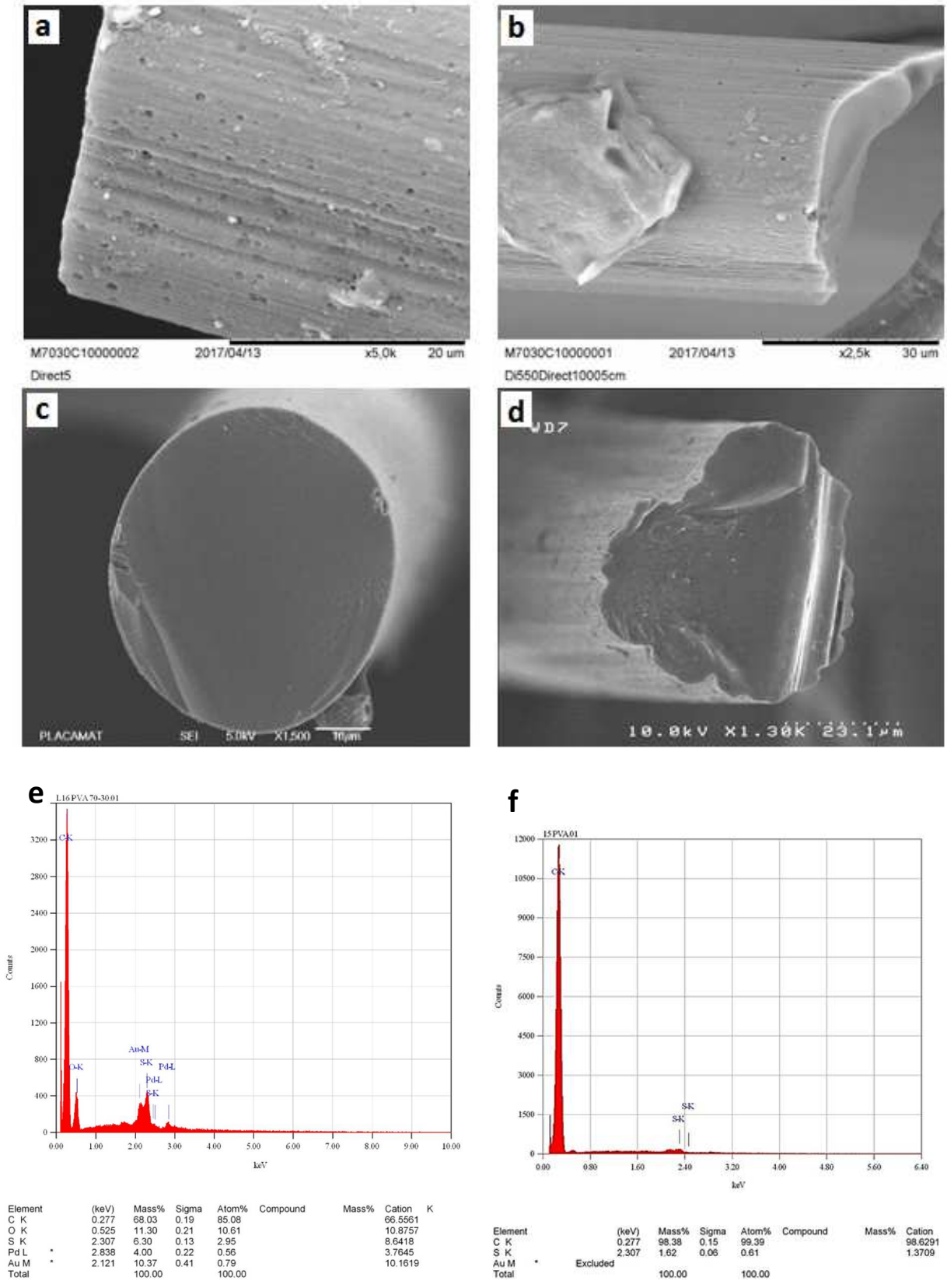

***Figure II-28**: SEM images of lignin-based carbon fibres: directly carbonized with stabilization at 250 °C (a, c), carbonized with tailor-made temperature program (b, d) and EDS analysis of precursor fibre (e) and carbon fibre (f)*

II.4.2 Structure of Lignin-Based Carbon Fibres

The structure of the obtained carbon fibres based on Kraft lignin and PVA was investigated with X-ray diffraction and Raman spectroscopy measurements. X-ray diffraction spectra were obtained from a Bruker Nanostar instrument operating in transmission mode at a wavelength of 1.54 Å (copper cathode) and measuring under vacuum. Raman spectroscopy was performed on carbonized samples by using an Xplora instrument from HORIBA Scientific. The used incident wavelength was 532 nm with a filter of 10 %. Before a measurement series, calibration was performed with HOPG (Highly Oriented Pyrolitic Graphite). On the fibre cross-sections, both the core- and skin zones have been analysed with Raman spectroscopy, revealing very similar spectra, which indicated homogeneous samples. In order to facilitate the measurements, the spectra presented in Figure II-29-b have been obtained from the fibre surfaces.

After carbonization of different precursor fibre samples at different temperatures, their resulting carbon structures were compared. A very disordered carbon structure was revealed through XRD- and Raman spectroscopy measurements (see Figure II-29). The obtained structure is a result of the amorphous nature of lignin, which is conserved during the carbonization process while PVA has disappeared (to be compared with *chapter II.2.4*). The XRD spectra do not show any distinct peak, but a very broad signal between 20-25°, corresponding to a disordered carbon structure independent of the temperature treatment from 250-1000 °C (see Figure II-29-a). The disordered carbon structure of lignin fibres heated to ≤ 1200 °C has also been reported in literature.[20, 27]

Up to 1000 °C, the D- and G-bands of the Raman spectra (see Figure II-29-b) were found similar in intensity, indicating a carbon structure with defects[27], which is in agreement with the obtained XRD results. Only after treatment at very high temperatures starting from 1500 °C, the peak widths for the D- and G-bands start to decrease with increasing temperatures. This trend indicates an increasing order within the carbon structure. Moreover, the G'-band appears in the Raman spectra. This band is typical for graphitic structures, which thus shows that lignin-based carbon can be somewhat ordered only at rather high temperatures due to structural rearrangement. More detailed investigations on amorphous carbon structures and their characterization by means of Raman spectroscopy have been performed by Ferrari & Robertson.[28]

Moreover, electrical conductivity measurements with a multimeter (Keithley 2000) were performed in order to indirectly assess the carbonization at different temperatures. The increase in electrical conductivity indicates an increased formation of sp^2 hybridized C-atom domains with increasing temperatures (see Figure II-30). This result is in agreement with the results obtained from Raman spectroscopy (see Figure II-29-b).

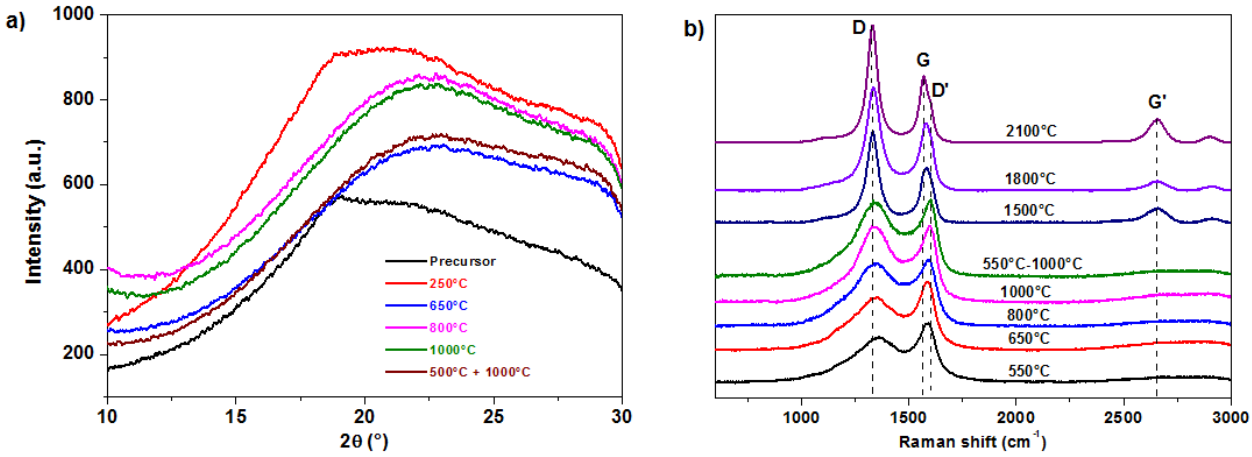

***Figure II-29**: Crystalline structure of lignin-based carbon fibres investigated by XRD (a) and Raman spectroscopy (b).*

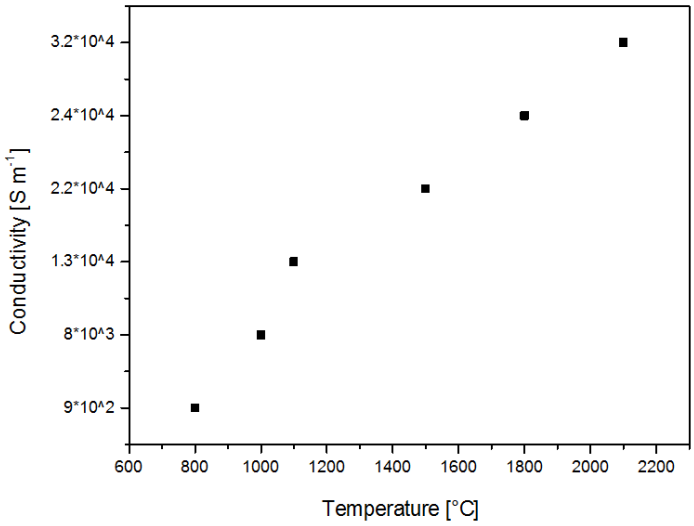

***Figure II-30**: Electrical conductivity of lignin-based carbon fibres after carbonization at different temperatures*

II.4.3 Mechanical Properties of Lignin-Based Carbon Fibres

The mechanical properties of the carbonized fibres were determined with a Zwick Roell Z2.5 tensile testing machine. The monofilament samples were glued onto paper frames in order to protect them from breaking during insertion into the clamps. The length of the samples was 20 mm and the frames were cut open directly before the measurement, in order to pull only on the fibres. The applied strain rate was 1 mm min^{-1} and no preload was applied due to a high fibre rigidity.

The precursor fibres were stabilized at 300 °C (2 °C min^{-1} + 1 h isotherm) and carbonized at 1000 °C (+ 1 h isotherm) with an increase in heating rate from 2 °C min^{-1} to 5 °C min^{-1} at 550 °C. Comparing the mechanical properties of precursor-, stabilized- and carbon fibres, it can be recognized that the mechanical properties increased through carbonization, while they did not change through stabilization (see Figure II-31-a). Besides, a dependency between the

fibre diameter and its resulting properties became evident. With smaller diameters, fibres generally became stronger (see Figure II-31-b). This relationship could be due to a higher surface-to-volume-ratio for thinner fibres and a higher amount and size of critical defects in thicker fibres, which can weaken their mechanical properties.[21]

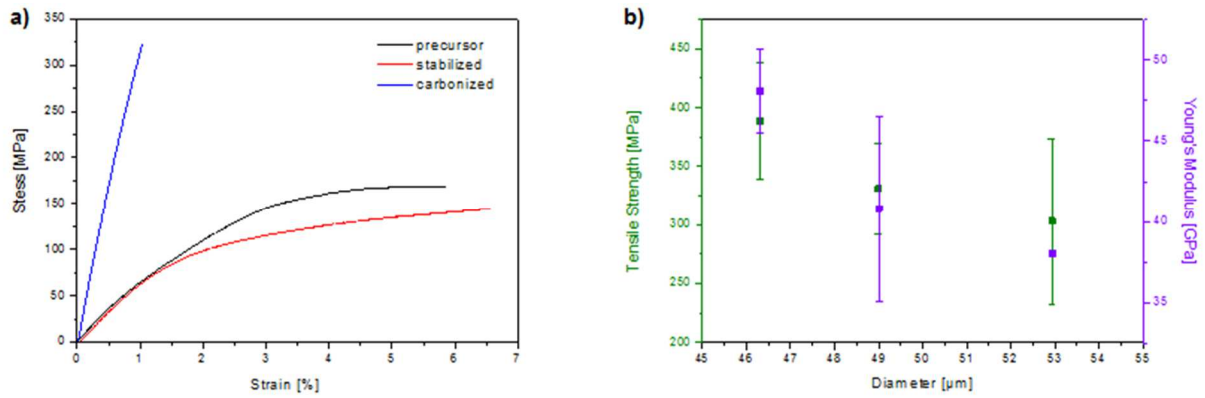

Figure II-31 *: Stress-Strain curves of lignin-based precursor-, stabilized- and carbon fibres (a) and relationship between carbon fibre diameter and obtained mechanical properties (b)*

Another study was performed in which the reference fibre KL-PVA 70:30 was carbonized under different conditions and the resulting mechanical properties were compared afterwards. A direct heating process to 1000 °C at 5 °C min^{-1} was compared to another process to which a stabilization under oxygen at 250 °C has been added. The third process within the comparison is the tailor-made carbonization program, which was called “complex”. As shown in Figure II-32, the thermo-oxidative stabilization alone did not significantly improve the mechanical properties of the reference fibre carbonized without stabilization (black curve vs. red curve). However, an entire adaptation of the carbonization program to the degradation behaviour of the fibre (see Figure II-27, blue and green lines) clearly led to improved mechanical properties (tensile strength: 351 ± 108 MPa and Young’s modulus: 44.5 ± 9.6 GPa for a fibre mean diameter of 37 µm). Through an optimized carbonization program, the porosity and amount of defects inside the carbon fibres potentially gets reduced, which consequently leads to higher mechanical strengths.

Overall, the obtained mechanical properties of the carbon fibres remained rather weak (see overview in Table II-6), mainly due to the amorphous molecular structure of lignin and a high degree of porosity induced during the carbonization process. However, there is still room for improvement on the processing conditions of the precursor fibres presented in this thesis. As shown in chapter *II.2.5*, an improved processing of the precursor fibres directly increases their mechanical properties, thus it should also improve the properties of the resulting carbon fibres.

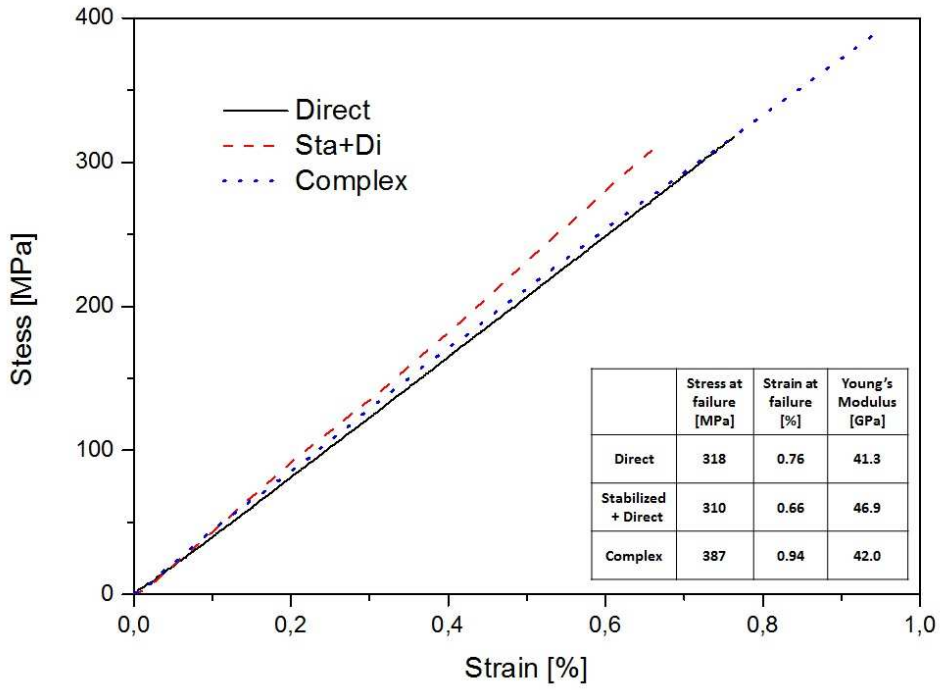

***Figure II-32**: Stress-Strain curves of lignin-based carbon fibres obtained with different carbonization temperature programs*

Table II-6: Summary of obtained mechanical properties of precursor fibres, stabilized fibres and carbon fibres

Sample	Tensile Strength [MPa]	Strain [%]	Young's Modulus [GPa]	Mean diameter [µm]
Precursor (L-PVA 70:30)	154 ± 25	4.8 ± 1.0	6.09 ± 0.99	67 ± 4
Stabilized 250°C (air)	112 ± 32	5.0 ± 1.8	5.63 ± 1.44	75 ± 13.
Heated to 1000°C (no stab.)	304 ± 58	0.8 ± 0.2	40.6 ± 7.4	41 ± 8
Stabilized at 250°C + 1000°C	336 ± 149	1.1 ± 0.4	36.2 ± 11.0	48 ± 11
Stabilized at 250°C + 550°C + 1000°C (5°C min^{-1})	331 ± 39	0.9 ± 0.2	40.8 ± 5.7	49 ± 9
Stabilized at 250°C + 550°C + 1000°C (complex)	351 ± 108	0.9 ± 0.3	44.5 ± 9.6	37 ± 10

Another possibility to improve the mechanical properties of the obtained lignin-based carbon fibres could be graphitization. As has been demonstrated by Raman spectroscopy results (see Figure II-29-b), graphitic structures start to be formed within the carbon fibres at temperatures ≥ 1500 °C. This change in structure can also lead to increased mechanical properties, especially to increased Young's moduli.

Usually, fibres comprised of several hundred filaments of a small diameter acting together within a fibre strand exhibit higher mechanical properties compared to monofilaments of larger diameters. Besides, the handling of a multifilament strand during processing is easier than for monofilaments. Lignin-PVA multifilaments have successfully been spun within the framework of this thesis (see *chapter II.3*). However, due to the lack of an optimized spinning setup, the multifilaments were found to adhere between each other after complete drying of the filaments. Therefore, the mechanical properties of the precursor fibres were found to be rather weak, since all the filaments behaved as one single fibre of a giant diameter.

Carbonization trials of some of the multifilaments of IAT-PVA195K 70:30 were still performed in order to study their behaviour during the process. Carbonization was performed under nitrogen in a static carbonization oven (Nabertherm) and the multifilaments were inserted vertically so that they were subjected to the high temperatures in hanging state. To equilibrate the fibre shrinkage, a small weight corresponding to the maximum force demonstrated during tensile testing was attached to one fibre end, whereas the other end was fixed at the entrance of the oven (see Figure II-33). As shown by the SEM images in Figure II-33, the multifilaments did not separate from each other during carbonization. Except a slightly decreased diameter, only the high porosity on their surface clearly identifies the carbonized samples. Given the high brittleness of the obtained multifilament carbon fibres, they could not be tested in terms of mechanical strength.

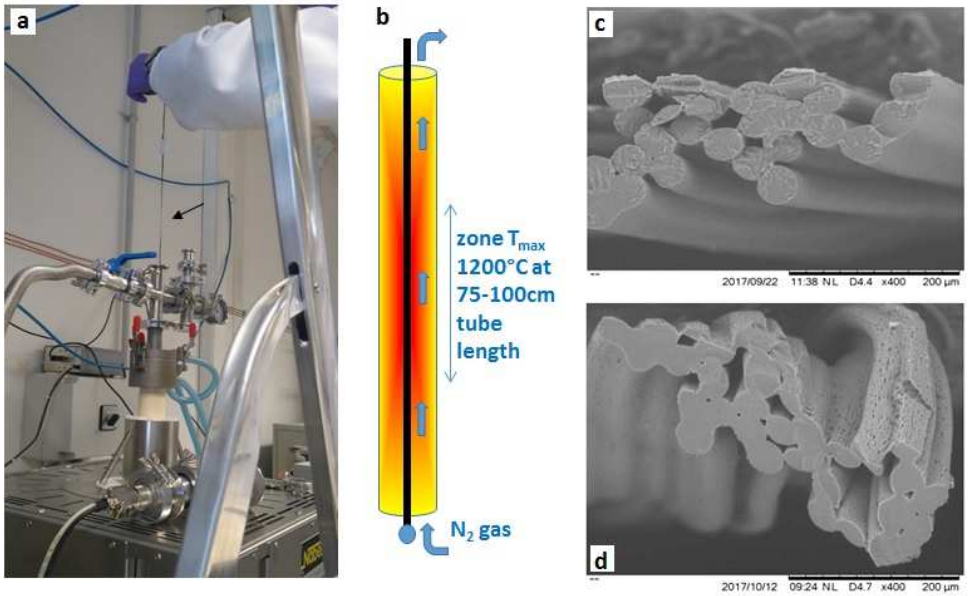

***Figure II-33**: Insertion of precursor fibre into static carbonization oven (a), schematic representation of oven (b) and SEM images of IAT-PVA195K 70:30 multifilaments before (c) and after carbonization (d), scale bars 200µm*

II.5 Conclusion

Lignin-polyvinyl alcohol (PVA) precursor fibres have been successfully prepared by a simple and economical wet-spinning process. An upscale from manual spinning on laboratory scale and continuous spinning of monofilaments on intermediate scale to multifilament spinning on pilot scale has been performed. The spinning trials on pilot scale have been performed with a commercially available lignin grade. The obtained results have shown that the two polymers lignin and PVA are only partially miscible in solution and that they form metastable states within solid blend films and -fibres. Precursor fibres containing a Kraft lignin-PVA ratio of 70:30 have been spun continuously under optimized processing conditions. Their mechanical properties were found suitable for the carbonization stage. By means of thermogravimetric results, a tailor-made temperature program has been created, bearing lignin-based carbon fibres with tensile strengths of up to 400 MPa and Young's Moduli of 50 GPa. The globally still low mechanical properties have been found due to a disordered carbon structure within the fibres because of the amorphous nature of the lignin precursor. Different approaches to further improve the structure and mechanical properties of the carbon fibres include graphitization and incorporation of carbonaceous liquid crystalline particles inside the precursor fibres. The latter is presented and evaluated in *chapters III* and *IV*.

References

[1] J. Zakzeski, P. C. A. Bruijnincx, A. L. Jongerius, and B. M. Weckhuysen, 'The Catalytic Valorization of Lignin for the Production of Renewable Chemicals', *Chem. Rev.*, vol. 110, no. 6, pp. 3552–3599, Jun. 2010.

[2] J. Sameni, S. Krigstin, and M. Sain, 'Solubility of Lignin and Acetylated Lignin in Organic Solvents', *BioResources*, vol. 12, no. 1, pp. 1548–1565, 2017.

[3] W. Fang, S. Yang, X.-L. Wang, T.-Q. Yuan, and R.-C. Sun, 'Manufacture and application of lignin-based carbon fibers (LCFs) and lignin-based carbon nanofibers (LCNFs)', *Green Chem*, vol. 19, no. 8, pp. 1794–1827, 2017.

[4] D. A. Baker, N. C. Gallego, and F. S. Baker, 'On the characterization and spinning of an organic-purified lignin toward the manufacture of low-cost carbon fiber', *J. Appl. Polym. Sci.*, vol. 124, no. 1, pp. 227–234, 2012.

[5] S. Kubo and J. F. Kadla, 'Kraft lignin/poly(ethylene oxide) blends: Effect of lignin structure on miscibility and hydrogen bonding', *J. Appl. Polym. Sci.*, vol. 98, no. 3, pp. 1437–1444, 2005.

[6] J. Luo, 'Lignin-based carbon fiber', 2010.

[7] V. Gupta and V. Kothari, *Manufactured fibre technology*. Springer Science & Business Media, 2012.

[8] H. Fujiwara, M. Shibayama, J. H. Chen, and S. Nomura, 'Preparation of high-strength poly (vinyl alcohol) fibers by crosslinking wet spinning', *J. Appl. Polym. Sci.*, vol. 37, no. 5, pp. 1403–1414, 1989.

[9] E. Otsuka and A. Suzuki, 'A simple method to obtain a swollen PVA gel crosslinked by hydrogen bonds', *J. Appl. Polym. Sci.*, vol. 114, no. 1, pp. 10–16, 2009.

[10] H. Hoshino, S. Okada, H. Urakawa, and K. Kajiwara, 'Gelation of poly(vinyl alcohol) in dimethyl sulfoxide/water solvent', *Polym. Bull.*, vol. 37, no. 2, pp. 237–244, Aug. 1996.

[11] S. Kubo and J. F. Kadla, 'The Formation of Strong Intermolecular Interactions in Immiscible Blends of Poly(vinyl alcohol) (PVA) and Lignin', *Biomacromolecules*, vol. 4, no. 3, pp. 561–567, 2003.

[12] J. D. Hoffman and J. J. Weeks, 'Rate of spherulitic crystallization with chain folds in polychlorotrifluoroethylene', *J. Chem. Phys.*, vol. 37, no. 8, pp. 1723–1741, 1962.

[13] P. J. Flory, 'Thermodynamics of crystallization in high polymers. IV. A theory of crystalline states and fusion in polymers, copolymers, and their mixtures with diluents', *J. Chem. Phys.*, vol. 17, no. 3, pp. 223–240, 1949.

[14] M. Föllmer, C. Mercader, W. Neri, S. Jestin, A. Derré, P. Poulin, 'Patent Application No. BFF17P0617', 2017.

[15] Y. Wang, C. Wang, and M. Yu, 'Effects of different coagulation conditions on polyacrylonitrile fibers wet spun in a system of dimethylsulphoxide and water', *J. Appl. Polym. Sci.*, vol. 104, no. 6, pp. 3723–3729, 2007.

[16] J. Chen, H. Ge, H. Liu, G. Li, and C. Wang, 'The coagulation process of nascent fibers in PAN wet-spinning', *J. Wuhan Univ. Technol.-Mater Sci Ed*, vol. 25, no. 2, pp. 200–205, 2010.

[17] J. G. Cook, *Handbook of textile fibres: man-made fibres*. Elsevier, 1984.

[18] P. Miaudet, 'Structure et propriétés de fibres de nanotubes de carbone à haute énergie de rupture', 2007.

[19] P. Guttmann *et al.*, 'Nanoscale spectroscopy with polarized X-rays by NEXAFS-TXM', *Nat. Photonics*, vol. 6, p. 25, Nov. 2011.

[20] L. M. Steudle *et al.*, 'Carbon Fibers Prepared from Melt Spun Peracylated Softwood Lignin: an Integrated Approach', *Macromol. Mater. Eng.*, vol. 302, no. 4, pp. 1600441–n/a, 2017.

[21] Olsson Carina, Sjöholm Elisabeth, and Reimann Anders, 'Carbon fibres from precursors produced by dry-jet wet-spinning of kraft lignin blended with kraft pulps', *Holzforschung*, vol. 71, no. 4, p. 275, 2017.

[22] S. P. Maradur, C. H. Kim, S. Y. Kim, B.-H. Kim, W. C. Kim, and K. S. Yang, ‘Preparation of carbon fibers from a lignin copolymer with polyacrylonitrile’, *Synth. Met.*, vol. 162, no. 5–6, pp. 453–459, 2012.
[23] P. J. Bissett and C. W. Herriott, ‘Lignin/polyacrylonitrile-containing dopes, fibers, and methods of making same’, Jan-2012.
[24] M. Zhang, ‘Carbon Fibers Derived from Dry-Spinning of Modified Lignin Precursors’, 2016.
[25] I. Brodin, M. Ernstsson, G. Gellerstedt, and E. Sjöholm, ‘Oxidative stabilisation of kraft lignin for carbon fibre production’, *Holzforschung*, vol. 66, no. 2, pp. 141–147, 2012.
[26] I. Norberg, ‘Carbon fibres from kraft lignin’, 2012.
[27] E. Frank, L. M. Steudle, D. Ingildeev, J. M. Spörl, and M. R. Buchmeiser, ‘Carbon Fibers: Precursor Systems, Processing, Structure, and Properties’, *Angew. Chem. Int. Ed.*, vol. 53, no. 21, pp. 5262–5298, 2014.
[28] A. C. Ferrari and J. Robertson, ‘Interpretation of Raman spectra of disordered and amorphous carbon’, *Phys Rev B*, vol. 61, no. 20, pp. 14095–14107, May 2000.

Chapter III Structuration of Lignin through Liquid Crystalline Graphene Oxide

This chapter presents the approach of combining lignin with graphene oxide (GO) flakes in order to introduce a higher crystallinity and orientation inside its amorphous carbon structure. In a first step, the phase behaviour of GO in presence of different lignin grades in solution is studied and demonstrated by phase diagrams. The second step comprises the preparation of lignin-GO films in different ratios as well as the wet-spinning of lignin-GO fibres. The impact of the GO flakes on the films and fibres after their carbonization is demonstrated. The thereby resulting structure and properties of the films and fibres are presented and compared with respect to their different preparation methods.

III. 1 Lignin-Graphene Oxide Solutions

The combination of lignin with graphene oxide (GO) for wet-spinning applications has first been studied in solution. The miscibility of the two components and the phase behaviour of GO in presence of lignin has been investigated. As shown in *chapter I.3.5*, the formation of liquid crystalline phases of GO in solution possibly leads to a higher orientation inside wet-spun fibres. The potential of this approach for possible spinning dopes made from lignin and graphene oxide was evaluated in this subchapter.

III.1.1 Introduction to Liquid Crystals and Phase Behaviour of Graphene Oxide

Along with the solid, liquid and gas state, the liquid crystalline state discovered in 1888 by Friedrich Reinitzer is often considered a forth state of matter. As the name implies, liquid crystals exhibit different phases considered as intermediate states between liquids and solid crystals (see Figure III-1, upper part). The building blocks forming liquid crystalline (LC) phases are anisotropic objects whose shape can for instance be elongated/"calamitic" (as in Figure III-1) or disk-like.[1-2]

Liquid crystals include the following mesophases, among others not presented here[3] (see Figure III-1, lower part):

- **Nematic Phase**: long range orientational order, the molecules all point in the same direction (one director).
- **Smectic Phase**: orientational- and positional order, thus arrangement in layers
- **Cholesteric or Chiral Nematic Phase**: long range orientational order with rotating director, the molecular orientation twists with a certain periodicity (rotation of a full circle corresponding to the so-called "pitch length")
- **Columnar Phase**: assembly of flat, usually disk-like molecules into cylindrical structures

On the one hand, a transition between the different mesophases can occur with temperature changes for "thermotropic" liquid crystals. On the other hand, so-called "lyotropic" liquid crystals organize in the respective phase depending on their concentration in solution.[2]

Anisotropic objects with a certain orientation such as liquid crystals possess birefringent properties. Birefringence can be visualized between two crossed polarized filters of an optical microscope (POM).

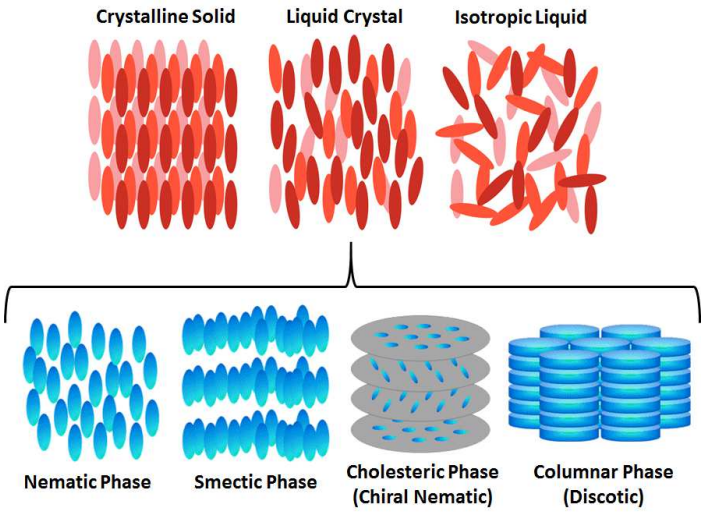

***Figure III-1**: Examples of liquid crystalline states between crystalline solid and isotropic liquid (above) and molecular orientation of possible liquid crystalline phases (below) [image based on **[4]**)*

Carbon-based liquid crystals are of particular interest for the development of novel carbon materials. For instance carbon nanotubes and mesophase pitch are already being used as precursor materials for carbon fibres. Graphene oxide represents another material class capable of forming liquid crystals in solvents, rendering them attractive for solution processing. The oxygenated monolayers of GO possess a very large surface area and widths of several micrometres but a thickness within the nanometre range, thus resulting in an anisotropic shape with high aspect ratios of ≥ 700.[5] Due to carboxyl- and hydroxyl groups on their surface (negatively charged), the GO layers are separated through electrostatic repulsive forces and can thus easily be dissolved in water and in polar organic solvents.[6] Nematic phases and isotropic-nematic phase transitions in GO solutions were first reported by Xu&Gao in 2011.[7] The phase transitions were found to be dependent on the concentration of GO sheets (volume-/mass fraction), their size, aspect ratio and the pH value or salt concentration of the solvent. The transition from isotropic to nematic phase depending on GO concentration is demonstrated in Figure III-2.

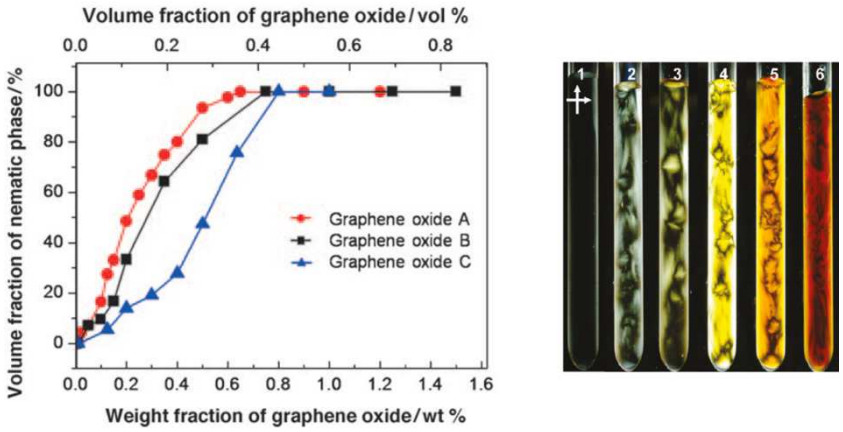

***Figure III-2**: Nematic phase volume fraction vs. GO concentration (decreasing GO flake sizes from A to C, left **[4]**) and birefringence of GO-solutions between crossed polarizers (increasing concentrations from 1-6, right* [7]*)*

III.1.2 Lignin-Graphene Oxide Phase Diagrams

A possible and common way to study and visualize the interactions between two components in a mixture is the preparation of a phase diagram. Various phase diagrams of pure graphene oxide (GO) already exist, for instance depending on its concentration in solution or its flake size (see Figure III-2). A few studies of the interaction between GO and polymeric compounds are also reported in literature. For instance, a phase diagram for mixtures of GO and polyethylene glycol (PEG) has been prepared by Shim et al.[8] However, mixtures of lignin and GO as well as their interactions in solution have not been reported yet. Within the framework of this thesis, phase diagrams of lignosulfonate and GO (in water and in DMSO) and of Kraft lignin and GO (in DMSO) have been prepared depending on the concentration of the two components inside the mixture.

The lignin-GO mixtures were prepared from two separate stock solutions of lignin and GO in water or in DMSO. From different mixing trials of lignin solutions with the initial GO solution it became clear that both components should be dissolved in the same solvent prior to mixing in order to assure a homogeneous blend solution. As a consequence, a water-based system of lignosulfonate (LS, Tembec) and GO as well as DMSO-based systems of LS with GO and Kraft lignin (KL, FCBA) with GO were investigated. The commercial GO solution at 0.4 wt% in water (Graphenea) was concentrated by two centrifugation steps (1400 g, 20 min + 50440 g, 60 min). The first centrifugation was used to separate and remove aggregated GO flakes from the solution. The supernatant was then used for the second centrifugation, during which a concentrated GO-gel was formed at the bottom of the tubes. The GO-gel was collected after removal of the supernatant (clear water) and its concentration was determined by dry extract (4 ± 0.5 wt%). For the two systems in DMSO, an exchange of solvent was thus performed from water to DMSO by means of centrifugation. Additionally to the centrifugation of GO in water, two more centrifugation steps were performed (each at 50440 g for 120 min). Before the second and third centrifugation, the water-based supernatant was removed and replaced with DMSO inside the tubes respectively. The GO gel was then re-dissolved inside the tubes by manual stirring and by using a vortex until the solution showed a homogeneously dark colour. After two re-dissolution steps with subsequent centrifugation, it was assumed that all water residues had been removed with the supernatants, leaving behind a GO-gel in DMSO. Due to the exchange of solvent however, the GO-gel in DMSO was found to exhibit a lower concentration (1.6-1.8 wt%, determined by dry-extract under vacuum) than the GO-gel in water.

The lignin solutions in water and DMSO were prepared by direct dissolution of the raw materials at 10, 20, 30 and 40 wt%. Afterwards, they were mixed with the prepared GO-gels (diluted to different concentrations) in ratios of 1:9 with magnetic stirrer bars at room temperature, as shown by equation III-1:

$$C_{dope} = C_L + C_{GO} = \frac{X(0.1m_{total})}{m_{total}} + \frac{Y(0.9m_{total})}{m_{total}} \qquad (III\text{-}1)$$

[X being the lignin solution at 10, 20, 30 or 40 wt%]
[Y being the GO solution e.g. at 0.45, 0.89, 1.34 wt% in DMSO / 1.12, 2.23, 3.34, 4.45 wt% in H_2O)]

The phase behaviour of the blend solutions was investigated by polarized optical microscopy (POM) between crossed polarizers.

- Lignosulfonate – Graphene Oxide

As already mentioned in *chapter II.1* (see Table II-2), the used lignosulfonate ("L12" extracted from maritime pine, Tembec) was found to be soluble in water and in DMSO at concentrations of up to 40 wt%. The phase behaviour of lignosulfonate (LS) - graphene oxide (GO) blend solutions was thus studied for a system in water and a system in DMSO.

As shown in the phase diagrams (see Figure III-3), the LS-GO solutions were found to change from an isotropic to a nematic state with increasing GO concentrations in both solvent systems. Thereby, the addition of LS did not seem to alter the phase transitions of GO when evaluated by POM images. For both systems, a broad transition range with coexisting isotropic and nematic phase was found, herein called as "biphasic" phase. The large biphasic area can be explained by the high polydispersity of the GO flakes, since larger flakes (higher anisotropy) tend to form nematic phases at lower concentrations than smaller flakes.[5] As already mentioned, the GO obtained in DMSO after the solvent exchange was less concentrated than the GO in water, thus the phase diagram based on DMSO (Figure III-3-b) covers only GO concentrations of up to 1.6 wt%. Comparing the two diagrams, the biphasic to nematic phase transition in DMSO seems slightly shifted to higher concentrations. This phenomenon could be due to different interactions of GO with the solvent. However, it has to be clearly stated that variations in this transitional concentration range are more likely related to the broad polydispersity of the GO flakes.[7] The low transition point between the isotropic and biphasic phase was possibly observed because of a large aspect ratio of the used GO flakes.[6] It has to be mentioned that the phase transitions found in Figure III-3 may differ from the findings of Xu&Gao due to less oxidized GO flakes. Xu&Gao report an additional oxidation step performed after the classical Hummer's method, in which graphite is typically oxidized by e.g. sulfuric acid. The obtained graphite oxide is then exfoliated into graphene oxide by sonication or mechanical stirring.[7]

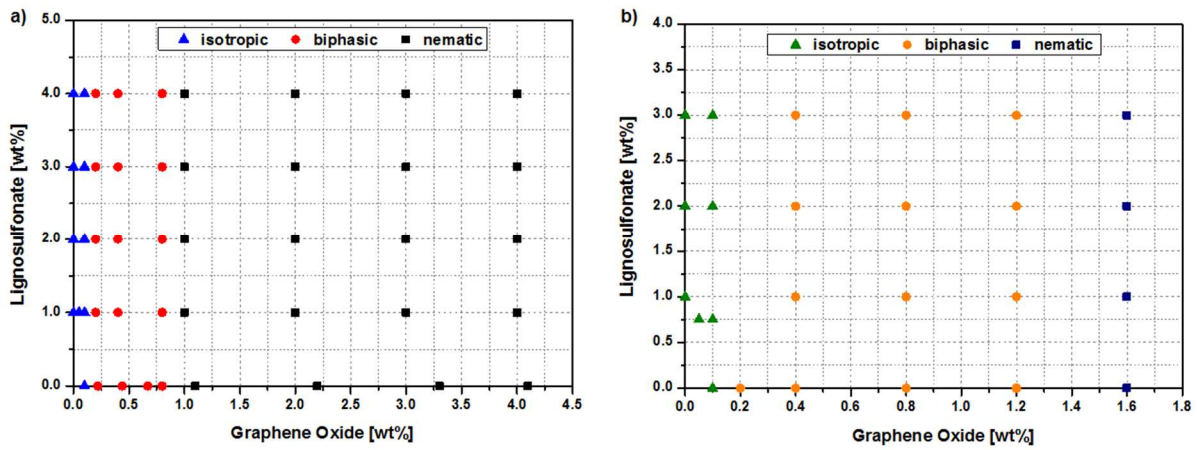

***Figure III-3**: Phase diagrams of lignosulfonate and graphene oxide in water (a) and in DMSO (b)*

By means of crossed polarizers in POM, birefringence of liquid crystalline phases can usually be visualized (see *chapter III.1.1*). In the isotropic phase and thus at low concentration of GO flakes, a lack of molecular orientation results in completely dark images, since all of the light waves are blocked by the crossed polarizers. Some bright spots which were found in the samples indicate GO aggregates, polarizing the light waves to a certain extent. Within the biphasic transition range at higher concentrations, typical birefringent Schlieren textures can be recognized in some areas of the POM images taken between crossed polarizers (see Figure III-4-a.2 and -b.2).[5] At even higher concentrations in the nematic phase, large areas of Schlieren textures suggest a more uniform and regular orientation of the GO flakes throughout the whole sample. In some areas, even more ordered, parallel banded textures were found in the LS-GO solutions, suggesting the partial formation of a lamellar phase (as proposed by Xu&Gao[7]).

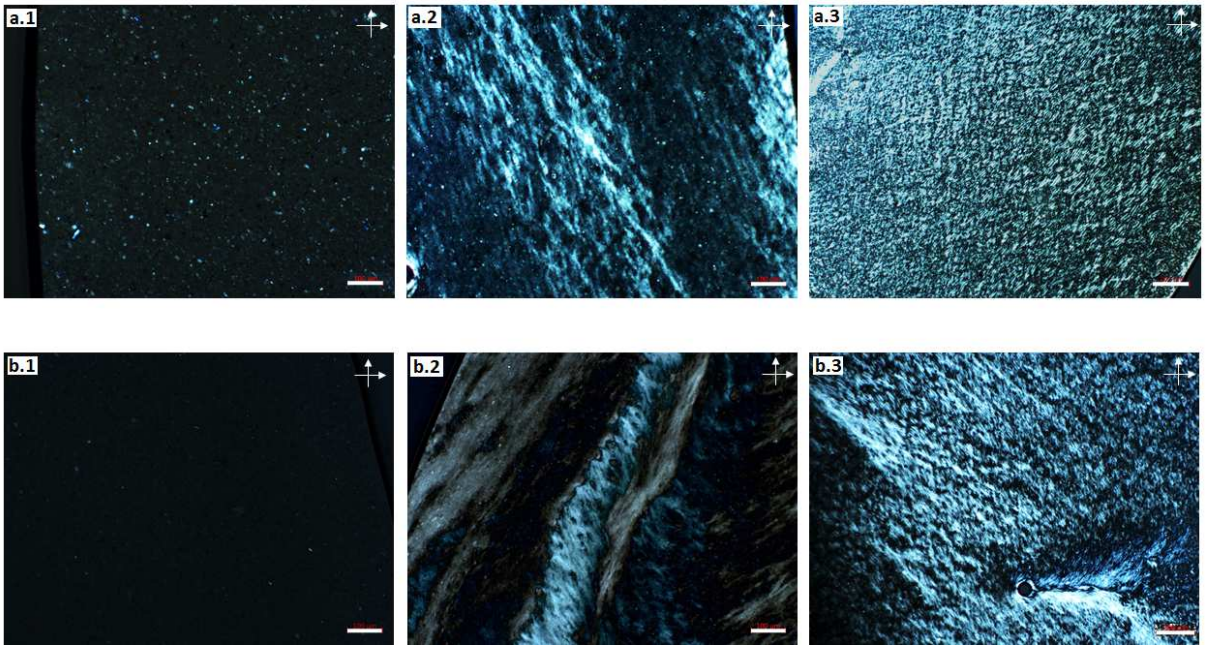

Figure III-4*: POM images of lignosulfonate-GO solutions in water (a) and in DMSO (b): in isotropic phase (1, scale bars 100µm), in biphasic phase (2, scale bars 100µm) and in nematic phase (3, scale bars 200µm)*

- Kraft lignin – Graphene Oxide

Softwood Kraft lignin (“L16” extracted from pine, FCBA) was found to be soluble in DMSO at high concentrations (see *chapter II-1*, Table II-2). In order to prepare mixtures with GO, a solvent exchange from water to DMSO was thus performed for the GO solution. The maximum concentration of the solution in DMSO being limited, GO concentrations only up to 1.8 wt% (and less in the mixtures) were investigated. The resulting phase diagram shows the GO liquid crystalline phase as a function of GO- and Kraft lignin (KL) concentration (see Figure III-5). Despite the presence of KL in high concentrations, liquid crystalline phases of GO were recognized on POM images. The transitions from isotropic to biphasic and from biphasic to nematic phase were found at similar concentrations as in the previous diagrams. Compared

to the system of lignosulfonate and GO in DMSO, KL-GO formed a nematic phase at lower concentrations. A possible explanation could lie in slightly different sizes of the GO flakes from different batches.

As for the systems lignosulfonate-GO in water and in DMSO, birefringent Schlieren textures were visualized by POM between crossed polarizers at increasing GO concentrations. The POM images did not show any significant differences of the KL system compared to LS. However, it has to be mentioned that the evaluation of the POM images with subsequent categorization into a respective phase was generally difficult to perform. Due to a lack of resolution of the microscope and because of only small differences between the samples, the phase diagrams should rather be considered as tendencies. Many factors influencing the phase behaviour of the investigated systems (GO polydispersity and aspect ratio, charge density, aggregation due to centrifugation etc.) further complicate the evaluation. The trend of the obtained phase diagrams however became clear: the phase transitions of GO in presence of LS or KL do still exist. This result suggests that lignin and GO are compatible in a way that homogeneous materials (e.g. films and fibres) can be prepared from blend solutions.

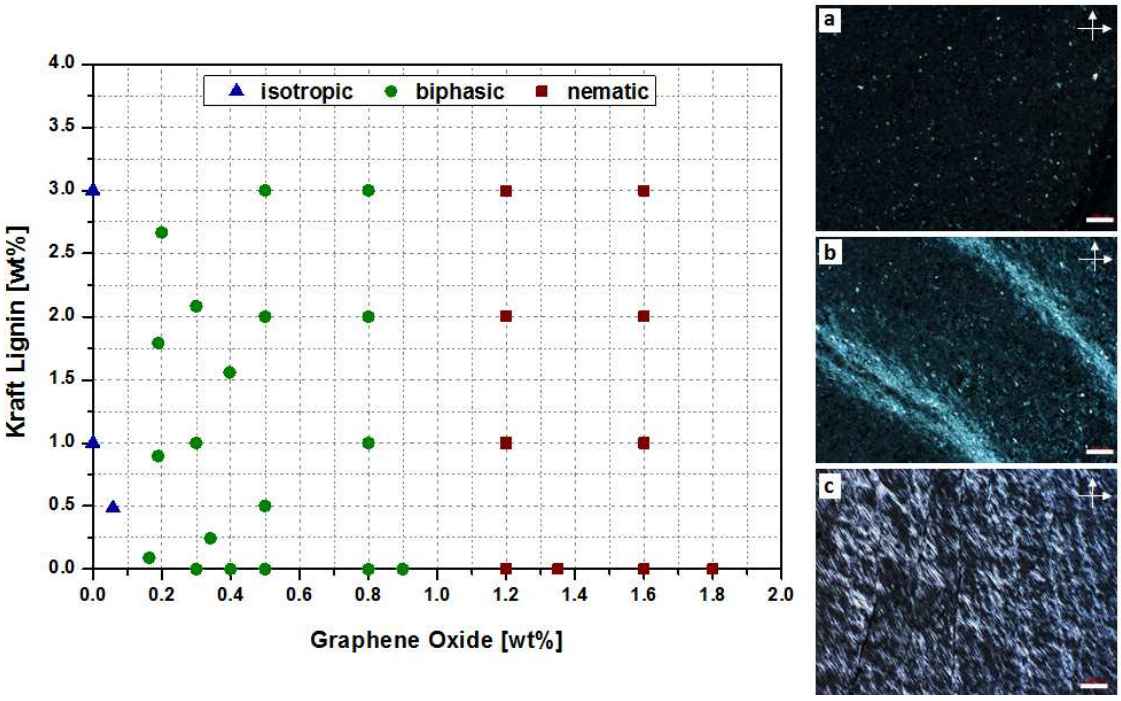

***Figure III-5**: Phase diagram of Kraft lignin and graphene oxide in DMSO (left) and POM images of solutions (right) in isotropic phase (a), biphasic phase (b) and nematic phase (c), scale bars: 100µm.*

III.1.3 Investigation of Graphene Oxide-Polymer Interactions by SAXS

As described in literature, graphene oxide (GO) flakes can be dissolved in water or in polar organic solvents. Due to negatively charged functional groups at their surface, the flakes are stabilized by electrostatic repulsion interactions. When the concentration is increased to a certain threshold, the GO layers self-assemble into liquid crystalline phases.[7]

Regarding the interaction between GO and different polymers in solution, several investigations are reported in literature. The self-assembly of GO with e.g. amphiphilic molecules forming micelles above a certain concentration has been investigated. Meng et al. studied the complexation behaviour of GO and cetyltrimethylammonium (CTAB).[9] The group discovered different structures of GO-CTAB complexes by means of small angle X-ray scattering (SAXS) measurements.[9] Similarly, Hsieh et al. studied the interactions between functionalized GO and sodium dodecyl sulphate (SDS) in order to stabilize GO solutions at the lowest possible SDS ratio.[10] Besides, Zamora et al. worked on the stabilization of reduced graphene oxide layers in water by means of bile salts and demonstrated stable dispersions by SAXS measurements.[11] The phase behaviour of GO and interacting polymers in solution, especially the structural evolution of liquid crystalline GO-polyethylene glycol (PEG) mixtures over 3-12 months, has been reported by Shim et al.[8] Besides, GO-dextran coatings for steel wires have been prepared by Hou et al., who reported hydrogen bonding between GO and dextran.[12]

Generally, non-covalent interactions between components inside colloidal solutions can be of attractive or repulsive nature. In the case of GO with an interacting polymer, attractive forces between the two components on the one hand can lead to a high compatibility and thus homogeneous mixtures. The polymer is then found to exhibit a so-called adsorbing behaviour, which is independent of the polymer concentration (see Figure III-6-a). On the other hand, repulsive forces between GO and a polymer can lead to domains of excluded volume. In this case, when the polymer concentration is increased, an aggregation of GO flakes can be induced, which is driven by a depletion effect (see Figure III-6-b). Depletion is normally visible in phase diagrams through an enlarged biphasic phase at high polymer concentrations.

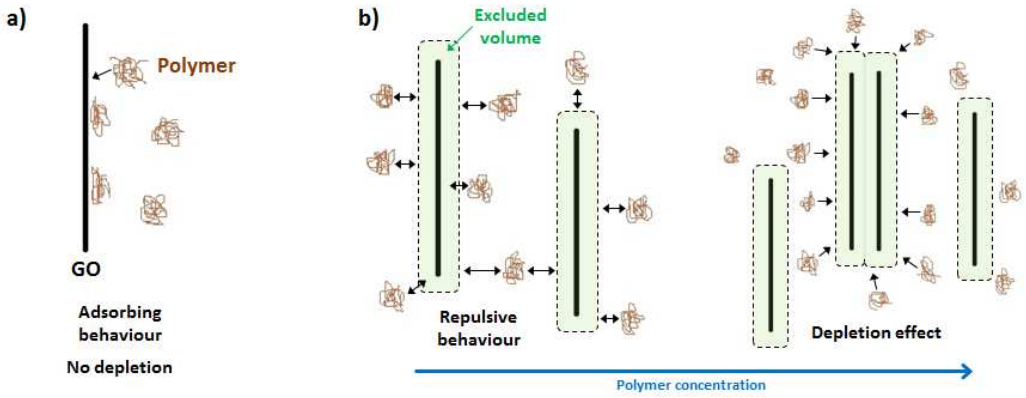

***Figure III-6**: Adsorbing behaviour (a) and repulsive behaviour of polymer molecules in presence of GO flakes (b), the latter one leading to a depletion effect at high polymer concentrations*

As shown in the previous subchapter, phase diagrams of GO and Kraft lignin (KL) as well as GO and lignosulfonate (LS) were prepared based on various mixtures of the two components. The liquid crystalline phase of the mixtures was evaluated based on POM images respectively. However, this method was lacking precise boundaries and resolution of the optical microscope. In order to get a deeper understanding of the interactions between these lignin grades and GO flakes, SAXS measurements were performed on mixtures at 3 wt% of GO and 3 wt% of lignin. In order to evaluate the obtained results and to compare them with those of other interacting polymers, mixtures of GO with PEG (35.000 g mol^{-1}, Sigma Aldrich), dextran (144.000 $gmol^{-1}$, Sigma Aldrich) and SDS (288 g mol^{-1}, Sigma Aldrich) have been prepared at the same time as the GO-lignin mixtures.

The samples of GO and the above mentioned polymers were first mixed at low concentrations (1.5 wt%) respectively and afterwards the homogeneous mixtures were concentrated by gradual evaporation of the solvent. At a known initial amount of components, the solvent was evaporated at room temperature under vacuum until the desired final concentration of 6 wt% in total (3 wt% GO + 3 wt% polymer) was reached. This preparation method was chosen based on the work of Shim et al.[8] (description in supporting information of [8]). The solvent used for the pure GO solution and the mixtures GO-PEG, GO-dextran, GO-SDS and GO-LS was water, whereas DMSO was used for the GO-KL solution.

The SAXS measurements were performed on a Bruker Nanostar instrument operating in transmission mode at a wavelength of 1.54 Å (copper cathode) under vacuum. The prepared mixtures were inserted into quartz capillaries and sealed immediately in order to avoid interactions with the environment (e.g. solvent evaporation) before being analysed. In the case of GO-KL in DMSO, no signal could be recorded with the instrument, possibly due to a different contrast in electron density of DMSO compared to water. Therefore, only the results for the water-based solutions could be evaluated within this thesis. The presence of a peak at small scattering angles, e.g. at a wave vector q^* of 0.026 $Å^{-1}$ for the pure GO sample (see Figure III-7), indicates an ordering in the sample corresponding to a lamellar/nematic phase. Besides, a second order diffraction peak can be recognized around 0.052 $Å^{-1}$, also indicating a lamellar ordering of GO flakes. The interlayer spacing d of the flakes can be calculated to around 24 nm by using the relationship $d = 2\pi/q^*$.[11] The two mixtures of GO-PEG and GO-Dex show the same scattering behaviour as pure GO in water (see Figure III-7). The small shift of both peaks towards higher scattering angles could indicate a beginning depletion effect, which may increase over time, but the shift could also be related to minor differences in GO concentration. From the spectra it can be concluded that pure GO and the GO-PEG/GO-Dex mixtures have a very similar scattering behaviour in solution. These two polymers do not seem to alter the phase behaviour of GO and they seem to act like adsorbing molecules.

In contrast to PEG and dextran, the GO samples containing SDS and LS show spectra with a strongly shifted diffraction peak (see Figure III-7). In the case of SDS, first- and second order diffraction peaks can still be found, but they are strongly shifted to higher q values. This shift to 0.067 $Å^{-1}$ indicates a decrease in interlayer spacing between single GO flakes with respect to the pure GO solution, meaning that the flakes approach each other up to a distance of 9 nm.

This observation thus confirms that depletion of GO flakes induced by SDS molecules took place in the sample. However, in the sample containing LS and GO, the GO diffraction peak was found shifted and broadened at the same time. The shifted diffraction peak suggests a phase separation within the system. The negatively charged sulfonate groups within the LS molecular structure (see Figure III-8-b) are likely to interact with the negative charges of GO through electrostatic repulsion. This repulsion between LS molecules and GO flakes may induce the observed depletion mechanism and thus a phase separation. The broadened shape of the diffraction peak could e.g. indicate a less uniform spacing of the GO flakes or smaller liquid crystalline domains. This is possible if the system is not yet at full thermodynamic equilibrium because of its viscosity and because of the polydispersity of the GO flakes.

The SAXS results could also depend on time scales, as found by Shim et al.[8]. Generally, the mixtures prepared for the phase diagrams and SAXS measurements were visualized by POM images directly after their preparation. However, the SAXS analysis was performed automatically for one sample after the other, taking 10 hours per sample. The LS-GO sample was thus measured only after 40 hours. It could thus be possible that the mixture is metastable, meaning that it forms a nematic phase upon mixing, but a phase separation by depletion takes place over time. This explanation could be in agreement with Shim et al. who measured GO-PEG solutions only 3 months after their preparation. Since GO is known to be chemically unstable over time, it is likely that the chemical nature of GO evolved over these 3 months. Shim et al. thus recognized clear depletion effects in their POM images, whereas SAXS measurements performed for this thesis only shortly after mixing did not indicate a depletion effect between GO and PEG.

In contrast to the observations made by POM, the SAXS results demonstrate an influence of LS on the phase behaviour of GO. The flakes can still form ordered liquid crystalline domains, due to the fact that birefringence can be observed in the mixtures by POM. However, the system can be considered as biphasic, since the SAXS spectra indicate a phase separation.

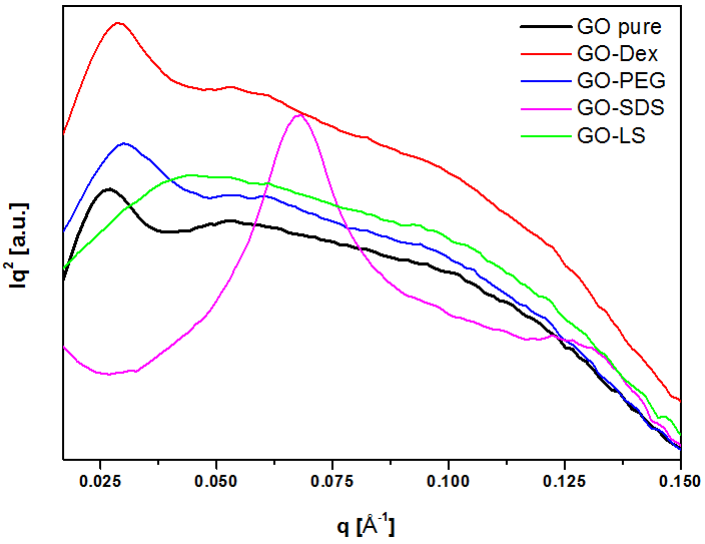

***Figure III-7**: SAXS spectra of scattered intensity with respect to the scattering wave vector q for aqueous solutions of pure GO (3 wt%) and of mixtures GO-Dex, GO-PEG, GO-SDS and GO-LS at 6 wt% (3wt%-3wt%)*

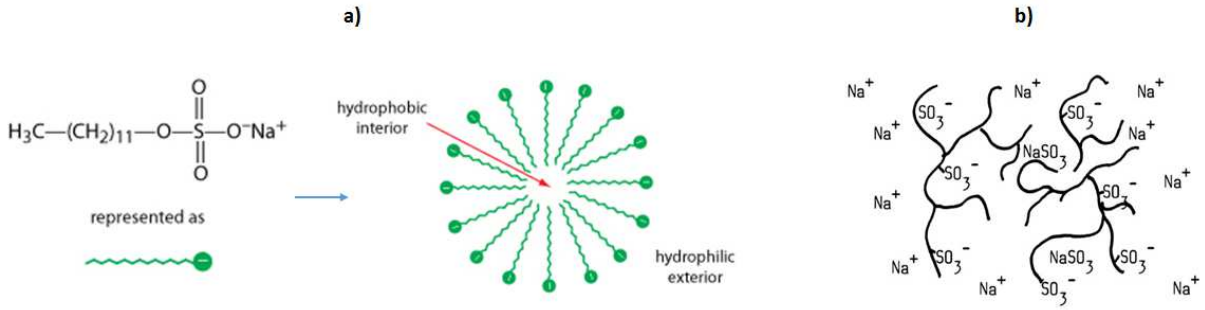

Figure III-8: Molecular structure and self-assembly of sodium dodecyl sulfate (SDS) into micelles (a) and generalized molecular structure of lignosulfonate (b)

As demonstrated in Figure III-7, the peak for the GO-SDS sample is shifted to larger angles, meaning that the GO flakes still form a pseudo-lamellar phase but with a reduced spacing between them. The system is therefore biphasic. The phase separation and decreased spacing between the flakes reflect an attractive interaction between them. This attraction can be ascribed to depletion induced by the surfactant micelles, which form at a concentration (CMC) of $8x10^{-3}$ mol l^{-1} corresponding to 0.23 wt% (see Figure III-8).[13]

In order to confirm this effect, SAXS measurements have been performed for several GO-SDS mixtures at different SDS concentrations. The stock solution of GO (0.4 wt%, Graphenea) was mixed with aqueous SDS stock solutions at 1-6 wt% respectively in a ratio of 1:1. After gentle stirring with magnetic stirrer bars at room temperature, the mixtures were concentrated by centrifugation at 50440 g for 60 min and removal of the supernatants. Assuming that all GO present in the mixture was concentrated at the tube bottoms while the SDS concentration stayed equal in centrifugate and supernatant, the resulting concentrations within the centrifugate were calculated to 3 wt% of GO and 0.5-3 wt% of SDS. It was observed that the mixtures with higher amounts of SDS could be more easily concentrated upon centrifugation. Despite the fact that the systems were not at true thermodynamic equilibrium after centrifugation, this behaviour confirms the effect of attractive interactions between the GO flakes. This attraction being stronger with increasing SDS contents, the flakes can be more easily packed and their interlayer distance decreases, as shown by the SAXS spectra in Figure III-9.

The phase separation of GO and SDS was rather difficult to recognize by means of POM. Regarding the mixtures of LS and GO, a clear effect on the GO flakes did not become evident through POM images either. For our case, optical microscopy hence does not seem to be a suitable method to determine the phase boundaries of GO with interacting polymers. A different method should be chosen in future studies to prepare phase diagrams for lignin and GO of higher accuracy.

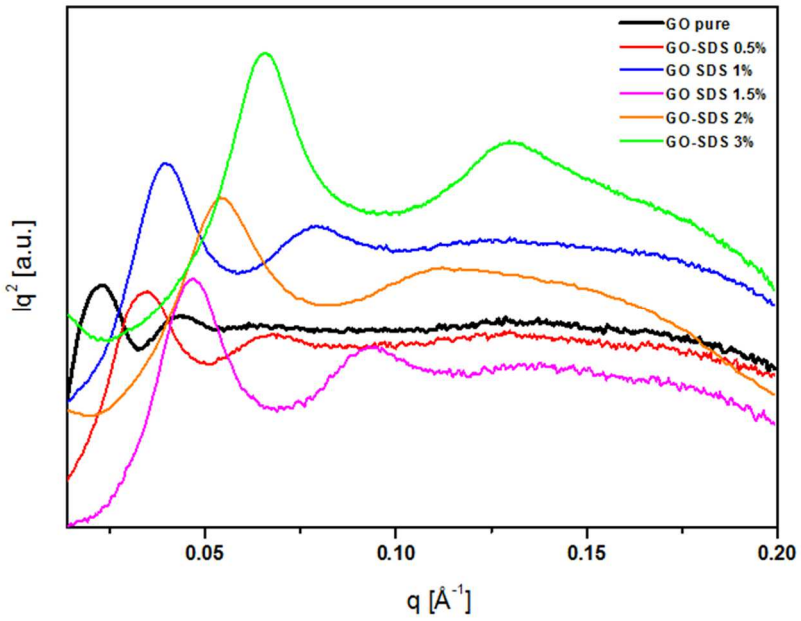

***Figure III-9**: SAXS spectra showing the scattered intensity as a function of the scattering wave vector q for aqueous solutions of pure GO (3 wt%) and GO-SDS solutions (3 wt% of GO and 0.5-3 wt% of SDS)*

III.2 Lignin-Graphene Oxide Films

Based on the results obtained for blend solutions of lignin (Kraft lignin and lignosulfonate) and graphene oxide, some of the combinations were selected to prepare composite films. The structure and the properties of the obtained lignin-graphene oxide films were investigated and are presented in this subchapter.

III.2.1 Preparation and Carbonization of Films

Blend solutions of lignosulfonate (LS) and graphene oxide (GO) in water and of Kraft lignin (KL) and graphene oxide (GO) in DMSO were prepared in different ratios based on selected points within the phase diagrams (see *chapter III.1.2*). The proportions in the blend solutions are listed in Table A-III-1 (see annex). Pure lignin- and GO stock solutions were prepared separately with subsequent addition of the lignin solutions into the GO solution. The two components were mixed with magnetic stirrer bars at room temperature until homogeneous blend solutions were obtained. By optical microscopy under normal light and polarized light, the homogeneity and the phase behaviour of the mixtures were evaluated. The blend solutions were then filled into Teflon® moulds (see Figure III-10-a) and subsequently dried under vacuum. By evaporation of the solvents at 45 °C (for water-based solutions) and 100 °C (for DMSO-based solutions) at 80 mbar for 12-16 h, solid lignin-GO films were prepared (see proportions in Table A-III-1).

The dried films were subsequently heated to 1200 °C under argon for carbonization by means of a static carbonization oven (Adamel Lhomargy FN 50 No. 4992). The films were placed inside a ceramic mould and protected with ceramic plates to prevent them from moving with the argon gas flux (see Figure III-10-b). Different heating rates were applied to study their influence on the quality of the obtained carbon films based on lignin and GO. Two linear heating ramps (2.5 °C min^{-1} and 5 °C min^{-1}) and one heating ramp divided in two parts (0.5 °C min^{-1} until 400-450 °C and 1 °C min^{-1} until 1200 °C) were applied. The latter one was selected based on the thermal degradation profiles of the films obtained by thermogravimetric analysis (TGA) under nitrogen, such as indicated in Figure III-11. The different lignin-to-GO ratios led to very similar carbon residues of the two GO-KL or GO-LS films after heating under nitrogen at 1200 °C. The pure lignin- and GO components demonstrated carbon residues of around 40 % (pure KL: 43 %, pure LS: 37 %, pure GO: 41 %). A direct comparison between the pure components and the films is given in Figure A-III-1 (see annex). It can be stated that the carbon residues of the KL-GO films (at both ratios of 20:80 and 80:20), were found to be at around 52 % and thus higher than those of pure KL and pure GO. This result suggests a synergistic effect between these two components, which does not seem to exist for GO and LS. It could be possible that additional bonds are created upon mixing of KL and GO due to a high affinity between the two materials, which gives their films a higher resistance against degradation.

Regarding the carbonization process in general, the high mass loss at temperatures below 450 °C indicates an increased degradation of matter and evaporation of gaseous elements

within this temperature range (see Figure III-11). Zhao et al., described the thermal decomposition of softwood lignin in three stages.[14] The mass loss at temperatures below 180 °C could mainly be attributed to the release of physically adsorbed water. Between 180 °C and 300 °C, phenolic compounds were found to be some of the main volatiles released, while during the third pyrolysis stage at temperatures above 300 °C, mostly CO_2 and CH_4 gaseous compounds were detected. The formation of these gases was mainly attributed to cleavage of lignin functional groups (methoxyl-, ether-, carboxyl- and carbonyl groups).[14] Consequently, the heating rate for this temperature range was decreased in order to provide more time for the samples to undergo the pyrolysis process.

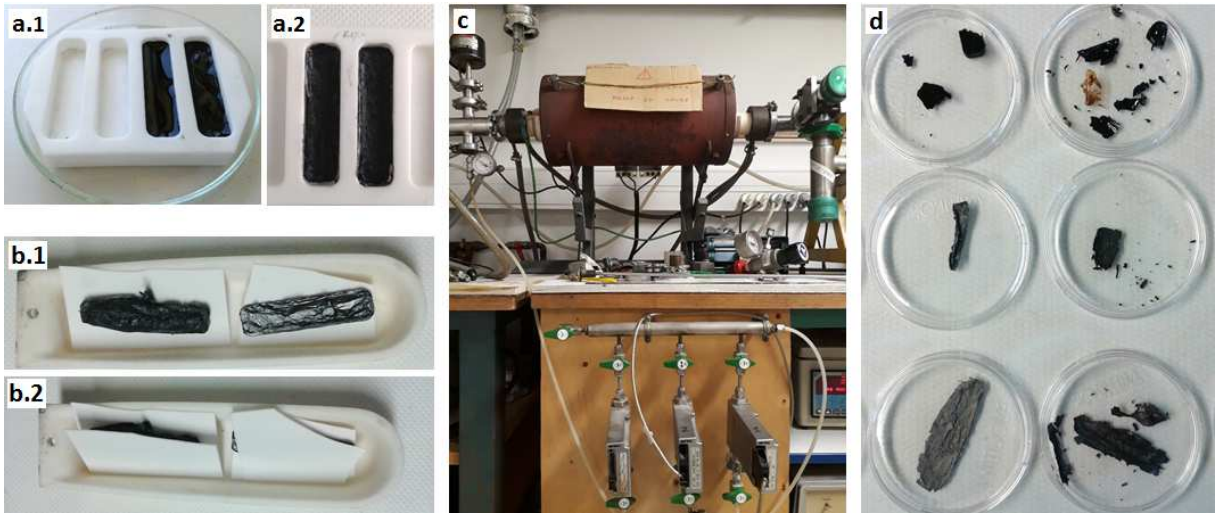

Figure III-10 *: Preparation and carbonization of lignin-graphene oxide films: Teflon mould with solutions and dried films (a), ceramic mould for placing the samples (b), static carbonization oven (c) and different morphologies of obtained carbon films based on lignin and graphene oxide after heating to 1200°C under argon (d)*

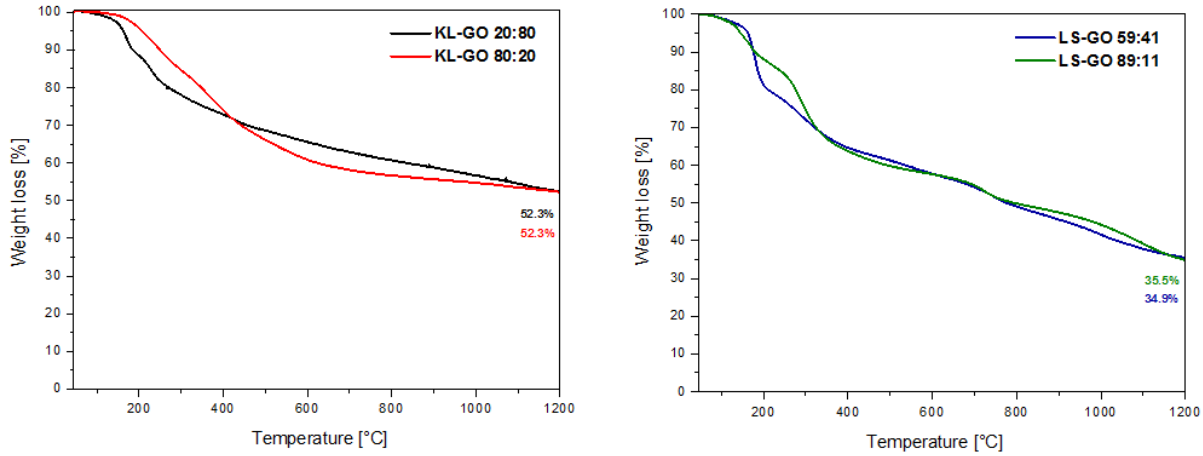

Figure III-11 : *Thermogravimetric analysis (TGA) results of selected films from Kraft lignin (KL) and graphene oxide (GO) (left) and from lignosulfonate (LS) and graphene oxide (GO) (right); measurements were performed under nitrogen*

III.2.2 Film Morphology

The morphology of the obtained films before and after carbonization was visualized with a scanning electron microscope (SEM) HITACHI TM3030 after gold-palladium metallization with a Quorum SC7620 to enhance the image contrast. The samples were fixed on a sample holder in a way that the cross-sections and the surfaces of the films could be characterized respectively.

By observation with bare eyes, it was recognized that the brittleness of the carbonized films strongly increased with increasing lignin contents (see Figure III-10-d). The high brittleness of lignin, which has also been observed during fibre spinning (see *chapter II.1.1*), is likely to be related to its amorphous molecular structure. The SEM images revealed a homogeneous morphology of the lignin-GO films, but depending on their composition, more or less pronounced porosity could be observed on their surfaces. Besides, a crumpled structure was observed for films at GO contents ≥ 40 % (see Figure III-12-b,-e,-f). This morphology suggests an organization of GO planes in several layers, whereby these were found more densely packed within the film cross-sections with increasing GO concentrations. The pure lignin films showed significantly different morphologies depending on the used lignin type. Whereas the film prepared from Kraft lignin (KL) showed a smooth and dense surface, the lignosulfonate (LS) film was found highly porous and cracked after carbonization (see Figure III-12-c and -d). The difference could be related to the higher content of impurities within LS compared to KL. According to TGA measurements under air performed up to 1100 °C, the remaining residue was found to be around 22 % (see Figure A-III-2-a in annex). A pyrolysis under air usually represents the quantity of inorganic components contained in the sample. In comparison, KL showed a residue of only 0.6 % under air. The inorganic substances within LS could provoke the formation of cracks during the carbonization process. However, by combining LS with GO, the crack formation was found inhibited (see Figure III-12-f.) and the addition of KL to GO even seemed to densify the obtained films.

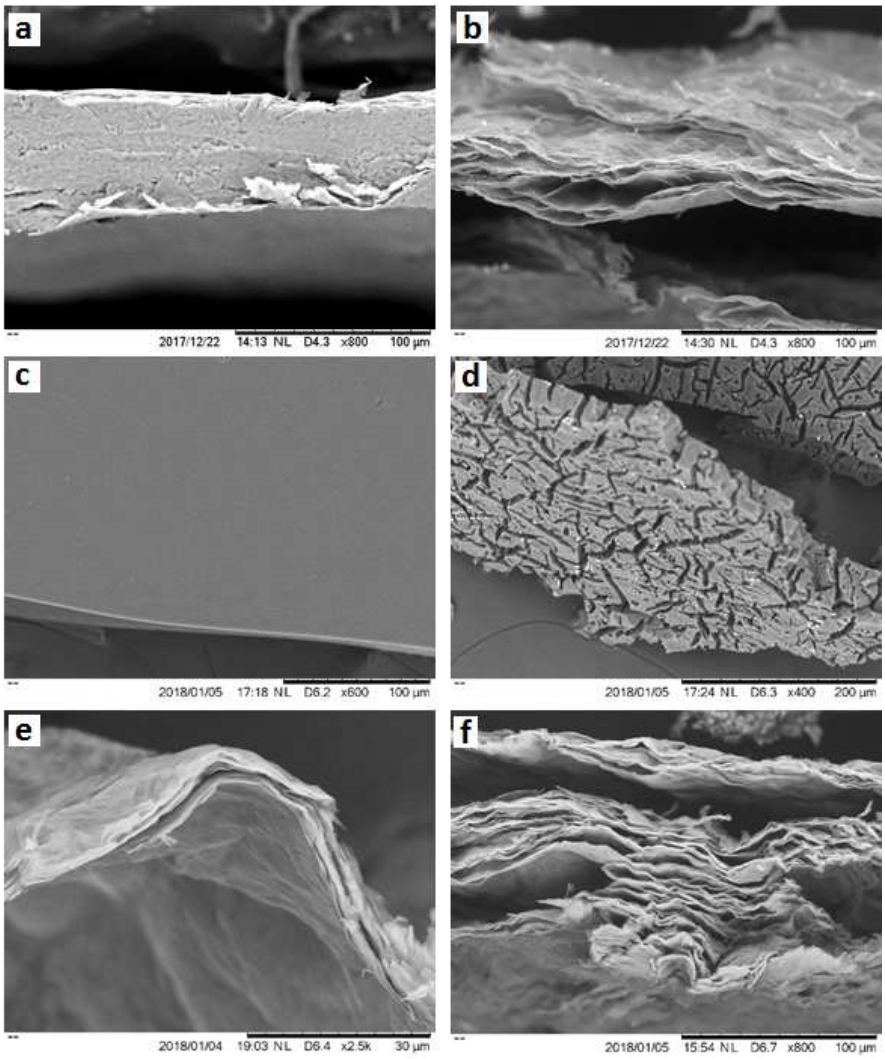

***Figure III-12**: Films of pure GO before (a) and after carbonization (b); and films after carbonization: pure KL (c), pure LS (d), GO-KL 50:50 (e) and GO-LS 41:59 (f)*

However, no clear orientation provoked by a liquid crystalline phase became evident for the lignin-GO films. This stands in contrast to the observations made by Xu&Gao[7], who characterized freeze-dried GO solutions with SEM images and found more oriented GO textures for samples prepared from more concentrated GO solutions. During the freeze-drying process, the state of the dissolved GO flakes can be considered as “frozen” and by direct conversion into a solid, it should be conserved for the SEM observation. It can be assumed that upon slow solvent evaporation, as performed in this thesis, all the blend solutions passed into a nematic phase before solidification into films, regardless of their initial concentration. As shown by the phase diagrams (see Figures III-3 and III-5), a fully nematic crystalline phase within a lignin-GO blend solution is starting to form at GO concentrations as low as 1.5 wt%.

As mentioned in the previous subchapter, different heating rates were applied to GO-LS and GO-KL films in order to study the influence on the obtained carbon structure. Two different compositions with different ratios of GO-LS (41:59 and 11:89) and GO-KL (80:20 and 20:80) were characterized. The films containing GO and LS generally showed a high amount of bright spots on their surface, both before and after carbonization (see Figure III-13). The particles

are thus assumed to be inorganic substances such as salts or minerals, due to the fact that they are still present after carbonization. Furthermore, TGA measurements under air revealed a high amount of inorganic components within LS (see Figure A-III-2-a in annex). These are considered as impurities, which may not only lead to residues on the film surfaces, but also to the formation of pores inside the films.[15] Thus, the high amount of impurities in LS can be considered a potential explanation for a high porosity in the films containing LS.

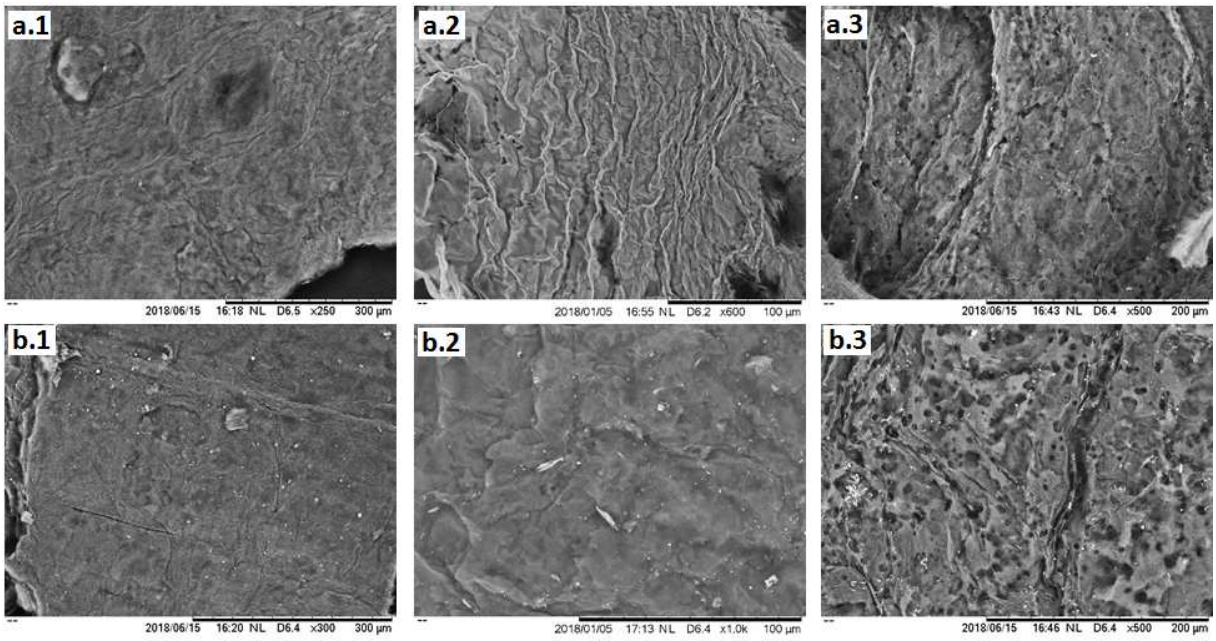

Figure III-13 *: Carbonized films of GO-LS at ratios 41:59 (a) and 11:89 (b) prepared at different heating rates: 5°C/min (1), 2.5°C/min (2) and 0.5°C/min + 1°C/min (3)*

Besides, the heating rate also seems to have an important impact on the porosity of the obtained films, since larger pores were found at lower heating rates. The films heated at a fast rate of 5 °C min^{-1} did not show any pores at a given SEM resolution, although it is possible that very small pores would become visible when characterizing the films at higher resolution. However, it can be stated that the pore size within GO-lignin carbon films seems to be related to the heating rate used for carbonization. At lower heating rates (0.5-1 °C min^{-1}), the films undergo a slower decomposition and thus may form larger pores, whereas at higher rates (5 °C min^{-1}), the decomposition process may be accelarated in a way that smaller pores are formed.

In the case of GO-LS films, larger pores seem to be created at higher LS contents (see Figure III-13), whereas the opposite behaviour was found for GO-KL films (see Figure III-14). Due to the fact that pure KL films did not show any porosity at the given resolution, KL seems to have a positive effect on the overall porosity of GO-KL composite films. Due to a low impuritiy content of KL and possibly a high compatibility with GO in solution (see *chapter III-1*), films based on KL and GO seem to be a promising candidate to obtain homogeneous and dense carbon structures with an increased orientation.

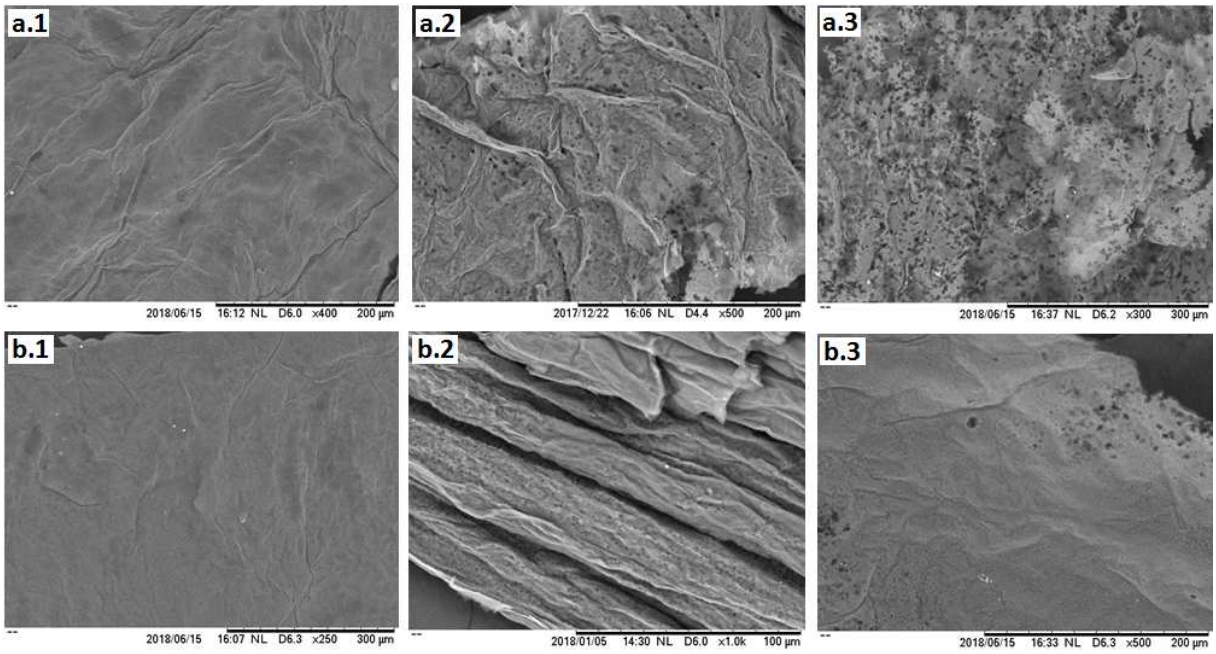

***Figure III-14**: Carbonized films of GO-KL at ratios 80:20 (a) and 20:80 (b) prepared at different heating rates: 5°C/min (1), 2.5°C/min (2) and 0.5°C/min + 1°C/min (3)*

III.2.3 Carbon Structure of Lignin-Graphene Oxide Films

The impact of graphene oxide (GO) flakes on the carbon structure of lignin was studied by X-ray diffraction (XRD) measurements. Films made from GO-lignosulfonate (LS) and from GO-Kraft lignin (KL) at different ratios were characterized by means of a Rigaku Nanoviewer (MicroMax 007HF) with a rotating anode coupled to a confocal Max-Flux® Osmic mirror operating at a wavelength of 1.5418 Å. The spectra of pure GO, pure lignin and different GO-lignin films were compared before and after carbonization. From the graphs in Figure III-15-a and III-16-a respectively, a clear diffraction peak at a scattering angle 2-Theta of 10-11° corresponding to the crystalline structure of GO can be recognized for the pure GO films before carbonization. In the case of GO-LS 67:33, this GO peak is found to be broadened and shifted towards lower scattering angles. The peak position and -shape suggest that LS molecules could be present between GO flakes, pushing them apart (see Figure III-15-a, orange curve). At higher LS contents, the GO peak was found to disappear, whereas many small peaks, possibly due to inorganic impurities, appear in the spectra at 20-35°. Besides, diffraction peaks at 42° were found in all samples except the pure lignin films, both before and after carbonization (compare spectra on left and right side). This scattering angle usually corresponds to the in-plane ordering of a hexagonal lattice (d_{100} of graphite), indicating that GO flakes are detected in these samples.

Considering the XRD spectra of the films after carbonization (Figures III-15-b and III-16-b), the diffraction peak of graphite at 26°, corresponding to $d_{002,}$ can be detected in all films containing GO. The position at 26° thus indicates an existence of dense graphitic domains in all GO-lignin films, whose possible arrangement is depicted in Figure III-17. In comparison, the pure LS and

pure KL films seem to exhibit only small carbon crystals with a low density. Depending on the GO-lignin ratios, the intensity of the graphite diffraction peak seems increased and its width slightly decreased at higher GO contents. These results suggest larger graphitic domains with larger carbon crystal sizes in films with higher GO contents. The concept of an improved ordering in lignin-based carbon through GO flakes seems valid even for a low GO content of 11 %. However, the broad overall shape of the diffraction peaks still indicates a poor crystallinity of the graphitic domains inside the films.

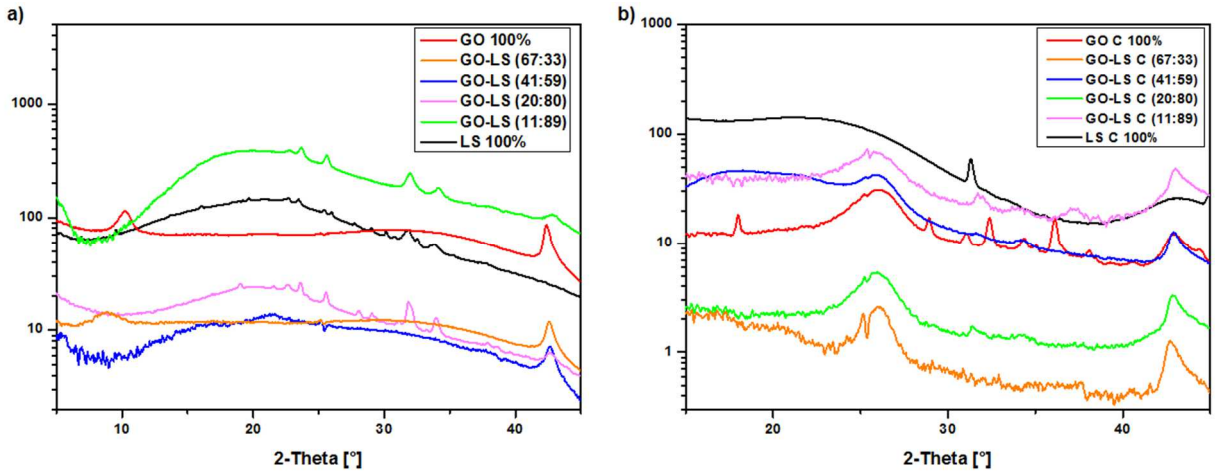

***Figure III-15**: XRD spectra showing scattered intensity depending on the scattering angle (2-Theta) of graphene oxide-lignosulfonate (LS) films before (a) and after carbonization (b)*

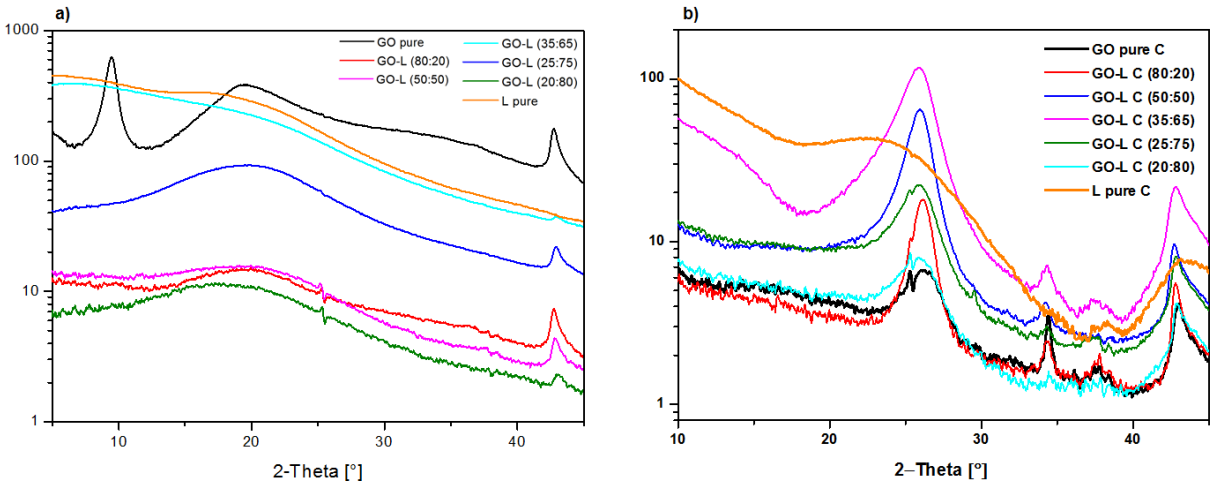

***Figure III-16**: XRD spectra showing scattered intensity depending on the scattering angle (2-Theta) of graphene oxide (GO)-Kraft lignin (KL) films before (a) and after carbonization (b)*

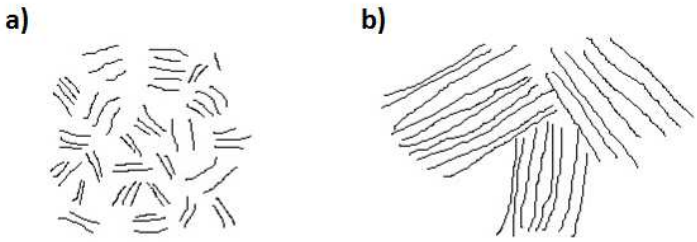

***Figure III-17**: Schematic structures of lignin-based carbon planes (a) vs. graphene oxide-lignin carbon planes (b)*

The impact of the heating rates used for carbonization on the obtained XRD spectra was investigated for the carbon films GO-KL 80-20 and 20-80. Three different heating rates were applied (5 °C min^{-1}, 2.5 °C min^{-1} and 0.5 +1 °C min^{-1}) and from SEM images an increased pore size in the carbon films after slow carbonization was observed (see *chapter III.2.2*). It becomes clear that for both ratios within GO-KL films, the films carbonized at 2.5 °C min^{-1} exhibited the sharpest diffraction peaks at 26°, suggesting the existence of graphitic domains (see Figure III-18). It can be noted that these domains are found larger and of larger crystal size at a higher GO content (see Figure III-18-a) compared to a higher KL content. After a fast heating rate during carbonization (5 °C min^{-1}), the resulting diffraction peaks are potentially shifted towards lower angles of ≤ 20°, whereas at a slow carbonization (0.5 +1 °C min^{-1}), a peak at 26° of reduced intensity and a peak around 20° seem to coexist. These results suggest on the one hand that a fast heating process may not provide enough time for the formation of graphitic domains during carbonization. On the other hand, a very slow heating process may provoke an increased degradation of the samples, thus hindering the carbon structure formation. Consequently, an intermediate heating rate was found to be the most suitable way to obtain large and dense graphitic domains within carbonized GO-KL films. According to the film morphologies, this rate also led to the lowest porosity on the carbon film surfaces (see *chapter III.2.2*). It can thus be concluded that a carbonization rate of 2.5 °C min^{-1} resulted in lignin-GO-based carbon films with the highest quality.

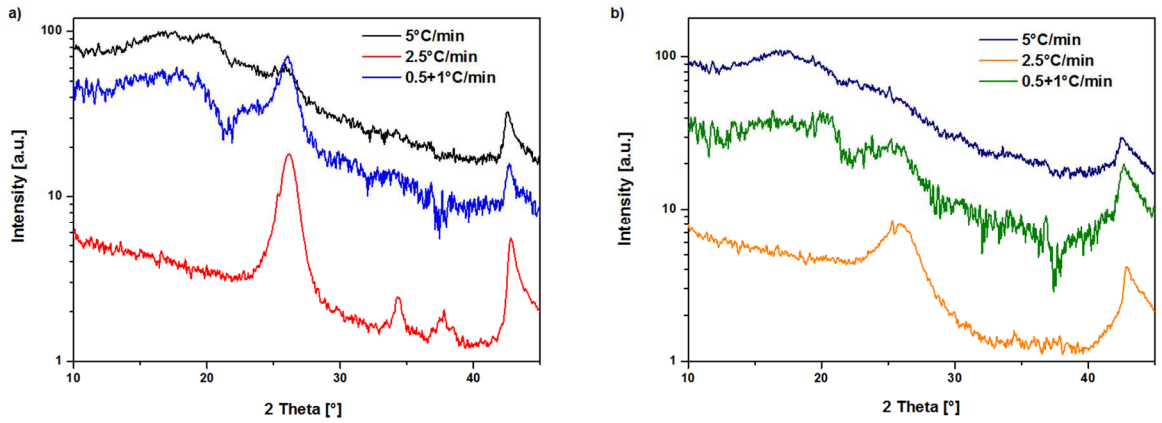

***Figure III-18**: XRD spectra showing scattered intensity depending on the scattering angle (2-Theta) of graphene oxide (GO)-Kraft lignin (KL) films carbonized at different heating rates (5°C/min, 2.5°C/min and 0.5°C/min+1°C/min) in ratios GO-KL 80-20 (a) and GO-KL 20:80 (b)*

Generally, it can be concluded that graphitic domains based on GO flakes can be introduced inside films made of amorphous lignin-based carbon. The poor alignment of these domains could be related to the preparation method of the films, since no particular direction is induced during solvent evaporation. However, regarding carbon fibre applications, an alignment of GO liquid crystals can be expected during wet-spinning, thus promising an oriented graphitic carbon structure for lignin-GO composite fibres.

III.2.4 Electrical Conductivity of Lignin-Graphene Oxide Films

Additionally to XRD measurements, the orientation of carbon planes within a given sample can be investigated by measuring the sample's electrical conductivity. The carbonized lignin-graphene oxide films were cut into rectangles and two opposing sides were fixed by means of conducting silver ink onto a glass substrate (see Figure III-19). Based on Ohm's law (equation III-2), the electrical resistance *R* of the films was measured with an electrometer (Keithley 6517B) operating at 0.1 V. The sample geometry (length and width) was determined with a sliding calliper, whereas the sample thickness was measured based on SEM images. From the obtained values, the cross-sectional surfaces *S* of the samples were calculated respectively. Based on equation III-3, the resistivity ρ was calculated from the measured values, which is inversely proportional to the electrical conductivity σ (see equation III-4).

$$U = R \cdot I \qquad (III\text{-}2)$$

(, where *U* is the applied tension [V], *R* the resistance [Ω] and *I* the electric current [A].)

$$R = \frac{\rho \cdot L}{S} \qquad (III\text{-}3)$$

(, where *R* is the resistance [Ω], ρ the resistivity [Ω·m], *S* the cross-sectional surface [m²] and *L* the length [m] of the sample.)

$$\sigma = \frac{1}{\rho} \qquad (III\text{-}4)$$

(, where σ is the electrical conductivity [S m^{-1}] of the sample.)

The electrical conductivity of carbon-based materials in bulk is much lower compared to metals. Their conductivity generally depends on their molecular structure and the availability of delocalized π-electrons (sp^2 hybridized structures).[16] Diamond is an insulator (10^{-13} S m^{-1}) since all outer electrons of each C-atom are localized (sp^3 hybridized carbon), whereas graphite possesses one delocalized electron per C-atom (sp^2) and is thus a conducting material (10^5 S m^{-1}).[17] Graphene by itself is highly conductive on the microscopic scale (10^5 S m^{-1}), but when assembled into macroscopic materials, its conductivity is usually decreased (e.g. graphene fibres 10^4 S m^{-1}).[18] Graphene oxide can be considered as an

insulator in its original state, but by chemical- or thermal reduction methods, it can be easily converted into electrically conductive graphene.[7]

The carbonization process of graphene oxide-based materials can be considered as thermal reduction. Upon heating, a high and drastic mass loss in thermogravimetric measurements can be observed around 180 °C, corresponding to the thermal reduction process of graphene oxide (GO) into reduced graphene oxide (rGO) (see Figure A-III-2-b in annex). Therefore, the electrical conductivity of the pure GO film was measured before and after carbonization. As expected, the electrical conductivity obtained for the GO film before carbonization was within the range of 10^{-1} S m^{-1}, thus an insulating material. After carbonization at 1200 °C, the conductivity of the GO film increased to $2x10^{4}$ S m^{-1}, hence GO was transformed into a conductive material. Since all the films prepared from GO and lignin were found insulating before carbonization, only the electrical conductivities of the carbonized films were evaluated.

As can be recognized from the film cross-sections (see *chapter III.2.2*), in some cases the films were found to consist of several layers of GO and lignin. Depending on the packing density of these layers, the overall film cross-section was found inflated or swollen in some cases, with air in between the layers. The sample thickness was thus difficult to evaluate and only approximate thickness ranges could be determined based on measurements at the densest parts. These thickness ranges were used to evaluate the electrical conductivity range. The obtained values should only be considered as indication and not as absolute values (see error bars in Figure III-19). With respect to the evaluation, only tendencies and ranges of magnitude are compared.

Figure III-19 demonstrates the electrical conductivity values obtained for the carbonized films with respect to the lignin concentration within the films. The electrical conductivity of GO-Kraft lignin (KL) films was found higher than that of the GO-lignosulfonate (LS) films. This could be related to the denser morphology found for the carbonized KL film compared to the carbonized LS film (see *chapter III.2.2*). A denser carbon structure usually leads to higher electrical conductivities. Due to the fact that the highest conductivities ($3\text{-}7x10^{4}$ S m^{-1}) were found for films containing KL ratios of 55-75 %, a synergistic effect between GO and KL could be assumed. In the case of GO-LS, the initial GO conductivity was rather decreased upon combination with LS. As already stated in *chapter III.1.3*, this observation could suggest a phase separation between GO and LS, thus decreasing the conductivity of GO through large insulating LS domains. The electrical conductivity values of pure GO and GO-lignin films was generally found within the reference range of graphene fibres ($2.5x10^{4}$ S m^{-1}), whereas pure KL- and LS films showed conductivities around the reference value of amorphous carbon (see Table III-1). These findings are in agreement with the amorphous- and crystalline molecular structure of lignin and GO respectively.

Four selected films were carbonized at different heating rates and their resulting electrical conductivities were directly compared. As shown in Figure III-20, the electrical conductivity range seems slightly decreased for the films carbonized more slowly (at 0.5 °C min^{-1} + 1 °C min^{-1}) both for GO-KL and GO-LS films. The films carbonized at 2.5 °C min^{-1} and

5 °C min^{-1} showed electrical conductivities within the same order of magnitude. As has been observed on SEM images, the films carbonized at the lowest heating rate exhibited the highest porosity (largest pore size). Based on this observation, it can be assumed that the density of these films is lower than for the other films, thus leading to a decreased conductivity. The corresponding electrical conductivity values presented in Figure III-20 are listed in the annex (see Table A-III-2).

Table III-1: Reference values for electrical conductivity of carbon-based materials (left side [17], [18]) and experimental results of lignin-graphene oxide films

References	
Material class[17]	**Electrical Conductivity [S m^{-1}]**
Insulators	< 10^{-8}
Semi-Conductors	10^{-8} - 10^{3}
Conductors	> 10^{3}
Carbon-based conductors	**Electrical Conductivity [S m^{-1}]**
Amorphous Carbon[17]	1.3-2x10^{3}
Graphene Fibres[18]	2.5x10^{4}
Graphitic Carbon (parallel planes)[17]	2-3x10^{5}

Lignin-Graphene Oxide-based Carbon Films	
GO – KL	**Electrical Conductivity [S m^{-1}]**
100-0	2.1x10^{4}
80-20	1.1-3.2x10^{4}
50-50	1.3-5.3x10^{4}
35-65	4.5-9x10^{4}
25-75	6.0x10^{4}
20-80	9.5x10^{3} -2.5x10^{4}
0-100	5.8x10^{3}
GO – LS	**Electrical Conductivity [S m^{-1}]**
100-0	2.1x10^{4}
67-33	2.6x10^{3}
41-59	4.7x10^{3}-2.5x10^{4}
20-80	5.6x10^{3}
11-89	1.2-4.4x10^{4}
0-100	2.7x10^{2}

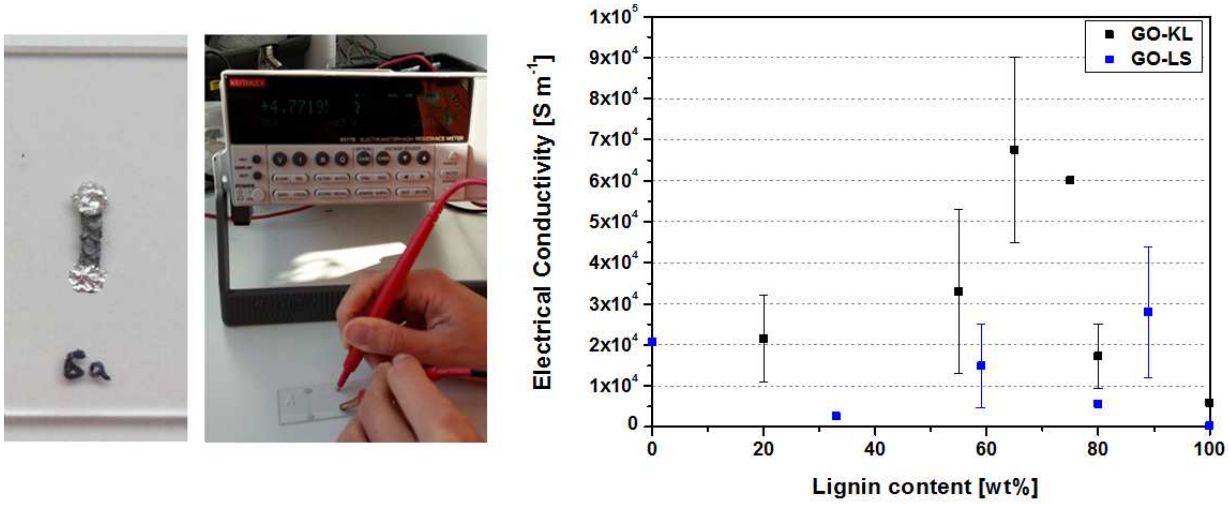

***Figure III-19**: Electrical conductivity measurements: setup (left) and results obtained for carbonized films of graphene oxide-Kraft lignin (right, black points) and graphene oxide-lignosulfonate (right, blue points)*

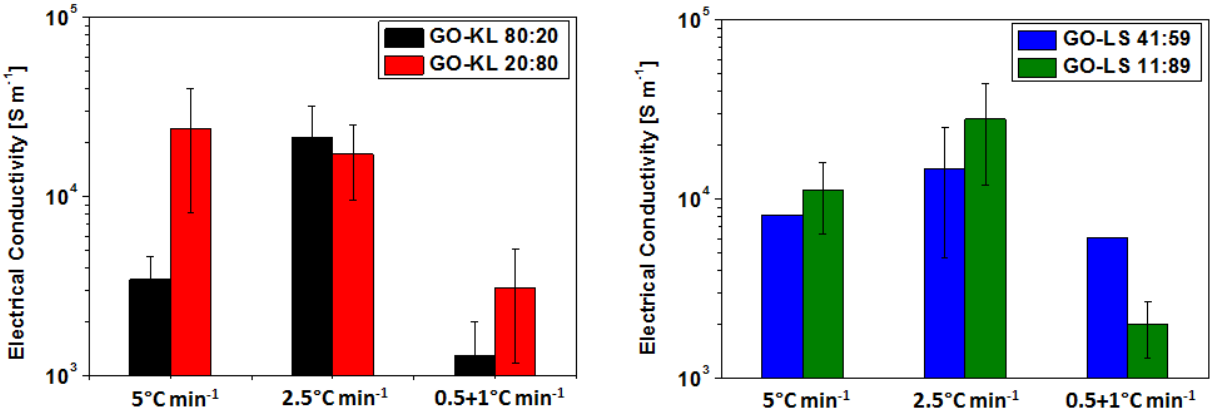

***Figure III-20**: Electrical conductivity obtained for films carbonized at different heating rates (5°C min^{-1}, 2.5°C min^{-1} and 0.5°C min^{-1}+1°C min^{-1}): graphene oxide-Kraft lignin films at ratios 80-20 and 20-80 (left) and graphene oxide-lignosulfonate films at ratios 41-59 and 11-89 (right)*

It can be concluded that composite films prepared from lignin and graphene oxide are electrically conductive after carbonization at 1200 °C. Their conductivity lies within the same range of graphene fibres, even at high lignin ratios. A dense carbon structure of GO-KL films was found, whereas carbonized GO-LS films exhibited a high porosity. Therefore, the conductivity of the GO-LS films was found slightly decreased.

In order to characterize these systems in more detail and to confirm the findings, their preparation method may have to be adjusted for future trials. On the one hand, the films should be prepared by an evaporation of a defined quantity of solution or by coating on a substrate. On the other hand, the drying process of the films should be improved to avoid swelling of the film layers or creation of pores due to the solvent evaporation. A different technique to measure the film thicknesses could also be useful to obtain more exact conductivity values and to decrease the length of the error bars. Further experiments could also include chemical reduction or doping of the films in order to enhance the performance of the GO-lignin composite films in terms of electrical conductivity.

III.3 Lignin-Graphene Oxide Fibres

In order to investigate whether the principle of introducing graphene oxide (GO) into lignin can also be transferred to fibre spinning applications, the wet-spinning of Kraft lignin (KL) and lignosulfonate (LS) in combination with GO has been performed on laboratory scale. The obtained fibres were characterized regarding their morphology before and after carbonization and the electrical conductivity of carbonized LS-GO fibres was determined. The results are presented in this subchapter.

III.3.1 Wet-Spinning of Lignin-Graphene Oxide Fibres

The lignin solutions were prepared by dissolution in water (LS) or in DMSO (KL and LS) at room temperature at 1-10 wt%. An aqueous GO solution (Graphenea) at 0.4 wt% was concentrated to 3-5 wt% by two centrifugation steps (1400 g, 20 min + 50440 g, 60 min). The two separate stock solutions were then mixed in different ratios depending on the desired concentration in the dried fibres (see Table III-2). Mixing was performed with magnetic stirrer bars at room temperature until homogeneous blend solutions were obtained. By optical microscopy under normal light and polarized light, the homogeneity and the phase behaviour of the mixtures were evaluated.

The micrographs in Figure III-21 show three selected dope solutions of LS and GO in different ratios (KL-GO dope solutions can be found in annex, Figure A-III-3). The total concentration within the dopes and the LS concentration decrease from left to right, thus leading to an increasing GO ratio. The upper micrographs were taken under normal light and they indicate homogeneous mixtures with only few aggregates within the dopes (see Figure III-21-a.1 and -b.1). The lower micrographs were taken under polarized light with crossed polarizers, revealing birefringent Schlieren textures. These structures indicate an organization of GO into a nematic liquid crystalline phase. Additionally, a shear was applied on the samples by moving the glass coverslips in a defined direction, thus simulating the flow direction during spinning. The alignment of GO flakes can clearly be recognized.

Rheology measurements are a common way to demonstrate the alignment of GO flakes under shear. Due to a limited amount of sample solutions, no rheology measurements were performed on the lignin-GO solutions presented in this thesis. However, from literature (e.g. Gao et al.,[7] see Figure III-22) it is known that liquid crystalline dope solutions show a strong shear-thinning behaviour due to the alignment of anisotropically shaped crystals in the flow direction.[7] This alignment should thus considerably enhance the flow behaviour of lignin solutions at high shear rates (e.g. 100 s^{-1}), while increasing their viscosities at low shear rates (e.g. 0.1 s^{-1}).

Generally, it is also possible to study the orientation of GO flakes in solution by means of small angle X-ray scattering (SAXS) as shown in *chapter III.1.3*. However, the concentration of GO in the spinning dopes used for this thesis was not high enough to obtain a signal on the given SAXS instrument (Bruker Nanostar).

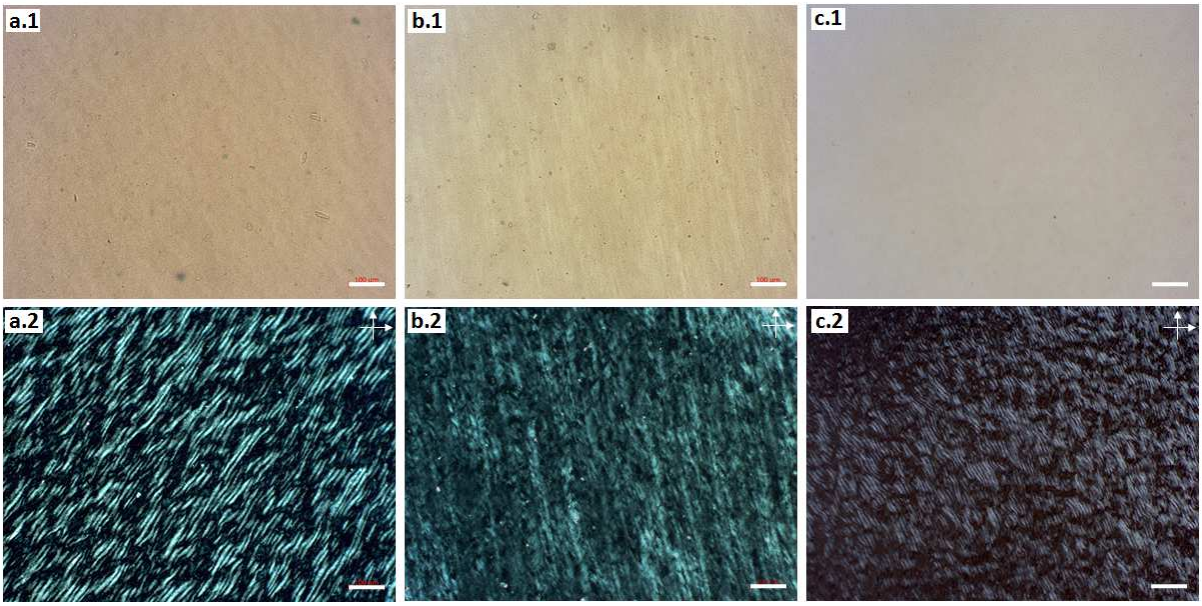

Figure III-21 : *Optical micrographs of lignosulfonate-graphene oxide dope solutions at ratios 7.5wt%-0.8wt% (a), 3.3wt%-1.7wt% (b) and 0.6wt%-1.5wt% (c) under normal light (1) and under polarized light at crossed polarizers (2), scale bars: 100µm*

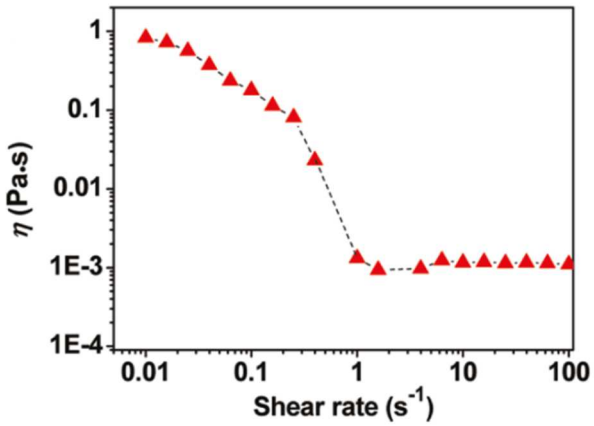

Figure III-22*: Viscosity of GO aqueous solution at 0.005 wt% as a function of shear rate (graph from [7])*

It can be assumed that during the spinning process used for our lignin-GO fibres, the GO flakes start to align in flow direction due to the applied shear upon entering into the tube or needle (see Figure III-23). The shear rate $\dot{\gamma}$ applied on our dope solutions flowing at a rate Q of 10-15 ml/h through a cylindrical die at a radius R of 150 µm was calculated to 1050-1570 s^{-1} by using equation III-5:[19]

$$\dot{\gamma} = \frac{4Q}{\pi \cdot R^3} \qquad \textit{(III-5)}$$

With respect to Figure III-22, it can be recognized that at shear rates within this high dimension, the GO flakes within the dope should be completely aligned upon exiting the die and hence right before coagulation.

The incorporation of GO flakes into a lignin dope should thus facilitate the spinning process and improve the structural properties of the fibres before and after carbonization.

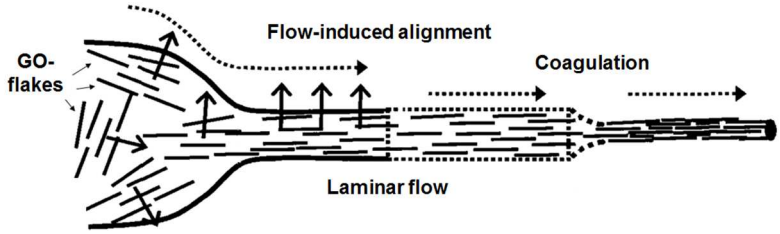

Figure III-23 *: Possible flow pattern of graphene oxide (GO) flakes in wet-spinning solutions (adapted from [18])*

The L-GO spinning dopes were injected by means of a syringe pump into a turning beaker containing the coagulation bath (see scheme in Figure III-24 and Figure III-24-a). The used counter-solvents for LS-GO and KL-GO fibres were ethanol and aqueous $CaCl_2$ (1 wt%) respectively. Regarding the overall spinning performance, the LS-based solutions showed a higher ease of spinnability than the solutions containing KL. The obtained LS-GO fibres were generally longer and more flexible compared to the KL-GO fibres (see Figure III-24-d1 and –d2). Especially upon drying, the KL-GO fibres showed extremely high brittleness (see Figure III-24-b1 compared to b2). This result could be related to the different counter-solvents, such as that ethanol represents a more suitable counter-solvent for LS-GO than $CaCl_2$ for KL-GO. However, a more suitable counter-solvent for the KL-GO dope solutions has not been found. Coagulation worked well, especially for LS-GO dopes, but often the as-spun fibres were found to break under their own weight when removed from the bath. As described in Table III-2, the coagulation process was generally found facilitated with increasing GO contents within the spinning dopes. The longest fibres were obtained from the dopes containing the highest GO ratios (73-77 %), as shown in Figure III-24-a and –c. These results indicate an improved wet-spinning performance of LS and KL upon combination with GO liquid crystals. An overview of the tested spinning dope compositions and their processing parameters is given in Table III-2.

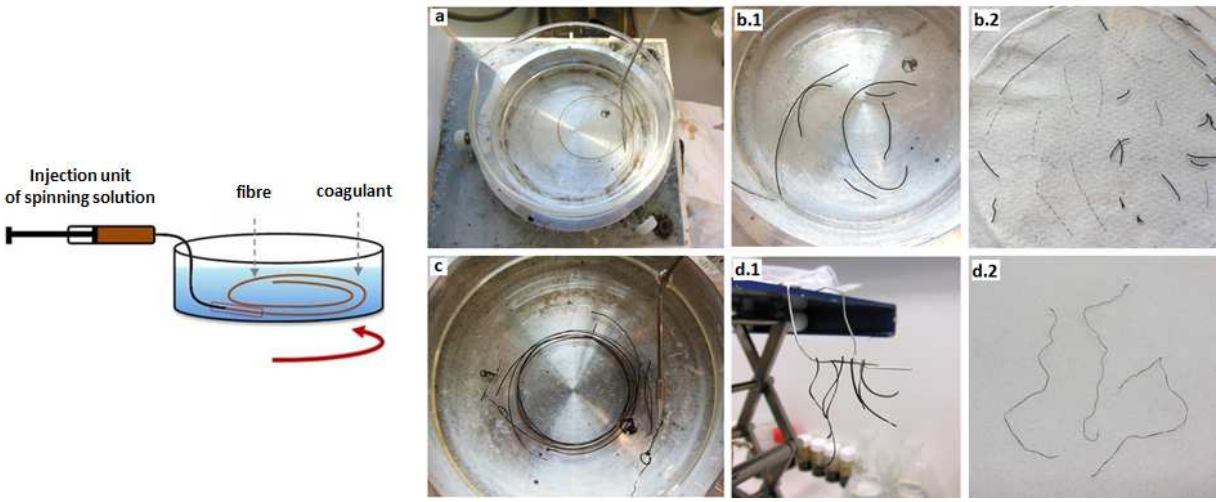

Figure III-24*: Scheme and photo of spinning setup with injection unit and turning coagulation bath (a), continuous wet-spinning of LS-GO fibres (c), as-spun KL-GO (b) and LS-GO (d) fibres in wet state (1) and after drying (2)*

Table III-2: Compositions and preparation parameters of wet-spun fibres from lignosulfonate-graphene oxide (LS-GO) and Kraft lignin-graphene oxide (KL-GO) solutions

Concentration in solution			**Concentration in fibre**		**Coagulation medium**	**Comments**
LS	**GO**	**total**	**LS**	**GO**		
7.5%	0.8%	12.6%	90%	10%	ethanol	coagulation difficult
3.3%	1.7%	5.2%	66%	34%	ethanol	good coagulation
0.6%	1.5%	2.2%	27%	73%	ethanol	very good coagulation
KL	**GO**	**total**	**KL**	**GO**		
4.3%	0.9%	5.2%	83%	17%	$CaCl_2$ (1 wt%)	coagulation difficult
5%	4.7%	9.7%	52%	48%	$CaCl_2$ (1 wt%)	coagulation difficult
0.6%	1.5%	2.2%	23%	77%	$CaCl_2$ (1 wt%)	good coagulation but brittle in dry state

III.3.2 Morphology of Lignin-Graphene Oxide Fibres

The obtained lignin-graphene oxide fibres were characterized with a scanning electron microscope (SEM) HITACHI TM3030 (after gold-palladium metallization with a Quorum SC7620 for increased image contrast) in order to visualize their morphologies. The fibres were fixed on a sample holder in a way that images of both cross-sections and surfaces could be taken respectively.

Figure III-25 depicts the composite fibres made of lignosulfonate (LS) and graphene oxide (GO), which have been coagulated in ethanol. Despite the different ratios used, the morphologies of the wet-spun LS-GO fibres have a similar appearance. The crumpled structure, especially on the fibre surfaces, strongly resembles the morphology of pure GO fibres.[18] It can be noted that at 90 % of LS, the fibre cross-section seems denser than the cross-sections of the fibres with higher GO contents (see Figure III-25-a1). Besides, a high amount of impurities can be found at the surface of the fibre containing 90 % of LS (see Figure III-25-a2). The high content of inorganic components within LS (around 22 %) has been demonstrated by TGA measurements (see Figure A-III-2-a, in appendix).

Comparing the fibres made from the two different lignin grades lignosulfonate (LS) and Kraft lignin (KL), the fibres based on KL and GO seem to have a denser structure than the LS-GO fibres. Besides, slightly less wrinkles could be found on their surfaces (see Figure III-26). Generally, the KL-GO fibres show rather flat cross-sections, which could be related to their drying process. In contrast to the LS-GO fibres, which could be dried in hanging state under a fume hood, the drying of KL-GO fibres was performed on a flat surface, since these fibres were too brittle to be manipulated otherwise (see Figure III-24-b2). Despite the fact that the denser structure of KL-GO fibres could be more suitable for composite applications, this route has not been pursued further due to a too high brittleness of these fibres.

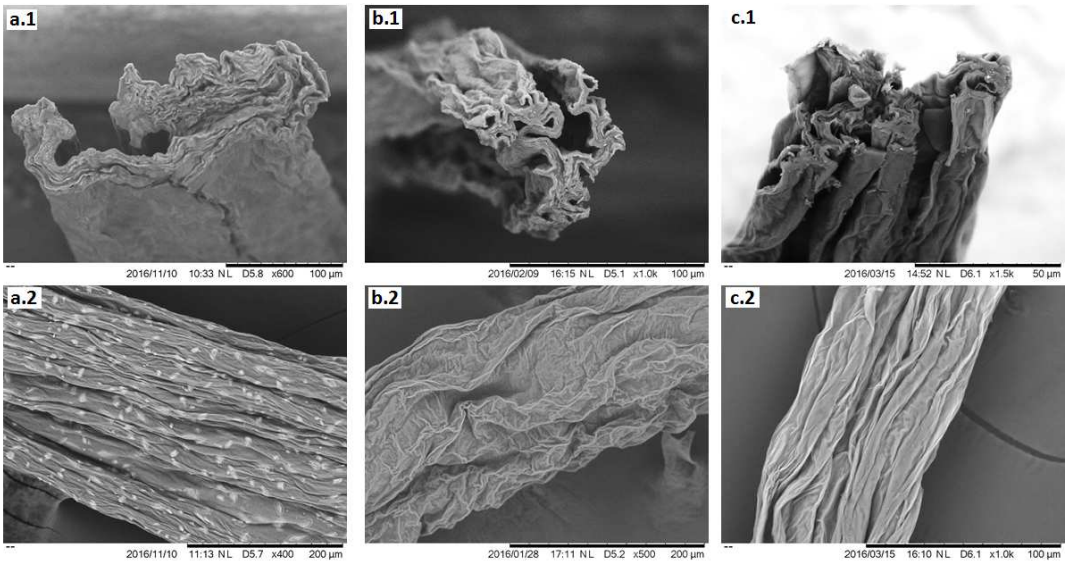

Figure III-25: *SEM images of lignosulfonate (LS)-graphene oxide (GO) fibre cross sections (1) and surfaces (2), ratios: 90%-10% (a), 66%-34% (b) and 27%-73% (c)*

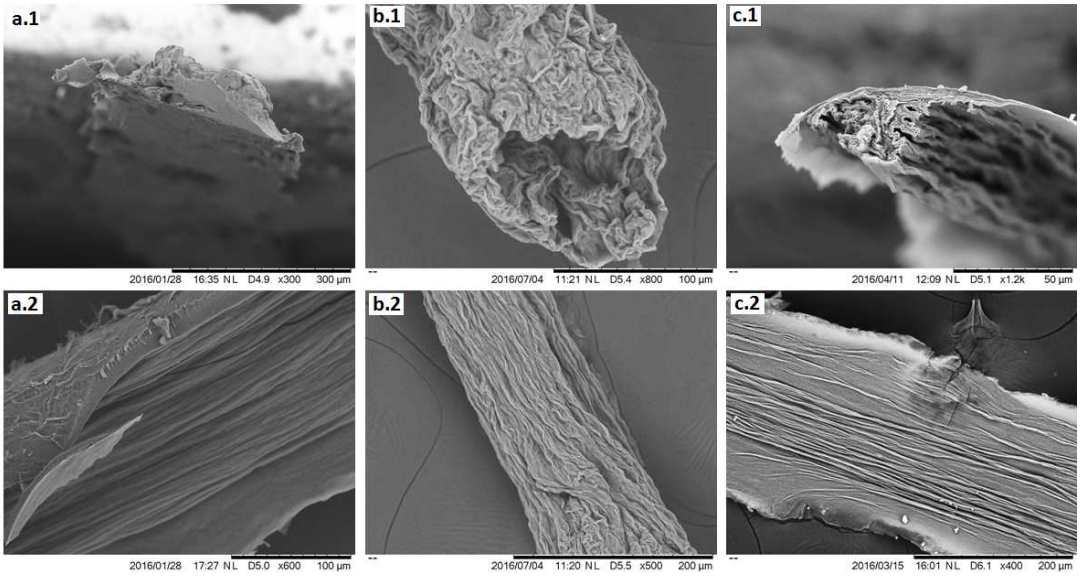

Figure III-26*: SEM images of Kraft lignin-graphene oxide fibre cross sections (1) and surfaces (2), ratios: 83%-17% (a), 52%-48% (b) and 27%-73% (c)*

III.3.3 Electrical Conductivity and Structure of Obtained Carbon

Due to high brittleness of the Kraft lignin-graphene oxide (GO) fibres, which made their manipulation too difficult, only the lignosulfonate (LS)-GO fibres were further characterized. The aim of introducing GO into lignin was to obtain a more organized and more crystalline carbon structure compared to the amorphous carbon structure of pure lignin. Similarly to the films characterized in *chapter III.2.4*, electrical conductivity measurements after carbonization gave an indication about the carbon structure within the LS-GO fibres.

Two types of LS-GO fibres with ratios 90-10 and 27-73 were placed inside a ceramic sample pan (see Figure III-25-d) and heated to 1200 °C under nitrogen inside a static carbonization oven (Nabertherm). The chosen temperature programme comprised the following steps: 20-280 °C (7.5 °C min^{-1}) + 280-360 °C (2 °C min^{-1}) + 360-480 °C (5 °C min^{-1}) + 480-1200 °C (7.5 °C min^{-1}). Due to a lack of sample quantity, TGA measurements could not be performed on these samples, which is why this standardized method for bio-based fibres at CANOE was used for carbonization.

The morphology of the carbonized LS-GO fibres was visualized by SEM images in the same manner as for the precursor fibres (see *chapter III.3.2*). As shown in Figure III-27-a-c, no significant morphological differences can be found between the precursor- and the carbon fibres (to be compared with Figure III-25). This result indicates that the crumpled surface and the cross-section composed of more or less compressed layers are conserved during the carbonization process, which is in agreement with literature.[20]

In order to obtain a better understanding of the crystallinity and the carbon structure of the LS-GO fibres after carbonization, their electrical conductivity was characterized. As described in *chapter III.2.4*, both fibre ends were fixed onto a glass substrate with conducting silver ink and the electrical resistance *R* of the samples was measured with an electrometer (Keithley 6517B). Based on equation III-3 and III-4, the electrical conductivity was calculated by taking into account the fibre length and cross-sectional area. The results presented in Figure III-27-e show that the LS-GO fibres with a higher GO content exhibit an increased electrical conductivity compared to the fibres with a higher LS content. More specifically, the conductivity was found to increase by one order of magnitude. This result can be explained by the amorphous structure of lignin compared to the lamellar/graphitic structure of GO planes, which is conserved during carbonization. As becomes clear from the results, an electrical current can flow more easily through a crystalline than through an amorphous material. Interestingly, at LS contents of 27 % within the precursor fibre, an electrical conductivity in the range of 10^4 S m^{-1}, and thus almost as high as the value for pure graphene fibres, was obtained. These results indicate the potential of the concept presented in this thesis and they indicate various possibilities for applications of LS-GO fibres in electronic applications.

Finally, the electrical conductivity values of the carbonized LS-GO films presented in *chapter III.2* were found within the same orders of magnitude than those of the LS-GO-based carbon fibres. Given their different preparation methods, improved properties would have been expected for the fibres due to the alignment of GO flakes induced during spinning, which does not occur for the films. However, it has to be noted that a direct comparison of the presented films and fibres is not possible since different heating rates were used for carbonization. Besides, slightly different LS-to-GO ratios were used, so that the obtained results should only be considered as indications. A direct comparison between lignin- and GO-based films and -fibres will be evaluated in the following chapter.

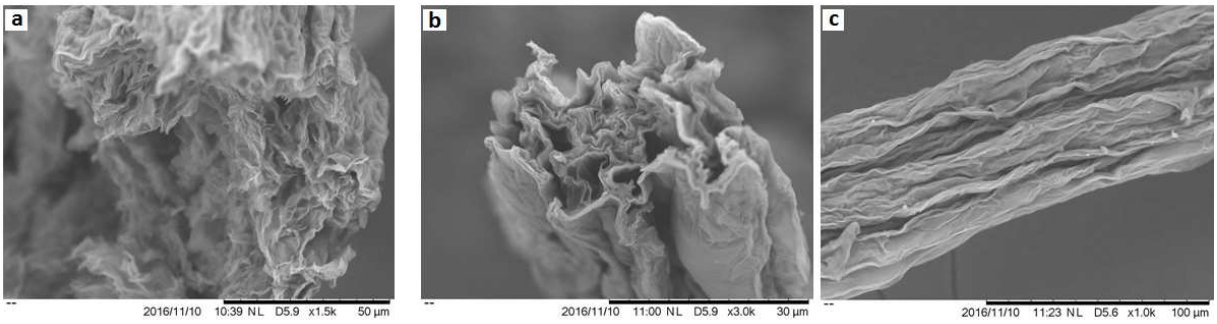

e

Carbonized Sample	Electrical Conductivity [S m^{-1}]
90% LS + **10% GO**	3.4-4.2 x $\mathbf{10^3}$
27% LS + **73% GO**	1.3-2 x $\mathbf{10^4}$
pure graphene fibre[18]	2.5 x $\mathbf{10^4}$

***Figure III-27**: SEM images of carbonized LS-GO fibres: 90%-10% (a), 27%-73% (b+c); sample pan used for carbonization (d) and electrical conductivity of given fibres (e)*

III.4 Conclusion

Different combinations of lignin (Kraft lignin, KL and lignosulfonate, LS) and graphene oxide (GO) have been prepared in solutions as well as in solid films and –fibres. The resulting properties of the lignin-GO films and –fibres have been characterized before and after carbonization. POM images of the solutions have revealed an alignment of GO flakes in presence of lignin and the formation of a nematic phase. This phase was found transferred into carbonized films and fibres since graphitic domains were demonstrated by XRD spectra. Furthermore, increased electrical conductivities indicated an increased crystallinity in the samples.

However, a high micro-porosity was recognized on the surfaces of the carbonized films and fibres due to degradation reactions induced by the heating process (see *chapter III.2.1* and *III.2.2*). The porosity was mainly found to be influenced by the amount of impurities inside the lignin grades and the heating rate used for carbonization. Its impact on the resulting carbon structure and -properties was shown through less pronounced XRD peaks and decreased electrical conductivities. An intermediate heating rate of 2.5 °C min^{-1} for carbonization of the lignin-GO films led to the best result in terms of decreased pore sizes and most pronounced graphitic domains. The micro-porosity of amorphous carbon being a general constraint for structural applications, further characterization should be performed in order to gain a better understanding of the mechanisms creating it. As also explained in *chapter II.4.1*, a possible reduction of the porosity could be achieved through an oxidative stabilization under air.

Regarding fibre wet-spinning applications, the approach of a GO reinforcement is promising since it would lead to lignin-based carbon fibres with enhanced structure. Unfortunately, the impact of the dope flow behaviour on the spinning performance could not be investigated in more detail due to only limited sample quantities. Rheology measurements on lignin-GO spinning solutions should be performed in the future. Besides, further samples should be prepared in order to directly compare the electrical conductivities of LS-GO films and –fibres.

The lignin-GO fibres, especially made from KL, were found to exhibit a very high brittleness in dried state, despite good spinning performances. The brittleness of these fibres can be considered as a strong restriction for industrial applications. The mechanical properties of the lignin-GO fibres could not be characterized due to high brittleness and limited sample quantity. Therefore, the use of a plasticizer is recommended and necessary in order to obtain flexible fibres that can be manipulated more easily up to the carbonization process. Despite the fact that such a system including three components would be very difficult to create and to characterize, it could open new market perspectives towards low-cost carbon fibres with enhanced structures. First attempts to create these fibres are presented in the last chapter of this thesis.

References

[1] P.-G. De Gennes and J. Prost, *The physics of liquid crystals (international series of monographs on physics)*, vol. 2. 1995.

[2] M. J. Stephen and J. P. Straley, 'Physics of liquid crystals', *Rev Mod Phys*, vol. 46, no. 4, pp. 617–704, Oct. 1974.

[3] D. Andrienko, 'Introduction to liquid crystals', *IMPRS Sch. Bad Marienb.*, 2006.

[4] T. Kato, Y. Hirai, S. Nakaso, and M. Moriyama, 'Liquid-crystalline physical gels', *Chem. Soc. Rev.*, vol. 36, no. 12, pp. 1857–1867, 2007.

[5] J. E. Kim *et al.*, 'Graphene oxide liquid crystals', *Angew. Chem. Int. Ed.*, vol. 50, no. 13, pp. 3043–3047, 2011.

[6] F. Lin, X. Tong, Y. Wang, J. Bao, and Z. M. Wang, 'Graphene oxide liquid crystals: synthesis, phase transition, rheological property, and applications in optoelectronics and display', *Nanoscale Res. Lett.*, vol. 10, no. 1, p. 435, 2015.

[7] Z. Xu and C. Gao, 'Aqueous Liquid Crystals of Graphene Oxide', *ACS Nano*, vol. 5, no. 4, pp. 2908–2915, 2011.

[8] Y. H. Shim, K. E. Lee, T. J. Shin, S. O. Kim, and S. Y. Kim, 'Wide concentration liquid crystallinity of graphene oxide aqueous suspensions with interacting polymers', *Mater Horiz*, vol. 4, no. 6, pp. 1157–1164, 2017.

[9] W. Meng *et al.*, 'Structure and Interaction of Graphene Oxide– Cetyltrimethylammonium Bromide Complexation', *J. Phys. Chem. C*, vol. 119, no. 36, pp. 21135–21140, 2015.

[10] A. G. Hsieh, S. Korkut, C. Punckt, and I. A. Aksay, 'Dispersion stability of functionalized graphene in aqueous sodium dodecyl sulfate solutions', *Langmuir*, vol. 29, no. 48, pp. 14831–14838, 2013.

[11] C. Zamora-Ledezma *et al.*, 'Liquid Crystallinity and Dimensions of Surfactant-Stabilized Sheets of Reduced Graphene Oxide', *J. Phys. Chem. Lett.*, vol. 3, no. 17, pp. 2425–2430, 2012.

[12] X. Hou *et al.*, 'Novel dextran/graphene oxide composite material as a sorbent for solid-phase microextraction of polar aromatic compounds', *RSC Adv.*, vol. 5, no. 28, pp. 21720–21727, 2015.

[13] Kirk-Othmer, *Kirk-Othmer Chemical Technology of Cosmetics*. John Wiley & Sons, 2012.

[14] J. Zhao, W. Xiuwen, J. Hu, Q. Liu, D. Shen, and R. Xiao, 'Thermal degradation of softwood lignin and hardwood lignin by TG-FTIR and Py-GC/MS', *Polym. Degrad. Stab.*, vol. 108, pp. 133–138, 2014.

[15] Olsson Carina, Sjöholm Elisabeth, and Reimann Anders, 'Carbon fibres from precursors produced by dry-jet wet-spinning of kraft lignin blended with kraft pulps', *Holzforschung*, vol. 71, no. 4, p. 275, 2017.

[16] J.-C. Charlier and J.-P. Issi, 'Electrical conductivity of novel forms of carbon', *J. Phys. Chem. Solids*, vol. 57, no. 6–8, pp. 957–965, 1996.

[17] A. M. Helmenstine, 'Table of Resistivity and Conductivity at 20°C', *ThoughtCo. Table Table of Resistivity and Conductivity*. [Online]. Available: https://www.thoughtco.com/table-of-electrical-resistivity-conductivity-608499.

[18] Z. Xu and C. Gao, 'Graphene fiber: a new trend in carbon fibers', *Mater. Today*, vol. 18, no. 9, pp. 480–492, 2015.

[19] A. Y. Malkin and A. I. Isayev, *Rheology: concepts, methods, and applications*. Elsevier, 2017.

[20] Y. Li *et al.*, 'Highly Conductive Microfiber of Graphene Oxide Templated Carbonization of Nanofibrillated Cellulose', *Adv. Funct. Mater.*, vol. 24, no. 46, pp. 7366–7372, 2014.

Chapter IV Preparation and Characterization of Lignin-Nanocomposite Films and -Fibres

This chapter can be considered as a conclusion of the work presented in this thesis, combined from the ideas, approaches and results of *chapter II* and *chapter III*. More specifically, graphene oxide (GO) flakes were incorporated into the system of Kraft lignin (KL) and polyvinyl alcohol (PVA) which was found suitable for continuous wet-spinning and for carbonization. The impact of GO on the amorphous structure of industrially processable lignin fibres was thus demonstrated for the first time. Furthermore, cellulose nanocrystals (CNCs) were evaluated as another possible anisotropic filler material for lignin-PVA fibres. The three-component dope solutions were used to prepare nanocomposite films and well as nanocomposite fibres with subsequent carbonization. By characterizing and comparing the obtained structures and properties of the carbon films and carbon fibres, their potential for future industrial applications was evaluated.

IV. 1 Lignin-PVA-GO and Lignin-PVA-CNC Films

As a conclusion of the work presented in this thesis, the systems of Kraft lignin (KL) and polyvinyl alcohol (PVA) (see *chapter II*) as well as Kraft lignin (KL) and graphene oxide (GO) (see *chapter III*) have been combined for wet-spinning applications of KL-based fibres with enhanced structuration. Spinning dopes containing KL, PVA and GO have thus been used to prepare nanocomposite fibres and –films. Additionally, cellulose nanocrystals (CNCs) have been evaluated as structural reinforcement for KL-PVA fibres and -films. The preparation and characterization of nanocomposite films made from KL-PVA-GO and KL-PVA-CNC solutions are presented and evaluated in this subchapter.

IV.1.1 Preparation of Solutions and of Nanocomposite Films

Two different compositions of KL-PVA-GO and KL-PVA-CNC solutions in DMSO were prepared for wet-spinning trials. Fixing the desired concentration of GO and CNC inside the dried fibres and films to 5 % and 10 % respectively, four different solutions were prepared. Thereby, the KL-to-PVA ratio inside the remaining 90-95 % of the fibres and films was kept at 70:30, as chosen for the pure KL-PVA fibres in *chapter II*. In order to keep the solid content inside the dope solutions as high as possible, the preparation protocol was changed with respect to the KL-PVA and KL-GO spinning dopes of *chapters II* and *III*. Previous spinning trials had shown that spinning dopes at low concentrations were more difficult to coagulate into fibres. Therefore, the KL powder was directly introduced into the GO- or CNC solutions prior to mixing with a PVA solution.

At first, a GO solution in DMSO was prepared as described in *chapter III.1.2* by an exchange of solvent and subsequent concentration by three centrifugation steps. The initial commercial 0.4 wt% aqueous GO solution (Graphenea) was hence transformed into a GO solution in DMSO at 1.67 wt%. CNCs (University of Maine, USA) were dissolved in DMSO at 2.8 wt% with a tip sonicator (Sonics 500/750 W) during 2 x 45 min at an amplitude of 25 % (pulse on: 2 s, pulse off: 1 s) at room temperature. The KL powder (from softwood, FCBA) was added into the GO- and CNC solutions in the respective quantities and stirred with magnetic stirrer bars at room temperature for 24 h. Afterwards, a PVA solution at 11.4 wt% in DMSO (prepared as explained in *chapter II.1.2*, p.57) was added to the mixtures and stirred at room temperature for 30 min. The quantities for the sample preparation and the resulting concentrations within the four samples are listed in detail in Table A-IV-1 (see annex). The following four dope solutions were used to prepare the composite fibres and films:

- “KL-PVA-GO 5 %” (**16 wt%** in solution; **66% KL, 29% PVA, 5% GO** in dried state)
- “KL-PVA-GO 10 %” (**11 wt%** in solution; **63.5% KL, 26% PVA, 10.5% GO** in dried state)
- “KL-PVA-CNC 5 %” (**20 wt%** in solution; **66% KL, 29% PVA, 5% CNC** in dried state)
- “KL-PVA-CNC 10 %” (**15 wt%** in solution; **63.5% KL, 26% PVA, 10.5% CNC** in dried state)

The dope solutions were characterized by optical microscopy both under normal light and under polarized light with crossed polarizers (POM). The micrographs of Figure IV-1 were taken directly after mixing and after applying shear on the glass coverslips located on top of the samples.

From the images taken under normal light, it becomes clear that the samples consist of homogeneous mixtures with only a few aggregates. The aggregates (see Figure IV-1-a) were also found to be present in the initial GO solution in DMSO, possibly due to the centrifugation processes during the solvent exchange. In general however, the images suggest that the three components KL, PVA and GO formed homogeneous and well-dissolved, miscible systems in a monophasic state. The same observation was made for the two systems of KL, PVA and CNCs (see Figure A-IV-1 in annex). However, it has to be noted that the optical micrographs of the KL-PVA-GO and –CNC solutions were taken immediately after mixing and that a biphasic system with separate KL- and PVA phases slowly started to form after some time. Besides, the dope solutions were found to form gels after 4-5 hours. These findings are in agreement with the “reference” KL-PVA system in DMSO at a ratio of 70:30 presented in *chapter II*. The GO- and CNC solutions in combination with KL and PVA can thus be considered as miscible, but metastable systems.

In optical micrographs with crossed polarizers, the birefringent properties of the liquid crystalline phase of anisotropic particles, such as GO and CNCs, can usually be visualized. For the dope solution at 0.8 wt% GO, 10.6 wt% KL and 4.6 wt% PVA (see Figure IV-1-a), a certain orientation induced by the applied shear can be recognized. Compared to the phase diagram of KL-GO solutions without PVA (see *chapter III.1.2*, p. 101), a solution at 0.8 wt% of GO in the presence of KL was found to be in the phase transition range between isotropic and nematic. This state seems still valid upon addition of PVA into the dope solution. However, for the sample at 1 wt% GO, 7 wt% KL and 3 wt% PVA, the texture of GO flakes was found modified (see Figure IV-1-b). In this case, it is possible that PVA molecules affect the liquid crystalline behaviour of GO, hindering an alignment of GO flakes under shear. Moreover, it is possible that the dissolution of KL powder directly inside the GO- and CNC solution leads to less homogeneous systems, in which the formation of a nematic phase is found hindered.

Although rod-like CNCs generally form liquid crystalline phases which even include cholesteric phases,[1] the most concentrated initial solution at 2.8 wt% in DMSO used for composite films and -fibres was found in an isotropic state (see dark micrographs of Figure A-IV-1 in annex). Depending on the aspect ratio of the cellulose nanocrystals, the concentration of the isotropic-to-nematic phase transition typically varies from < 1 wt% to about 5 wt%.[1] Knowing that rather short rods (150-200 nm) at low aspect ratios (30-40) were used for the samples, the concentration of the CNC solution at 2.8 wt% was found too low for a self-assembly into a nematic phase.[1] This CNC type is known to form liquid crystalline phases at only around 10 wt%. Besides, a small CNC size and a lack of resolution of the optical microscope could also contribute to the fact that no CNCs could be recognized in Figure A-IV-1. Trials to prepare more concentrated CNC solutions have been performed in DMSO, but at concentrations above 2.8 wt%, aggregates were found with bare eyes.

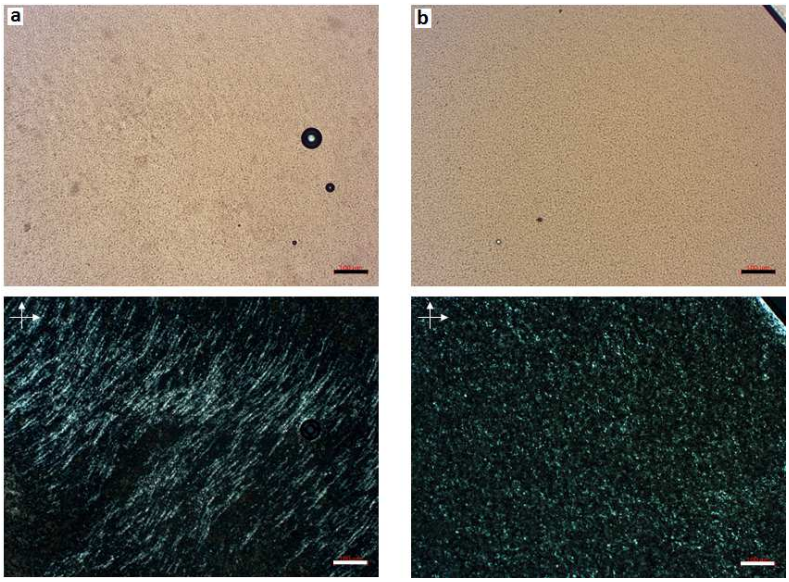

Figure IV-1: *Optical micrographs of dope solutions containing 0.8 wt% GO, 10.6 wt% KL and 4.6 wt% PVA in DMSO (a) and 1 wt% GO, 7 wt% KL and 3 wt% PVA in DMSO (b); under normal light (above) and polarized light (below); scale bars: 100 µm.*

Based on the KL-PVA-GO and KL-PVA-CNC dope solutions shown in Figure IV-1 and Figure A-IV-1, solid nanocomposite films were prepared by evaporation of DMSO at 45 °C for 3 days under vacuum (80 mbar). A Teflon mould and a polyethylene sheet were used as substrates respectively. A strong smell indicated remaining DMSO inside the films, despite the drying under vacuum. The temperature used for drying was kept as low as possible to avoid thermal degradation of CNCs, since colour changes of some CNC solutions had already been noticed at temperatures around 40-50 °C.

From the results and the experience obtained in *chapter II* and *III*, it becomes clear that the optical micrographs of the KL-PVA-nanocomposite dope solutions presented in Figure IV-1 do not represent an ideal base for fibre spinning and for well-structured carbon materials. Optimization trials in the future should include an alternative dope preparation method in order to obtain systems with a higher total concentration and systems whose concentrations are easily tuneable. Besides, a detailed study of the 4-component systems (including DMSO) should be performed, for instance by preparation of phase diagrams (as has been done in *chapter II* and *III*).

IV.1.2 Thermal Properties and Carbonization of Nanocomposite Films

As for some of the films made from lignin and GO (see *chapter III.2.1*), the prepared nanocomposite films were characterized by thermogravimetric analysis (TGA) with a TGA 5500 instrument (TA Instruments) in order to investigate their thermal degradation behaviour. The nanocomposite films were also compared to the reference film composed of KL and PVA in a ratio of 70:30. All samples were heated at 5 °C min^{-1} to 1200 °C under nitrogen with an isotherm at 45 °C during 1 h to remove potentially adsorbed water.

In TGA measurements performed on the pure components, KL powder shows a carbon residue of 43 % at 1200 °C (if 5 % of adsorbed water are removed beforehand, to be compared with Table II-6). In comparison, PVA exhibited only 0.06 % of carbon residue when heated to 1200 °C under inert atmosphere (see Figure IV-2-a). This result indicates that PVA molecular chains alone do not withstand high temperatures without degrading. Unless covalent bonds are introduced during mixing, the combination of KL with PVA should thus lower the overall carbon yield, as demonstrated by the KL-PVA film in Figure IV-2-a. However, the obtained residue of 37 % for this film is higher than the theoretically expected value, which would be around 30 %. On the one hand, the real residue could be due to partial bonding between KL and PVA, hence increasing the carbon yield to a certain extent. A high compatibility between KL and PVA in a ratio of 70:30 has already been demonstrated by the DMA results shown in *chapter II.1.3* and a small synergistic effect is thus possible.

Regarding the TGA evaluation, it also needs to be considered that DMA measurements revealed DMSO residues inside the films before carbonization, due to insufficient drying (see *chapter II.1.3*). The high mass loss of the KL-PVA film around 200 °C is thus associated to evaporating DMSO residues. Therefore, the actual carbon yields of the films could be even higher than the ones measured by TGA. However, the exact quantity of remaining DMSO was not determined within the framework of this thesis.

The thermal degradation of the KL-PVA reference film and of the KL-PVA-GO and KL-PVA-CNC nanocomposite films is compared in Figure IV-2-b. Similar quantities of DMSO residues (mass loss around 200 °C) are assumed for all the films due to an identical preparation method. The TGA results demonstrate that the carbon residue of the reference film is slightly decreased upon addition of CNCs, whereas it is significantly increased by addition of GO. TGA analysis of pure, freeze dried GO revealed a carbon residue of 41 %, whereas commercial cellulose is known for carbonization yields of only 10-20 %. The decrease of the KL-PVA carbon yield by CNCs is thus a logical consequence. However, since the carbon residue of pure KL and pure GO are within the same range, the strong increase in carbon yield by GO possibly indicates a synergistic effect between GO and KL or GO and KL+PVA. Functional groups such as hydroxyl-, carbonyl- or carboxyl groups, which can generally be found in lignin molecules, can also be present on the surface of GO flakes, thus creating possible bonding sites between the two materials. In any case, the increased TGA residue is a promising result with respect to a carbonization process on an industrial scale, where increased carbonization yields potentially decrease production- and material costs of the carbon fibres.

Additionally to the high mass loss around 200 °C (mostly due to DMSO), the second temperature range of high mass loss was found between 300 and 400 °C. Above these temperatures, only minor degradation seems to occur. Based on these results, carbonization of the nanocomposite films was performed under argon in two different steps: at first, heating was performed from room temperature up to 550 °C at a linear rate of 2 °C min^{-1} and afterwards, the films were heated up to 1200 °C at a faster rate of 5 ° min^{-1}.

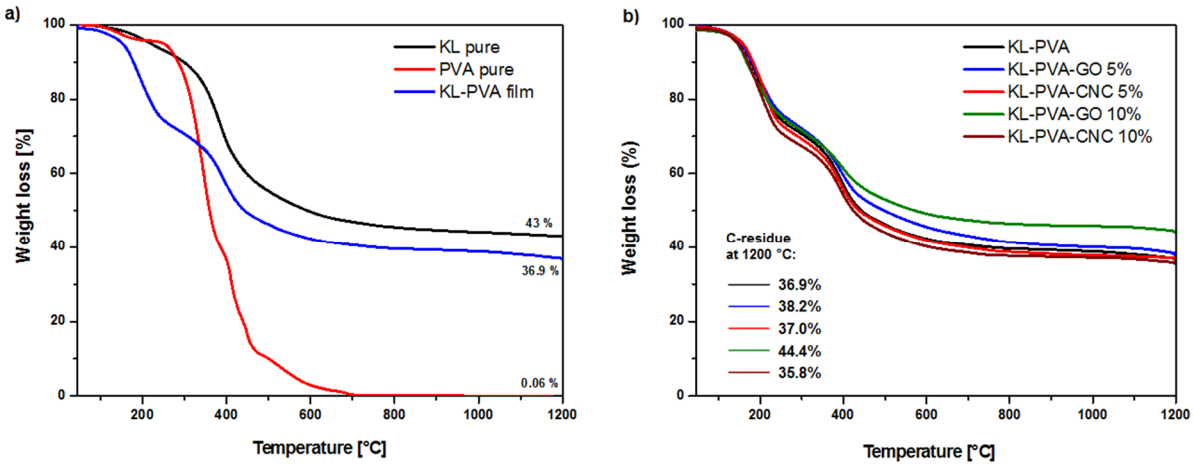

Figure IV-2 : *Thermogravimetric analysis (TGA) results (under nitrogen) and carbon residues at 1200 °C of pure KL, pure PVA and KL-PVA film (a) in comparison to KL-PVA-nanocomposite films (b)*

Based on these results, the morphology of the nanocomposite films was characterized before and after carbonization and the obtained structure within the carbonized films was investigated by means of XRD- and electrical conductivity measurements.

IV.1.3 Morphology of Nanocomposite Films Before and After Carbonization

As for the lignin-GO films (see *chapter III.2.2*), the morphology of the KL-PVA-GO and KL-PVA-CNC nanocomposite films was visualized with a scanning electron microscope (SEM) HITACHI TM3030 after gold-palladium metallization with a Quorum SC7620. The surfaces and the cross-sections of the films were characterized respectively.

The morphology of the reference film made from KL and PVA in a ratio of 70:30 was characterized in detail. Thereby, the micrographs of the films taken before and after carbonization were directly compared. As shown in Figure IV-3-a, a droplet-shaped phase can be recognized on the surface of the KL-PVA film before carbonization. This texture strongly resembles the emulsion of the initial solution, which has been used to prepare the films. Two phases were visualized within the KL-PVA blend solution in DMSO by optical microscopy, but also in solid KL-PVA films and –fibres by TEM imaging (see *chapter II.1.3*). Figure IV-3-a thus shows the biphasic state of the reference film KL-PVA 70:30 in SEM images. However, this state was not found anymore in the SEM images after carbonization of the films (at the given SEM resolution). According to TGA measurements, PVA should disappear during carbonization, thus theoretically leaving behind a monophasic carbon film based purely on KL. A high porosity was found on the surface of the obtained films after carbonization, which could be an indication for the PVA removal (see Figure IV-3-b1). The cross-sections however were found dense with only a low degree of porosity (see Figure IV-3-b2).

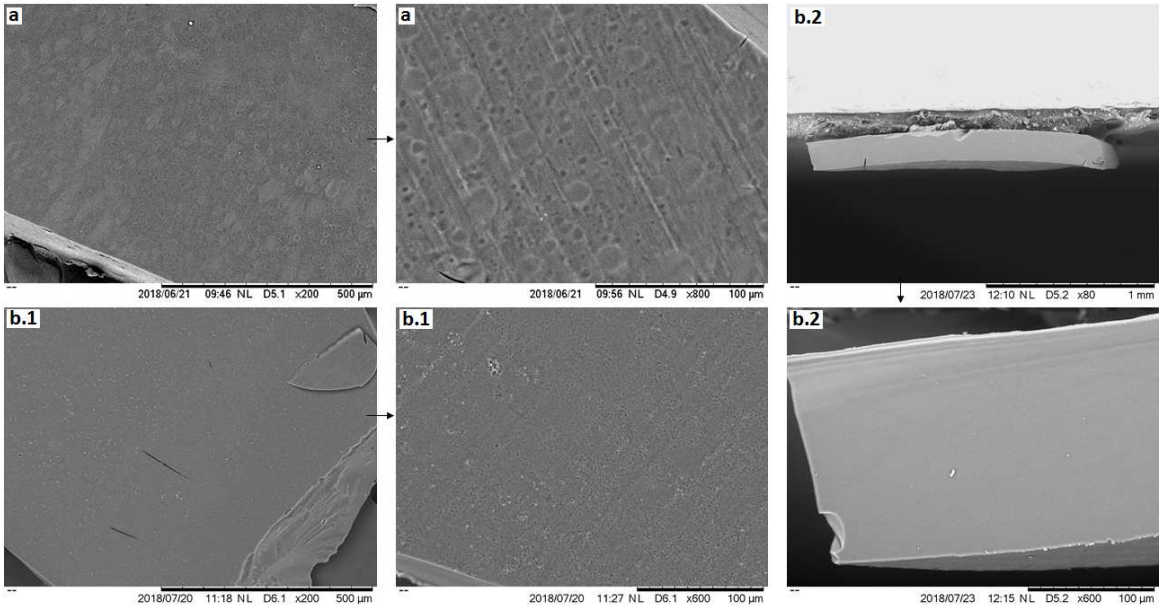

***Figure IV-3** : SEM micrographs at different magnifications of the reference film KL-PVA 70:30 before (a) and after carbonization (b): surface (b.1) and cross-section (b.2)*

Regarding the nanocomposite films, the morphology of their surfaces was found similar before and after the carbonization process. Besides, the surface morphologies of the films containing GO were found smooth and homogeneous. Their cross-sections seemed slightly less dense after carbonization. The structure composed of stacked layers was found more visible after the carbonization process than before. This structure lightening within the cross-sections could be explained by the removal of certain functional groups, gaseous compounds and possibly PVA during carbonization. Similar observations were made for the surfaces and the cross-sections of KL-PVA-CNC films, both at 5 % and at 10 % of CNCs. However, especially the cross-sections of KL-PVA-CNC 5 % were found denser than those of the films containing 5 % and 10 % of GO (see Figures A-IV-2 and A-IV-3 in annex).

Comparing the KL-PVA films with and without GO, the SEM images demonstrate that GO induces stacked layers inside the films, whereas the films without GO have a more uniform and dense morphology. The arrangement in layers is likely due to the molecular geometry of GO planes which are stacked on top of each other during the drying process of the films.

A deeper understanding of the film morphologies before and after carbonization could be gained by observation at higher resolutions. Besides, elemental analysis (EDS) could indicate more details about the film homogeneities.

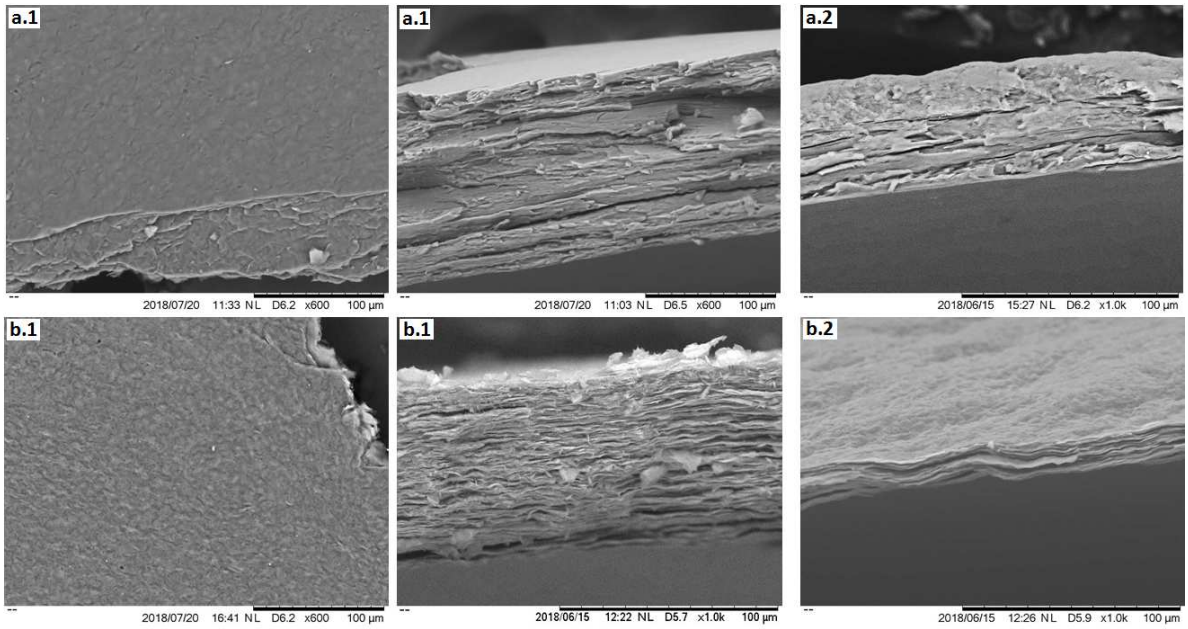

***Figure IV-4**: KL-PVA-GO film at 5% GO before (a.1) and after carbonization at 1200°C (b.1) and KL-PVA-GO film at 10% GO before (a.2) and after carbonization at 1200°C (b.2)*

IV.1.4 Carbon Structure of Nanocomposite Films

The obtained carbon structure of the films KL-PVA-GO 5%/10% and KL-PVA-CNC 5%/10% after carbonization was characterized by means of X-ray diffraction (XRD) and electrical conductivity experiments.

The XRD analysis was performed on a Rigaku Nanoviewer (MicroMax 007HF) with a rotating anode coupled to a confocal Max-Flux® Osmic mirror operating at a wavelength of 1.5418 Å. Different CNC- and GO concentrations as well as the carbonization temperature of the nanocomposite films have been varied and their impact on the obtained carbon structure was evaluated. From both graphs in Figure IV-5 it becomes clear that the reference film KL-PVA 70:30 shows a broad peak at a scattering angle 2θ of around 24°, representing a poorly oriented carbon structure. This is in agreement with the findings of *chapter II.4.2* (p. 87), in which the structure of KL-based carbon fibres has been studied as a function of different carbonization temperatures. However, the shape and position of the peak found for the KL-PVA film do not seem to be altered for films carbonized at 1000 °C and carbonized at 1200 °C (compare Figure IV-5-a and -b).

Regarding the carbon films containing CNCs, it becomes clear that for concentrations ≥ 10 % the peak position is slightly shifted to higher angles. Whereas a broad diffraction peak at around 25° was found for a purely CNC-based carbon film, the combination of KL, PVA and CNC led to a small shift towards 26° and to a decreased peak width. The effect was not found for the composite film containing 5 % of CNCs. This result indicates that at a certain quantity of CNCs inside the KL-based carbon films, the crystallinity within the samples may increase. Approaching the diffraction peak of graphite at 2θ = 26°, denser carbon domains seem to be

created within the films by incorporation of CNCs with respect to the KL-PVA film. However, the broad shape of the peak still indicates a poorly graphitized carbon structure. Comparing the carbonization temperatures of 1000 °C and 1200 °C for a film containing KL, PVA and CNCs, similar diffraction peaks and thus carbon structures were found.

The carbon films based on KL, PVA and GO show diffraction peaks shifted to 26° with respect to the diffraction peak of the reference film without GO. At low GO concentrations of ≤ 5 %, the peak shows a rather low intensity and a large width, thus indicating graphitic domains of a small size within the carbon film. However, the carbon film containing 10 % of GO shows a similar diffraction pattern than a film made from pure GO (compare Figure IV-5-b). This result clearly indicates a creation of large graphitic domains (2θ = 26°) within the film prepared from KL, PVA and GO after carbonization at 1200 °C. Compared to the results presented in *chapter III.2.3* (see Figure III-16) the peak width of the film KL-PVA-GO 10.5 % seems to be slightly higher than for films prepared only from KL and GO. It is thus possible that the presence of PVA during the carbonization process could alter or hinder the organization of GO into graphitic domains to a certain extent.

The two-dimensional lattice spacing of graphite (d_{100}) appears around 2θ = 42°.[2] A clear diffraction peak of d_{100} can be found for the pure GO film after carbonization (see Figure IV-5-b). The signal is also visible within all the carbonized films, whereby it is found less pronounced in the KL-PVA reference film and more pronounced for the films containing GO and CNCs. Since this diffraction peak indicates in-plane ordering, its enhancement suggests an increased ordering of the KL-based amorphous carbon in the case of the films KL-PVA-CNC 10 %, (see Figure IV-5-a), KL-PVA-GO 5% and -10 % (see Figure IV-5-b).[2]

From Figure A-IV-4 (see annex) an influence of the carbonization temperature in the case of KL-PVA-GO 10 % becomes clear. The sample carbonized at 1200 °C shows a clearer diffraction peak than the sample carbonized at 1000 °C. Based on this observation, it is possible that a carbonization at even higher temperatures could lead to larger crystalline domains within the carbon films containing GO. Regarding the resulting properties, the approach bears a high potential especially for lignin-based carbon fibres with GO reinforcement.

Additionally to the XRD results, the electrical conductivity of the films was determined to further indicate the crystallinity and structural organization of the given samples, a higher conductivity being associated to a more graphitized structure. Electrical resistivity measurements were thus performed on the carbonized films as described for the lignin-GO films in *chapter III.2.4*. The respective electrical conductivity values were determined based on the equations III-3 and III-4 (see p. 115). An increased electrical conductivity of the carbonized KL-PVA film ($5x10^3$ S m^{-1}) upon combination with CNCs and GO is demonstrated by the graph in Figure IV-6. The composite films containing 10 % of CNCs or GO generally show higher conductivities than the films at 5 %, but they are within the same order of magnitude (10^4 S m^{-1}). A synergistic effect generally seems to exist between KL and the nanoparticle fillers. Besides, the conductivity of KL-PVA-GO 10 % was found to increase with higher carbonization temperatures (1000 °C

compared to 1200 °C, see overview in Figure IV-6), which is in accordance with the XRD results (see Figure A-IV-4). A trend towards enhanced lignin-based carbon structures of increased crystallinity induced by GO and CNCs can thus be confirmed.

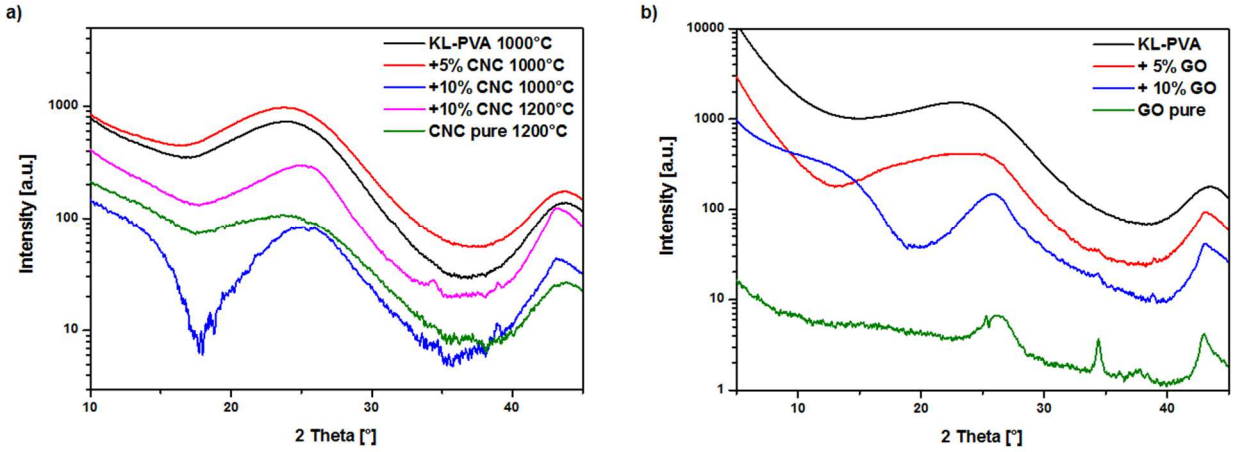

Figure IV-5: *XRD spectra showing scattered intensity depending on the scattering angle (2-Theta) of carbonized nanocomposite films: KL-PVA-CNC films after carbonization at 1000°C/1200°C (a) and KL-PVA-GO films after carbonization at 1200°C (b)*

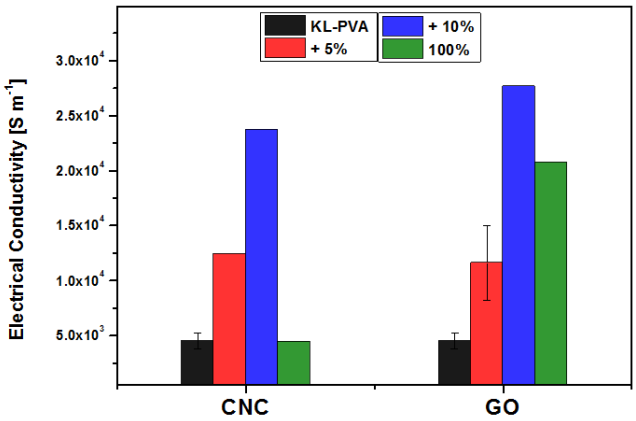

Carbon films made from Kraft lignin (KL), polyvinyl alcohol (PVA) and cellulose nanocrystals (CNC) or graphene oxide (GO)	
KL-PVA-CNC (1000°C)	**Electrical Conductivity [S m^{-1}]**
KL-PVA 70:30	3.8-5.2x10^{3}
KL-PVA-CNC 5%	1.2x10^{4}
KL-PVA-CNC 10%	2.4x10^{4}
CNC 100%	4.5x10^{3}
KL-PVA-GO (1000°C)	**Electrical Conductivity [S m^{-1}]**
KL-PVA 70:30	3.8-5.2x10^{3}
KL-PVA-GO 5%	8.2x10^{3}-1.5x10^{4}
KL-PVA-GO 10%	2.8x10^{4}
GO 100%	2.1x10^{4}
KL-PVA-GO (1200°C)	**Electrical Conductivity [S m^{-1}]**
KL-PVA 70:30	6.7x10^{2}-2.2x10^{3}
KL-PVA-GO 5%	6.2x10^{3}-1.5x10^{4}
KL-PVA-GO 10%	4.2x10^{4}

Figure IV-6 *: Electrical conductivities of KL-PVA-CNC and KL-PVA-GO films after carbonization at 1000 °C (left) and overview of electrical conductivity values (right)*

IV.2 Lignin-PVA-GO and Lignin-PVA-CNC Fibres

The dope solutions used for nanocomposite films have also been used to prepare nanocomposite fibres based on Kraft lignin (KL), polyvinyl alcohol (PVA) and graphene oxide (GO) or cellulose nanocrystals (CNCs) by coagulation. A combination of the three components theoretically allows the creation of precursor fibres at reduced cost and high carbonization yields (high lignin content) which can be easily manufactured (PVA used as plasticizer) and which possibly exhibit enhanced crystallinity with graphitic domains after carbonization (incorporation of GO and CNC liquid crystalline nanoparticles). In this subchapter, the preparation and characterization of these nanocomposite fibres are described and the results are directly compared with those obtained for nanocomposite films (shown in *chapter IV.1*).

IV.2.1 Coagulation and Carbonization of Nanocomposite Fibres

The preparation of the spinning dopes based on KL, PVA and GO as well as KL, PVA and CNCs was performed as described in *chapter IV.1.1*. Both systems in solution were entirely based on DMSO. All the dope solutions were coagulated in isopropanol in order to compare their spinning performance with the reference fibres made from KL and PVA (70:30) described in *chapter II*.

As already mentioned, the fact of mixing three components “diluted” the overall concentration in the systems. Besides, the concentration of nanoparticles within the mixture was limited by technical constraints, such as the exchange of solvent for GO (from water to DMSO) and the low dispersibility of CNCs in DMSO. Regarding the coagulation of polymer dope solutions during wet-spinning, high dope concentrations are generally advantageous for the process. In our case however, lower concentrations rendered the coagulation into composite fibres more difficult. Especially the systems containing GO could only be prepared at a low overall concentration of 11-16 wt%. Therefore, nanocomposite fibres at 10 % of GO and 10 % of CNCs (in dried state) were only spun by hand by means of coagulation inside a beaker (see principle in *chapter II.1.2*, p. 58). This method generally allows the wet-spinning of fibres at low dope quantities and simplified parameters. Drying of these fibres was performed under tension overnight under a fume hood. Composite fibres at 5 % of GO and 5 % of CNC contents were also spun by hand in order to compare them with those at 10 % of GO and 10 % of CNCs. Additionally, continuous spinning trials (see principle in *chapter II.2.1* p. 67) were performed on the systems containing 5 % of GO and 5 % of CNCs.

The four dope solutions were found homogeneous, as can be recognized from Figure IV-1 and Figure A-IV-1 (see annex). However, as already mentioned, only a limited liquid crystalline behaviour of CNCs and GO was found within the dope solutions. In the case of CNCs, the absence of a liquid crystalline phase could be due to a particle concentration below the phase transition. Regarding GO, only partial nematic domains were found within the systems, suggesting a biphasic state. The formation of a fully nematic phase of GO could have been

hindered either by a low concentration (0.8-1 wt%) or by the presence of PVA inside the system.

The influence of both GO- and CNC anisotropic particles on the flow behaviour of the reference spinning solution containing 14 wt% of KL and 6 wt% of PVA in DMSO was characterized. Rheology measurements were performed on dope solutions with very low particle contents (0.002-0.7 wt%) on a rheometer (Malvern Kinexus pro+) with a plate-plate geometry at a gap size of 0.3 mm. From the graphs in Figure A-IV-5 (see annex), it becomes clear that at low shear rates (0.1-0.2 s^{-1}) the viscosity of the solutions strongly increases with increasing nanoparticle concentrations. At shear rates ≥ 10 s^{-1} however, the viscosity decreases to a similar level for all the tested spinning dopes due to a strong shear thinning behaviour. Although shear thinning was observed for all spinning dopes, it was found amplified with increasing GO- and CNC contents. Unfortunately, the rheology measurements do not include the spinning dopes used to prepare the fibres containing 5 % and 10 % of GO and CNCs due to a limited sample quantity. However, the obtained results should also be valid for higher nanoparticle concentrations (0.8-1.6 wt%) and the expected shear thinning effect might be even stronger.

The shear rate at the inner wall of the die during the continuous spinning trials (see Figure III-23) was calculated to 630 s^{-1} by using equation III-5 (see *chapter III.1.3*). The KL-PVA spinning dopes at 0.8 wt% of GO and 1 wt% of CNCs in DMSO are thus likely to exhibit low viscosities just before coagulation because of a strong shear thinning effect which possibly leads to a high alignment of the particles.

Generally, the systems made from KL, PVA and CNCs showed a high ease of spinnability upon the coagulation in isopropanol. With respect to the reference system KL-PVA 70:30, no significant differences regarding the coagulation behaviour were noticed. Besides, during the continuous wet-spinning of KL-PVA-CNC 5 %, high draw ratios of up to 3.4 in dried state (DR_2) (see *chapter II.2.1*, p. 67) could be applied on the fibres. This system thus showed a similar stretching- and drying behaviour as the KL-PVA system without CNCs. Regarding the spinning process, an improved KL-PVA spinnability induced by the CNC fillers did not become evident.

The dope solutions of KL-PVA-GO 5 % and -10 % were generally found more difficult to coagulate in isopropanol. Even upon coagulation by hand, the process seemed slower compared to the coagulation of KL-PVA 70:30 fibres and the obtained fibres seemed softer and less resistant in wet state. This coagulation behaviour indicates that isopropanol cannot be considered as an ideal coagulant for these two systems. It is possible that the presence of GO flakes inside the systems would necessitate another coagulant. Pure GO fibres for instance are generally coagulated in aqueous solutions containing acids, bases or salts.[3] The GO flakes being negatively charged, coagulation of aqueous GO solutions into fibres can be provoked by counter-solvents containing charges as well, such as calcium chloride ($CaCl_2$)- or sodium hydroxide (NaOH) solutions.[3, 4] In this case, positively charged calcium ions (Ca^{2+}) or sodium ions (Na^+) assist the coagulation process. Consequently, salts which can be dissolved in alcohols would be an ideal candidate for coagulation of the KL-PVA-GO systems. However,

it also needs to be considered that the low solid content (11-16 wt%) within the dope solutions might have contributed to a decreased spinning performance of these systems.

The continuous spinning of KL-PVA-GO 5 % fibres and the manual spinning of KL-PVA-GO 5 % and -10 % was found very difficult due to a high fibre brittleness both in wet- and in dried state. The high brittleness could thus be due to a low solid content in the spinning dope or an insufficient coagulation of the dope in isopropanol. During the continuous spinning, draw ratios of only 2.8 (DR_1) and 2.2 (DR_2) could be applied, which are much lower compared to the ones used for the KL-PVA fibres.

The carbonization of the as-spun precursor fibres was performed as described in *chapter II.4.1* (p. 83). Stabilization under air was performed up to 300 °C at 2 °C min^{-1} with an isotherm of 1 h. The subsequent carbonization was performed under argon from room temperature to 550 °C at 2 °C min^{-1} and from 550 °C to 1000 °C at 5 °C min^{-1}, with an isotherm at 1000 °C of 1 h. The fibres were attached to a graphite frame with carbon-based glue in order to perform both stabilization and carbonization under tension. However, the tension could not be controlled during the process. Besides, due to a high brittleness of the KL-PVA-GO fibres, the carbonization step was found to be a delicate task. The fibres broke very easily under small stresses during manipulation or during the carbonization process. Therefore, only limited quantities of intact carbon fibres could be recovered from the frames for the subsequent characterization of their properties.

IV.2.2 Morphology of Nanocomposite Fibres

The cross-sections and the surfaces of the nanocomposite fibres were visualized with a scanning electron microscope (SEM) HITACHI TM3030 after gold-palladium metallization with a Quorum SC7620. The morphologies of the precursor- and the carbon fibres were directly compared.

Significantly different morphologies between the composite fibres containing graphene oxide (GO) and those containing cellulose nanocrystals (CNCs) become clear from Figures IV-7 and A-IV-6 (see annex). The fibres based on Kraft lignin (KL), polyvinyl alcohol (PVA) and CNCs have very similar morphologies to the ones of the KL-PVA reference fibres without nanoparticles. In other words, at the given resolution, CNCs did not become evident within the fibres and thus they do not seem to have an impact on the fibre morphology of the KL-PVA (70:30) system. However, the morphology of the KL-PVA-GO composite fibres is clearly influenced by GO. The fibre cross-sections and surfaces show a crumpled structure (see Figure IV-7), which stands in contrast to the smooth surface and dense cross-section of the KL-PVA fibres presented in *chapter II.2.2*.

Besides, the different coagulation behaviour between fibres containing CNCs or GO (as mentioned in *chapter IV.2.1*) becomes also clear from the cross-sections of the composite fibres. The KL-PVA-CNC fibres possess a circular or bean-shaped and smooth cross-section, whose shape likely depends on the amount of solvent (DMSO) inside the coagulation bath

(isopropanol), as explained in *chapter II.2.2*. The preparation method (discontinuous spinning by hand or continuous spinning) does not seem to have an impact on the cross-sectional shape. In the case of the KL-PVA-GO fibres however, it became clear that the fibres prepared manually in a discontinuous manner show cross-sections of an undefined shape, whereas continuously spun fibres were found rather bean-shaped. It is thus possible that coagulation happened faster upon continuous injection into the coagulation bath for the case of KL-PVA-GO 5 %. It can also be stated that the coagulation behaviour was found very unstable in isopropanol and thus insufficient for continuous spinning trials of fibres containing 10 % of GO and very difficult for 5 % of GO. The instability of the coagulation might be reflected in the randomly shaped cross-sections depicted in Figure IV-7-a and –b.

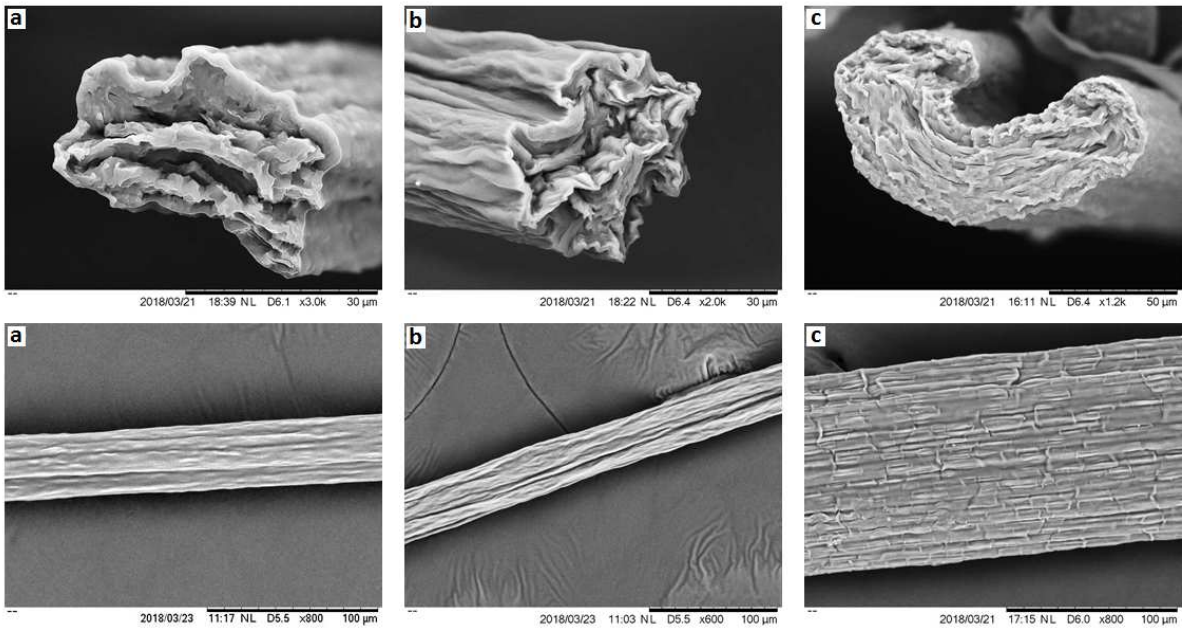

Figure IV-7: *SEM micrographs of KL-PVA-GO 5% (a) and -10% precursor fibres spun by hand (b) and continuously spun KL-PVA-GO 5% precursor fibres (c)*

Comparing the fibre morphologies before and after carbonization, no significant differences were found for the KL-PVA-CNC fibres (see Figure A-IV-6 in annex). In the case of KL-PVA-GO fibres however, the carbonized fibres seem densified with respect to the precursor fibres. By comparing Figures IV-7 (precursor) and IV-8 (carbon fibres), the mass loss occurring during carbonization becomes evident since the fibre sizes are reduced. However, the structure of the carbon fibres seems denser than the structure of the precursor fibres. Besides, an increased porosity on the surface of carbonized KL-PVA-GO 5 % fibres was recognized with respect to their precursor fibres (at the given resolution). Similarly as for the nanocomposite films, the increased porosity could be due to the removal of PVA and volatile components during carbonization (see *chapter IV.1.3*). As explained in *chapter III.2.2*, the size of the pores created during the process is dependent e.g. on the heating rate and/or on the sample composition.

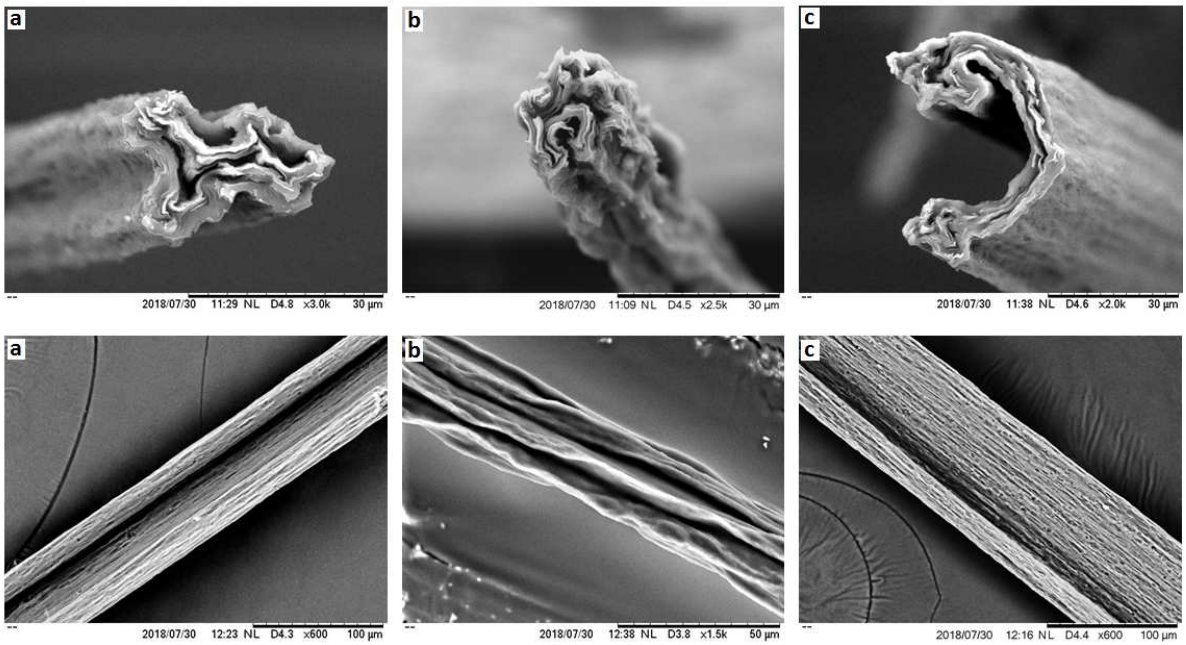

***Figure IV-8**: SEM micrographs of carbonized KL-PVA-GO 5% (a) and -10% fibres (spun by hand) (b) and continuously spun KL-PVA-GO 5% after carbonization (c)*

IV.2.3 Carbon Structure of Nanocomposite Fibres

The structures obtained within the nanocomposite fibres after carbonization were investigated by means of X-ray diffraction (XRD) measurements in order to study them in the same manner as the composite films. The XRD spectra were recorded on a Rigaku Nanoviewer (MicroMax 007HF) with a rotating anode coupled to a confocal Max-Flux® Osmic mirror operating at a wavelength of 1.5418 Å. The carbonized fibres were cut into small pieces and inserted into 0.2 mm glass capillaries in order to assemble the fibres into larger surfaces suitable as samples for the XRD analysis. The spectra of the fibres were obtained by subtracting the scattering pattern of an empty capillary. Since a high quantity of fibres was necessary to obtain a clear diffraction signal, only the continuously spun fibres were used for these measurements.

As shown in the patterns of Figure IV-9, the carbon fibres based on KL-PVA and KL-PVA-CNC 5 % exhibited diffraction peaks at around 22°, whereas the peak is shifted towards 24° for the KL-PVA-GO 5 % fibres. As for the nanocomposite films based on the same materials, the fibres containing GO exhibited diffraction peaks with their maximum at the highest scattering angles. The obtained diffraction peak can be considered as an approach towards the scattering angle of graphite at 2θ = 26°, which suggests a beginning formation of graphitic domains within the carbon fibres. A position around 22° however rather suggests a less dense and amorphous carbon structure of the fibres, which was not found modified by an addition of CNCs.

Comparing the spectra obtained for nanocomposite films and –fibres (see Figure IV-5 and IV-9), it should be mentioned that the diffraction peaks of the films were generally found at higher angles (2θ: 24-25°) than those of the fibres (2θ: 22-24°). The sample composition being

identical, possible explanations could lie in the different sample geometries. The shape and dimensions of a precursor material can generally have an influence on its thermal behaviour during the carbonization process.

The obtained results thus indicate that lignin-based carbon fibres containing 5 % of GO may exhibit a higher ordering of carbon crystals, approaching the properties of graphitic domains. However, the results also suggest that the low GO content is rather limiting the effect. As shown in composite films, the size and the density of graphitic domains within the obtained carbon can be increased at GO contents of 10 % (see Figure IV-5). Unfortunately, the quantity of KL-PVA-GO 10 % fibres which was carbonized within the framework of this thesis was not high enough to perform XRD measurements and thus to demonstrate the concept. The results obtained for nanocomposite films however give rise to the high potential of these fibres with respect to more crystalline and more aligned carbon structures.

The electrical conductivity of the carbon fibres obtained from KL-PVA, KL-PVA-CNC 5 % and KL-PVA-GO 5 % was obtained as described in *chapter IV.1.4*. For all measured samples, the conductivities were found within the range of 1.2-1.8x10^3 S m^{-1}. These results being in the same order of magnitude suggests only small structural differences between the three samples. However, these values were found rather low given the fact that the conductivity of the nanocomposite films was found to rise to 10^4 S m^{-1} by incorporation of 5 % of CNCs or 5 % of GO. This difference could be related to different densities of the carbon structure within films and fibres.

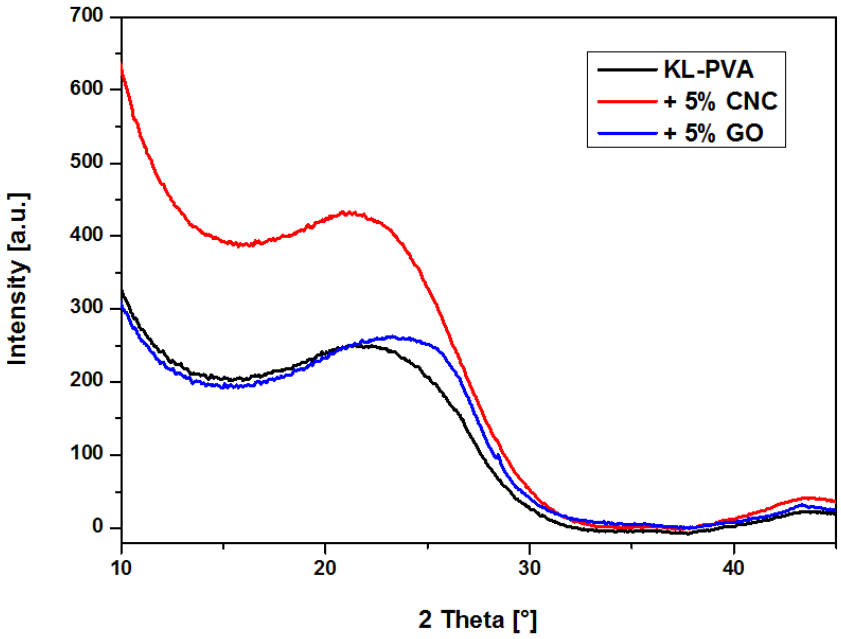

***Figure IV-9**: XRD spectra showing scattered intensity depending on the scattering angle (2-Theta) of nanocomposite fibres after carbonization at 1000°C: continuously spun KL-PVA reference fibre (70:30) and continuously spun KL-PVA-CNC 5% and KL-PVA-GO 5% nanocomposite fibres*

Comparing the diffraction pattern and electrical conductivities between films and fibres, the obtained results are rather surprising. Originally, a higher alignment of nanoparticles due to flow and shear stress during spinning was expected within the fibres, whereas the particles within the films were thought to self-assemble without a directing movement. The results obtained in this subchapter however suggest a higher organization and crystallinity within the films than within the fibres. Different sample preparation techniques (coagulation vs. evaporation) and the additional oxidative stabilisation performed for fibres may have a strong impact on the resulting carbon structure. In order to evaluate the obtained results more precisely, the organization process of GO and CNCs into nematic (fluid state) and graphitic domains (solid state) within lignin-based nanocomposite films and -fibres should be studied in more detail.

IV.2.4 Mechanical Properties of Nanocomposite Fibres

Compared to the lignin-graphene oxide (GO) fibres presented in *chapter III.3*, the nanocomposite fibres presented in this chapter were prepared with polyvinyl alcohol (PVA) as a spinning aid and plasticizing agent. Consequently, the resulting precursor fibres were found flexible and resistant enough to perform tensile tests both on precursor- and carbon fibres. The mechanical properties of lignin-based fibres in presence of anisotropic nano-carbon particles (graphene oxide flakes and cellulose nanocrystals) were thus characterized for the first time.

- *Precursor fibres*

The mechanical properties of Kraft lignin (KL)-polyvinyl alcohol (PVA) fibres in a ratio of 70:30 and nanocomposite fibres made from KL, PVA and CNC- or GO particles at different concentrations (maintaining a KL-PVA ratio of 7:3) have been investigated. The tests were performed on a Zwick Roell Z010 tensile testing machine with pneumatic jaws to clamp the fibres at sample lengths of 20 mm according to ISO 5079. A preload of 0.05 N was applied in order to tighten the fibres inside the clamps prior to performing the tests at strain rates of 50 % min^{-1}. The elongation of the fibres and the force at rupture were recorded respectively and the surfaces of the fibre cross-sections were determined from SEM images. The tensile stress was calculated from equation II-4 and the Young's modulus was calculated from the slope of the obtained stress-strain curves at strain values between 0.05 % and 0.25 %. For each sample, 5-10 fibres were measured and the average values were compared respectively.

An influence of CNCs and GO flakes on the mechanical properties of manually spun KL-PVA precursor fibres becomes clear from Figure IV-10. Both the average tensile strengths and moduli were found increased by the incorporation of nanoparticle fillers. In the case of the KL-PVA-CNC fibres, the presence of CNCs seems to increase the average tensile strength by at least 100 % (from around 40 MPa to ≥ 80 MPa) and the average moduli by around 150 % (from around 2 GPa to around 5 GPa). Thereby, the highest mechanical properties (on average) were obtained for fibres containing 5 % of CNCs with a strength of around 120 MPa and a modulus of around 6 GPa. However, the average tensile strength and modulus were not found

to increase linearly with increasing CNC concentrations (see Figure IV-10-a). The higher elongation obtained for a CNC content of 5 % could be due to fluctuations in the manual spinning- and stretching process. Globally however, the mechanical properties of the fibres containing 1, 5 and 10 % of CNCs were found within the same range of magnitude.

The mechanical properties of KL-PVA-GO precursor fibres evolved in a different way compared to the KL-PVA-CNC fibres. On average, the tensile strength as well as the modulus were found to increase progressively with increasing GO contents (see Figure IV-10-b). Whereas at 1 % of GO the obtained properties were found similar to those of the KL-PVA reference fibres, the average tensile strength increased from around 40 MPa to around 90 MPa upon addition of 5 % of GO and to around 130 MPa for 10 % of GO. The average moduli were found to increase from around 2 GPa to around 7 GPa and 13 GPa for 5 % and 10 % of GO respectively. These results clearly indicate a reinforcing effect of the KL-PVA fibre matrix by incorporation of GO flakes, leading to improved mechanical properties depending on the GO concentration.

Additionally to the nanoparticle filler concentration, an influence of the processing conditions on the mechanical properties of the nanocomposite precursor fibres was found. Thereby, the properties obtained for precursor fibres coagulated discontinuously (by hand) and continuously were compared for the systems containing 5 % of GO and 5 % of CNCs. Regarding the KL-PVA-GO 5 % precursor fibres, the preparation technique does not seem to have an impact on the resulting mechanical properties. Manually- as well as continuously spun fibres showed tensile strengths within the range of 90-100 MPa and moduli of 6-7 GPa (see Figure IV-11). For precursor fibres containing CNCs however, a strong influence can be recognized depending on the chosen spinning process. Comparing manually- and continuously spun fibres, it became clear that continuously spun fibres exhibit slightly higher tensile strengths from 120 to 150 MPa and a much higher elongation at break (see Figure IV-11). This result indicates a higher elasticity of continuously spun fibres and it could be due to different draw ratios applied during the different spinning techniques. Unfortunately, the stretching was not quantified during manual spinning so that the draw ratios of the two systems cannot be compared directly. Regarding the KL-PVA-GO 5 % fibres, no difference between the two spinning techniques became evident in their mechanical properties. This result could be related to their difficult coagulation behaviour (see *chapter IV.2.1*), allowing only minor draw ratios in wet state for both techniques.

Additionally, hot-stretching tests were performed on the continuously spun KL-PVA-CNC 5 % fibres at 120 °C by applying draw ratios of 100 %. The resulting mechanical properties of these fibres were found strongly increased with respect to the unstretched KL-PVA-CNC 5 % reference fibres (see Figure IV-11, green vs. orange curve). An increase of the average tensile strength from around 150 MPa to around 280 MPa suggests an increased alignment of molecular chains in fibre direction within the hot-stretched samples. Since the tests were performed above the glass transition of PVA (T_g: 75 °C), it is assumed that mostly PVA chains were aligned during the treatment. The impact of hot-stretching on the orientation of KL chains is considered as rather small due to their amorphous nature. Based on the strongly increased

tensile strengths for KL-PVA-CNC 5 %, additional hot-stretching experiments should be performed on KL-PVA-GO 5 % precursor fibres since they may lead to a similar increase in mechanical properties.

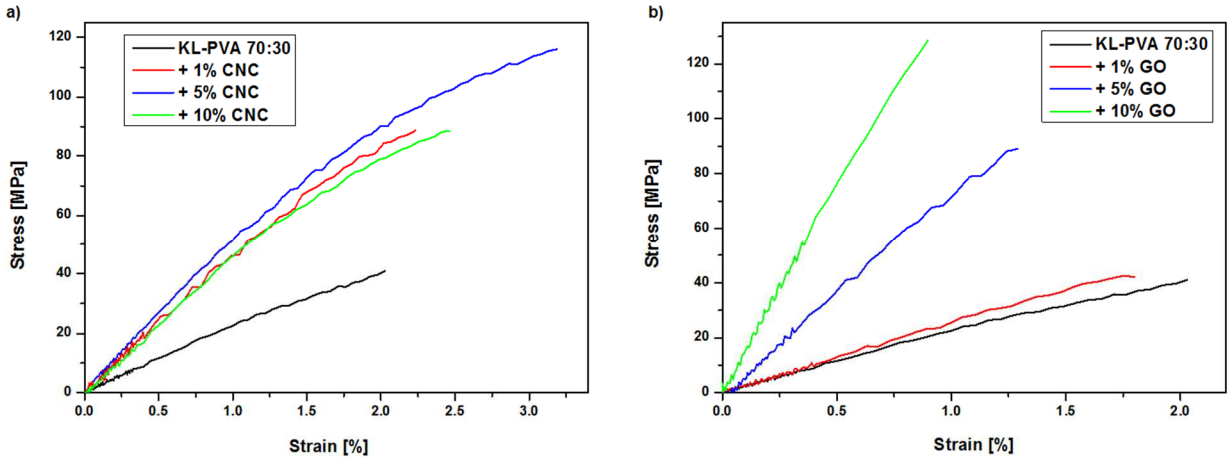

***Figure IV-10**: Influence of nanoparticle filler contents on the mechanical properties of manually (discontinuously) spun KL-PVA (70:30) precursor fibres: for KL-PVA-CNC composite fibres (a) and for KL-PVA-GO composite fibres (b). The graphs are representative of the average values obtained from 10 samples.*

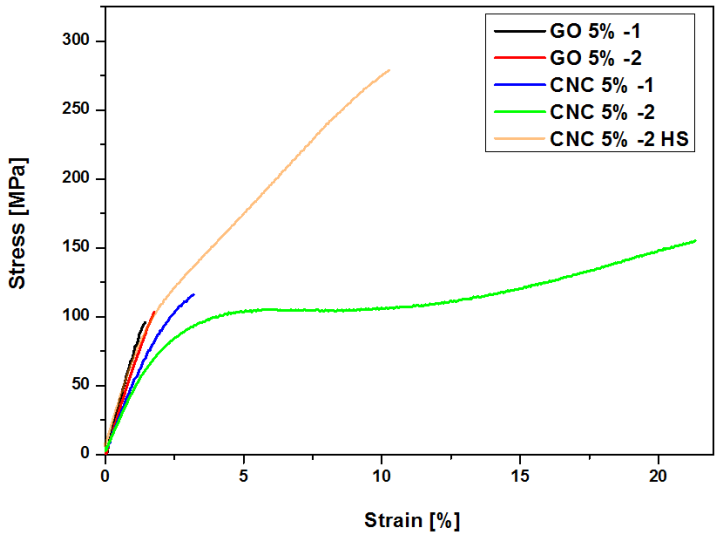

***Figure IV-11**: Influence of the spinning process on the mechanical properties of KL-PVA-CNC 5 % and KL-PVA-GO 5 % precursor fibres: discontinuous spinning by hand (1), continuous spinning (2) and hot-stretched sample (HS). The graphs are representative of the average values obtained from 10 samples.*

- *Carbon fibres*

The mechanical properties of the carbonized nanocomposite fibres were determined on a Zwick Roell Z2.5 tensile testing machine. The fibres were glued into paper frames leaving an open sample length of 20 mm. The frames stabilised the samples when clamped inside the jars and were cut open prior to the measurements. The strain rate was chosen to 1 mm min^{-1}

without applying a preload. The tensile stress and -strength, fibre elongation and Young's modulus were determined in the same manner as for the precursor fibres.

Due to the fact that the PVA present inside the precursor fibres is assumed to be removed during carbonization, the resulting carbon fibres containing only KL or KL and CNC/GO were found to possess a very high brittleness. The manipulation of the carbonized fibres was thus found rather difficult. Therefore, only three samples were considered for the tensile tests respectively, thus resulting in high deviations of the obtained values. Therefore, the results presented in this section can only be considered as indications for possible mechanical properties and thus for the potential of the carbon fibres.

Mainly the carbon fibres obtained from continuously spun precursor fibres, namely the KL-PVA 70:30 reference fibre and the fibres KL-PVA-CNC 5 % and –GO 5 %, were characterized regarding their mechanical properties. Comparing the three samples, the highest average tensile strength of around 650 MPa was obtained for the fibres based on KL, PVA and GO at 5 %. In contrast to the KL-PVA-CNC 5 % fibre showing around 200 MPa on average, the GO flakes seem to reinforce the properties of the reference KL-based carbon fibre exhibiting strengths of only around 300 MPa. Although CNCs were found to weaken the fibres' tensile strengths, they slightly increased the carbon fibre modulus to around 50 GPa (on average) compared to the other two samples showing 40-42 GPa. Globally however, GO seems more suitable as reinforcing material than CNCs due to the strong increase in tensile strength of KL-based carbon fibres. An overview of the obtained mechanical properties for all samples is given in Table IV-1.

Comparing the manually spun fibres containing 5 % and 10 % of GO, preliminary results show that it is possible to further increase the tensile strength of the carbon fibres by at least 30 %. If a continuous spinning of precursor fibres containing KL, PVA and 10 % of GO was possible prior to carbonization, even higher tensile strengths (≥ 650 MPa) could be expected due to the increased amount of GO. Besides, a more graphitic carbon structure within KL-PVA-GO 10 % films compared to KL-PVA-GO 5 % films has already been demonstrated by XRD- and electrical conductivity results. Further developments to improve the spinning performance of KL-PVA-GO fibres containing at least 10 % of GO thus represent one of the most promising approach to increase the mechanical properties of KL-based carbon fibres.

Similarly to the precursor fibres, an improved tensile strength was found for the hot-stretched fibres made from KL, PVA and 5 % of CNCs after carbonization. This result indicates an increased alignment of CNCs induced by the hot-stretching tests, which seems to be conserved during carbonization. However, XRD measurements should be performed in order to confirm this hypothesis, since an increased alignment of CNCs within the carbon fibres should lead to a modified diffraction pattern.

Table IV-1: Overview of mechanical properties obtained for nanocomposite precursor and – carbon fibres with respect to fibre diameter (average over 3-10 tests for each fibre sample)

	Precursor fibres				Carbon fibres			
Fibre sample	**Tensile Strength [MPa]**	**Young's Modulus [GPa]**	**Elongation at Break [%]**	**Fibre diameter [µm]**	**Tensile Strength [MPa]**	**Young's Modulus [GPa]**	**Elongation at Break [%]**	**Fibre diameter [µm]**
KL-PVA 70:30 (hand)	36.5 ± 6.1	1.7 ± 0.6	2.2 ± 0.4	58	-	-	-	-
KL-PVA 70:30 (on roll)	154 ± 25	6.1 ± 1.0	4.8 ± 1.0	67.0 ± 4.0	331 ± 39	40.8 ± 5.7	0.9 ± 0.2	49.5 ± 9.1
KL-PVA 70:30 (hot-stretched)	195 ± 51	5.8 ± 0.9	5.4 ± 2.4	57	264 ± 183	32.3 ± 11.7	0.69 ± 0.4	43.6 ± 3.6
+ GO 5% (hand)	89.7 ± 13.1	7.3 ± 1.5	1.7 ± 0.6	33.0 ± 3.8	346 ± 45	52.8 ± 9.5	0.7 ± 0.04	31.7 ± 3.8
+ GO 5% (on roll)	99.8 ± 22.1	6.0 ± 1.4	2.4 ± 1.4	64.1 ± 6.0	**658** ± 70	42.5 ± 6.6	1.6 ± 0.2	49.7 ± 1.1
+ GO 10% (hand)	127 ± 86	12.8 ± 6.5	1.0 ± 0.2	32.9 ± 7.4	448	34-80?	0.55	19.8 ± 1.5
+ NCC 5% (hand)	139 ± 47	6.2 ± 1.9	15.1 ± 16.7	41.4 ± 11.4	-	-	-	-
+ NCC 5% (on roll)	155 ± 37	4.9 ± 0.9	23 ± 19	63.9 ± 6.2	177 ± 48	**50.7** ± 2.5	0.38 ± 0.08	42.9 ± 0.9
+ NCC 5% (hot-stretched)	**278** ± 43	6.8 ± 0.9	12.7 ± 2.5	55.1 ± 3.5	**478** ± 15	**51.6** ± 3.3	0.96 ± 0.06	34.8 ± 0.7
+ NCC 10% (hand)	77.4 ± 19.4	4.6 ± 1.0	2.2 ± 0.5	52.4 ± 10.1	-	-	-	-

Compared to the mechanical properties of lignin-based fibres which are already reported in literature, the values obtained in this thesis are within the intermediate range. The highest mechanical properties have been obtained by Compere et al. (Oak Ridge National Laboratory ORNL, USA) who reported tensile strengths of up to 1.03 GPa and Young's moduli of 83-109 GPa for melt-spun lignin-based carbon fibres.[5] Although it has to be kept in mind that the used spinning technique differs from ours, it also should be noted that their carbon fibres showed diameters of only 10-14 µm. The carbon fibres obtained in this thesis however exhibit diameters which are 3-5 times higher. As already mentioned in *chapter II.4.3* for instance, the mechanical properties of fibres tend to increase with decreasing diameter. Therefore, an important objective for future spinning trials is to decrease the diameters of our precursor- and our carbon fibres. The precursor fibre diameter can be decreased either by injecting the spinning dope through smaller spinneret holes or by increasing the draw ratios during the spinning process. Besides, the diameter of the final carbon fibres can be further decreased by applying a carbonization process under tension. Typically, industry envisions the spinning of multifilament strands (see *chapter II.3*) with filament diameters of around 15 µm, leading to carbon fibres with a diameter of ≤ 7 µm. If this objective would be accomplished, the resulting mechanical properties could theoretically by far exceed the highest strengths and moduli ever reported.

IV.3 Conclusion

Two different methods have been chosen to prepare nanocomposite films and -fibres from dope solutions based on dimethyl sulfoxide (DMSO). The solutions contained Kraft lignin (KL), polyvinyl alcohol (PVA) and carbonaceous nanoparticle fillers, namely graphene oxide (GO) flakes and cellulose nanocrystals (CNCs). It has been shown that the nanoparticles assembled, at least partially, into liquid crystalline phases within the dope solutions. Upon evaporation of DMSO on the one hand, nanocomposite films were prepared from the solutions. On the other hand, the dope solutions were used for coagulation in isopropanol in order to prepare nanocomposite fibres. Both films and fibres were subjected to carbonization and the resulting structure and properties before and after carbonization were characterized.

The carbonization yield of nanocomposite films can be significantly increased by addition of GO flakes inside the KL-PVA matrix. Furthermore, an increased crystallinity was found for films containing 5 and 10 % of GO, which became evident by increased electrical conductivities. X-ray diffraction (XRD) patterns also indicated graphitic domains within the samples. Similar results were obtained for the structure of composite films containing CNCs, although the structuration effect was found less pronounced.

Regarding the wet-spinning process of nanocomposite fibres, isopropanol was found a suitable coagulant for KL-PVA-CNC fibres. However, the coagulation behaviour of the KL-PVA-GO dopes was found more difficult, possibly due to the absence of ions within isopropanol. Despite a rather poor spinning performance, the fibres containing GO flakes still showed promising properties. After carbonization, the nanocomposite fibres generally exhibited less pronounced graphitic domains and lower electrical conductivities than the nanocomposite films. Tensile tests of the precursor fibres however revealed an increased tensile strength and Young's modulus by incorporating nanoparticle fillers. Regarding the carbon fibres, only 5 % of CNCs or GO within continuously spun fibres led to improved mechanical properties. Especially GO was found a promising reinforcement, leading to tensile strengths of up to 650 MPa for KL-based carbon fibres and thus an improved performance by more than 100 %.

In order to further improve the properties of the KL-PVA-GO fibres, optimization trials in the future should include an alternative dope preparation method to obtain systems with a higher total concentration and systems whose concentrations are easily tuneable. Different GO sources with larger flake sizes and different methods for the solvent exchange could also improve the properties of the dopes. Besides, a detailed study of the 4-component systems, including DMSO, should be performed, for instance by preparation of phase diagrams. The coagulation of the nanocomposite fibres containing GO should also be improved in order to evaluate their potential for a scalable wet-spinning process.

References

[1] J. P. F. Lagerwall *et al.*, 'Cellulose nanocrystal-based materials: from liquid crystal self-assembly and glass formation to multifunctional thin films', *Npg Asia Mater.*, vol. 6, p. e80, Jan. 2014.
[2] X. Ma, C. Yuan, and X. Liu, 'Mechanical, microstructure and surface characterizations of carbon fibers prepared from cellulose after liquefying and curing', *Materials*, vol. 7, no. 1, pp. 75–84, 2013.
[3] Z. Xu and C. Gao, 'Graphene fiber: a new trend in carbon fibers', *Mater. Today*, vol. 18, no. 9, pp. 480–492, 2015.
[4] R. Jalili *et al.*, 'Formation and processability of liquid crystalline dispersions of graphene oxide', *Mater. Horiz.*, vol. 1, no. 1, pp. 87–91, 2014.
[5] A. Compere, W. Griffth, C. Leitten Jr, and J. Pickel, 'Evaluation of lignin from alkaline-pulped hardwood black liquor', *ORNL*, vol. 118, pp. 6–97, 2005.

Overall Conclusion and Perspectives of this Thesis

The results of this thesis demonstrate a successful preparation of lignin-based fibres by means of coagulation, which can be converted into low-cost and “green” carbon fibres. The properties of these fibres can be tailored by optimization of the spinning process, adaptation of the carbonization process and incorporation of reinforcing nanocarbon filler materials such as graphene oxide (GO) and cellulose nanocrystals (CNCs). The obtained results confirm a promising potential of our fibres.

The first experimental part of this thesis mainly consisted in the preparation and characterization of wet-spun precursor fibres from softwood Kraft lignin (KL) and polyvinyl alcohol (PVA). Our results have shown that the two polymers are only partially miscible in solution and that they form metastable states within solid blend films. Monofilaments containing a KL- to PVA ratio of 70:30 have been spun continuously under optimized processing conditions. Our developed spinning method for lignin-PVA fibres led to a filed patent application in October 2017. The obtained KL-PVA fibres demonstrated a homogeneous, biphasic morphology with bean-shaped or round cross-sections and a smooth surface. The precursor fibres exhibited mechanical properties which were found sufficient for the subsequent carbonization step. TGA results revealed a potential carbonization yield of around 30 %, and allowed the creation of a tailor-made temperature program. The precursor fibres were thus attached to graphite frames and heated to 1000 °C in a static carbonization oven under argon. The obtained lignin-based carbon fibres exhibit tensile strengths of up to 400 MPa and moduli of up to 50 GPa at rather large monofilament diameters of 40-75 µm. Future spinning trials will include further drawing steps in order to decrease these fibre diameters. As has been shown, smaller fibre diameters potentially increase the mechanical properties. Furthermore, the effect of hot-stretching of the precursor fibres on the resulting carbon fibre structure and –properties will be studied in more detail for lignin. In the case of linear polymers, hot-stretching is a classic tool to improve the fibres’ molecular orientation and thus their mechanical properties.

Besides, it was shown that the carbonization process itself has a crucial influence on the resulting fibre morphology and properties. Especially the microporosity on the fibre surfaces can be tailored by addition of an oxidative stabilization treatment and/or adjusted heating rates during carbonization. A quantitative study of the porosity, e.g. by means of SAXS measurements could be performed in the future. Regarding the obtained carbon structures within our fibres, XRD results revealed a highly disordered carbon with a very poor orientation. This structure is linked to the amorphous nature of lignin itself and it is the main reason for the fibres’ low mechanical- and electrical properties. At carbonization temperatures above 1500 °C, Raman spectroscopy results revealed a beginning formation of graphitic domains inside our fibres. A graphitization of the fibres at even higher temperatures will thus be performed in future studies in order to show its effect on the fibre properties. Furthermore, a carbonization process under tension might lead to more aligned carbon structures and thus improved mechanical properties of our fibres. Such a carbonization oven is already being used for cellulose-based carbon fibres at the Research and Technology Transfer Platform CANOE.

A different approach to induce a higher structuration inside lignin-based carbon fibres has been proposed in the second experimental part of this thesis. The combination of lignin with graphene oxide (GO) flakes or colloidal rod-like cellulose nanocrystals (CNCs), which form liquid crystalline phases in solution, revealed highly promising results. In principle, phase diagrams demonstrated a good compatibility between lignin and GO, whereby GO flakes are able to form nematic phases in presence of lignin molecules. The two components being compatible in solution, lignin-GO films at different ratios were prepared by evaporation of the respective solvent. TGA measurements demonstrated an increased carbonization yield of the films induced by GO. Their characterization showed that denser and larger graphitic domains are created within the carbonized films at higher GO contents. Similarly, GO leads to an increased electrical conductivity of the carbonized lignin films.

The lignin-GO solutions were also used for coagulation into composite fibres, whereby PVA was finally added as a plasticizing agent. An alignment of the anisotropic particles during wet-spinning theoretically induces a more ordered structure within the fibres than in the films. Although improved KL-PVA fibre performances were observed upon incorporation of GO- and CNC particles, the films were found to exhibit larger graphitic domains and a higher crystallinity than the fibres. These findings indicate that the carbonization process does not only depend on the sample composition, but also on its geometry. A more detailed comparison between films and fibres should thus be performed in future studies. Besides, a deeper understanding of the impact of PVA on the liquid crystalline phase inside the dope solution should be gained. Possible cross-linking reactions between lignin and PVA during the carbonization process could also be evaluated, e.g. by modulated-DSC measurements.

Regarding the use of GO for our spinning dopes, other GO sources and dissolution methods should be found and exploited in order to facilitate the dope preparation and lower the costs. The solutions based on DMSO were difficult to prepare and could not be highly concentrated in GO. However, higher dope concentrations containing GO could considerably facilitate the spinning process. GO types of larger flake sizes might also improve the fibres' performances and the ease of spinnability. Even though GO was found an efficient reinforcing element for lignin fibres, it has to be paid attention to keep the fibre raw materials at a low price. Eventually, a chemical reduction of GO could also be envisioned to study its influence on the fibre properties.

Only 5 % of GO or CNCs within continuously wet-spun KL-PVA precursor fibres already improved the mechanical properties of the resulting carbon fibres. The highest tensile strengths were found around 650 MPa for carbonized KL-PVA-GO fibres. This value corresponds to an increase of 100 % on average with respect to our carbon fibres without GO. The tensile tests of composite fibres containing 10 % of GO or CNCs are still ongoing. Higher ratios of carbonaceous filler materials within lignin fibres may even further increase their mechanical properties.

The highest tensile strengths and moduli obtained within the framework of this thesis, namely 650 MPa and 50 GPa, are comparable to other lignin-based carbon fibres and can be considered as elevated. Especially given the fact that our chosen spinning method is still

limited to rather large fibre diameters of 30-50 µm, a decrease in diameter would improve these properties even further. The highest mechanical properties ever reported for lignin-based carbon fibres do not exceed tensile strengths of 1.03 GPa and Young's moduli of 83-109 GPa. These values were obtained at Oak Ridge National Laboratory (USA) based on melt-spun lignin fibre blends. Advantages of our wet-spun fibres compared to these melt-spun fibres may include higher carbonization yields due to higher lignin contents and a more economical processing since no stabilisation is required for our infusible lignin grade. These two factors are important aspects which potentially decrease the fibres' production costs.

As already mentioned, further work on our systems will include the decrease of the precursor fibre diameters through the spinning process. A common way to do so is the production of multifilaments, which contain hundreds of thin filaments combined into a fibre strand. This principle was validated for our fibres during multifilament wet-spinning trials on pilot scale (100 filaments). However, the drying process of the fibres was found difficult, presumably due to DMSO residues. A replacement of our DMSO-based solution by solvents with lower boiling points, which are compliant with economical- and safety requirements, would be ideal to avoid this problem. A homogeneous dispersion of Kraft lignin, for instance in water, would represent an alternative spinning dope whose solvent would be easier to evaporate from the resulting fibres.

In conclusion, a wet-spinning method was presented in this thesis which allows the simple production of commercially available lignin grades. Besides, the principle was found suitable for multifilament spinning on pilot scale. This potential for a large scale production of precursor fibres at lower costs than conventional precursors will allow for commercial applications in the future. The current demand for low-cost carbon fibres combined with the interest of paper manufacturers to valorise their lignin is favourable for further developments in the field. Our wet-spinning method was found suitable for different Kraft lignin grades provided by different paper manufacturers from the Aquitaine region (France). In principle, the wet-spinning ability of these grades covers a huge amount of potential raw materials. Furthermore, a novel carbonization line especially designed for bio-based precursors is currently being installed at CANOE in southern France. It will have a capacity to produce up to one ton of carbon fibres per year. The chances are high that, one day, lignin-based multifilaments will continuously be carbonized on this pilot plant. Ultimately, the possible applications for these fibres (composite parts, energy storage, electronics, …) are endless.

List of Chemicals

Solvents:

- Butan-1-ol & Butan-2-ol, Acros Organics (CAS No. 71-36-3) and *Scharlau (*CAS *No.* 78-83-1)
- Dimethyl Ethylene Urea (**DMEU**)/ 1,3-dimethyl-2-imidazolininone, *Kermel*, CAS No. 80-73-9
- Dimethyl Formamide (**DMF**), *JT Baker,* CAS No. 68-12-2
- Dimethyl Sulfoxide (**DMSO**), *Scharlau (CAS No. 67-68-5) and VWR International,* reagent grade ACS
- Ethanol (**EtOH**), *VWR International*, CAS No. 64-17-5
- Ethylene Glycol (**EG**), *Scharlau*, CAS No. 107-21-1
- Isopropanol (2-Propanol), *Brenntag (CAS No. 67-63-0) and VWR International,* reagent grade ACS (CAS No. 67-63-0)
- 4-methylmorpholine N-oxide (**NMMO**), 50% in water, *Acros Organics*, CAS No. 7529-22-8
- Water, demineralized

Polymers:

- Kraft Lignin “L16” (**KL**), softwood from maritime pine, extracted by *FCBA*, black liquor provided by *Smurfit Kappa*
- IndulinAT® Kraft lignin “L9” (**IAT**), softwood, purchased from *MeadwestVaco* (CAS No. 8068-05-1)
- Lignin Alkali KRAFT “Aldrich”, purchased from *Sigma Aldrich (CAS No. 8068-05-01)*
- Lignosulfonate Arbo N18 “L12” (**LS**), maritime pine, purchased from *Tembec*
- Alginate (Alginic Acid Sodium Salt), *Sigma Aldrich* (CAS No. 9005-38-3)
- Dextran, 144 kg mol^{-1}, *Sigma Aldrich* (CAS No. 9004-54-0)
- Polyethylene glycol (**PEG**), 35 kg mol^{-1}, *Sigma Aldrich* (CAS No. 25322-68-3)
- Polyvinyl Alcohol “PVA195K” (**PVA**): Mowiol® 56-98,195 kg mol^{-1}, 98 % hydrolysis degree, *Sigma Aldrich* (CAS No. 9002-89-5)
- Polyvinyl Alcohol “PVA61K”, Mowiol® 10-98, 61 kg mol^{-1}, 98 % hydrolysis degree, *Sigma Aldrich*
- Polyvinyl Alcohol “PVA205K” (**PVA2**) Fluka PVA 40-88, 205 kg mol^{-1}, 88 % hydrolysis degree, *Sigma Aldrich* (CAS No. 9002-89-5)
- Polyvinylpyrolidone (**PVP**), CAS No. 9003-39-8, *Sigma Aldrich*
- Thermoplastic polyurethane (**TPU**), Elastollan® C 80 A, *BASF*

Filler Materials:

- Cellulose nanocrystals (CNCs), purchased from *University of Maine Process Development Center*
- Graphene Oxide (GO), aqueous solution of 4 mg ml^{-1}, *Graphenea*

Salts (for preparation of aqueous solutions):

- Aluminium sulfate ($Al_2(SO_4)_3$), *Fluka* (CAS No. 16828-11-8)
- Ammonium Sulfate ($(NH_4)_2SO_4$), Sigma Aldrich (CAS No. 7783-20-2)
- Calcium chloride ($CaCl_2$), *Fisher* (CAS No. 10035-04-8)
- Calcium sulfate ($CaSO_4$), *Sigma Aldrich* (CAS No. 10101-41-4)
- Sodium chloride (NaCl), *JT Baker* (CAS No. 7647-14-5)
- Sodium dodecylsulfate (SDS), *Sigma Aldrich* (CA No. 151-21-3)
- Sodium hydroxide (NaOH), *Scharlau* (CAS No. 1310-73-2)
- Sodium tetraborate decahydrate “Borax”, *Sigma Aldrich* (CAS No. 1303-96-4)
- Sodium sulfate (Na_2SO_4), ACS Reagent > 99 % anhydrous powder, *Sigma Aldrich* (CAS No. 7757-82-6)
- Boric Acid, *Fisher (*CAS No. 10043-35-3)

Annex

Chapter II:

Table A-II-1: Results of coagulation screening of 7 different lignin solutions in chosen counter-solvents: water (H_2O), ethanol (EtOH) and aqueous salt solutions (at 0.1 wt%, 1 wt% and 10 wt%)

L12: lignosulfonate (Tembec); L16: Kraft lignin (FCBA); L6: Soda Lignin Protobind 2400 (Green Value); L4: Organosolv Alcell (Fraunhofer CBP); L7: Soda Lignin Protobind 6000 (Green Value); L9: Kraft lignin (IndulinAT®, Mead WestVaco)

x: solution dissolves ~: solution solidifies ✓: fibre is formed

Lignin solution	H_2O	EtOH	NaOH		NaCl		Na_2SO_4		$CaSO_4$ 0.1%	$(NH_4)_2SO_4$		$Al_2(SO_4)_3$		$CaCl_2$ 1%
			1%	10%	1%	10%	1%	10%		1%	10%	1%	10%	
L12 in DMSO (40 wt%)	✗	✓	✗	✗	✗	✗	✗	✗	✗	✗	✗	✗	✗	✗
L16 in DMSO (30 wt%)	✓	✗	✗	✗	✓	✓	✓	✓	✓	✓	✓	✓	✓	✓
L6 in DMSO (30 wt%)	✓	✗	✗	✗	✓	✓	✓	✓	~	✓	✓	✓	✓	✓
L4 in DMEU (30 wt%)	✓	✗	✗	✗	~	✓	✓	✓	✓	✓	✓	~	~	✓
L7 in NMMO (20 wt%)	✗	✗	✗	✗	✗	✓	✗	~	~	✗	✓	~	✓	~
L9 in EG (20 wt%)	~	✗	✗	✗	~	✓	✓	✓	~	~	✓	~	✓	~
L12 in H_2O (40 wt%)	✗	~	✗	✗	✗	✗	✗	✗	✗	✗	✗	✗	✗	✗

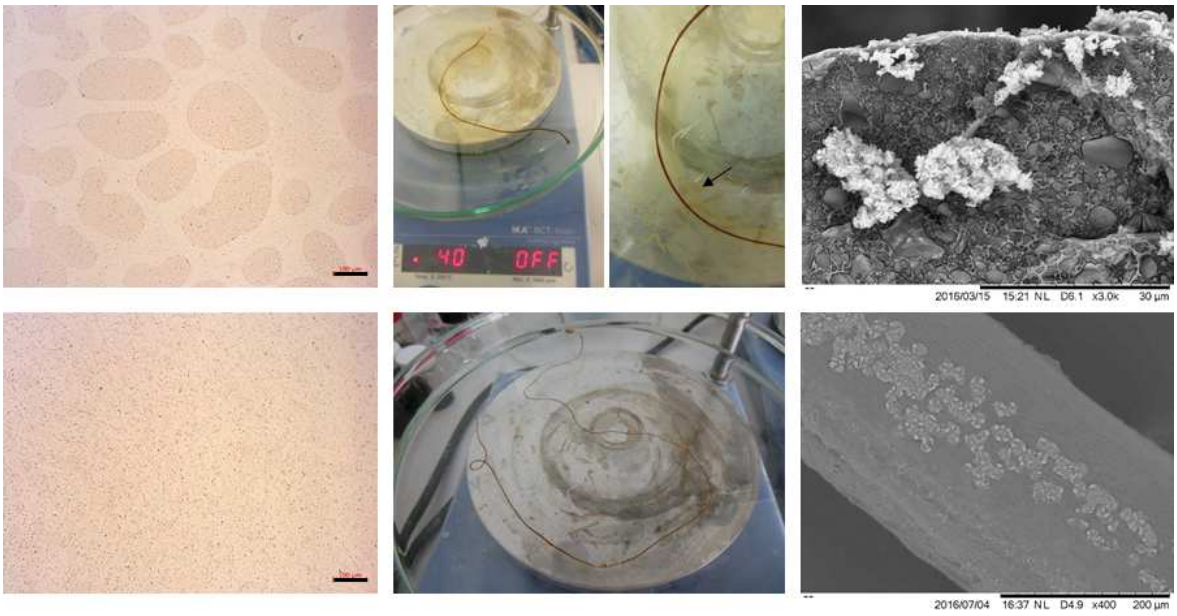

***Figure A-II-1**: Dope solutions (scale bars 100µm), coagulation and SEM-characterization of lignosulfonate-PVA fibres (from left to right). Row above: dope solution in water and coagulation in sodium sulphate (Na_2SO_4); row below: dope solution in water + Borax ($B_4Na_2O_7$) and coagulation in sodium hydroxide (NaOH).*

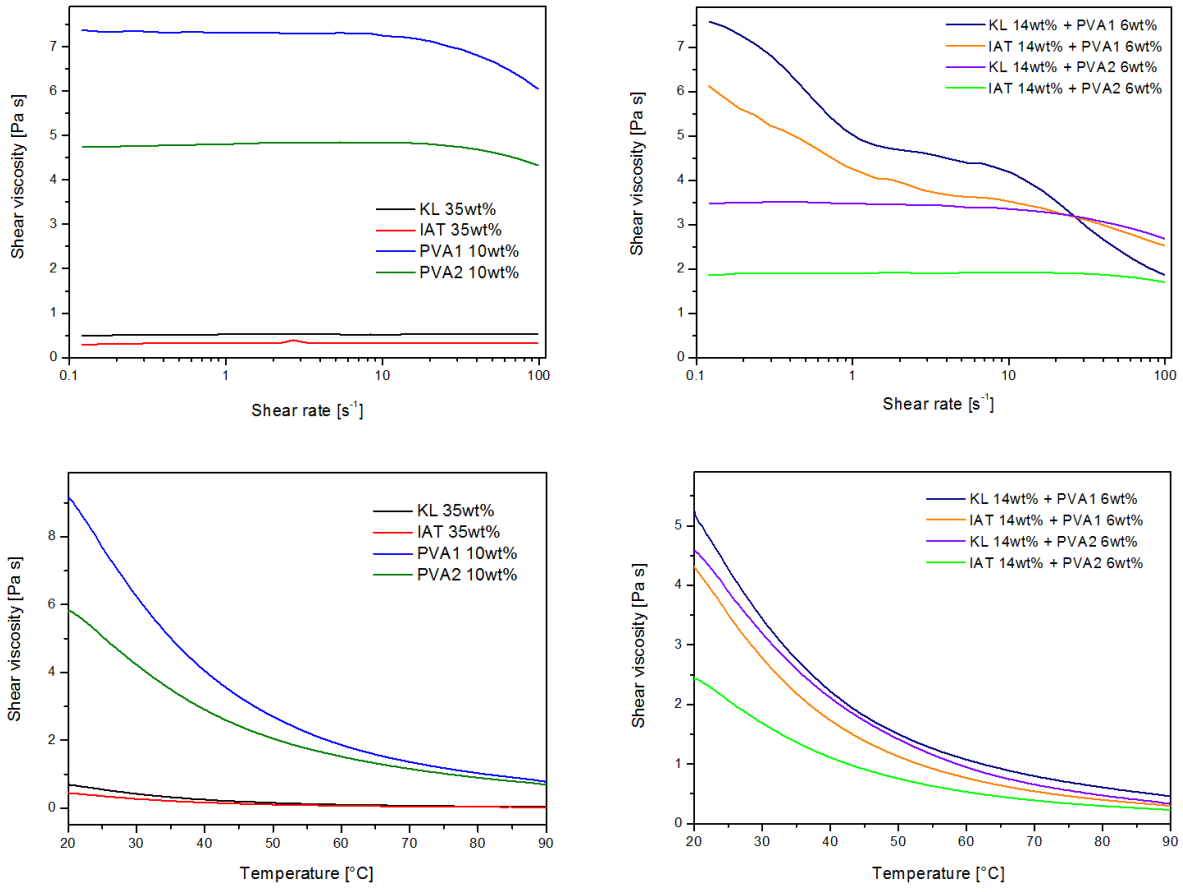

***Figure A-II-2:** Shear viscosity as a function of shear rate (above) and of temperature (below) for lignin- and PVA solutions before (left) and after mixing (right): the used lignin grades were Kraft lignin "KL" (L16, FCBA) and Kraft lignin IndulinAT® "IAT" (MeadWestVaco); the used PVA grades were PVA195K with degree of hydrolysis of 98% ("PVA1) and PVA205K with degree of hydrolysis of 88% ("PVA2")*

Table A-II-2: Quantities of lignin- and PVA solution and resulting ratios inside mixture and dried films

Lignin solution at 35 wt% [g]	PVA solution at 10 wt% [g]	Concentration in solution L - PVA [wt%]	Concentration in dried film L – PVA [wt%]
2	3	14 - 6	70 - 30
1	3.5	7.8 – 7.8	50 - 50
0.5	4.1	3.8 – 8.9	30 - 70

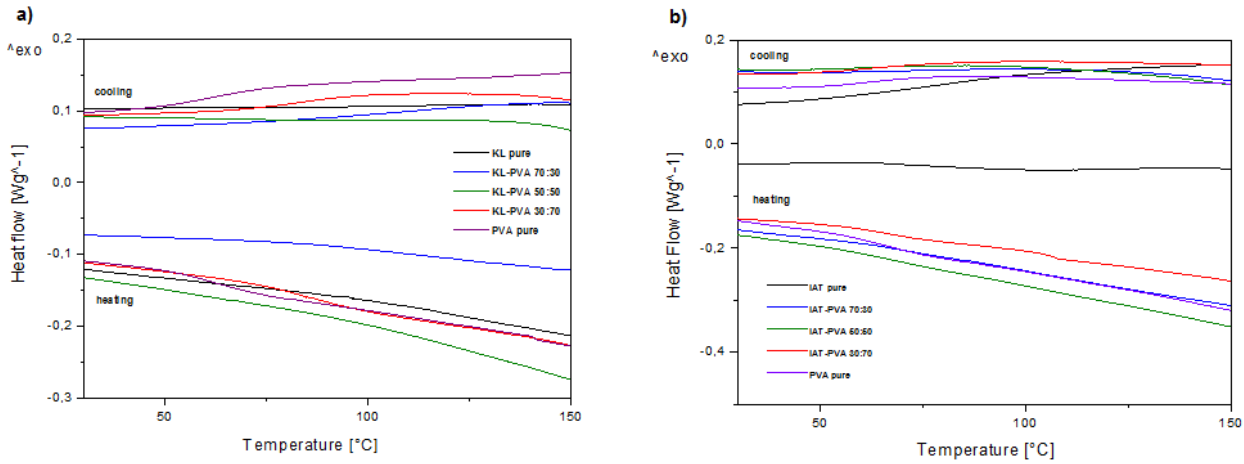

Figure A-II-3: *DSC heating- and cooling cycles of films KL-PVA (a) and IAT-PVA (b): pure components and different ratios (70:30, 50:50 and 30:70). Zoomed into glass transition temperature range.*

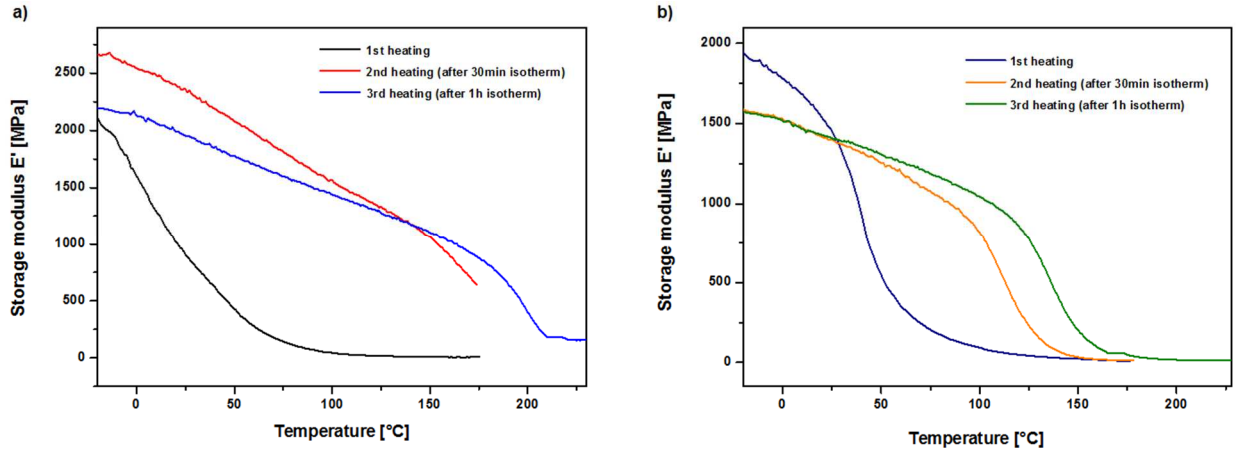

Figure A-II-4: *DMA heating cycles of films KL-PVA 70:30 (a) and 30:70 (b) depicting the increasing storage modulus E' after isotherms of 30min and of 1h at 180°C*

Chapter III:

Table A-III-1: Combinations of graphene oxide (GO) with Kraft lignin (KL) and lignosulfonate (LS) in solutions and in dried films

Concentration in solution [wt%]			Concentration in dried film [%]			Solvent
Graphene Oxide	**Kraft lignin**	**Total**	**Graphene Oxide**	**Kraft lignin**	**Total**	
1.8	-	1.8	100	-	100	DMSO
1.6	0.4	2	80	20	100	DMSO
1	1	2	50	50	100	DMSO
1.6	3	4.6	35	65	100	DMSO
1	3	4	25	75	100	DMSO
0.5	2	2.5	20	80	100	DMSO
-	35	35	-	100	100	DMSO
Graphene Oxide	**Lignosul -fonate**	**Total**	**Graphene Oxide**	**Lignosul -fonate**	**Total**	
3.2	-	3.2	100	-	100	water
2	1	3	67	33	100	water
2.8	4	6.8	41	59	100	water
1	4	5	20	80	100	water
0.5	4	4.5	11	89	100	water
-	40	40	-	100	100	water

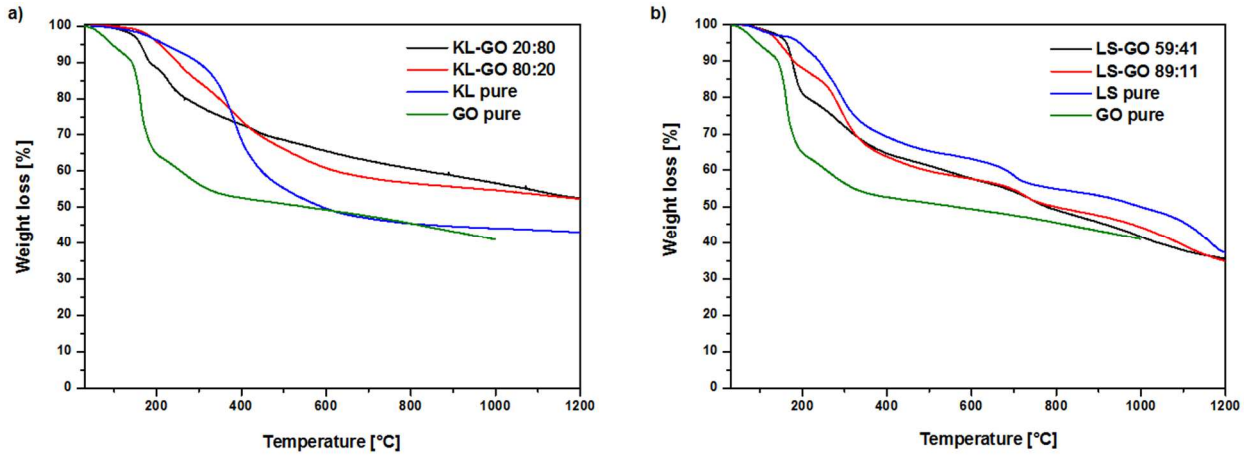

Figure A-III-1: *Results of thermogravimetric analysis (TGA) performed under nitrogen on selected films from Kraft lignin (KL) and graphene oxide (GO) (a) and from lignosulfonate (LS) and graphene oxide (GO) (b); the carbon residues were directly compared with those of the pure components*

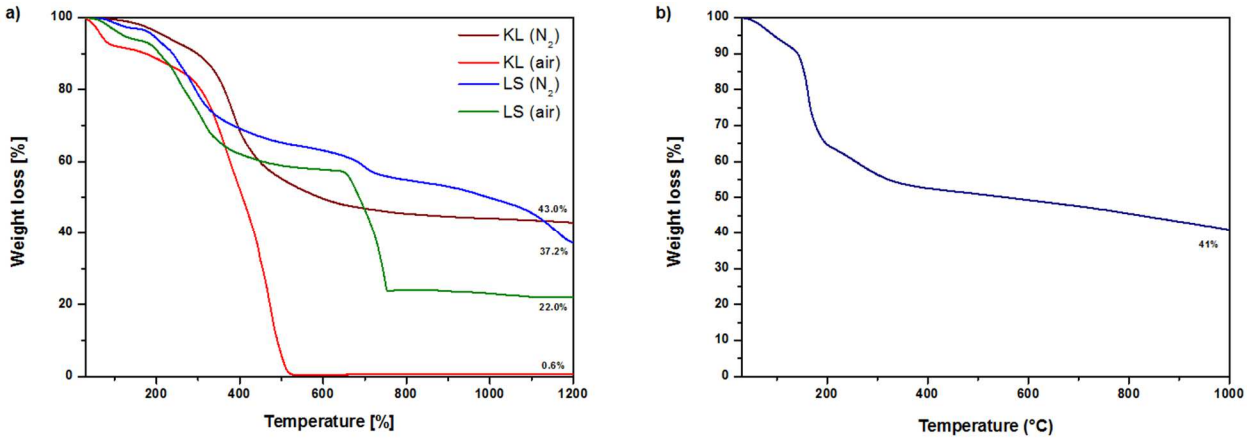

Figure A-III-2: *Results of thermogravimetric analysis (TGA) performed on Kraft lignin (KL) powder and lignosulfonate(LS) powder under nitrogen (N_2) and under air (a) and TGA analysis of freeze dried graphene oxide (GO) under nitrogen (b). GO was subjected to an isotherm of 1h at 30°C before the measurement to remove adsorbed water.*

Table A-III-2: Electrical conductivity ranges (in S m^{-1}) with respect to the heating rates used for carbonization of graphene oxide-Kraft lignin films (GO-KL) and graphene oxide-lignosulfonate films (GO-LS) consisting of two different ratios respectively

Carbonization at 5 °C min^{-1}	
Film sample	**Electrical Conductivity [S m^{-1}]**
GO – KL 80:20	$2.3\text{-}4.6\times10^{3}$
GO – KL 20:80	$8.1\times10^{3}\text{-}4.0\times10^{4}$
GO – LS 41:59	8.2×10^{3}
GO – LS 11:89	$6.4\times10^{3}\text{-}1.6\times10^{4}$
Carbonization at 2.5 °C min^{-1}	
Film sample	**Electrical Conductivity [S m^{-1}]**
GO – KL 80:20	$1.1\text{-}3.2\times10^{4}$
GO – KL 20:80	$9.5\times10^{3}\text{-}2.5\times10^{4}$
GO – LS 41:59	$4.7\times10^{3}\text{-}2.5\times10^{4}$
GO – LS 11:89	$1.2\text{-}4.4\times10^{4}$
Carbonization at 0.5 °C min^{-1} + 1 °C min^{-1}	
Film sample	**Electrical Conductivity [S m^{-1}]**
GO – KL 80:20	$5.9\times10^{2}\text{-}2.0\times10^{3}$
GO – KL 20:80	$1.2\text{-}5.1\times10^{3}$
GO – LS 41:59	6.1×10^{3}
GO – LS 11:89	$1.3\text{-}2.7\times10^{3}$

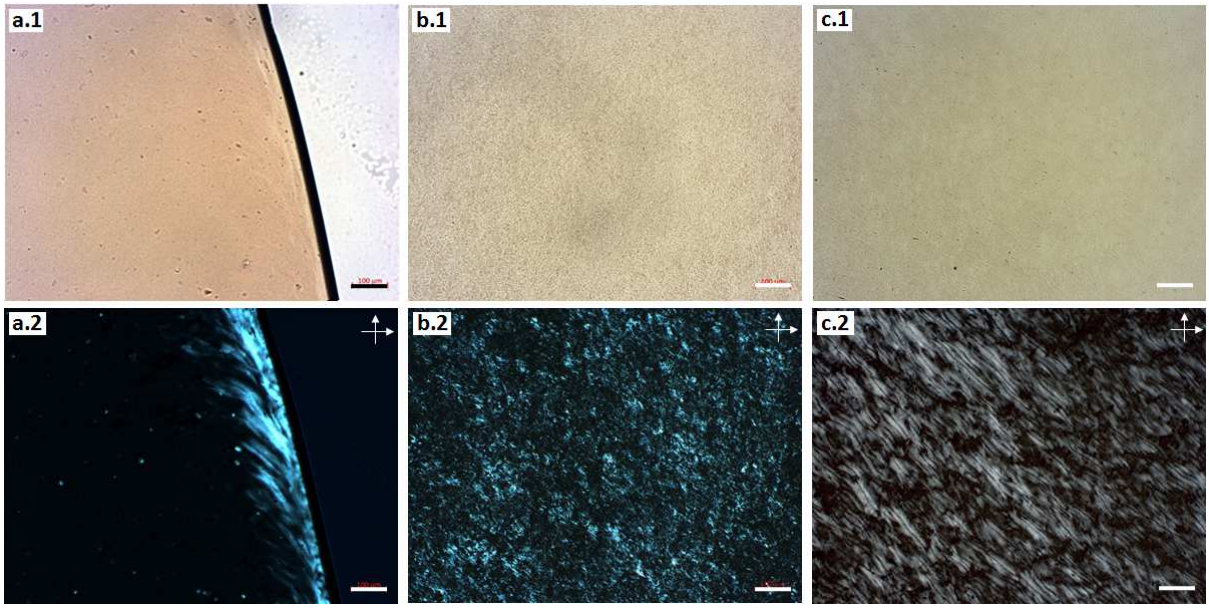

Figure A-III-3: *Optical micrographs of Kraft lignin-graphene oxide dope solutions at ratios 4.3wt%-0.9wt% (a), 5wt%-4.7wt% (b) and 0.5wt%-1.7wt% (c) under normal light (1) and under crossed polarizers (2)*

Chapter IV:

Table A-IV-1: Composition of Nanocomposite films- and fibres: Kraft lignin (KL), polyvinyl alcohol (PVA), graphene oxide (GO) and cellulose nanocrystals (CNC), all solutions are based on DMSO

Quantities for solution preparation [g]			**Concentration in solution [wt%]**				**Concentration in dried film or fibre [%]**		
GO (1.7 wt%)	**KL powder (100%)**	**PVA (11.4 wt%)**	**GO**	**KL**	**PVA**	**Total**	**KL**	**PVA**	**GO**
1.98	0.43	1.66	0.8	10.6	4.6	16.0	66.0	29.0	**5.0**
3.38	0.34	1.23	1.1	6.9	2.8	10.8	63.5	26.0	**10.5**
CNC (2.8 wt%)	**KL powder (100%)**	**PVA (11.4 wt%)**	**CNC**	**KL**	**PVA**	**Total**	**KL**	**PVA**	**CNC**
2.20	0.80	3.03	1.0	13.3	5.7	20.0	66.0	29.0	**5.0**
3.93	0.67	2.40	1.6	9.6	3.9	15.1	63.5	26.0	**10.5**

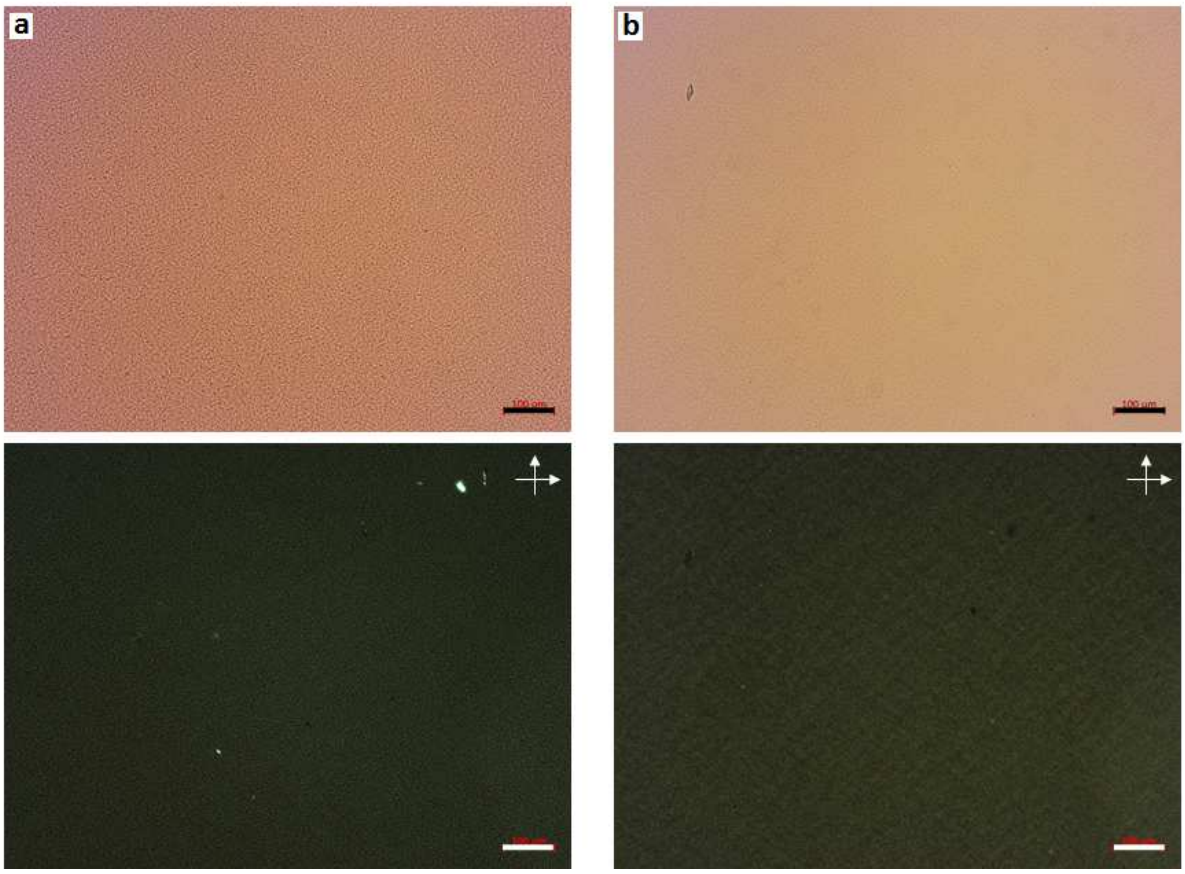

Figure A-IV-1: *Optical micrographs of dope solutions containing 1.0 wt% CNC, 13.3 wt% KL and 5.7 wt% PVA (a) and 1.6 wt% CNC, 9.6 wt% KL and 3.9 wt% PVA (b) based on DMSO, under normal light (above) and polarized light (below)*

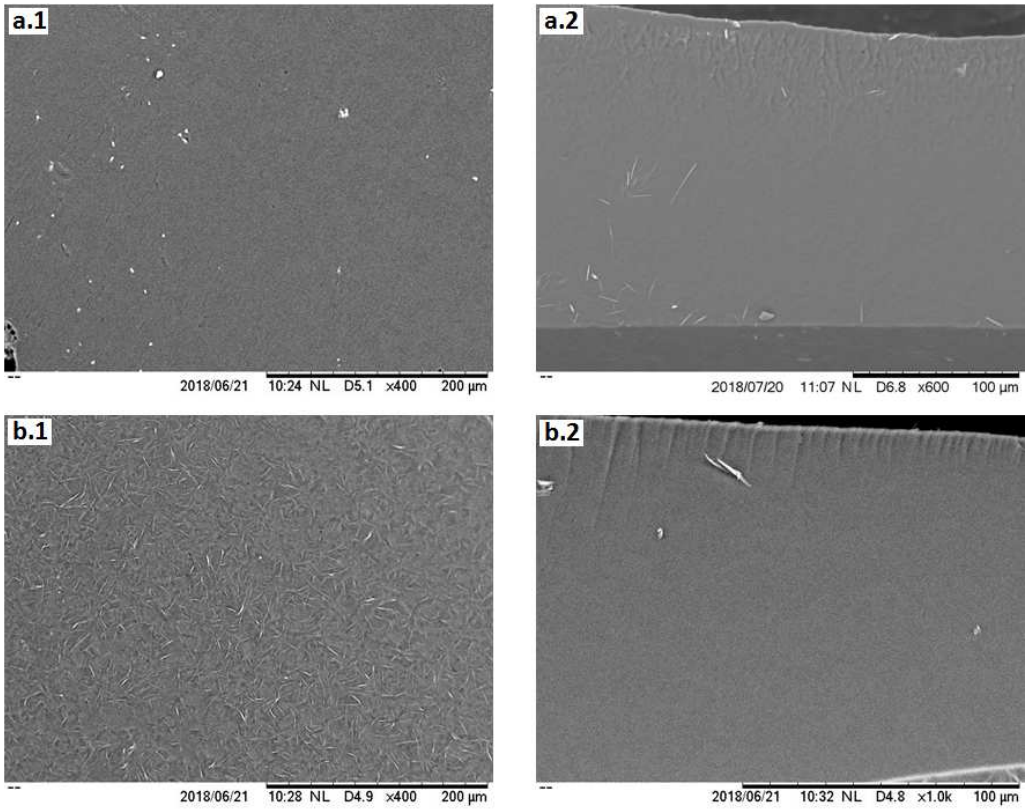

Figure A-IV-2: *KL-PVA-CNC film at 5% CNC: surface before (a.1) and after carbonization at 1200°C (b.1) and cross-section before (a.2) and after carbonization at 1200°C (b.2)*

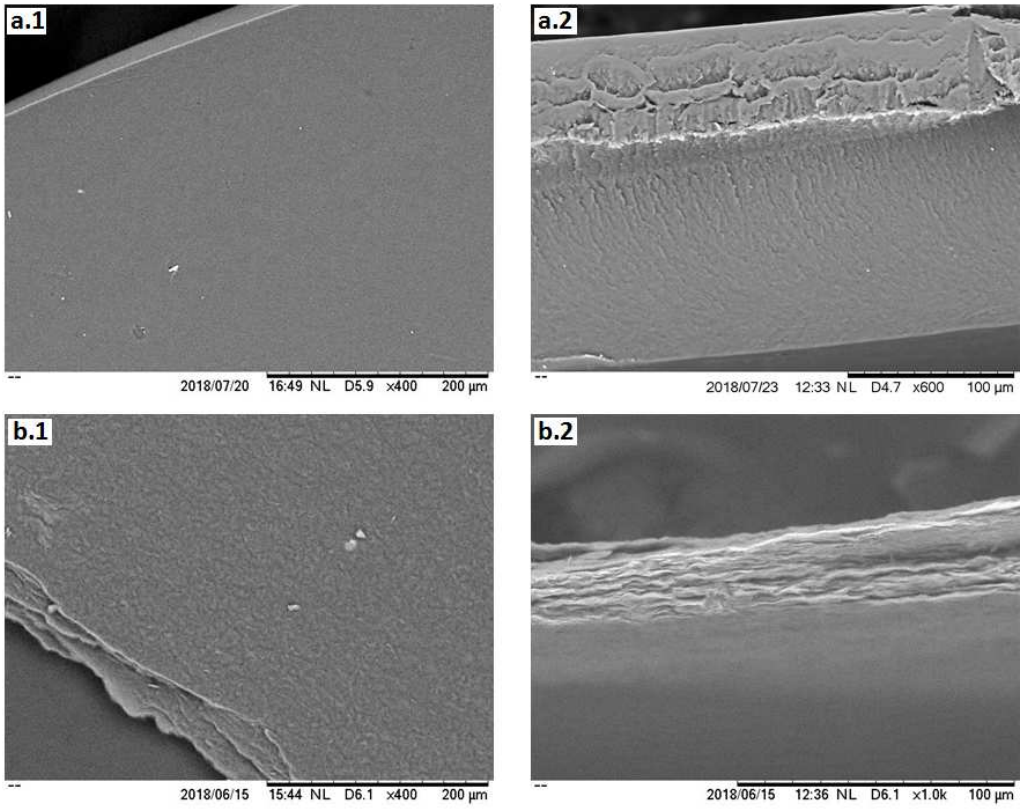

Figure A-IV-3: *KL-PVA-CNC film at 10% CNC: surface before (a.1) and after carbonization at 1200°C (b.1) and cross-section before (a.2) and after carbonization at 1200°C (b.2)*

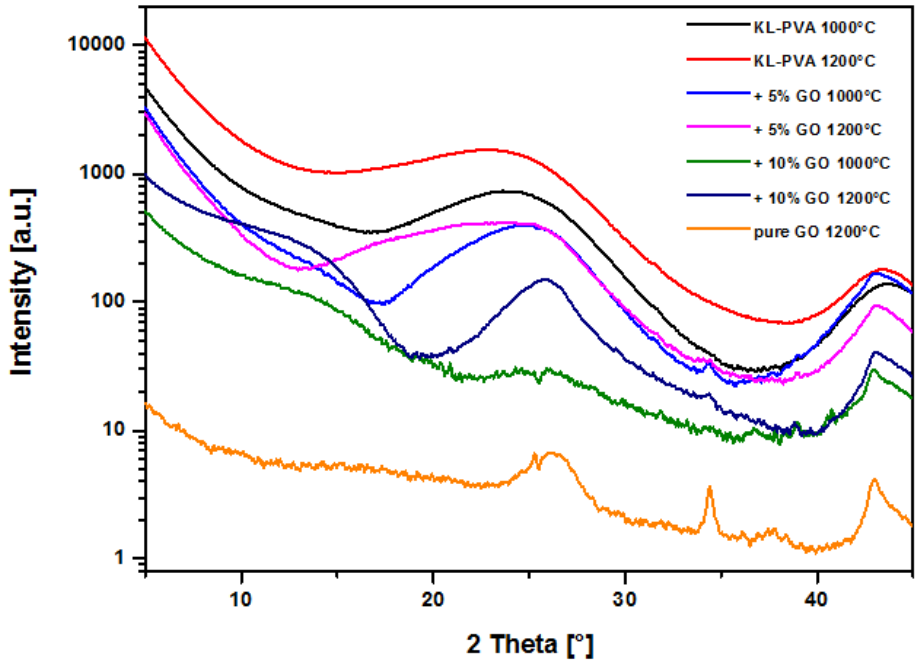

Figure A-IV-4: *XRD spectra of films: KL-PVA 70:30, pure GO and KL-PVA-GO 5% and -10% carbonized at 1000 °C and 1200 °C*

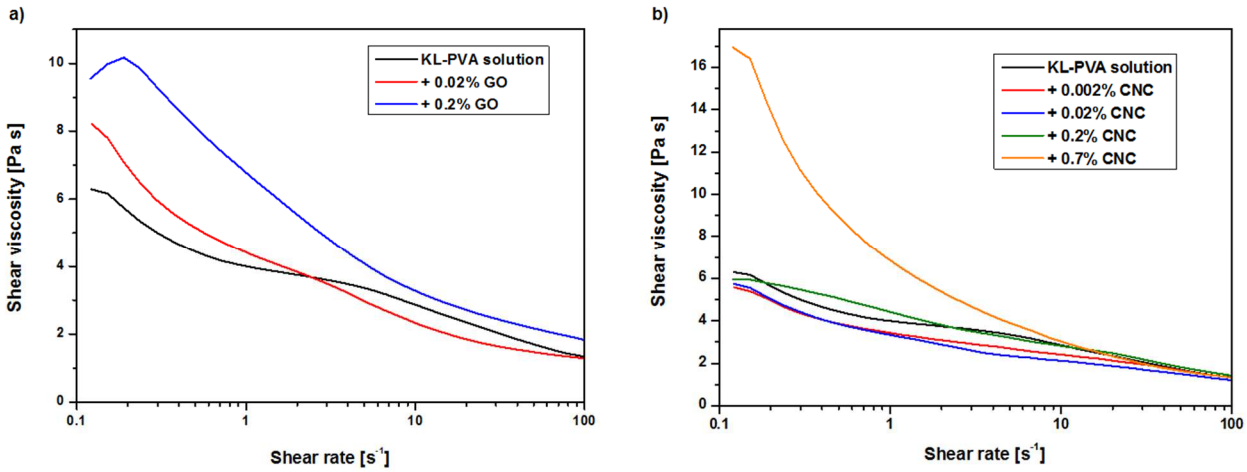

Figure A-IV-5: *Shear viscosity with respect to shear rate of dope solutions used for wet-spinning: influence of graphene oxide (GO) flakes (a) and cellulose nanocrystals (CNCs) (b) at different concentrations (in wt%) on the rheology of a spinning dope containing 14 wt% Kraft lignin (KL) and 6 wt% polyvinyl alcohol (PVA) in dimethyl sulfoxide (DMSO)*

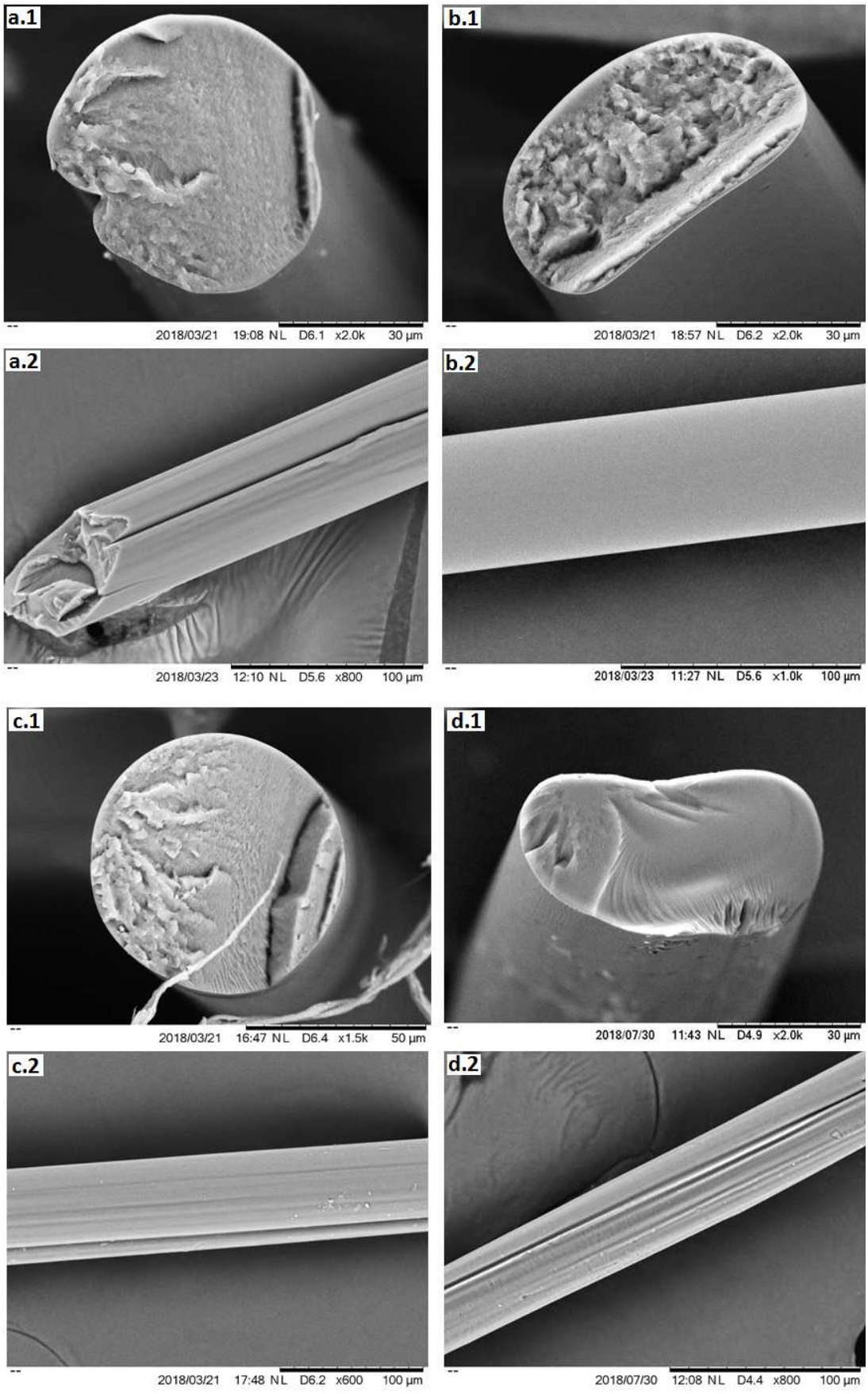

Figure A-IV-6: *SEM micrographs of KL-PVA-CNC 5% (a) and -10% precursor fibres spun by hand (b) and of continuously spun KL-PVA-CNC 5% precursor- (c) and carbonized fibres (d): cross-sections (1) and surfaces (2)*